l. 165, November 1, 1984
mplete in one issue

ISSN 0003-2670

ANALYTICA CHIMICA ACTA

International journal devoted to all branches of analytical chemistry

ELSEVIER

ANALYTICA CHIMICA ACTA

International journal devoted to all branches of analytical chemistry
Revue internationale consacrée à tous les domaines de la chimie analytique
Internationale Zeitschrift für alle Gebiete der analytischen Chemie

PUBLICATION SCHEDULE FOR 1984

	J	F	M	A	M	J	J	A	S	O	N	D
Analytica Chimica Acta	156	157/1	157/2	158/1 158/2	159	160	161	162	163	164	165	16

Scope. *Analytica Chimica Acta* publishes original papers, short communications, and reviews dealing with a aspect of modern chemical analysis, both fundamental and applied.

Submission of Papers. Manuscripts (three copies) should be submitted as designated below for rapid and effi handling:

Papers from the Americas to: Professor Harry L. Pardue, Department of Chemistry, Purdue University, West Lafay IN 47907, U.S.A.

Papers from all other countries to: Dr. A. M. G. Macdonald, Department of Chemistry, The University, P.O. Box Birmingham B15 2TT, England. Papers dealing particularly with computer techniques to: Professor J. T. C Universität Bern, Pharmazeutisches Institut, Baltzerstrasse 5, CH-3012 Bern, Switzerland.

Submission of an article is understood to imply that the article is original and unpublished and is not being consic for publication elsewhere. Upon acceptance of an article by the journal, authors will be asked to transfer the copy of the article to the publisher. This transfer will ensure the widest possible dissemination of information.

Information for Authors. Papers in English, French and German are published. There are no page cha Manuscripts should conform in layout and style to the papers published in this Volume. Authors should co Vol. 160 for detailed information. Reprints of this information are available from the Editors or from: Elsevier Edi Services Ltd., Mayfield House, 256 Banbury Road, Oxford OX2 7DH (Great Britain).

Reprints. Fifty reprints will be supplied free of charge. Additional reprints (minimum 100) can be ordered. An a form containing price quotations will be sent to the authors together with the proofs of their article.

Advertisements. Advertisement rates are available from the publisher.

Subscriptions. Subscriptions should be sent to: Elsevier Science Publishers B.V., Journals Department, P.O. 211, 1000 AE Amsterdam, The Netherlands. Tel: 5803 911, Telex: 18582.

Publication. *Analytica Chimica Acta* appears in 11 volumes in 1984. The subscription for 1984 (Vols. 156–16 Dfl. 2145.00 plus Dfl. 231.00 (p.p.h.) (total approx. U.S. $914.00). All earlier volumes (Vols. 1–155) except Vol and 28 are available at Dfl. 215.00 (U.S. $82.70), plus Dfl. 15.00 (U.S. $6.00) p.p.h., per volume.

Our p.p.h. (postage, packing and handling) charge includes surface delivery of all issues, except to subscribe Australia, Brazil, Canada, China, Hong Kong, India, Israel, Japan, Malaysia, New Zealand, Pakistan, Singapore, S Africa, South Korea, Taiwan and the U.S.A. who receive all issues by air delivery (S.A.L. — Surface Air Lifted) extra cost. For the rest of the world, airmail and S.A.L. charges are available upon request.

Claims for issues not received should be made within three months of publication of the issues. If not they cann honoured free of charge.

For further information, or a free sample copy of this or any other Elsevier Science Publishers journal, readers i U.S.A. and Canada can contact the following address: Elsevier Science Publishing Co., Inc., Journal Inform Center, 52 Vanderbilt Avenue, New York, NY 10017, U.S.A., Tel: (212) 916-1250.

Pyrolysis Mass Spectrometry of Recent and Fossil Biomaterials

Compendium and Atlas

by H. L. C. MEUZELAAR, *Salt Lake City, UT, U.S.A.*, J. HAVERKAMP, *Amsterdam, The Netherlands and* F. D. HILEMAN, *Dayton, OH, U.S.A.*

Techniques and Instrumentation in Analytical Chemistry, Vol. 3

Since the 3rd International Symposium on Analytical Pyrolysis in 1976, the importance of pyrolysis mass spectrometry (Py-MS) as an analytical method has increased considerably. Specially designed Py-MS systems using galvanically heated filament or direct probe pyrolysis have been quite successful in structural investigations and kinetic studies involving synthetic polymers and model compounds. The Curie-point Py-MS has, however, made a lasting impression on the field, being unique in those applications that require maximum reproducibility. This book presents an in-depth discussion of basic principles (including sample requirements, short- and long-term reproducibility problems and data processing approaches) of Py-MS techniques.

The Compendium has been put together by authors who have themselves been deeply involved in an extensively used fully-automated Py-MS system. It is thought that this system, particularly useful in characterising bacteria, could revolutionise clinical methods which have not changed since Pasteur.

The advent of commercially available Curie-point Py-MS systems has prompted the authors to include a small Atlas of over 150 reference spectra of carefully selected biomaterials which should help users of these systems to "tune" their instruments to the existing systems and to evaluate unknown spectra.

An asset to any chemistry library and particularly useful to those scientists considering the application of Py-MS techniques to their own specific problems in the analysis and data processing of biomaterials.

Contents: Part I. Compendium of Basic Principles and Applications. 1. Origins and Development of Pyrolysis Mass Spectrometry of Biomaterials. 2. From Fingerprinting to Structural Investigation. 3. Pyrolysis Mechanisms in Biomaterials. 4. The Technique of Curie-Point Py-MS. 5. Reproducibility in Curie-Point Py-MS. 6. Data Analysis Procedures. 7. Selected Applications to Biomaterials. **Part II. Atlas of Selected Pyrolysis Mass Spectra.**

1982 xiv + 294 pages
US $ 61.75/Dfl. 145.00
ISBN 0-444-42099-1

ELSEVIER SCIENTIFIC PUBLISHING COMPANY
P.O. Box 211
1000 AE Amsterdam, The Netherlands.

ELSEVIER SCIENCE PUBLISHING CO. INC.
52 Vanderbilt Avenue
New York, NY 10017, U.S.A.

7246A

ANALYTICA CHIMICA ACTA
VOL. 165 (1984)

ANALYTICA CHIMICA ACTA

International journal devoted to all branches of analytical chemistry

ELSEVIER Amsterdam–Oxford–New York–Tokyo

0003-2670/84/$

Printed in The Netherlands

Analytica Chimica Acta, 165 (1984) 1—29
Elsevier Science Publishers B.V., Amsterdam — Printed in The Netherlands

QUALITY ASSURANCE IN BIOMEDICAL NEUTRON ACTIVATION ANALYSIS

Report of an Advisory Group[a] of the International Atomic Energy Agency, Vienna, Austria

(Received 27th March 1984)

SUMMARY

Evidence from various sources leads to the conclusion that all current methods for the determination of trace elements in biological materials may, as currently practised, be subject to significant error, even as large as several orders of magnitude. This report, prepared by an Advisory Group convened by the International Atomic Energy Agency, examines possible sources of error arising in the application of neutron activation analysis to biomedical materials, and attempts, in the light of current knowledge, to recommend practical and effective means to avoid them. The topics discussed include sampling and sample preparation, standards, the activation of samples and standards, chemical separations, γ-ray spectrometry, and general methods of internal and external quality assurance.

Neutron activation analysis (n.a.a.), in both its instrumental (i.n.a.a.) and radiochemical (r.n.a.a.) forms, is an important method for the in vitro determination of trace elements, and is widely applied to specimens of biomedical origin. Partly on account of difficulties caused by the low concentrations involved, which may be only of the order of a $\mu g\ kg^{-1}$ or less, these analyses are often accompanied by significant errors. This is an important problem, not only because of the confusion and waste of time caused by erroneous data, but also because vital decisions may depend on the accuracy of such data, for example in medical diagnosis and in the implementation of governmental regulations pertaining to the levels of toxic substances in foods and tissues.

The report that follows represents an attempt to identify some of the possible sources of error in in vitro n.a.a. and to advise on practical means to avoid them. It stems from an Advisory Group Meeting convened by the

---

[a]Members of the Group were: Dr. H. J. M. Bowen (U.K.), Dr. M. de Bruin (Netherlands), Dr. A. R. Byrne (Yugoslavia), Dr. R. Dybczynski (Poland), Prof. J. J. M. de Goeij (Netherlands), Prof. V. P. Guinn (U.S.A.) chairman, Dr. K. Heydorn (Denmark), Dr. G. V. Iyengar (Federal Republic of Germany), Dr. M. Sankar Das (India), and Dr. J. Versieck (Belgium). Dr. V. D. Anand (U.S.A.) was present as an observer. The IAEA's Secretariat was represented by Drs. R. M. Parr (secretary) and L. Pszonicki. Address for reprints: Dr. R. M. Parr, International Atomic Energy Agency, P.O. Box 100, A-1400 Vienna, Austria.

0003-2670/84/$03.00

International Atomic Energy Agency (IAEA) in September 1982 as well as from subsequent exchanges between the contributors.

Working papers prepared by members of the Group have been compiled in a Technical Report published by the IAEA [1]. A limited number of copies of this publication is available on request. The interested reader is referred to this publication for further details on all the topics discussed below.

BACKGROUND TO PRESENT REPORT

The analysis of biological materials for trace elements is at present undertaken on a large scale in many countries around the world. Although it is difficult to quote well documented data on the actual numbers of determinations done, it is almost certain that they are to be measured in tens of millions per year on a world-wide basis. Neutron activation analysis plays an important role in such work (especially for some of the less commonly measured trace elements), and the IAEA has for many years promoted and supported its applications through technical cooperation, analytical quality control services, etc.

Neutron activation analysis has a number of favourable characteristics that account for its important role in trace element work, particularly its very low detection limits (for most, though not all, of the elements of biomedical interest), its relative freedom from contamination problems and matrix effects, and its potential for multi-element determinations. Research nuclear reactors of a kind suitable for n.a.a. are now relatively accessible to scientists in a large number of countries; according to a recent report there are at present 163 such reactors in operation in 41 countries [2]. The wide applicability of n.a.a. is exemplified by the fact that it has been indicated to be capable of yielding results of medium or high precision ($\approx$10% relative s.d. or better) under optimum conditions for as many as 26 elements of interest (mostly trace elements) in a variety of biological reference materials; this is more than for any other trace analysis method [3]. Moreover, in several recent IAEA intercomparisons, n.a.a. was the only method of analysis which yielded results for some trace elements (e.g., Ag, Au, Ce, Cs, Eu, Ga, Pt, Sb, Sc and W) [4, 5]. The same intercomparisons have also consistently shown a high frequency of use of n.a.a., and a high percentage of the total number of elements that could be determined by this method, a fact which is further confirmed by reports of measurements on biological reference materials available from the U.S. National Bureau of Standards (NBS) [6].

For more than 10 years, the IAEA has been conducting interlaboratory comparisons in this field, all of which, despite the good accuracy and precision expected of n.a.a., have revealed wide discrepancies between the results reported by different laboratories for many of the elements of interest. These findings, which are by no means confined to n.a.a., but rather appear to be typical of all current methods of trace element analysis, have frequently

been confirmed even when consideration is restricted to a selection of "experienced laboratories". The magnitude of the discrepancies depends somewhat on the concentration levels involved, and is generally higher the lower the concentration. As a general rule, it appears that results for Ca, Cl, Cu, Fe, Mg, Na, Se and Zn exhibit the smallest variability, but even for these elements a significant fraction of participating laboratories report erroneous results. Elements occupying an intermediate (and rather poor) position as regards analytical variability include As, Hg, I and Mn, while Cd, Co, Cr, Mo and Sb typically show extreme variability (up to several orders of magnitude). Table 1 illustrates some of these findings for two biological reference materials recently issued by the IAEA. The data reported refer to measurements by n.a.a. and its principal competitor as a method for determining trace elements, atomic absorption spectrometry (a.a.s.).

The lack of progress in recent years in achieving a significant improvement in the level of performance of laboratories participating in the IAEA's programmes points to the need for more radical solutions to these problems, which almost certainly cannot be found just in the organization of more intercomparisons. It appears to be necessary instead to convince each individual analyst of the necessity of identifying the sources of error affecting his own measurements, and then of taking appropriate steps to correct them.

The report that follows is intended as guidance for all involved in analysis, including sample collection and preparation. The analytical procedure is here broken down into its component steps and, for each of these, an attempt is made to describe what, in the light of current knowledge, may be considered to be "good laboratory practice". The report also attempts to identify potential sources of error in each of these steps and to recommend effective means to avoid them. Where appropriate, advice is offered on specific checks and adjustments that might help to ensure a proper functioning of procedures and equipment.

All these recommendations constitute part of "quality assurance" which, borrowing the definition of Taylor [7], is here taken to encompass the two concepts "quality control" and "quality assessment". Quality control is the mechanism established to control errors, while quality assessment is the mechanism used to verify that the analytical procedure is operating within acceptable limits.

Although this report deals mainly with problems that arise when n.a.a. is applied to biomedical materials, many of its recommendations are of a general character and also have relevance to other analytical methods and other kinds of analytical samples. The term "biomedical" is mainly used in the broad sense, including both its biological and medical aspects; however, most of the discussion and examples refer specifically to medical specimens (e.g., human tissues). Broadly similar analytical considerations apply also to many other kinds of biological materials, though some of the details may differ.

TABLE 1

Illustration of poor results for selected elements in two IAEA intercomparison materials: milk powder (A-11) and animal muscle (H-4)
The results considered in each data set are the laboratory means reported by participants in the intercomparisons; all concentration values are in mg kg^{-1} (note the wide range and the poor agreement, in many cases, between the mean and the median)

Element	Method[a]	Material	No.[b]	Median	Mean	Range	Max/min
As	R.n.a.a.	A-11	6	0.0056	0.12	0.004—0.54	122
		H-4	11	0.0061	0.037	0.004—0.20	55
Cd	A.a.s.	A-11	7	0.47	0.60	0.001—1.66	1446
		H-4	9	0.090	0.25	0.003—0.96	295
	R.n.a.a.	H-4	5	0.056	0.12	0.01—0.42	43
Co	I.n.a.a.	A-11	6	0.091	0.60	0.005—2.90	575
		H-4	16	0.004	0.012	0.0015—0.046	31
	R.n.a.a.	A-11	6	0.0056	0.0075	0.004—0.016	4
		H-4	5	0.013	0.016	0.001—0.040	28
Cr	A.a.s.	A-11	7	0.76	8.15	0.032—52	1656
		H-4	8	0.098	0.20	0.015—0.71	47
	I.n.a.a.	H-4	6	0.25	0.31	0.02—0.80	40
	R.n.a.a.	A-11	6	0.049	3.07	0.016—18.1	1138
		H-4	5	0.020	0.049	0.012—0.12	10
Hg	A.a.s.	A-11	5	0.095	0.20	0.001—0.67	500
	R.n.a.a.	A-11	6	0.003	0.022	0.002—0.12	52
		H-4	8	0.013	0.013	0.005—0.021	4
Mn	A.a.s.	A-11	17	0.67	3.99	0.20—55	279
		H-4	11	0.56	1.16	0.43—3.9	9
	I.n.a.a.	H-4	13	0.55	0.75	0.41—2.05	5
	R.n.a.a.	A-11	7	0.256	0.295	0.12—0.58	5
		H-4	6	0.44	0.35	0.08—0.45	6
Mo	R.n.a.a.	H-4	8	0.051	0.12	0.032—0.38	12
Sb	I.n.a.a.	H-4	8	0.008	0.030	0.004—0.16	44
	R.n.a.a.	A-11	5	0.004	0.21	0.001—1.01	777
		H-4	6	0.004	0.072	0.002—0.41	175

[a]I.n.a.a. = instrumental n.a.a.; r.n.a.a. = radiochemical n.a.a.; a.a.s. = atomic absorption spectrometry. [b]Number of laboratory means in the data set (no data are quoted for <5 such values).

QUALITY ASSURANCE OF SAMPLING, SAMPLE PRESERVATION AND PREPARATION

Sampling

Proper selection of nature, number, and site of procurement of primary samples. It is well established that factors such as age, sex, nutritional status, pregnancy, lactation, and environmental or occupational exposure, may contribute to the overall variability of trace element levels in biomedical samples.

These influences can be grouped under the heading "presampling factors" [8], all of which need to be taken into consideration in the planning stage of any study on trace elements in biomedical materials.

Ideally, sampling should be done in such a way that the original properties of the sampled material are fully retained, with no contamination, and with all necessary documentation pertaining to the sample itself. In practice, however, compromises are almost always necessary; in such cases the sampling design has to be tailored according to the actual objectives of the study.

The number of primary samples and the locations from which they are taken in a given organ depend, of course, not only on the objectives of the study but also on the characteristics (anatomical structure, physiological function) of the material that is selected for analysis. As a rule, in the biomedical field, it is considerably more difficult to meet analytical requirements as to the number (e.g., replicates) and size of samples than in most other areas of trace element research. For successful work, close collaboration between the analytical and biomedical communities is mandatory, or the investigator must combine both functions, because elemental determinations in arbitrarily selected materials, without due consideration of their potential biomedical relevance, can lead only to an accumulation of largely useless data.

The relative ease with which some specimens (e.g., hair and nails) can be collected and preserved should not be allowed to obscure the fact that there may be considerable difficulties in interpreting any analytical data subsequently obtained. There is no doubt that hair analyses may provide useful information in some selected situations. However, it is now well documented that a wide variety of largely uncontrollable factors may markedly affect the observed results.

Control of contamination. Many factors may invalidate the results of trace element research. It cannot be emphasized too strongly that, in spite of recent improvements in the sensitivity and selectivity of the analytical methods used, the reliability of an analytical value still depends strongly on the quality of the sample. No amount of care during the measurement can guarantee reliable information if an error has been introduced earlier.

Many trace elements of interest are present at very low concentrations ($\mu g\ kg^{-1}$ or less) in biomedical samples, and their determination is particularly susceptible to errors from inadvertent extraneous additions, i.e., contamination [9—11]. This is a problem for all analytical methods, though n.a.a. has the unique advantage that sample contamination after the irradiation does not affect the final outcome.

A striking, but by no means atypical, illustration of this problem is provided by observations on inadequately collected and processed serum samples intended for the determination of manganese [12]. In 9 samples transferred with an automatic dispenser (inadequate procedure), the following figures were obtained: a mean of 4.83 ± 5.17 (s.d.) $\mu g\ l^{-1}$ with a range of 0.61—16.83 $\mu g\ l^{-1}$. In contrast, in 9 adequately handled samples from the same

serum pool, using exactly the same radioanalytical procedure, the following values were obtained: a mean of 0.72 ± 0.10 (s.d.) $\mu g\ l^{-1}$ with a range of 0.56—0.89 $\mu g\ l^{-1}$, i.e. a factor of almost 7 lower in mean value, and a 52-fold improvement in standard deviation.

No universal set of rules for avoiding problems of this kind can be given, apart from general advice to work in a clean environment with reproducible, non-contaminating tools. Many of the recommendations on sample preparation are relevant in this respect. However, if, for any reason, it is impossible to collect the specimen under completely adequate conditions, then a sufficient amount should always be obtained to permit later removal, in the analytical laboratory, of the contaminated surfaces (though this, of course, is not possible for fluid samples).

Various other factors, in addition to contamination, also threaten the integrity of the sample, e.g., losses by adsorption or volatilization. They are considered further below.

Post-mortem samples. Autopsy sampling from human cases always involves a certain lapse of time between death and sample collection. When normal metabolic processes stop and active transport through membranes ends, passive diffusion may cause profound changes in trace element distribution. In addition, autolysis may cause detrimental changes. These problems cannot be completely avoided, but their effects can be minimized by standardizing sampling conditions, especially the time factor [8, 13].

Preservation and storage

Preservation and storage are not interchangeable terms because preservation also includes retaining the morphological features of a specimen, whereas storage, especially from the point of view of trace element studies, may be understood to imply an overall safe, contamination-free and non-degraded containment.

Preservation of a sampled specimen is governed by several factors, particularly the matrix itself. For example, preservation of bone, hair or nail is relatively simple compared with that of brain, liver, lung or kidney. Preservatives such as formaldehyde are generally unacceptable for trace element work because of problems of leaching and contamination. Therefore, the method of preservation by freezing is emerging as a better choice. For short term preservation (up to a few days) samples can be kept at ≈0°C, or even at refrigerator temperature. Long-term preservation (extending from several weeks to years) requires temperatures of −20°C or below. For storage up to several years, many workers recommend a temperature of around −80°C, while for specimen banking purposes it may even be advisable to store at liquid nitrogen temperature. If possible, whole organs or chunks of tissues should be procured, sealed in clean polyethylene (PE) bags, and packed in clean plastic containers, before freezing. The samples should be frozen as quickly as possible. In any case, they need to be kept under cool conditions until they can be frozen.

One disadvantage of preservation by freezing is the uncertainty that may arise in determining the wet weight of the specimen if it is subsequently allowed to thaw (because of loss of water vapour and possible cell lysis during storage). Moreover, the method is not suitable for all biological fluids. For example, whole blood, once frozen, cannot be used to obtain samples of serum or of packed cells. Whole blood can be preserved for only a few days at refrigerator temperature, and requires the addition of an anticoagulant, which is a potential source of contamination.

As regards storage, where applicable, it is good practice to freeze-dry, or oven-dry at relatively low temperatures (e.g., 80°C), because storing dry substances is less complicated. Storage containers made of PE or PTFE are adequate for most purposes, but should be thoroughly cleaned before use [10, 14]. Low humidity and a dust-free environment are absolutely essential. If suitably packed, dry samples can be stored for long periods of time under cold storage [13].

Sample preparation

In many laboratories, the first time an analyst becomes acquainted with the sample is when it arrives at the laboratory. Before accepting it for analysis, however, he should familiarize himself with the prior history of the specimen (which should be adequately recorded) and be confident of its integrity.

Elements such as Cr, Mn and Pb are highly susceptible to airborne contamination and, unless "clean room" or "clean bench" facilities are available, analysts intending to determine these elements should consider carefully whether their laboratory facilities are adequate for the purpose. It is in general good practice to assess all possible sources of error experimentally, especially those arising from contamination within the working environment, to take measures to minimize such errors and to conduct periodic monitoring. For example, contamination introduced by leaching, or losses by adsorption, can be studied by preparing a particular type of sample in containers fabricated from different materials.

The primary concern from the point of view of sample handling is to use tools and containers made of materials containing very low concentrations of the trace elements of interest. However, it should be recognized that the objective is not necessarily to eliminate contamination entirely, but merely to reduce it to a level at which it is no longer significant. For some trace elements, such as Cu and Zn, contamination may be insignificant even when no special precautions are taken. At the present time, for ultratrace work, the recommended materials for tools and containers are plastics, silica and high-purity metals such as titanium. If the problem of obtaining a durable sharp edge for tools made of titanium could be overcome (e.g., by use of a suitable alloy made with non-contaminating elements), this would be an important step forward in producing a standard kit for handling tissues.

Several steps, such as washing, drying, ashing and homogenization, may be

needed for handling solid samples to prepare them for analysis. Each of these may be a source of contamination. The rationale for washing some types of samples, such as hair and nail, and even autopsy specimens, prior to analysis is to remove external contamination from the former, or to minimize the effect of residual blood in the latter. For hair and nail, a washing step is generally deemed to be necessary, though it is not feasible to prescribe a universal treatment that satisfies the requirements for all the elements of interest. For autopsy samples, washing with water has both advantages and disadvantages, and its utility is therefore questionable [13].

Freeze-drying is basically well suited for removing water from biological samples, but care should be taken that the sample is prefrozen before placement in the freeze-dryer and that an adequate vacuum is maintained. In oven-drying, it is important to maintain the temperature below 100°C to avoid matrix decomposition and subsequent losses of elements such as Sn and Hg. A temperature of around 500°C is effective for dry ashing even relatively big samples, but has the serious disadvantage of causing losses by volatilization of a number of elements. Low-temperature ashing (below 150°C) with nascent oxygen is effective only for small samples, and is also not totally safe for volatile elements. For more details on the relative merits of various drying procedures, the reader is referred to a recent review [15].

Biological samples are inherently inhomogeneous, both macroscopically and microscopically, because of their complex and intricate structure. Depending on the aim of the investigation, it may or may not be necessary to reduce the effect of macroscopic inhomogeneity by a specific homogenization step. This is particularly necessary for reference materials, composite meals and faeces, but may also be required for human tissue samples that need to be divided into aliquots prior to analysis. Such homogenization may be applied to both the wet and dry specimens by the use of cryogenic techniques [14].

Biological fluids are susceptible to bacterial growth in the unfrozen state, and sample preparation should therefore be finished within a few hours. If possible, they should be aliquoted in the fluid state, because it is then relatively simple to retain homogeneity. Freshly thawed samples should be stirred well before aliquoting, to overcome concentration gradients [15].

In conclusion, it may safely be said that inadequate sample collection and manipulation can be the source of more serious errors than any other step in the analytical procedure. Low-level trace element research imposes strict requirements on its practitioners. The analyses must be conducted under rigorously controlled conditions to protect the sample from artefacts from the containers, the reagents, or the ambient air. As a consequence, no programme of low-level trace element analyses should be started before adequate contamination control procedures have been developed (sample collecting and handling devices, container cleaning techniques, "clean room" facilities, etc.).

Pre-irradiation separations

Separations prior to irradiation are sometimes used to achieve (1) differentiation of the matrix as to cell types or cell constituents, (2) chemical speciation of the analyte, (3) removal of interfering elements and/or concentration of the element to be determined, and/or (4) reduction of high radiation levels arising during processing of the subsequently irradiated specimens. However, the introduction of pre-irradiation separations deprives n.a.a. of one of its main advantages, i.e., the virtual absence of the analytical blank. Especially for solid samples, it is rather difficult at low trace levels to prove that no losses or contamination have occurred and, if so, to correct for them. Therefore, pre-irradiation separations should be avoided as much as possible. While separations for the reasons mentioned under (1) and (2) are unavoidable, this is not the case for the other groups. For instance, by developing fast radiochemical separations, pre-irradiation separations can sometimes be avoided, or replaced by a simple pretreatment such as ashing.

QUALITY ASSURANCE IN REACTOR NEUTRON ACTIVATION ANALYSIS OF BIOMEDICAL SAMPLES

Possible causes of poor performance as evidenced by IAEA intercomparisons

Causes of the poor performance of some laboratories that have participated in IAEA intercomparisons are difficult to identify because the participants have usually not described their analytical procedures in sufficient detail. Even if they had done so, however, the tracking down of the sources of error in individual cases would mostly have been of a speculative character.

One obvious source of error, however, is the choice of an inappropriate analytical method, e.g., a method with a potential capability (detection limit) close to the concentration level of the elements being determined. Even if the choice of method is correct, an inappropriate version of the method is sometimes chosen (e.g., i.n.a.a. instead of r.n.a.a., which, for some intercomparison materials, seems to have been the case for elements such as As, Co, Cr, Hg, Mn and Sb). Every step in the procedure may be a source of error if the execution is poor; thus many errors are, in fact, human errors.

In addition to the possible sources of error discussed in the remainder of this report, some further causes are: (a) uncritical expectation of the multi-element capabilities of n.a.a., i.e., not taking into account that, for some elements determined in a given run, irradiation, cooling, separation, or measurement conditions may be very far from the optimum, and the interferences may be excessive; and (b) trivial human errors in making the calculations, copying the data and reporting the results (typing errors, etc.).

Optimization of analytical parameters

In many instances of n.a.a. studies (particularly i.n.a.a.), the elements of interest are not measured under the best conditions for those elements in that particular matrix. This situation leads to unnecessarily poor measurement

precisions, and sometimes even to systematically erroneous values (e.g., unrecognized overlapping photopeaks), and to the use of samples too small to give good counting statistics, or too large for the counting-rate limitations of the Ge γ-ray spectrometer used. These same difficulties may also apply to r.n.a.a., if groups of elements are separated and counted on the spectrometer, rather than individually separated elements.

In order to avoid the difficulties mentioned above, in i.n.a.a. work, one has essentially two choices: (1) to conduct a series of exploratory measurements, before proceeding to the final sample analyses, in order to deduce approximately optimum combinations of sample weights and irradiation and decay conditions for the elements of interest in such a matrix, or (2) to use a computer program that supplies similar information, in most cases without the necessity of making any exploratory experimental measurements. The exploratory approach is the older approach, and is time-consuming. However, its use is far better than making no effort at all in the direction of optimization, if for any reason the computer approach is not accessible.

An i.n.a.a. Advance Prediction Computer Program (APCP) [16] is now available that helps one to select, in advance, optimum combinations of sample size and irradiation (t_i), decay (t_d), and counting (t_c) times for the measurement of any particular element of interest in any type of sample matrix for which even rather approximate average elemental composition input data are available from the literature (including also major and minor elements). Such input data can be obtained from any analytical methods, not just n.a.a. Using permanently stored nuclear data and experimental response curves for any given Ge detector, the APCP calculates, for any selected thermal-neutron flux and for each selected combination of t_i, t_d, and t_c, the maximum allowable sample weight, all cumulative Compton levels and Compton edges, and all statistically significant photopeaks (including escape peaks and the 511-keV peak) and their respective standard deviations. Photopeaks that overlap with one or more other peaks are flagged in the print-outs, as well as those that fall on significant Compton edges. For elements of interest not in the input, or input elements that are not detectable, the program also prints out their respective minimum detectable concentrations, for any selected measurement precision (e.g., $\pm 30\%$).

The APCP is also very useful in planning the preparation of optimum element standards, and can readily simulate pre- or post-irradiation chemical separations (by eliminating separated elements from the input). By scanning the outputs for all the selected sets of conditions, one can rapidly see whether a given element will be detectable at all in that matrix, and if so, the best set of conditions for its determination, the precision then attainable, and which of the (n,γ) products of the element, and which of its γ-rays, give the best precision. If the i.n.a.a. output is unfavourable for any particular element, the need for some type of chemical separation is indicated. The program allows one to make calculations for i.n.a.a. with either epithermal, or thermal plus

epithermal neutrons. (A second, more elaborate program, in FORTRAN 4, also includes all fission-spectrum fast-neutron products.) The APCP has been checked experimentally (with various certified biological reference materials), with excellent agreement between predicted and observed results.

Use of advance prediction, such as by the APCP, not only provides guidance for subsequent experimental measurements that ensure they will be conducted in an approximately optimum manner, thus saving a great deal of time, but it also draws attention in advance to possible difficulties (e.g., overlapping peaks). The nature and usefulness of the APCP are described more fully elsewhere [16, 17].

Calibration

Direct and indirect calibration methods. The accuracy of the calibration is obviously crucial for the accuracy of the whole analysis, yet the preparation and use of standards are not always straightforward, and simple and regular tests to check for possible errors are often neglected.

Calibration can be done in various ways. Most commonly, direct irradiation standards are used consisting of known amounts of all elements to be determined, which are irradiated together with the samples. Another, indirect, way of calibration involves the use of a single-element comparator [18], also called a monostandard. In this approach, a particular element (e.g., Co) is irradiated together with the samples and measured afterwards without any chemical processing. The comparator is calibrated against the elements of interest in separate experiments, leading, under well-defined experimental conditions, to constants, often called k-factors. This method is discussed further below.

The use of certified reference materials as irradiation standards, though practised by many workers, is not to be recommended for the trace element analysis of biological materials, as the uncertainties in the certified values are too large for many elements. The high costs and limited stocks of these materials further support the argument that they should not be used in this way.

Preparation and treatment of irradiation standards. Aqueous chemical standards are widely used in n.a.a. (particularly r.n.a.a.) for, as well as offering convenience, they represent a good approximation to the (usually relatively small) neutron absorption properties of biological samples, and can closely mimic their size and position during irradiation. Checks on geometrical effects, confirming the absence of significant flux gradients, are easily done on clusters of standards.

Irradiation standards are normally prepared from working solutions obtained by dilution of stock solutions shortly before use. Stock solutions should be made up from stoichiometric compounds of high purity (especially with respect to elements that produce interfering radionuclides on irradiation), be simple to prepare, and possess good stability (long shelf-life). Acidification of stock and working solutions is usual to improve stability (against hydrolysis, biological spoilage and adsorption effects). Further details con-

cerning suitable stock solutions may be found in a working paper [19].

In the preparation of irradiation standards, two occasional sources of error should be kept in mind. The first may occur in the preparation of mixed multi-element standards containing trace amounts of particular elements with high activation cross-sections (e.g., gold and some rare earths), if the same elements are also present as impurities in other components of the mixture. The result may be a negative systematic error in the calibration. The other error involves differences in isotope ratios between sample and standard. Substantial differences may occur with commercially enriched or depleted elements such as Li, B and U, while small differences (up to tenths of a percent) may be observed with other elements (e.g., S and Ca) as a result of biological or geological fractionation.

Irradiation standards may be used directly as solutions, or dried first, especially for high-fluence irradiations. The use of supports such as filter paper, silica or charcoal (which must, of course, be of sufficient purity for the purpose), is recommended to define the geometry if the standard is to be measured directly, and to facilitate quantitative recovery if it is to be removed from the ampoule. Other types of standard such as labelled cellulose, gelatin, ion-exchange beads or polymerized resins are sometimes useful, but checking against the original aqueous solution is required. Possible losses during preparation (e.g., by drying or sputtering) should be examined with such secondary standards.

Irradiation standards should preferably not be processed, but their activities measured directly or after a minimal treatment to recover adsorbed activity quantitatively from the vial walls by leaching. If measured directly, the vial must be of sufficient purity that it does not introduce errors in the measurement of the standards. Geometric factors also need to be considered. Possible volatile forms of certain elements (e.g., Hg) must be trapped by cooling and absorption in acidified carrier solution. (It is good practice to make up all aqueous standards for activity measurement in acidified carrier solution to help avoid adsorption on the wall of the measurement vial.)

Selection of the calibration method. Usually, the selection of a particular calibration method depends not only on quality assurance requirements but also on practical considerations. Options to choose between are: direct versus indirect calibration; mixed multi-element standards versus collections of single element standards; processing of irradiation standards in the same way as samples versus direct measurement.

The direct measurement of irradiation standards brings various advantages such as a reduction in the number of radiochemical operations, including chemical yield determinations, and a lowering of the risk of contaminating the sample. For simplicity, the difference in counting geometry between sample and standard should be constant; if not, a determination in each analytical run is required. When Ge γ-ray spectrometry is applied, multi-element standards can often be used provided that the ratios of the elemental weights have been properly chosen and that the photopeaks of interest do not overlap.

The radiochemical processing of irradiation standards is not recommended if their primary function as direct comparators is to be retained. This is because there is no guarantee that the chemical yield of the separation (or its variability) is the same for both samples and standards. If yields are quantitative, high or reproducible, nothing is gained in most cases, whereas if they are irreproducible, the assumption of the same yield may be erroneous. Further, the overall uncertainty of the yield determination is increased, and the chances of cross-contamination between samples and standards in the equipment (especially automatic devices) is increased. When high accuracy is required, chemical yields should in any case be measured for each sample separately. When this is impractical (e.g., in multi-element r.n.a.a.), frequent control of yields using radiotracers and non-irradiated material of the same composition is advisable.

A useful practical measure of control over the chemical yield or correct functioning of the chemical separation procedure can often be achieved by radiochemical processing of an additional standard or aliquot of the standard. By comparing the activity of the processed standard with that of an unprocessed standard or a flux monitor, time-consuming chemical yield determinations for each element can be omitted, while a reasonable estimate of the chemical yield can still be obtained, and other factors, such as counting geometry, can be taken into account. The risk of cross-contamination may be reduced by using standards containing a small multiple of the amounts of trace elements present in the samples, and by rigorous cleaning procedures.

The use of a single element comparator in place of a multi-element one also has particular advantages. For instance, it may save space in the irradiation container (particularly if it replaces a number of single element standards or a bulky multi-element standard). Further, it can also save labour (no chemical processing, fewer fractions to be counted). When dealing with short-lived radionuclides, the single-element comparator eliminates the need for a rapid processing of the standards. However, the usefulness of the single-element comparator is fully determined by the degree of constancy of the k-factors. Variations in these values over a series of determinations may occur because of changes in the neutron energy spectrum or counting geometry. Regular checks are therefore needed to ensure that such variations are not occurring. In order to compensate for neutron energy spectrum changes with time, as often occur in high-power nuclear reactors, the principle of the comparator may be extended to include two or three elements with different resonance integrals [21].

The main sources of error in the preparation and use of standards are likely to arise from careless working and insufficiently regular checks on accuracy. Among the former can be included weighing, dilution and dispensing errors, evaporation losses and deterioration of solutions. As a check on these sources of error, as well as to monitor flux variations in the irradiation position, it is good practice to use a suitable flux monitor (e.g., Co, Fe or Zn), and to calculate the ratio of the decay-corrected specific activity of the

standard to the theoretically expected specific activity. This ratio need not be exactly unity (though a large discrepancy is an indication of error); however, it should remain constant from one irradiation to the next. The same objective can also be achieved by other, similar means [22].

Whenever fresh working solutions are prepared, the old and new solutions should be checked in a simultaneous irradiation. Stock solutions should be checked at less frequent intervals by making up an independent solution, preferably from a different compound by another analyst. Exchange of standard solutions between laboratories might be useful and revealing, especially in cases in which "round-robin" exercises are being made. Suitable stock solutions are now available commercially (mainly for use in atomic absorption spectrometry), but these should always be checked by some independent test.

Reactor activation of samples

For the most accurate work by n.a.a., the sample and the standard are irradiated together. In this step the factors that should receive special attention to minimize the errors in the analysis are: (a) flux gradients in the irradiation position (spatial distribution of flux); (b) effect of the unmoderated neutron spectrum producing the indicator radionuclides from threshold reactions; and (c) recoil transfer from the container to the sample on the one hand, and loss of indicator radionuclide from the sample to the container, on the other hand.

Spatial distribution of the neutron fluence. It is well documented that, in many reactor irradiation positions, the neutron flux density gradient, parallel to the core, is about 2—3% cm^{-1}. The perpendicular gradient can cause even greater errors, the flux density variation being exponential [23, 24]. Facilities for rotating the samples and the standards during irradiation are useful in minimizing such errors. In any case, it is good practice to characterize the irradiation positions for such flux density gradients by using appropriate monitors. Several elements or alloys suitable for monitoring different fluences have been reported in the literature [25]. The use of an independent fluence monitor to assess the reproducibility of the irradiation conditions is particularly important if, as is often the case when short-lived radionuclides are being measured, the sample and standard are irradiated separately. Further, the ability to obtain a consistent decay-corrected specific activity of the monitor is an assurance that reproducible irradiation conditions are being maintained in all situations.

Effect of the unmoderated component of the neutron spectrum. Two aspects have to be considered: (a) the effect of the epithermal component on the monoelement comparator approach of n.a.a., and (b) threshold reaction interferences.

Some of the advantages and limitations of the use of single-element comparators (monostandards) for multi-element n.a.a. have been discussed in the previous sections and in the literature [23]. This approach requires that the

epithermal component of the neutron fluence in the irradiation position be constant over a series of analyses because the specific activities of the individual radionuclides, which have different resonance integrals, are normalized with respect to that of the monostandard.

Interference from threshold reactions must be considered in the analysis of biological samples. Depending on the type of reactor and the exact location of the irradiation position relative to the core, there may be large differences in the neutron flux spectrum between different irradiation positions. Some of the important reactions of interest in the analysis of biological samples are: $^{23}Na(n,\alpha)^{20}F$, $^{31}P(n,\alpha)^{28}Al$, $^{56}Fe(n,p)^{56}Mn$, $^{54}Fe(n,\alpha)^{51}Cr$, $^{64}Zn(n,p)^{64}Cu$ and $^{63}Cu(n,\alpha)^{60}Co$. Particular attention is drawn to the possibility of interference in the determination of chromium in whole blood.

The extent of interference depends on the fast/thermal flux ratio in the reactor, which should be measured whenever the reactor parameters have been changed or if there is a change in the irradiation position. If one makes some assumptions about the fission component of the fast neutron fluence, it may be possible to estimate the extent of interference based on the reported excitation functions for the reactions of interest and a knowledge of the approximate composition of the sample in respect of the interfering elements. In many reactors, however, the hard component of the flux, which can be determined by the use of a set of threshold monitors recommended by the IAEA, deviates from a virgin fission spectrum. It is therefore more prudent to determine experimentally equivalent interference values by irradiating known amounts of the interfering elements under a cadmium shield and to use these values to correct the experimental data. Further details are discussed in the working paper [26].

Possible recoil and radiolysis effects. Absorption of γ-radiation and fast neutron moderation cause radiolysis of the organic material, and thereby also changes in the chemical status of the trace elements. In addition, the radiation dose to the sample causes its temperature to rise. Both effects may result in losses of particular trace elements (e.g., halogens, mercury) from the sample by diffusion and volatilization. Losses may be further enhanced by the recoil effect accompanying the nuclear transformations. A part of the trace elements lost from the sample may remain in the gaseous state or be deposited on the inner surface of the container.

During irradiation, biological material deteriorates, sometimes to tarry substances, with evolution of gaseous products. Pressure build-up may occur, especially after long irradiation periods in high neutron fluxes, sometimes being high enough to cause substantial losses of sample material on opening the container. During the irradiation, losses from silica vials are virtually absent, but they may occur from PE vials because of small leaks or porosity of the material (e.g., for iodine and mercury).

Another consequence of recoil effects is that radionuclides formed in the container material migrate. Thus, the inside surface of the container, even if initially clean, can become contaminated as a result of the irradiation. This

contamination is easily carried along with the sample during further processing. Therefore it is important that the vials should not only have clean inside surfaces, but also low levels of the trace elements of interest in the layer below the surface. Because trace elements tend to be enriched in the surface layer of silica tubing used for the fabrication of irradiation vials, it is recommended to remove a layer of about 20 μm by etching in hydrofluoric acid before use [27].

Post-irradiation chemical treatment

Radiochemical processing may be a source of error, both random and systematic. However, compared with the chemical processing required for other methods of trace element determination, it has some specific characteristics that facilitate error control. These are: (1) that contamination with stable isotopes of the elements of interest after the irradiation does not interfere; (2) that the chemical separations can be done with the optimum amount of material because of the possibility of carrier addition; (3) that the yield of the chemical separation does not need to be quantitative or reproducible, because it can be determined for each sample, thus allowing flexibility in the selection of a separation method with the desired characteristics; and (4) that it is a tracer technique in itself. Thus the induced radioactivity, as well as additional tracers, may give information on various phenomena such as tailing, decontamination, adsorption and volatility losses. Yet, some constraints may arise in radiochemistry that are absent in nonradiochemical work, and these may make operations more prone to error. For instance, high radiation levels may be involved, or work with short-lived radionuclides may demand very rapid operations.

The main radiochemical operations involved in r.n.a.a. are discussed below. They include transfer of the irradiated sample from the irradiation container, addition of carrier, mineralization of the sample, equilibration of the carrier, removal of the main interfering activities and/or separation of radionuclides of interest, preparation of the counting fraction, and determination of the chemical yield. For details on all these points, the reader is referred to the working paper [20].

It is self-evident that normal good analytical practice should be followed throughout all these steps. A special feature of r.n.a.a. is the possibility of radioactive contamination occurring at any of the stages listed. Cross-contamination must be prevented by good laboratory practice, involving adequate cleaning operations, separate glassware for standards and samples, or the use of disposable equipment. In the use of automated and mechanized equipment, the existence of memory effects should be checked by blank runs, and if present, reduced by cleaning runs.

Transfer of the irradiated sample from the irradiation container. Irradiation containers, especially when no double containment is used, can become contaminated during irradiation or subsequent handling. To avoid transfer of this contamination along with the sample, they should be cleaned externally before being opened.

As already mentioned, radiolysis of organic material during irradiation leads to a pressure build-up, which may be high enough to cause appreciable losses of sample material on opening the container. In addition, some radionuclides may be volatile, particularly as a result of radiation effects. Both types of loss can be minimized by cooling the container in liquid nitrogen before opening.

During irradiation, biological specimens may char to tarry substances; these stick to the container wall and mostly cannot be removed entirely by simple means, but instead require some kind of dissolution. This dissolution, which may be the first step in the mineralization of the entire sample, leads to the problem that radionuclides from the container wall may also be leached out, resulting in a positive systematic error. This error (which is one of the components of the overall analytical blank) may be reduced by thoroughly cleaning the inner container surface before irradiation, but one still has to take account of radionuclides recoiling from the inside surface of the container material into the sample. Moreover, when silica ampoules are used, the process of opening them leads to fresh fractures, which may add to the blank. When high-purity synthetic silica ampoules are used, the blank value is generally only a problem for a few trace elements at the lowest levels (e.g., Cr and Sb). However, in all cases, the blanks should be checked and steps should be taken to ensure that they remain insignificant. If the blank value is a significant fraction of the measured value, the analyst should be aware that the measured blank does not always provide an accurate estimate of the "real" blank.

Generally speaking, the above-mentioned problems are more severe for long irradiation periods and/or high fluences. Under moderate irradiation conditions, negligible decomposition of the sample occurs and PE containers can be used; this facilitates a direct transfer of the sample from the irradiation vial. Double encapsulation is advisable to reduce contamination.

Carrier addition and equilibration. It is important to add carrier, isotopic with the radionuclides to be separated, as early as possible in the radiochemical processing, preferably during transfer of the irradiated sample. It is always necessary to ensure that the carrier element and the radionuclide originating from the trace element are at some early stage converted to the same chemical form so that they behave identically in the ensuing separation. If the radionuclide to be separated has more than one valence state, the radiochemical separation should include an oxidation-reduction cycle as a first step. In many radiochemical processing procedures, this cycle is already built in, because the mineralization of organic material generally involves reductive conditions at the beginning and oxidative conditions at the end.

Mineralization of the sample. The mineralization of organic matrices is certainly one of the most critical points in the entire radiochemical processing. Losses before carrier-radionuclide exchange has taken place must be avoided, volatilization being the most frequent source.

Volatilization losses depend strongly on the experimental conditions

(temperature, time and reagents used). Sometimes the losses are also influenced by the amount of carrier added (e.g., Au). Trace elements easily lost are halogens and mercury. In the presence of particular compounds, other trace elements may be volatile, e.g., Cr (in hot perchloric acid) or Sb, Sn, As, Sb and Se (in concentrated halide systems).

The use of closed systems (e.g., "bombs", oxygen flask), and semi-closed (e.g., reflux) systems, generally provides sufficient protection against such losses. Total destruction of the matrix should occur and be checked (visual examination is not always sufficient). In certain samples containing high levels of insoluble inorganic constituents (e.g., silica, phosphates), separate dissolution may be called for if they are suspected of containing an appreciable fraction of the element to be determined. However, any precipitates thrown down after dissolution in the presence of carrier are generally not a problem, although they may lower the chemical yield (which must, in such cases, be determined separately for each sample).

Chemical separations. Once sample transfer, equilibration of the carrier, and mineralization of the sample have been done properly, there are only minor errors in the chemical separation steps involved. Variations in the chemical yield are not a problem, provided that they are measured and corrected for (only the uncertainty of the yield determination is introduced).

The choice of separation techniques should be appropriate to the level of the activity to be measured and the radionuclide purity required. In Ge γ-ray spectrometric measurements, a lower degree of radionuclide purity is acceptable, compared with that required for the more sensitive NaI(Tl) γ-ray spectrometry, where generally single (or dual) element fractions are counted. Gamma-ray spectrometry also permits the use of group separations, but at the expense of poorer precision in the signal measurement. A NaI(Tl) detector (especially the well-type) is called for when very low trace element levels are determined, because of its inherently superior detection efficiency.

Determination of the chemical yield. Most modern separation procedures, either manual or mechanical, are designed for a high and reproducible chemical yield of the added carrier. Therefore, a yield determination on each individual sample is generally not practised. A coefficient of variation of the yield of a few percent (e.g., $\approx 5\%$) is normal, and is generally quite acceptable in view of other sources of error in the n.a.a. procedure (e.g., flux gradients, counting statistics), as well as the biological variability of the majority of biological specimens. However, when the ultimate in accuracy and precision is required (e.g., for the certification of reference materials), individual yield determinations may be necessary. Another need for yield determinations is in speedy work with short-lived radionuclides or in complicated separations designed to achieve ultimate sensitivity, both of which carry the risk of unacceptably large variations in the yield.

Yield determinations can be based on various principles; in the most commonly used procedure, the recovery of added carrier is measured, either by classical analytical techniques, or by re-activation of the separated fraction,

using a suitable radionuclide (preferably short-lived) of the element involved. In the first approach, the yield determination is susceptible to the normal hazards of the analytical technique used (though these are normally quite precise, e.g., titrimetry), while in the second the main source of error is due to counting errors for the sample and comparator and possible flux differences between them. Another technique is that based on recovery of added radiotracer, provided that there is a suitable radioisotope, complementary to the one produced on activation. This method involves a compromise between good measurability of the added tracer and minimization of the deterioration of the γ-ray spectrum.

Gamma-ray spectrometry in n.a.a.

The measurement of radioactivity is an essential step in every n.a.a. procedure. Such measurements are almost exclusively based on γ- or x-radiation because these types of radiation are mono-energetic and relatively insensitive to attenuation phenomena. Three steps are involved: measurement, spectrum analysis and interpretation. In this discussion, attention is paid mainly to problems associated with the use of semiconductor (Ge and Ge(Li)) detectors. Scintillation detector spectrometers are less sensitive to errors relating to factors such as count rate, dead-time, pile-up and geometry; the most important errors usually arise in the spectrum interpretation step. For details on all these points, the reader is referred to the working paper [28]. A summary of suggested checks and adjustments is given in Table 2.

Measurement. The measurement of a radioactive sample as part of an activation analysis should result in a pulse-height distribution reflecting quanti-

TABLE 2

Suggested checks and adjustments for γ-ray spectrometry

Action	Frequency
Adjustment of γ-ray spectrometer components	Occasionally
Test of spectrometer count-rate capabilities (including dead-time and pile-up correction)	Occasionally
Test of spectrometer stability (time and temperature)	Before first analytical use of spectrometer
(Relative) efficiency calibration (including estimate of possible errors)	For each measuring geometry
Test of performance of procedure for spectrum analysis	For each procedure
Compilation of γ-ray spectrum catalogue	For each high-efficiency counting geometry
Energy calibration	Daily
Background measurement	Occasionally
Background monitoring (short measurements)	Daily
Check of energy resolution and peak shape	In each spectrum

tatively both the energies and intensities of the radiations emitted by the sample. This can only be achieved if the spectrometer energy response and efficiency are sufficiently stable under the expected measurement conditions.

The components of the spectrometer have to be interconnected according to the instructions in the manuals, and the spectrometer settings optimized for the relevant energy region and count-rate regime. The stability of the spectrometer characteristics should be tested prior to its first use in analyses. During actual use, care has to be taken that the limits of acceptable operating conditions of the spectrometer (count-rate, ambient temperature, etc.) are not exceeded. If this happens, the spectra must be disregarded, because they might be inaccurate. Moreover, regular (e.g., daily) tests are needed to verify spectrometer performance. Peak-shape deterioration can be regarded as an early warning of spectrometer malfunction.

In the next paragraphs some potential sources of error in γ-ray spectrometry are discussed. It is assumed here that the spectrometer components are free of technical defects, and that they have been adjusted carefully according to the manufacturer's recommendations.

Geometry. In order to achieve a high detection efficiency, samples are often counted very close to the detector. At short sample—detector distances, however, the efficiency becomes very sensitive to variations in this distance or in the sample dimensions. For a sample placed directly on the cap of a medium-size Ge detector, 1-mm changes in distance or sample height result in changes in efficiency of about 5% and 2%, respectively. Therefore, measurements close to the detector should be made only when both sample position and dimensions are precisely reproducible and identical for samples and standards. Otherwise, the measurements have to be made with larger sample—detector distances (i.e., greater than the detector diameter), where the geometrical errors are substantially lower. When there is a systematic difference between the geometry of samples and standards, the associated difference in efficiency can be determined experimentally and corrected for. The use of a well-type Ge detector may reduce geometrical errors to a great extent.

Sample self-absorption. When samples of finite size are measured, part of the radiation will be prevented from reaching the detector because of attenuation in the sample itself. This may lead to appreciable analytical errors when samples and standards are not identical in both dimensions and matrix composition. Such errors can be avoided by using special procedures for sample and standard preparation and/or mathematical corrections for the attenuation. These measures either require a priori knowledge of the sample composition or imply a considerable complication of the measurement or spectrum interpretation procedures. If no such special measures are taken, the sample size has to be so small that errors by self-absorption stay within the limits set by the analytical precision requirements. For water-equivalent materials, such as most biological materials, the error from self-absorption is in general less than 1% for γ-ray energies above 100 keV and sample sizes up to 1 g.

Bremsstrahlung. High-energy β-radiation emitted in the sample, for example by ^{32}P, may give rise to bremsstrahlung. This shows up in the spectrum as a continuous background and affects the precision of measurement of peaks, particularly at low energies. Bremsstrahlung can be reduced considerably by surrounding the sample with approximately 1 g cm^{-2} of thick absorber of low Z material (e.g., plastic). The β-particles lose their energy in such an absorber, mainly through inelastic collisions, and the generation of bremsstrahlung is thereby suppressed.

Dead-time and pile-up. Dead-time and pile-up constitute one of the most important problems of quantitative γ-ray spectrometry. Both effects lead to a change in the counting efficiency, depending on event rate, pulse-height distribution and instrument settings. The most commonly used methods of correction for dead-time and pile-up losses are: (a) the use of a time reference peak in the spectrum originating from a pulse generator or from a radioactive source; or (b) the use of the dead-time correction circuit in a multichannel analyzer, possibly also combined with a pile-up rejector.

Inappropriate correction may lead to appreciable errors, ranging from a few percent at count rates of 1000 s^{-1} to tens of percent for count rates above 10 000 s^{-1}, depending on the equipment and correction method used. The corrections based on a time reference peak are much better than those using a dead-time circuit [29], but special care should be taken when a reference pulser is used in combination with a pile-up rejector, because improper mutual adjustment may easily lead to excessive errors.

For each γ-ray spectrometer, the correction for dead-time and pile-up at increasing event rates should be measured prior to its first use in quantitative work. The count rates must be limited to values for which the correction for dead-time and pile-up losses has been proven to be adequate.

Additional problems occur when mixtures of radionuclides with strongly differing half-lives are measured, which decay considerably during the measurement. Even when the overall correction for dead-time and pile-up is appropriate, the correction of the count rates of the individual nuclides can be wrong [30]. Proper correction of the individual count rates requires the use of dedicated electronic units or additional computer processing of the measured spectra. Otherwise, the initial dead-time has to be limited to a few percent in order to avoid substantial errors.

Excessive event rates. If a significant fraction of the events occurring in the detector is not recorded in the spectrum, as can be the case in measuring a selected energy region, the actual event rate may be considerably higher than the observed count rate, and may exceed the limits for proper equipment performance without being noticed. Such a system overload may lead to errors caused, for example, by energy-dependent changes in the counting efficiency or to peak-shape deterioration. Therefore, in cases where the total event rate can be much larger than the count rate, the former should be monitored (e.g., with a fast scaler) so that proper action (e.g., changing the counting geometry) can be taken. In this respect, special attention should be

paid to spectrometers equipped with a preamplifier with pulsed optical feedback.

Analysis of γ-ray spectra. Spectrum analysis in γ-ray spectrometry comprises the detection of the peaks in the recorded spectrum, the calculation of peak positions and peak areas, and the conversion of these data into peak energies and (relative) intensities. It is self-evident that the statistical errors inherent in all radioactivity measurements have to be taken into account in the final analytical result, using the well-known error propagation laws.

Manual and computerized procedures based on some kind of integration of channel contents only yield reliable results for single free-standing peaks and should not be applied to overlapping peaks. For the calculation of areas and intensities of overlapping peaks, accurate results can be obtained only by using computer programs which include a peak-fitting routine. In general, the best results are obtained with computer programs based on a modified Gaussian distribution as the peak shape function. However, it should be noted that most procedures overlook a considerable part of the multiplets in a spectrum. This may seriously affect the reliability of the analytical results, unless it is kept in mind during spectrum interpretation that all observed peaks potentially contain more than one single peak, even when such a peak is not recognized as a multiplet in the spectrum analysis.

The choice of a procedure for calculation of peak position and area depends on the complexity of the spectra to be processed and on the available computer facilities. For simple spectra, manual or computer integration procedures may be appropriate, but for complex spectra, as are usually obtained in i.n.a.a., only methods based on the use of peak-fitting routines can be regarded as adequate. Once a method has been selected, its performance should be checked, e.g., by statistical analysis of the results (peak areas and positions and the errors reported for these quantities) obtained on applying the method to reference peaks [31].

Peak positions are converted to γ-ray energies by using an energy calibration curve. For most spectrometers, this curve deviates slightly from a straight line. It can be established with sufficient precision from measurements on approximately ten peaks with well-known energies more or less evenly spread over the relevant energy region (information on suitable radionuclides is regularly published in Nucl. Instrum. Methods). The error in an estimate of peak position is in general very small, but additional errors arise from uncertainties in the calibration curve and from possible gain shifts since the time of the last energy calibration. The total of these errors in the peak position should be taken into account in the spectrum interpretation procedure.

The conversion of peak areas into absolute intensities is only relevant for those n.a.a. techniques that are not based on direct comparison of the same elements in sample and standard. The conversion is done by using an efficiency calibration curve preferably based on at least ten points. As most methods of n.a.a. are based on direct comparison of the count rates in the

same peak of sample and standard, quantitative evaluation is possible without efficiency calibration. But for the verification of spectral purity or correction for spectral interferences, a knowledge of the energy-dependence of the efficiency (relative efficiency curve) is required. This curve can be measured very conveniently with two or three radionuclides emitting several γ-rays with known intensity ratios. Information on the efficiency calibration can be found in a recent review [32]. Large errors may occur when measurements are made close to the detector, where the efficiency is high. Under such conditions, peak areas can be influenced by summation in a hardly predictable way, leading to large systematic errors in the conversion of peak areas into γ-ray intensities. It is therefore advisable, for spectra measured with the sample close to the detector or in a well-type detector, to use the peak areas as such without conversion, and compare them directly with the spectra of standards measured under identical conditions. In this situation, standard spectra of all the relevant radionuclides have to be measured for each detector and each source-detector geometry.

Interpretation of γ-ray spectra

Identification of peaks. The peaks observed in the γ-ray spectrum are assigned to specific radionuclides by comparing their energies and intensities or peak area ratios with data tabulated in a γ-ray catalogue. Additional aids to identification can often be derived from consideration of half-lives and possible activation processes. All the observable peaks should be identified by these means, following which the analyst should consider carefully whether low-intensity γ-rays from the identified radionuclides may be contributing counts to the photopeak used for determining the element of interest. A sufficiently large energy window around the calculated peak energy should be used to account for the possible error in the peak position calculation and for the occurrence of spectrum shifts.

Peak purity. Every peak should be treated as a potential multiplet unless it can be proven that contributions from other nuclides are absent. This is particularly important for the broad peaks in spectra obtained with a scintillation detector. When such a detector is used, it is recommended to make an additional qualitative measurement with a Ge detector to verify spectral purity. If the sample activity is too low for a meaningful additional measurement, one has to rely on the selectivity of the radiochemical separation procedure and on a careful inspection of the γ-ray spectrum itself.

Additional peaks. It should be noted that, in addition to γ-ray photopeaks, a spectrum may contain various other kinds of peaks such as annihilation and escape peaks, x-ray peaks, γ-ray escape peaks, sum peaks and pile-up peaks.

The annihilation peak originating from positrons emitted by radionuclides present in the sample can be used for quantification, but it is necessary to be sure that all positrons are stopped and annihilate in, or very close to, the sample. This can be achieved by surrounding the sample closely with an absorber of sufficient thickness to stop the emitted positrons. The annihilation

radiation from positrons formed by pair-production during absorption of high-energy γ-rays in the sample and its surroundings does not reflect quantitatively any of the activities present in the sample. Its intensity depends on the intensities and energies of the emitted γ-rays, the size and composition of the sample, and the dimensions and composition of any objects near the sample or detector (e.g., the shield). Special care should therefore be taken in correcting for this contribution to the annihilation peak.

For sum peaks and escape peaks it should be noted that their intensities relative to other photopeaks depend not so much on nuclear properties as on characteristics of the detector, such as its efficiency. These peaks may only be used in a quantitative evaluation of γ-ray spectra by comparing them with peaks in spectra measured under identical conditions. Summation effects may lead to the appearance of unexpected peaks, arising from summation of coincident γ-rays or of coincident γ- and x-rays. Such peaks do not appear in any γ-ray catalogue and, when they are not recognized as sum peaks, they may be erroneously assigned to unrelated radionuclides.

The most effective way to avoid excessive errors resulting from summation effects is to prepare and measure the samples and standards under exactly the same geometrical conditions. If this is too laborious or impractical, the only alternative is to conduct all measurements at such large sample—detector distances that summation effects are negligible. However, the lower counting efficiency will lead to a loss of analytical sensitivity unless compensated by increased counting times.

Pile-up peaks do not usually lead to incorrect identification because they are easily recognized on the basis of their peculiar shapes.

Background radiation. The background radiation spectrum generally has two components, one constant and one variable. The constant part comes from cosmic radiation and natural activities present in the construction materials of the counting room and its equipment. Once this almost constant background has been measured, each spectrum can be corrected for it. The variable contribution to the background may arise from radioactive samples in or near the counting room, or from activity present as contamination of the detector. This component of the background spectrum may change significantly with time, and therefore needs regular monitoring. Daily background measurements will reveal the presence of time-dependent background contributions, so that proper action can be taken. Helmer [32] gives more detail on some of these points.

INTERNAL AND EXTERNAL QUALITY ASSURANCE

A result for which the uncertainty is unknown is worthless because it cannot be used to draw valid conclusions; worse, it is dangerous because it may be misused and lead to false conclusions. Quality assessment is needed to ascertain that the uncertainty of results reported by a laboratory does not exceed well defined limits, and quality control serves to detect unexpected deviations with a minimum delay.

Internal quality assurance is concerned with maintaining precision within a single laboratory, where the importance of keeping careful records and appropriate control charts is well established. External quality assurance involves reference materials obtained from an outside body, and is a method for testing the accuracy of laboratory results. In practice, internal quality assurance mainly has to do with laboratory precision, whereas external quality assurance mainly has to do with laboratory accuracy.

Internal quality assurance

Laboratories engaged in n.a.a. of biomedical samples do not produce the large number of results characteristic of a routine clinical chemistry laboratory. Internal quality control cannot therefore be directly based on the recommendations of the International Federation of Clinical Chemistry (IFCC) [33]. The use of the analysis of precision [34] makes quality control possible with a small number of results with variable precision and is particularly suited to n.a.a.

The precision of individual results is here determined from the totality of independent, random, errors associated with different stages of the analysis. These contributions should be determined by separate investigations of the random errors associated with the factors discussed in the preceding sections. The most significant relative source of variation, which is often the precision of the activation itself, must be estimated accurately. The most significant absolute sources of variation are associated with the sampling or the corresponding blank.

When all random sources of variation, $a, b, \ldots n$, have been estimated, the precision of the analytical result is expressed by its overall standard deviation $\hat{\sigma}$, where:

$$\hat{\sigma}^2 = \sigma_a^2 + \sigma_b^2 + \ldots\ldots\ldots \sigma_n^2 \qquad (1)$$

In activation analysis the useful range of the analytical method covers many orders of magnitude, and different components of the total variation dominate under different circumstances. In addition, the statistics of the counting process introduce a variance component into Eqn. 1. This contribution is usually referred to as the precision of counting statistics, and the pooled contribution from all other sources is called the a priori precision.

Quality control can be based on the duplicate analysis of a fraction (e.g., $\approx$20%) of the samples [35]. Results y_1 and y_2 for m duplicates are tested by the statistic

$$T = \sum^{m} [(y_1 - y_2)^2/(\hat{\sigma}_1^2 + \hat{\sigma}_2^2)] \qquad (2)$$

which is approximated by a χ^2 distribution with m degrees of freedom. As long as the value T is within the accepted control limits, the analysis is in a state of statistical control.

Lack of statistical control means that unknown errors are present, and that the results are not of the expected quality and should therefore be rejected

[7]. Identification of these unknown sources of variation is facilitated by applying the analysis of precision to separate stages of the analysis, such as the sampling [34], data processing [31], etc. [24]. Such errors may sometimes be extremely difficult to identify, and may call for considerable skill and intuition on the part of the analyst.

When all sources of variation have been brought into a state of statistical control, only strictly additive or multiplicative errors remain. These are assessed by the analysis of a certified reference material as described below.

External quality assurance

External quality assurance provides the main means to make an independent test of the accuracy of analytical results from a given laboratory, but it can also give an estimate of laboratory precision. It is based on analyses of certified reference materials (CRMs) such as those available from the IAEA and the NBS [36]. Ideally, several CRMs should be analysed, so as to cover a range of concentration of the elements determined. If the precision of the method has not been measured as described above, it should be investigated by measurements on at least four samples of each CRM. A plot of reported values against certified values shows the inaccuracy, or bias, of the results $(x_t - \bar{x})$, where x_t is the certified value and $\bar{x}$ the laboratory mean. It also illustrates the variation of precision with concentration, and if the graph is supplied with maximum allowable deviation (MAD) lines, one can see whether the results are acceptable (within the MAD lines) or not [37, 38]. Experience shows that laboratories can be trained to improve both accuracy and precision dramatically by a series of tests of this kind, alternating with intensive searches to remove systematic errors.

External quality control checks may be both open and blind. It is best for some external body to provide a randomized series of the CRMs for analysis, together with standards, if these are believed to contribute to the error, so that the test is largely blind. There is no agreement as to the frequency of such checks in routine analysis, but as much as 20% of the analytical effort may be devoted to quality control [39]. External quality control is a legal requirement for clinical analyses of Ca, Cl, K and Na in some U.S. states [40], using commercial reference sera, but is unlikely to become so for n.a.a. of trace elements.

Major problems are that current CRMs are rather expensive (about $10/g), that they are certified for too few elements, and that no CRMs are available at present with very low concentrations of trace elements such as occur in human serum [12, 41]. The overwhelming majority of elemental determinations in biological materials make no use of external quality control and are therefore of doubtful validity. It is recommended that further efforts be made to increase the use of external quality control, to increase the number of CRMs, and especially to increase the number of certified elements in selected CRMs with large available stocks.

CONCLUSIONS

This survey of the n.a.a. of biomedical samples by a group of scientists experienced in this field was instigated by the simple fact that numerous laboratory intercomparison studies of various reference materials have resulted, for a very large number of elements, in an extraordinarily wide range of reported values for a given element in a given material. This range in some cases spans one, two, or even more orders of magnitude. Because vastly better precision and accuracy than these should be attainable, the Advisory Group was requested to consider carefully every conceivable source of error, and then to arrive at recommendations designed to eliminate or greatly reduce them.

The main steps involved in such n.a.a. procedures that have been considered in detail by the Advisory Group are: (1) the procurement of representative, uncontaminated, samples; (2) the preservation of biological samples and their preparation for analysis; (3) the preparation of standards; (4) the reactor neutron activation of samples and standards; (5) the subsequent radiochemical separations (if necessary); (6) γ-ray spectrometry measurements; (7) the process of data reduction and reporting; and (8) internal and external quality assurance. Many sub-problems in each of these eight steps have been considered, details of which are presented in this report, and in even greater detail in the various working papers [1].

These considerations have resulted in a considerable number of recommendations which, if meticulously implemented, should at least greatly improve the degrees of precision and accuracy attained by activation analysts in actual practice. It is believed that the following ten recommendations, used as a reminder check list, will be of value:

(1) obtain representative, uncontaminated samples;

(2) carefully avoid additions or losses of elements during sample storage and in the preparation of analytical samples ("clean" benches or "clean" laboratories may be necessary for analyses at ultratrace levels);

(3) optimize the analytical parameters (activation time, decay time, sample weight, position in reactor, choice of detector, etc.) for the particular elements and matrices of interest;

(4) assess in advance whether r.n.a.a. must be employed, or pre-separations, or whether i.n.a.a. can provide equally good results;

(5) prepare accurate standards of the elements of interest rather than use certified reference materials as standards, and check that the decay-corrected specific activities are reproducible;

(6) if radiochemical separation is employed, take pains that all sources of error associated with this step are minimized;

(7) monitor the analytical blanks and ensure that they are suitably low and reproducible;

(8) conduct γ-ray spectrometric measurements and subsequent spectrum analysis carefully and properly;

(9) analyse at least some of the samples in replicate, and compare the estimated overall precision with the observed variability, so as to ascertain whether any unknown sources of error are operating; and

(10) check the accuracy of the overall analytical procedure by analysing certified reference materials of similar matrix compositions, and report the results obtained and the reference values used.

REFERENCES

1 International Atomic Energy Agency, Quality Assurance in Biomedical Neutron Activation Analysis, Report of an IAEA Advisory Group, IAEA-TECDOC-323, IAEA, Vienna, 1984.
2 International Atomic Energy Agency, Research Reactors in Member States, 1980 edn., Report IAEA-mf-1, IAEA, Vienna, 1980.
3 V. P. Guinn and J. Hoste, Elemental Analysis of Biological Materials, Current Problems and Techniques with Special Reference to Trace Elements, Ch. 7, Tech. Rep. Ser. No. 197, IAEA, Vienna, 1980, pp. 105—140; see also p. 367 of same report.
4 R. Dybczynski, J. Radioanal. Chem., 60 (1980) 45.
5 R. Dybczynski, Relative accuracy, precision and frequency of use of neutron activation analysis and other techniques as revealed by the results of some recent IAEA intercomparisons, in ref. 1.
6 E. S. Gladney, Anal. Chim. Acta, 118 (1980) 385.
7 J. K. Taylor, Anal. Chem., 53 (1981) 1588A.
8 G. V. Iyengar, Anal. Chem., 54 (1982) 554A.
9 V. D. Anand, J. M. White and H. V. Nino, Clin. Chem., 21 (1975) 595.
10 J. Versieck, F. Barbier, R. Cornelis and J. Hoste, Talanta, 29 (1982) 973.
11 M. Zief and J. W. Mitchell, Contamination Control in Trace Element Analysis, Wiley, New York, 1976.
12 J. Versieck, Collection and manipulation of samples for trace element analysis; quality assurance considerations, in ref. 1.
13 G. V. Iyengar, J. Pathol., 134 (1981) 173.
14 G. V. Iyengar, Preservation and preparation of biological materials for trace element analysis; quality assurance considerations, in ref. 1.
15 G. V. Iyengar and B. Sansoni, Elemental Analysis of Biological Materials, Current Problems and Techniques with Special Reference to Trace Elements, Ch. 6, Tech. Rep. Ser. No. 197, IAEA, Vienna, 1980, pp. 73—101.
16 V. P. Guinn, J. Leslie and L. Nakazawa, J. Radioanal. Chem., 70 (1982) 513.
17 V. P. Guinn, Optimization of reactor neutron activation analysis conditions, in ref. 1.
18 F. Girardi, G. Guzzi and J. Pauly, Anal. Chem., 37 (1965) 1085.
19 A. R. Byrne, The preparation and use of chemical irradiation standards, in ref. 1.
20 J. J. M. de Goeij, Error sources involved in radiochemical processing, in ref. 1.
21 F. de Corte, A. Speeke and J. Hoste, J. Radioanal. Chem., 3 (1969) 205.
22 V. P. Guinn and J. J. M. de Goeij, Trace Elements in Relation to Cardiovascular Diseases, Rep. IAEA-157, IAEA, Vienna, 1973, pp. 163—173.
23 D. de Soete, R. Gijbels and J. Hoste, in P. J. Elving and I. M. Kolthoff (Eds.), Neutron Activation Analysis, (Chem. Anal. Ser. Vol. 34), Wiley Interscience, London, 1972.
24 K. Heydorn, Aspects of precision and accuracy in neutron activation analysis, Rep. RISO-R-149 (1980), Riso National Laboratory, Roskilde, Denmark.
25 International Atomic Energy Agency, Neutron Fluence Measurements, Tech. Rep. Ser. No. 107, 1970.
26 M. Sankar Das, Sources of error in the activation of biological materials in research nuclear reactors, in ref. 1.

27 B. Mazière, A. Gaudry, J. Gros and D. Comar, Radiochem. Radioanal. Lett., 28 (1977) 155.
28 M. de Bruin, Gamma-ray spectroscopy in NAA; sources of error, in ref. 1.
29 H. Houtermans, K. Schaerf, F. Reichel and K. Debertin, Intercomparison of High Precision Gamma-Ray Spectrometry, Rep. ICRM Action 5/78, IAEA, Vienna, 1980.
30 M. Wiernik, Nucl. Instrum. Methods, 95 (1971) 13.
31 K. Heydorn, Computers in Activation Analysis and Gamma-Ray Spectroscopy, (Proc. Conf. Mayaguez, 1978), U.S. Department of Energy, CONF-780421 (1979), pp. 85—95.
32 R. G. Helmer, Nucl. Instrum. Methods, 199 (1982) 521.
33 J. Büttner, R. Borth, J. H. Boutwell, P. M. G. Broughton and R. C. Bowyer, Clin. Chim. Acta, 98 (1979) 129F.
34 K. Heydorn and K. Norgaard, Talanta, 20 (1973) 835.
35 K. Heydorn, Development of Nuclear-Based Techniques for the Measurement, Detection and Control of Environmental Pollutants, (Proc. Symp. Vienna, 1976), IAEA, Vienna, 1976, pp. 61—73.
36 R. M. Parr, Survey of currently available reference materials for use in connection with the determination of trace elements in biological materials, Report IAEA/RL/103, IAEA, Vienna, 1983.
37 L. Friberg and M. Vahter, Environ. Res., 30 (1983) 95.
38 H. J. M. Bowen, External quality control, in ref. 1.
39 J. Büttner, R. Borth, P. M. G. Broughton and R. C. Bowyer, Clin. Chim. Acta, 106 (1980) 109F.
40 N. W. Tietz (Ed.), Fundamentals of Clinical Chemistry, Saunders, Philadelphia, PA, 1976.
41 G. V. Iyengar, W. M. Kollmer and H. J. M. Bowen, The Elemental Composition of Human Tissues and Body Fluids, A Compilation of Values for Adults, Verlag Chemie, Weinheim, 1978.

Analytica Chimica Acta, 165 (1984) 31—49
Elsevier Science Publishers B.V., Amsterdam — Printed in The Netherlands

A PROGRAM FOR THE PROCESSING OF ANALYTICAL DATA (DPP)

P. VAN ESPEN

Department of Chemistry, University of Antwerp, U.I.A., Universiteitsplein 1, B-2610 Wilrijk (Belgium)

(Received 21st May 1984)

SUMMARY

Computer-assisted interactive data presentation and analysis facilities are needed to handle the vast amount of information produced by automated instruments. The data processing program, DPP, presented here is a FORTRAN-77 program designed to solve this problem. The program is equipped with a leading verb command language for input and job scheduling, thus providing an efficient and user-friendly operator/program interface, and with a data-base organization that accommodates a wide variety of data structures. Data presentation and analysis procedures include tabulation and plotting, regression analysis, non-linear least-squares fitting, polynomial fitting, principal component analysis, hierarchal clustering and non-hierarchal clustering. Data matrices with up to 10 000 data points, distributed over a maximum of 3000 variables and 3000 samples, can be examined. Because of the open-ended structure of the program, it is straightforward to incorporate additional data analysis procedures when they are needed. Recent applications are discussed.

Computerized data handling has become an established part of analytical practice. Two steps in the analytical process involve computers. In the measurement step, computers can control the instrument, process signals, and transform raw data into meaningful results such as concentrations. The second step, which is becoming more and more important, is the interpretation of results and presentation of the information in a form relevant to the problem under investigation. This interpretation may range from simply tabulating and plotting selected features from a data set to statistical analysis such as regression or factor analysis, or to mathematical manipulations and transformations. The necessity of automation in the second step is accentuated by the high sample throughput achieved by many modern instruments which can also generate a vast array of data on each sample. The data matrices, built up in this way, are often nearly incomprehensible to the investigator without computer assistance.

Typically, the computer used in the first step of the analytical process is a dedicated mini- or micro-computer with specialized instrument interfaces and job-specific software. The programs running on it are written for limited and repetitive jobs and must be highly efficient in time and hardware usage. For data interpretation, the computer requirements are quite different: one

0003-2670/84/$03.00

would prefer to use a general-purpose computer with a large memory, a variety of data storage and output devices such as hard disks, magnetic tapes, printers and plotters, and to use high-level programming languages so that large sets of data can be handled simultaneously, and the processing can be easily adapted to each new investigation. Because current technology can provide the physical resources in a laboratory mini-computer, the greatest difference between systems for data acquisition and those for thorough data interpretation lies in the software. Whereas the data acquisition and signal-processing software must be highly efficient in using computer resources (CPU time and memory space), the data analysis software must be highly efficient in the operator effort required to process a variety of data structures originating from many different experiments conducted in the laboratory, and must be efficient in the effort expended by the chemist in managing the programs.

Various software packages useful for data interpretation in analytical chemistry, have been described in the literature. The Statistical Package for the Social Sciences (SPSS) [1] has grown to a very large system and encompasses many of the statistical procedures relevant to analysing chemical data. Its interactive use, which is essential in a laboratory environment, is however limited by its basic structure, which was designed for batch-mode processing. Also, the means to instal, operate and maintain such a package are often not available in an analytical laboratory. The same drawbacks apply to the biomedical computer programs (BMD) [2]. Besides these two examples of general data-analysis packages originating from outside the field of analytical chemistry, several programs have been developed by and for analytical chemists. ARTHUR is a well known and widely used system [3], incorporating many and sophisticated data-analysis procedures, but it is difficult to operate as a general laboratory data-analysis program. Other programs have been written for specific statistical calculations, such as SIMCA for principal component modelling [4] and MASLOC for non-hierarchal cluster analysis [5].

A computer program specifically designed for interactive data analysis in the analytical laboratory is described in this paper. It incorporates a wide selection of calculation procedures with extremely flexible data input and output formats into a single system through which these can be executed according to need. This program, DPP (Data Processing Program) is written in FORTRAN 77 and is currently implemented on a VAX 11/780 (Digital Equipment Corporation) under the VMS operating system.

THEORY

In designing the program, the following requirements were taken into consideration: (a) the program should be easy to operate, even for an inexperienced computer user; (b) there should be virtually no limitations to the amount and type of data that can be handled; (c) the program must be

capable of dealing with many different jobs of data interpretation without need for reprogramming; (d) the structure should be open-ended, so that various data analysis routines can be added to the program; (e) the dependence of the program on specific processor, operating system and input/output devices should be minimal. To achieve these goals, the program was structured around four major blocks of code, responsible for program control, the organisation of the data, the actual data analysis procedures, and the program input-output. Special attention is paid to the I/O handling, in order to make the program as device-independent as possible.

Essentially, the program operates by executing a sequence of more or less independent tasks. Each job is initiated by input of a command line, read from the appropriate input device (terminal). This command line is interpreted and the requested operation is executed. These commands are related to input-output, to manipulation of the data base and to the various procedures for data analysis.

Program control

The program can be considered as a collection of mutually consistent modules (subroutines or groups of related subroutines) which execute in an order specified by the user. In order to do this, a leading verb command language [6, 7] is implemented. As input to the program, the operator provides one or more words to specify the desired job, optionally followed by a number of items that supply extra data required for this job. This input string is called a command line. To obtain a flexible and efficient controlling procedure, the command line syntax, depicted in the syntax diagram in Fig. 1, was adopted. The command specifier consists of one or more command words. Multi-word constructions are only used whenever one command word would be interpreted ambiguously in the context of the current program state. Thus PRINCIPAL_COMPONENT_ANALYSIS is considered as one word, specifying that principal component analysis must be done. The word SELECT must be followed by the word VARIABLES or by the word SAMPLES to construct an unambiguous command. The command specifier can be followed by a number of qualifiers. Each qualifier is made up of one word optionally followed by an equal sign and data. The function of the qualifier is to supply extra information for the job to be done. If absent, the default will be used. The command line ends with data that are specific for the command. Data can be entered as a list of items separated by commas. Each item can be a number, a range (two numbers separated by an underscore) or a character string. Examples of syntactically correct commands are:

```
SELECT VARIABLES mass
SELECT SAMPLES 1_20,24,oldsam
SORT SAMPLES\DESCENDING mass
READ_DATA\FORMAT=(10F10.0) file.dat
```

The first example is a command line with a datum specified as a string. The second line is a list of data items consisting of a range of numbers, a single

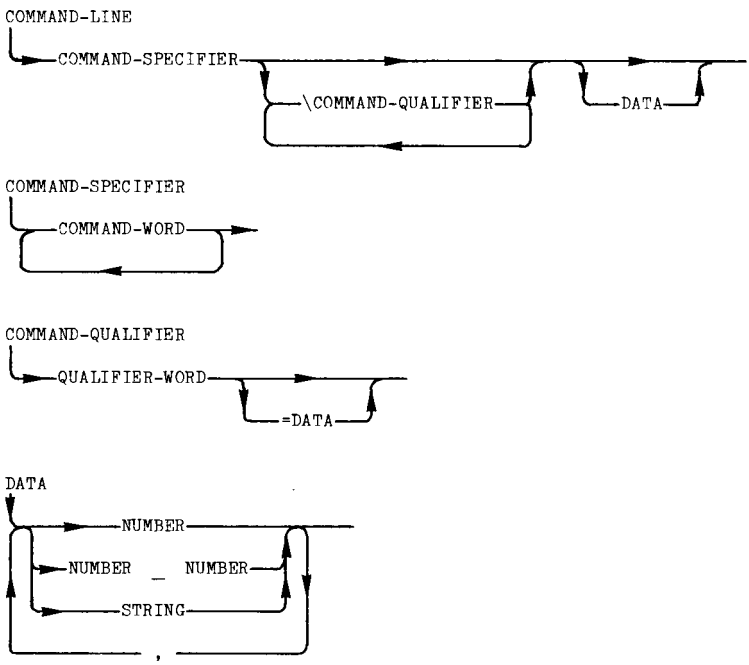

Fig. 1. Syntax diagram of the input command language implemented in DPP. This command language is used to control the operation of the program.

number and a string. These commands achieve, respectively, the selection of the variable with name "mass" and selection of samples 1–20, sample 24 and the sample with name "oldsam". The two remaining lines show examples of command lines with qualifiers. The qualifier \DESCENDING specifies that the samples have to be sorted in descending order, the \FORMAT qualifier is used to indicate the format specification that is to be used for reading the data file.

The command line is analysed for syntax and interpreted by using the appropriate command and qualifier tables. At the end of this process, when no syntax errors are encountered, pointers are set and control is transferred to the execution routine which reads the data from the command string.

This structure guarantees a high degree of flexibility so that even complex tasks can be controlled, while minimizing user input required for a standard call to a job. Commands and qualifier words are defined as meaningful English terms, so that the user of the program has little problem in learning them. Each word can be abbreviated to the minimum number of characters that is necessary to maintain unambiguity, e.g., the letter L suffices to specify the command LIST, but to read in a data matrix at least REA has to be entered as abbreviation for READ_DATA because of the existence of the command word REMOVE. It is our experience that any operator can learn this procedure of inputting data to a program much faster than a

conventional, sequential, preformatted input, because he has to be aware only of the possible inputs and the syntax and not of the order in which they have to be presented. A list of the commands available in the DPP is given in the appendix.

Data-base structure

Most data presentation tasks (e.g., tabulating and plotting) and also various data-analysis procedures can be regarded as operations on a two-dimensional data matrix. The columns of this matrix represent variables or attributes; the rows represent samples or objects. Plotting of two attributes measured on a number of samples becomes the plotting of two column vectors. Plotting of a spectrum is equivalent to plotting two column vectors, one holding the measured signal (in the y direction) and the other holding the value of the quantity (energy, wavelength) at which the signal is measured. This last column frequently is the step number (channel number) of the measurement. Most multivariate procedures (e.g., principal component analysis) are conducted on a 2-dimensional matrix holding the desired variables and samples. This two-dimensional data structure is implemented in DPP.

Data to be analysed must be contained in a formatted or an unformatted file. This file consists of a header which can contain information about the names of the variables and/or the samples, about the number of samples and variables and the type of data. The same command line syntax is used to process this header, making all entries position independent. If no names for variables or samples are given, default names (respectively V1, V2, ... and S1, S2, ...) are given by the program. After this header, the actual data matrix is stored, one record for each sample. A typical data file is shown below:

```
VARIABLE_NAMES CU,ZN,FE
#SAMPLES 12
LABEL TEST-DATA
END_HEADER
12. 34.5  7
 0.  1.  23.76
```

The program uses the information in the header to establish that there are three variables with the names CU, ZN and FE and 12 samples, the names of which will be S1 to S12. The data matrix is identified by the label TEST-DATA. END_HEADER terminates the header and the rest of the data file contains the actual data matrix. This data file is read in by the program when the command "READ_DATA file-name" is executed. For further processing, each variable and sample can be accessed by its name or by the number of the column or row of the data matrix.

Essential to the operation of the program is the concept of sample and variable groups. These groups are collections of some or all variables (samples) in the data base that are operated on at the same time. Only one variable group and one sample group are active at any time. Groups have both a name

and a number for reference. Sample group 1 (ALL_SAM) and variable group 1 (ALL_VAR) always encompass the entire data matrix. New groups can be created and variables or samples selected from the main group into the new groups. All subsequent data analysis will be done on the currently active variable and/or sample group.

Various operations are possible on the data matrix: definition of new items (variables or samples) in terms of those already present, partitioning of the data matrix by creating new groups and selecting variables and samples in them, transposition (rotation) of the data matrix and sorting of samples and variables. The definition of new items is done with the commands: "DEFINE SAMPLE name=arithmetic expression" or "DEFINE VARIABLE name= arithmetic expression". The arithmetic expression may be any legitimate algebraic expression containing the operators +, −, *, /, and ^ (addition, subtraction, multiplication, division and exponentiation), numbers, variable names (or sample names in the case of the definition of a sample) and function references. The standard algebraic functions: SIN, COS, TAN, LOG, LN, SQRT, EXP, ABS, INT for respectively sine, cosine, tangent, log base 10, log base e, square root, exponent, absolute value and integer value, are included. Besides these, a number of special functions of interest in data analysis and presentation are defined: MEAN and STDEV, returning the mean and the standard deviation of the items in the argument list, and INDEX, NUMBER and RAN, returning respectively the number (column or row) in the current group, the number in the original data matrix and a random number between zero and one. Examples of definitions are:

```
DEFINE VARIABLE LCON_FE=LOG(CONC_FE)
DEFINE SAMPLE AVER=MEAN(#1_#20)
```

which define a variable with name LCON_FE, the value of which is the logarithm of the value of the variable CONC_FE (the concentration of iron in the samples) and a sample with variables which will have a value equal to the mean of the values of the corresponding variables in samples 1—20. There is almost no limit to the complexity of the definition, and subsequent definitions may contain items that have been defined in a previous operation.

The partition of the data matrix is done by a series of operations invoked by the following commands: "CREATE SAMPLE_GROUP name" or "CREATE VARIABLE_GROUP name", to create a group with its associated name; "SELECT SAMPLES list" or "SELECT VARIABLES list", to place variables or samples into the currently active group; and "ACTIVATE SAMPLE_GROUP name" or "ACTIVATE VARIABLE_GROUP name", to make a previously created group the current group. In addition, selection of samples and variables can be achieved by using a logical expression as a condition, e.g.,

```
SELECT SAMPLES\CONDITION=FE.GT.100.AN.CU.LT.10*ZN
```

This command will select all samples for which the value of the variable FE is greater than 100 and the value of the variable CU is less than 10 times the value of the variable ZN into a sample group. Further, there are commands

for deleting defined items, removing items from a group and erasing entire groups.

Another useful operation is transformation of the data matrix. When the command TRANSPOSE is executed, all variables become samples and all samples become variables. This allows all data-analysis procedures to run on both the variables and the samples. A second TRANSPOSE command will then restore the data matrix to its original state. Finally, the SORT facility allows sorting in an ascending or descending order of samples (or variables) that are collected in a group according to the value of a variable (or sample).

Currently, the table size in the program is set to allow handling of 3000 variable names and 3000 sample names, with a limit of 10 000 points in the data matrix. Approximately 60 sample groups and 60 variable groups can be created.

Data analysis

The third major block of code in the program consists of the modules that provide the data representation and analysis. Each of these modules is invoked by a command line, specifying the desired procedure and optional parameters for the procedure. The selected module then reads the parameters from the command line and executes the analysis procedure on the currently active parts of the data matrix. Currently, subprograms for extensive data listing and plotting are implemented as well as the following data-analysis procedures.

Data screening. This calculates mean, median and variance of a variable in the current active sample group. Also a table and a plot of the frequency distribution of that variable can be obtained.

Polynomial regression analysis. This performs fitting of one variable in the data matrix with an arbitrary polynomial in another variable, listing of polynomial coefficients and statistical parameters, listing and plotting of fit and residuals, and distribution of residuals.

Multiple linear regression. The regression can be calculated between one variable in the data matrix chosen as dependent variable and one or many independent variables. The same information as in polynomial regression can be obtained.

Non-linear least-squares fitting. This fits one dependent variable to an arbitrarily defined (non-linear) function of an independent variable. The fitting function is supplied as part of the command string. The minimization of the sum of squares can be done by the simplex algorithm [8] or by the Marquardt algorithm [9].

Hierarchal cluster analysis. The Euclidian distances between the samples in the active sample group are calculated in the active variable space, and clustering is done by using one of the following variations [10]: nearest neighbour, furthest neighbour, group average, centroid, median, Ward's error sum, simple average and flexible strategy. The results of the clustering are presented as a tree, and the samples clustering at a certain level can be sorted automatically into sample groups of the data base for further analysis.

Non-hierarchal cluster analysis. The MASLOC program [11] was implemented with only a few minor modifications to adapt it to the structure of DPP.

Principal component analysis. A covariance or correlation matrix is calculated over the active sample and variable group and eigenvalues, eigenvectors and loadings are determined. Loadings, eigenvectors and calculated scores can be listed or plotted.

Input—output organisation

Because the program is designed for interactive use, special attention is given to the input-output structure and provisions are made to have control over this structure from within the program.

Input of the command line is normally done through the terminal. In order to ensure that long or repetitive sequences of commands can be dealt with efficiently, two control commands are available: BACKUP, which will cause DPP to write the subsequently entered commands in a back-up file. This file or any other file containing commands can then be executed in the current or later runs of the program, by typing the command COMMAND. followed by the name of the file. The program will execute all the commands in the file and return to the interactive command level afterwards.

During program execution, a large amount of information is produced, a portion of which the user usually wants to save for the record. In order to avoid the creation of a vast pile of hardcopy output, all results of analysis are first dumped in a scratch file. When the analysis is finished, the content of the scratch file is listed on the terminal screen. If the command REPORT is then entered, the same output is directed to the line printer file.

A similar procedure is employed for the output of graphic information. Each plot produced results in graphic information stored in an internal format in a scratch file. When the plot is complete, interpreter routines are invoked to transfer the picture to the selected output device. The interpreters handle the translation from the internal graphic format to the code for the selected graphics device. Three interpreters are currently installed, one producing code for a REGIS device (e.g., a DEC VT125 terminal), one issuing conventional pen-plotter subroutine calls, and one producing a low-resolution plot on a standard ASCII terminal or line printer. An example of the same plot produced on a Versatec V80 and on a line printer is shown in Fig. 2. Each plot produced will appear on the terminal screen either as a low-resolution plot on a standard terminal or as a high-resolution plot on the VT125. The command REPORT will produce the equivalent plot on the selected hardcopy device (line printer or Versatec). The desired output device is selected by using the commands "SET TERMINAL" and "SET PLOTTER".

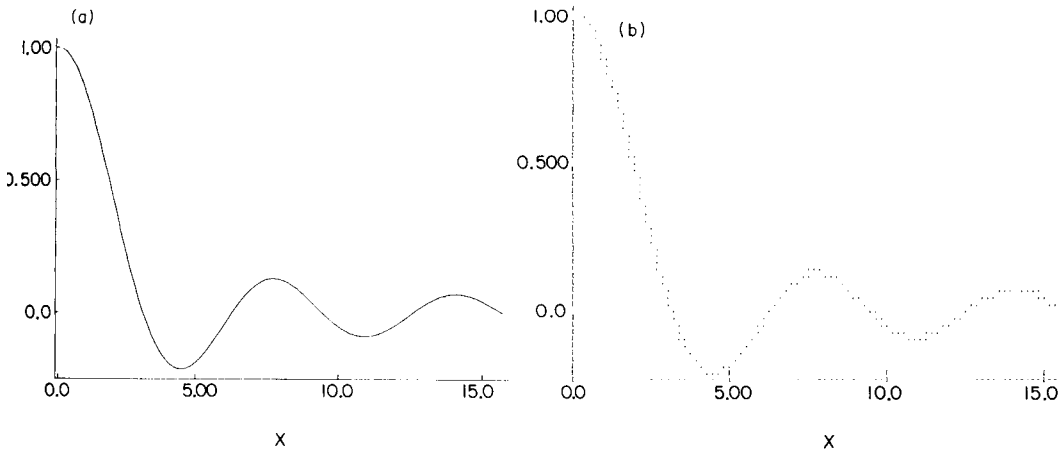

Fig. 2. Plots of the function $\sin(x)/x$: (a) produced by the program on a Versatec V80 plotter; (b) produced in low resolution on the line printer.

RESULTS AND DISCUSSION

The working principles of the program are illustrated by a few characteristic examples, which cover most of the aspects of the methodology used. For clarity, all commands are used without abbreviation. In normal practice, each word can be abbreviated to the minimum length needed to make it unambiguous, typically 1—3 characters. The ">>" sign is the prompt displayed by DPP on the terminal when it is ready to accept a new command. An exclamation sign (!) is used to continue a command on the next input line.

Non-linear fitting of data to an arbitrary function

This example illustrates the use of nonlinear least-squares fitting. The example is taken from a study of ion kinetic energy distributions as measured in laser microprobe mass spectrometry [12]. The input data are integrated intensities of the peaks between mass 24 and mass 120 (the variables denoted by M24 to M120) obtained in eleven mass spectra (the samples) taken with the laser microprobe mass analyser at different settings of the reflector potential of the instrument. The reflector voltage is also included as a variable in the data matrix.

The aim is to interpolate the ion intensities as a function of the reflector potential using an exponential distribution:

$$f(x) = A\{1 - \exp[-(x - B)/C]\} \qquad (x > 0)$$

$$f(x) = 0 \qquad (x < 0)$$

where A is the amplitude of the distribution, B the offset and C the exponential coefficient. This can be done in DPP by using the command

NON_LINEAR_FITTING with the fitting function supplied as part of the command line in the form: dependent-variable=fitting-function. The function is expressed in terms of the independent variable and parameters that have to be optimized. In this example, the dependent variable is the intensity of mass 24 (denoted by M24). The reflector potential (REFL) is the independent variable and the three parameters A, B and C are indicated by P(1), P(2) and P(3). Figure 3 shows the command line used and the output obtained. The last part of the function definition is used to set the function value to zero for negative values of the independent variable. The data points included in the fit are those selected in the current sample group, in this case all eleven spectra. The fit was started with initial parameter values of 922, −10 and 10 and a step size of respectively 10, 2 and 1. The minimization is done with the simplex algorithm. After 94 iterations a minimum was found corresponding to optimal values for the parameters. Figure 4 shows the plot of the fit. The simplex algorithm was used in this case because the fitting function has no continuous derivative for zero values of the independent variable, in which case the Marquardt algorithm cannot be used. A drawback

```
                        DPP command line

>>NON_LINEAR_FITTING\START=922,-10,10\STEP=10,2,1 !
>>M24=P(1)*(1-EXP((P(2)-REFL)/P(3)))*(ABS(REFL-P(2))+REFL-P(2))/(2*(REFL-P(2)))


                          DPP output

NON LINEAR LEAST SQUARES FITTING
********************************

Performed on : CARBON1.DPP
Sample group #     1      ALL_SAM     having         11 samples

Dependent variable   Y : M24
Independent variable X : REFL
Fitting function       :
    P(1)*(1-EXP((P(2)-REFL)/P(3)))*(ABS(REFL-P(2))+REFL-P(2))/(2*(REFL-P(2)))

Number of data points :      11

Minimization using the SIMPLEX algorithm stopped after
    94 iterations, requiring     168 function evaluations

SUM OF SQUARES =    2228.        LAST CHANGE =  8.0878E-03 %

PARAMETER ESTIMATES

P( 1) =    279.0
P( 2) =   -10.30
P( 3) =    7.607

DATA POINT          REFL            M24        FITTED VALUE   DIFFERENCE
 SAMPLE              X               Y            YFIT         Y-YFIT

    1 S1          -40.00        0.0000E+00     0.0000E+00    0.0000E+00
    2 S2          -30.00        0.0000E+00     0.0000E+00    0.0000E+00
    3 S3          -20.00        0.0000E+00     0.0000E+00    0.0000E+00
    4 S4          -10.00          8.900          11.41        -2.506
    5 S5        0.0000E+00        222.9          206.6         16.26
    6 S6          10.00           223.7          259.5        -35.79
    7 S7          20.00           286.9          273.8         13.10
    8 S8          40.00           288.4          278.7         9.677
    9 S9          60.00           291.7          279.1         12.62
   10 S10         80.00           263.4          279.1        -15.71
   11 S11         100.0           281.3          279.1         2.188
```

Fig. 3. Commands used and output obtained in least-squares fitting to an exponential distribution function.

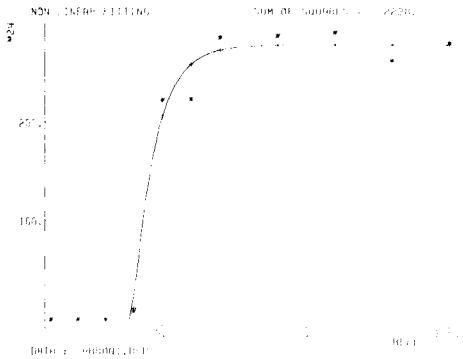

Fig. 4. Graphic representation of the fit of the exponential distribution function: (*) experimental points; (—) fitted function.

of the simplex method is that it generally requires a large number of iterations and function evaluations compared to the Marquardt method.

This example illustrates the capability of the program to fit any algebraic function to experimental data without the need for reprogramming; the fitting function can be specified explicitly in the command line, and can be stored in a command file for repeated use.

Processing of spectral data with DPP

The next example illustrates how DPP can be used to manipulate spectral data. Spectra obtained in, for example, x-ray fluorescence and mass spectrometry, are ordered arrays of numbers. The order represents the physical parameter for which the spectrum is taken, e.g., x-ray energy (keV) for x-ray spectra and mass in atomic mass units for mass spectra. It must be emphasized that this program was not initially developed for this type of application; the possibilities shown here are merely a consequence of the very general structure of the data base and the versatility of the commands that can be executed.

The data matrix is read as an unformatted file, each record being a 512-channel x-ray spectrum taken with a TRACOR Si(Li) detector installed on a JEOL-733 electron microprobe. The three records, or samples, are from three spectra S3010, S3008 and S3104. The variables are the contents of the 512 channels, and have default names V1 to V512. The initial command sequence to read in the data are as follows:

```
>>READ\DIRECT_ACCESS EMSPC.DAT
>>SHOW SAMPLES
  SAMPLE GROUP #     1       ALL_SAM
  INDEX        NAME     NUMBER
      1   S3010                1
      2   S3008                2
      3   S3104                3
```

In order to plot the spectral data (intensity vs. channel number), the data matrix is transposed:

```
>>TRANSPOSE
>>SHOW VARIABLES
  VARIABLE GROUP #      1      ALL_SAM
  INDEX        NAME    NUMBER
      1        S3010        1
      2        S3008        2
      3        S3104        3
```

Next a new variable is defined, representing the channel number. The DPP-function NUMBER(#1) is a function with a value equal to the column or row number of the data matrix, depending on its use in the definition of a variable or a sample. Thus: ">>DEFINE VARIABLE CHANNR=NUMBER(#1)". After this command, a spectrum can be plotted; the x-axis variable is the defined channel number, the y-axis variable is the intensities of spectrum number 3010. Thus: ">>PLOT\LINE CHANNR,S3010". The resulting plot on a Versatec plotter is shown in Fig. 5(a). To obtain a log plot with the x-axis expressed in x-ray energy (keV) the commands are

```
>>DEFINE VARIABLE LS3010=LOG(S3010)
>>DEFINE VARIABLE ENERGY=CHANNR*40/1000
>>PLOT\LINE\Y_LAB=SPECTRUM_3010 ENERGY,LS3010
```

The second line expresses the relation between channel number and energy in the spectrometer, one channel being 40 eV. The result is shown in Fig. 5(b). Other possible manipulations on spectral data are operations such as taking the sum, averages and ratios of spectra and the normalization of spectra.

Hierarchal cluster analysis on a large data set

In this example, a full two-dimensional data matrix is employed instead of only two variables. The electron microprobe was used to analyse 852 indi-

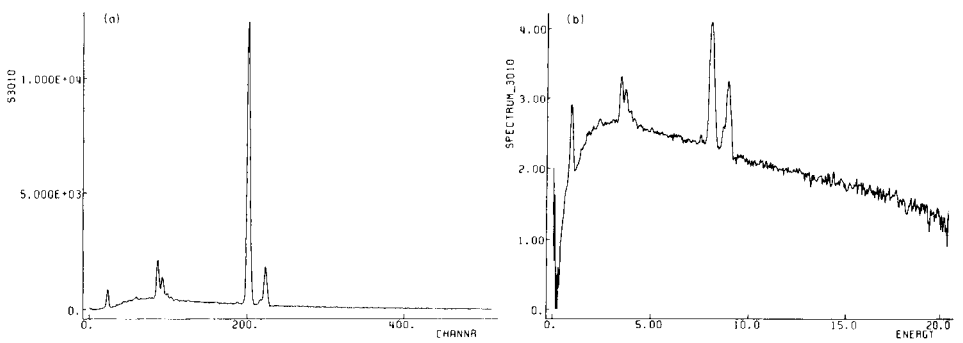

Fig. 5. Plots of an electron-induced x-ray spectrum: (a) number of counts versus channel number (the x-axis variable is produced by the program using the function NUMBER(#1)); (b) the x-ray intensity is log-transformed and the channel number is converted to x-ray energy in keV.

vidual aerosol particles. For each particle, an x-ray spectrum was taken and analysed. The individual results were transferred to a file for analysis by DPP. The data file consists of the net x-ray peak intensities for the 29 elements detected in the x-ray spectra and 7 variables pertaining to the particle size and shape, measured for the 852 particles. In the example, only the first 100 samples, selected from the sample group TEST, were used. The particles were classified in five groups by using hierarchal cluster analysis on the relative intensities of the elements Al, Si, P, S, Ca, Fe and Pb. In order to do this, new variables were defined with values equal to the relative intensity of the corresponding x-ray peak. Those variables were selected in a variable group, called NORM. The following command sequence was used:

```
>>CREATE SAMPLE_GROUP TEST
>>SELECT SAMPLES 1_100
>>DEFINE VARIABLE SUM=(AL+SI+P+S+CA+FE+PB)/100
>>DEFINE VARIABLE AL_N=AL/SUM
>>DEFINE VARIABLE SI_N=SI/SUM
>>DEFINE VARIABLE P_N=P/SUM
>>DEFINE VARIABLE S_N=S/SUM
>>DEFINE VARIABLE CA_N=CA/SUM
>>DEFINE VARIABLE FE_N=FE/SUM
>>DEFINE VARIABLE PB_N=PB/SUM
>>CREATE VARIABLE_GROUP NORM
>>SELECT VARIABLES AL_N,SI_N,P_N,S_N,CA_N,FE_N,PB_N
>>HIERARCHICAL_CLUSTER_ANALYSIS\STRATEGY=FURTHEST_NEIGHBOUR !
>>\NUMBER_OF_CLUSTERS=5
```

The clustering method selected was the furthest neighbour technique (complete linkage) [5]. The clustering tree diagram is shown in Fig. 6. The qualifier, "\NUMBER_OF_CLUSTERS=5", automatically initiates a procedure in which five sample groups are formed, holding the samples (particles in this case) that conglomerate in five clusters. The sample groups can then be used in further analysis. On the command "ACTIVATE SAMPLE_GROUP 3", the first cluster of particles becomes the active sample group. Figure 7 shows the commands used to work stepwise through these five groups and to list their average composition. Inspection of the output shows that the first cluster consists of particles rich in silicon, calcium and lead. The second group are calcium phosphate particles. The third group consists of two pure lead particles. The largest group is cluster four, containing particles rich in sulphur. The last cluster contains soil particles characterized by the presence of aluminium, silicon, calcium and iron.

Principal component analysis

The last example involves principal component analysis, used to investigate an environmental data set. During the period from December 1978 to July 1981, 37 aerosol samples were taken near Arica, Chile, by means of Battelle cascade impactors [13]. Each sample consists of aerosol material deposited at six different impactor stages, depending on the aerodynamic diameter of

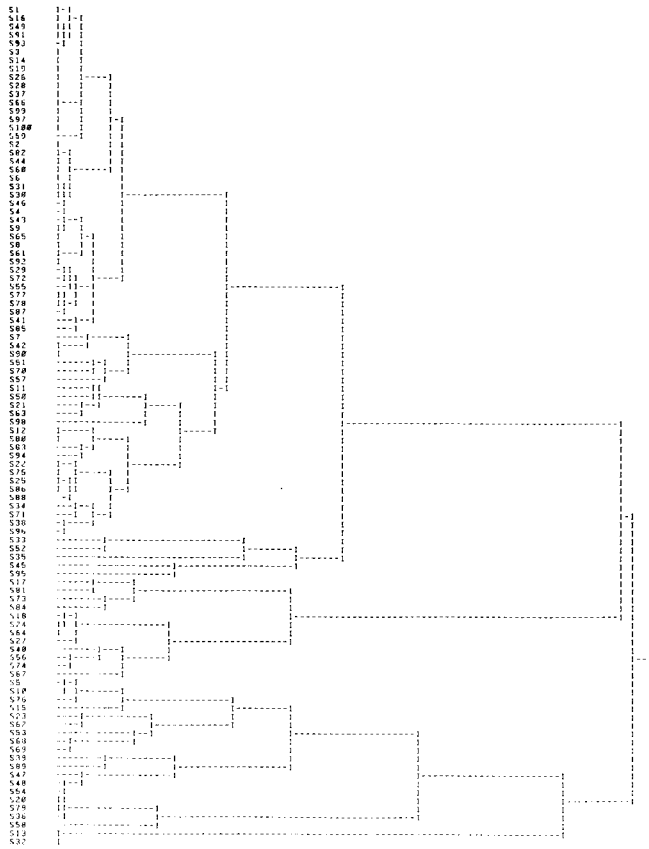

Fig. 6. Hierarchal clustering tree for 100 aerosol particles analysed with the electron microprobe.

the particulates. Stage one holds the material with a diameter greater than 16 μm, and the aerodynamic diameters are halved in each successive stage down to stage 6, where the very fine particles with diameters of 1—0.5 μm are retained. The elemental concentration of 24 elements was determined at each stage of the 37 impactor samples by energy-dispersive x-ray fluorescence spectrometry [14]. The data were organized into a 38 × 147 matrix; 37 rows were used to represent the samples and one row contained the detection limits. The columns are the 24 elements in stages 1—6 (denoted by AL_1, SI_1, ..., PB_1,AL_2,SI_2, ..., PB_2, ..., PB_6), the sampling volume, the sampling date and the sampling duration.

One of the applications of DPP on this data matrix was the use of principal component analysis to investigate whether there were different sources of lead in this background aerosol. A submatrix was created holding the 37 impactors as objects and the concentration of lead on the 6 stages and the average silicon concentration over the 6 stages as attributes. The eigenvectors

```
>>ACTIVATE SAMPLE_GROUP 3
>>LIST_DATA\NODATA\SAMPLE_STATISTICS
LISTING : AEROSOL_PARTICLES
Variable group #      2      NORM
Sample group   #      3      SG3
              AL_N          SI_N          P_N          S_N          CA_N          FE_N          PB_N
MEAN          Ø.Ø           1Ø.9Ø        1.136         Ø.Ø          42.83         Ø.Ø           45.14
ST. DEV.      Ø.Ø           13.88        4.251         Ø.Ø          11.96         Ø.Ø           16.43
#SAMPLES      14.ØØ         14.ØØ        14.ØØ         14.ØØ        14.ØØ         14.ØØ         14.ØØ

>>ACTIVATE SAMPLE_GROUP 4
>>LIST_DATA\NODATA\SAMPLE_STATISTICS
LISTING : AEROSOL_PARTICLES
Variable group #      2      NORM
Sample group   #      4      SG4
              AL_N          SI_N          P_N          S_N          CA_N          FE_N          PB_N
MEAN          Ø.Ø           Ø.Ø          35.7Ø        5.612         58.69         Ø.Ø           Ø.Ø
ST. DEV.      Ø.Ø           Ø.Ø          1.374        8.795         7.498         Ø.Ø           Ø.Ø
#SAMPLES      4.ØØØ         4.ØØØ        4.ØØØ        4.ØØØ         4.ØØØ         4.ØØØ         4.ØØØ

>>ACTIVATE SAMPLE_GROUP 5
>>LIST_DATA\NODATA\SAMPLE_STATISTICS
LISTING : AEROSOL_PARTICLES
Variable group #      2      NORM
Sample group   #      5      SG5
              AL_N          SI_N          P_N          S_N          CA_N          FE_N          PB_N
MEAN          Ø.Ø           Ø.Ø           Ø.Ø          Ø.Ø          Ø.Ø           Ø.Ø           1ØØ.Ø
ST. DEV.      Ø.Ø           Ø.Ø           Ø.Ø          Ø.Ø          Ø.Ø           Ø.Ø           Ø.Ø
#SAMPLES      2.ØØØ         2.ØØØ         2.ØØØ        2.ØØØ        2.ØØØ         2.ØØØ         2.ØØØ

>>ACTIVATE SAMPLE_GROUP 6
>>LIST_DATA\NODATA\SAMPLE_STATISTICS
LISTING : AEROSOL_PARTICLES
Variable group #      2      NORM
Sample group   #      6      SG6
              AL_N          SI_N          P_N          S_N          CA_N          FE_N          PB_N
MEAN          Ø.1799        5.115        1.174        83.95         7.16C         Ø.7979        1.621
ST. DEV.      Ø.9717        5.588        3.142        14.Ø8         8.822         4.623         4.824
#SAMPLES      68.ØØ         68.ØØ        68.ØØ        68.ØØ         68.ØØ         68 ØØ         68.ØØ

>>ACTIVATE SAMPLE_GROUP 7
>>LIST_DATA\NODATA\SAMPLE_STATISTICS
LISTING : AEROSOL_PARTICLES
Variable group #      2      NORM
Sample group   #      7      SG7
              AL_N          SI_N          P_N          S_N          CA_N          FE_N          PB_N
MEAN          1Ø.18         77.45        Ø.1381        7.851         2.684         1.697         Ø.Ø
ST. DEV.      11.85         17.42        Ø.4784        3.793         3.849         2.346         Ø.Ø
#SAMPLES      12.ØØ         12.ØØ        12.ØØ         12.ØØ         12.ØØ         12.ØØ         12.ØØ
```

Fig. 7. Listing of the average composition of the five clusters of the aerosol particles obtained by hierarchal clustering. User inputs are those lines starting with the ">>" sign.

of the correlation matrix were obtained and the first two principal component loadings were plotted. The command sequence was

```
>>CREATE SAMPLE_GROUP IMPACTOR
>>SELECT SAMPLES 1_37
>>DEFINE VARIABLE SI_MEAN=MEAN(SI_1;SI_2;SI_3;SI_4;SI_5;SI_6)
>>CREATE VARIABLE_GROUP LEAD
>>SELECT VARIABLES PB_1,PB_2,PB_3,PB_4,PB_5,PB_6,SI_MEAN
>>PRINCIPAL_COMPONENT_ANALYSIS
PCA>>PLOT LOADINGS 1,2
```

The resulting plot is shown in Fig. 8. The analysis confirms the observation reported previously [15] that there are two major sources of lead present in the remote South American aerosol: lead on coarse particles associated with crustal elements, and lead on fine particles (stages 5 and 6) that is probably of anthropogenic origin.

Conclusions

The software described gives the researcher a number of facilities to arrange, modify and investigate his experimental data. The program is specially designed so that these operations can readily be done interactively.

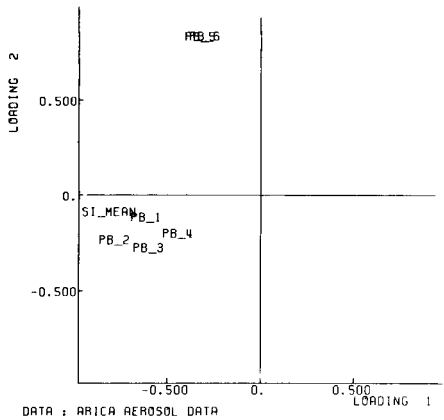

Fig. 8. Plot of loading of the first two components, resulting from a principal component analysis of lead concentrations in the six differently sized fractions and of the mean silicon concentration observed in a remote South American aerosol.

Experience in this laboratory has shown that people can master the program quickly, because of its uniform input syntax and the consistency of the program logic. The combination of operations related to the data base, and data-analysis procedures in one program greatly enhances the performance and applicability of the program. Because of the structure of the program, newly developed or already existing routines for data analysis are easily added when they are needed in the laboratory. One drawback is that the current version of the program requires a substantial amount of memory. A large portion of the data matrix and all the tables for names and pointers are resident in memory. A version in which the entire data structure would be resident on disk and only portions of it would lie in memory at any time is under development. In this way the program could be used on smaller mini-computers.

This work was supported by the National Science Foundation of Belgium (NFWO) and by the Interministerial Commission on Science Policy of Belgium through grant 80-85/10. The author is indebted to T. Mauney and B. Raeymaekers for their comments and for the use of the laser-microprobe and electron-microprobe data.

APPENDIX: DPP COMMANDS

This appendix contains the commands available in DPP. Words of the DPP vocabulary are shown in upper case, and data input in lower case. The word "ITEM" stands for SAMPLE or VARIABLE, "list" is a list of data separated by commas, "id" is the identification of an item by either its number or its name. The most important command qualifiers are listed under the command.

Commands related to the data base

Command	Meaning
>>READ_DATA file specification	Read in of data file
>>SET MISSING_VALUE value	Specify the value of missing data
>>SHOW "ITEM"	Show the items present in the currently active group
>>CREATE "ITEM" GROUP name	Create a group
>>ERASE "ITEM" GROUP id	Erase a group
>>ACTIVATE "ITEM" GROUP id	Make a group active
>>SELECT "ITEM" id-list	Select items in a group
\CONDITION=logical-expression	
>>REMOVE "ITEM" id-list	Remove items out of the current group
>>DEFINE "ITEM" name=arithm-expres	Define a new item
>>DELETE "ITEM" id-list	Delete a defined item
>>TRANSPOSE	Transpose the data matrix
>>SORT "ITEM" sort-item-id	Sort the items
\ASCENDING	
\DESCENDING	
\BY_NUMBER	

Commands dealing with data presentation and analysis

Command	Meaning
>>LIST_DATA	List the data in the current sample and variable group
>>PLOT variable-id-list	Plotting of data
\NUMBER_OF_GRAPHS	
\POINT	
\LINE	
\BARGRAPH	
\Y_ERROR_BARS	
\X_ERROR_BARS	
\SAMPLE_SYMBOL	
>>SCREEN_DATA variable-id	Perform a data screening over all data points in the current sample group
\TABLE_OF_DISTRIBUTION	
\HISTOGRAM	
>>POLYNOMIAL_REGRESSION list-of-powers	Perform a polynomial regression analysis on the data in the current sample group
\WEIGHTED	
>>NON_LINEAR_FIT variable=function	Non-linear fitting
\SIMPLEX	
\START_VALUES	
\STEP_SIZE	
>>PRINCIPAL_COMPONENT_ANALYSIS	Principal component analysis
\CORRELATION_MATRIX	
\COVARIANCE_MATRIX	
>>HIERARCHAL_CLUSTER_ANALYSIS	Hierarchal cluster analysis
\NEAREST_NEIGHBOUR	
\FURTHEST_NEIGHBOUR	
\GROUP_AVERAGE	
\CENTROID	
\MEDIAN	
\WARDS_ERROR_SUM	
\SIMPLE_AVERAGE	
\FLEXIBLE_STRATEGY	

>>MASLOC	Non-hierarchal cluster analysis by MASLOC
\BABEL	
\SHIFT_BABEL	
\EXACT	
\CORRELATION_DISTANCE	
\EUCLIDEAN_DISTANCE	
\MANHATTAN_DISTANCE	

Commands dealing with program control and input—output

Command	Meaning
>>COMMAND file-name	Instruct DPP to read commands from a file
>>STOP	Stop DPP
>>TYPE file-name	Type the content of a file on the terminal
>>SHOW STATUS	Show the current status of, and the computer resources used by, the program
>>SET BACKUP	Instruct DPP to back up all the commands entered
\ON	
\OFF	
>>SET BATCH	Set DPP in batch mode
\ON	
\OFF	
>>SET TERMINAL terminal-type	Identify the graphics mode of the terminal
>>SET PLOTTER plotter-type	Identify the plotter
>>REPORT	Make a hard copy (printer and/or plotter) from the results obtained with the current command

REFERENCES

1 N. H. Nie, C. H. Hull, J. G. Jenkins, K. Steinbrenner and D. H. Bent, SPSS, Statistical Package for the Social Sciences, McGraw-Hill, New York, 1975.
2 W. J. Dixon, BMD, Biomedical Computer Programs, University of California Press, Berkeley, 1971.
3 A. M. Harper, D. L. Duewer, B. R. Kowalski and J. L. Fasching, in B. R. Kowalski (Ed.), Chemometrics: Theory and Application, ACS Symposium Series 52, American Chemical Society, Washington, DC, 1977, p. 14.
4 S. Wold and M. Sjostrom, in B. R. Kowalski (Ed.), Chemometrics: Theory and Application, ACS Symposium Series 52, American Chemical Society, Washington, DC, 1977, p. 241.
5 D. L. Massart and L. Kaufman, The Interpretation of Analytical Chemical Data by the use of Cluster Analysis, Wiley, New York, 1983.
6 T. Mauney and P. Van Espen, in A. D. Romig and J. I. Goldstein (Eds.), Proc. 20th Ann. Meet. Microbeam Analysis Soc., Microbeam-84, San Francisco Press, 1984, p. 295—298.
7 W. M. Newman and R. F. Sproull, Principles of Interactive Computer Graphics, McGraw-Hill, New York, 1973.
8 J. A. Nelder and R. Mead, Comput. J., 7 (1965) 308.
9 D. W. Marquardt, J. Soc. Ind. Appl. Math., 11 (1963) 431.
10 P. M. Mather, Computational Methods of Multivariate Analysis in Physical Geography, Wiley, London, 1976.

11 L. Kaufman and D. L. Massart, MASLOC Users' Guide (Version 1), Internal Report, HWPR/025, Vrije Universiteit Brussel, Brussels.
12 T. Mauney and F. Adams, Int. J. Mass Spectrom. Ion Proc., in press.
13 R. J. Mitchell and J. M. Pitcher, Ind. Eng. Chem., 51 (1959) 1039.
14 P. Van Espen, F. Adams and W. Maenhaut, Bull. Soc. Chem. Belg., 90 (1981) 305.
15 P. Van Espen and F. Adams, Anal. Chim. Acta, 150 (1983) 153.

Analytica Chimica Acta, 165 (1984) 51—59
Elsevier Science Publishers B.V., Amsterdam — Printed in The Netherlands

EXTRACTION OF MASS SPECTRAL INFORMATION BY A COMBINATION OF AUTOCORRELATION AND PRINCIPAL COMPONENTS MODELS

S. WOLD
Department of Chemistry, University of Umeå, S-901 87 Umeå (Sweden)
O. H. J. CHRISTIE*
Rogaland Research Institute. P.O.B. 2503 Ullandhaug, N-4001 Stavanger (Norway)
(Received 24th May 1984)

SUMMARY

In mass spectrometry, pattern recognition can be used for high-precision chemical structure classification provided that the mass spectra have been transformed to counteract the effect of mass spectral shifts. Autocorrelation transforms can be employed for this purpose. This transform gives results which are interpreted in terms of periodicities in the mass spectra, i.e., the loss of certain fragments from various ions.

Mass spectrometry is commonly used for identification of organic compounds. Because of its specificity, this technique is often the only one feasible for compounds present in small quantities, hence its frequent use in connection with gas chromatography, liquid chromatography and pyrolysis.

The identification of previously analysed compounds is usually based on search and matching techniques against a library of mass spectra of known compounds (e.g. [1—3]). Even in well investigated problem areas, however, previously unrecorded compounds often appear. Because their mass spectra are not present in the library, matching techniques may be less useful. Classification methods based on similarities and dissimilarities between the "unknown" spectrum and reference compounds are then preferable. Classification methods, if working properly, might also be useful to diminish the search through large libraries of tens of thousands of spectra by rapidly directing the search to smaller subclasses of the library [4, 5].

CLASSIFICATION AND PATTERN RECOGNITION

The problem of using spectra of known reference compounds for the classification of a spectrum of an unknown compound can be formulated as a pattern recognition problem. A training set of spectra of reference compounds of known classes is first used to develop classification rules. In the second phase, those rules are used to assign the spectrum of the "unknown" compound to one of the "known" classes.

0003-2670/84/$03.00

Pattern recognition methods can be divided into two broad categories: syntactic (grammatical) methods and statistical methods. When applied to mass spectrometry, the former are often called interpretative methods (DENDRAL [6, 7], STIRS [8], and SISCOM [9]). Here, grammatical rules are derived from libraries of compounds with known structural features. For the spectrum of the "unknown" compounds, one searches for a structure that, subject to the rules, would give a spectrum that matches the given spectrum as closely as possible. There is a variety of search algorithms [2, 5], some of which have been tested against each other by Henneberg [9].

With statistical pattern recognition methods, each mass spectrum is represented as a point in a p-dimensional space in the hope that spectra from compounds with similar structure will cluster closely in this space (Fig. 1). This space is called M-space (multivariate space or measurement space). However, this statistical pattern recognition approach presents three main sets of problems in mass spectrometry, as outlined below.

(1) The class homogeneity and spectral representation

Statistical pattern recognition is based on the assumption that each class is homogeneous with respect to the p variables. Thus, each structural class should occupy a small part of M-space. A situation indicated in Fig. 2 makes all pattern recognition methods for mass spectral classification break down.

The direct representation of mass spectra by their intensities at different mass numbers is commonly used in pattern recognition [5, 10]. This is not

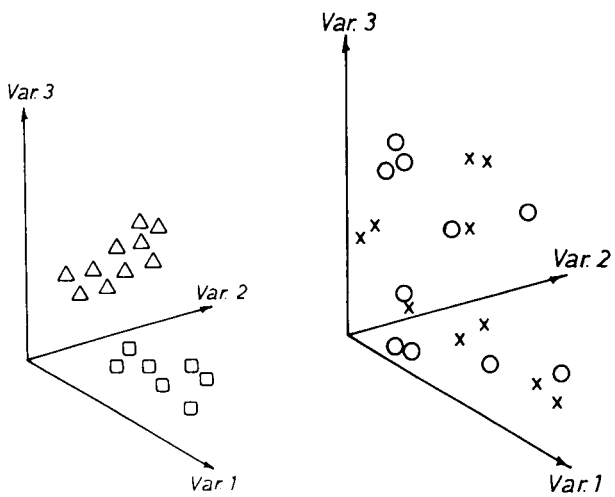

Fig. 1. Two homogeneous classes of objects well separated in M-space; the ideal case for pattern recognition.

Fig. 2. The classes must be homogeneous and not, as here, spread out "randomly" in M-space. A failure to recognize the "natural" grouping of mass spectra may give this undesired picture.

correct, as is evident from the following argument. Two compounds which differ only by the replacement of one hydrogen by deuterium are considered. Clearly, parts of the spectra of the D compound are shifted one mass unit with respect to the H compound. This makes variable j of the deuterated compound correspond to variable j of the non-deuterated compound for many values of $j + 1$. In the M-space this corresponds to a grand rotation and the two points will thus be far from each other in M-space (Fig. 3). Consequently, the structural class is scattered among different parts of M-space rather than being concentrated in a small part.

Because a change in a few substituents from, say, CH_3 to C_2H_5, or NH_2 to $NHCH_3$ does not necessarily represent a significant change of chemical structure, it can be concluded that the representation of spectra by their intensities at different mass number is unsuitable for statistical pattern recognition.

A better way to represent the spectra would be to use their periodic transforms such as Fourier, Hadamard or autocorrelation transforms. They have indeed been tried in pattern recognition for mass spectrometry [11—13]. However, the use of the linear learning machine in these studies is unfortunate for the reasons mentioned below, and the possible advantages of the transforms were masked by the choice of an unsuitable data analytical method.

Clerc and Szekely [14] have recently argued against such transformations for mass spectra. However, the approach is preferred here because of the following arguments. The transformed data are invariant to a translation of the original spectrum. The transformations reveal periodicities because of the loss of the same fragment ion from various ions. Hence, this solution adopts the easily perceptible features of mass spectra as routinely observed by the mass spectroscopist, and the transformed data should be better suited for pattern recognition than are the original data.

(2) The class specification

Because pattern recognition can only recognize classes that in some way have an objective existence in the given data, one has to specify the classes in a multivariate sense according to mass spectral knowledge. This has been done very little so far. Most applications of pattern recognition to mass spectrometry has been made with the naive objective of recognizing functional groups such as amines, alcohols, esters, nitro groups, etc. It has

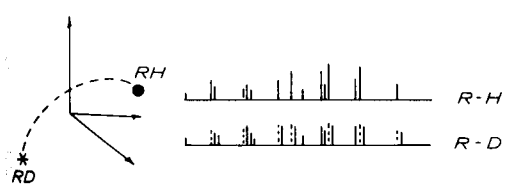

Fig. 3. If a mass spectrum of a compound is represented as the intensities at different *m/z* values, the spectra of a compound and its deuterated analogue are in different quadrants in M-space, despite the fact that they are chemically very similar.

been pointed out that mass spectrometry is a method mainly giving information about the molecular skeleton rather than the functional groups [15].

(3) The number of variables

Most pattern recognition methods traditionally used in chemistry and in mass spectrometry, notably the linear learning machine (LLM), have the unfortunate property that the number of samples in a study must be substantially larger than the number of variables in order to avoid spurious correlations. Ordinary mass spectra usually have many peaks (variables). If a total number of 250 peaks is to be accounted for, the necessary number of spectra would be around 1000. The resulting 1000 × 250 data matrices are unmanageable even for large computers. Hence shortcuts reducing the number of variables, hopefully without losing the information in the data, have been tried. Usually the data reduction is made by selecting variables that separate the given classes. This may increase the chance for spurious correlations dramatically and so far few investigations have been published demonstrating statistically reliable results [4, 16—18].

However, pattern recognition methods have been developed which are not hampered by a large number of variables in relation to the number of objects. In the present paper, the SIMCA method is used [19—21]. This method derives A-dimensional principal components (PC) models in the p-dimensional M-space for each class of objects. Because $A(p + n - 1)$ parameters are estimated from $p \times n$ data elements in the class matrix, the estimation is statistically stable as long as A (the number of components in the model) is substantially smaller than both the number of variables and the number of objects in the class. This condition is always easy to meet. Hence, our approach overcomes the difficulty of the small number of samples versus variables of methods. Evidently, the sum of intensities of the shifts may easily differ from that of the untransformed data. Thus, an increase of one m/z value at the expense of another one would leave the sum of intensities unchanged, whereas this would not be the case for the sum of transformed intensities. This restricts the present approach to classification purposes and makes it unsuitable for absolute quantification. It is not difficult to modify the transformation to make it suitable also for quantification, however.

PROPOSED METHOD

In the present investigation, a small data set (21 spectra) is used to investigate the feasibility of the autocorrelation transform in combination with the SIMCA method. This would possibly handle problems (1) and (3) above. With respect to problem (2), the specification of the classes is made tentatively in consistence with knowledge of mass spectrometry (alkanes, cycloalkanes, aromatics, etc.), but efforts will be made to check the correctness of this class specification.

Autocorrelation transform

The intensity at mass number i is denoted by x_i. The modified autocorrelation technique which for long has been successfully used for spectral noise reduction (e.g. [22]) forms a new set of variables, v_m, by a sequential multiplication series of the original variables x_i

$$v_m = x_i x_{i-m}/(p-m) \quad (1)$$

Thus, the new variables v_m can be seen as the normalized product of a spectrum and the same spectrum shifted by m mass numbers.

Autocorrelated variables are used here because we believe that significant information for mass spectral information is related to periodicities in the spectra. Thus, the loss of a CH_2^+ group will give a high autocorrelation for shift 14 because peaks 14 units apart will have a tendency to be high simultaneously. This makes the data analysis of autocorrelated spectra easy to interpret from the chemical point of view, and the present pattern recognition solution is in principle an alternative to the fundamental homologue observation utilized in, for example, the SISCOM system [9].

Data

A set of mass spectra of hydrocarbons with eight carbon atoms was used: eight alkylpentanes, seven alkylcyclopentanes and six alkylcyclohexanes. All the spectra were collected from the NIH library of the VG-7250 integrated g.c./m.s./d.s. system. The 13 most intense mass-spectral lines of each compound constitute the source data for the present work (Table 1). It is not difficult to separate alkylpentanes from alkylcycloalkanes, but the mass spectra of alkyl-cyclopentanes and -cyclohexanes are usually very similar. Thus, the data set constructed contains classification problems with different degrees of difficulty.

The mass-spectral source data were subjected to an autocorrelation transform according to Eqn. 1, producing the initial set of shifts. In order not to exaggerate any class separation, all resulting shift variables with value zero for all compounds in any class were deleted. It must be emphasized that this leads to a loss of information which would not be recommendable in practice. Because, however, all possibilities of artifacts in the present demonstration are better excluded, this information reduction is deliberately made to remove the possibility of overoptimistic class separation.

The transformation of the 13 mass spectral lines into 35 shift values means that the dimensionality of M-space has been expanded from 13 to 35. This is a technique contrary to the commonly encountered data reduction whereby the dimensionality is lowered. In reality, however, all mass numbers have a defined intensity and the autocorrelation transform has the same dimensionality as the original spectrum.

TABLE 1

Residual standard deviation for compounds 1—14 refitted to the one-component models of class 1 (open chain) and 2 (cyclopentane)

Plot	Compound	(Class)	Distance to Class 1	Distance to Class 2	Variances	
					1	2
12	1: 2,2,4-TMP	(1)	0.289	3.213		
13	2: 2,2,3-TMP	(1)	0.311	2.688		
14	3: 2,3,4-TMP	(1)	0.746	2.182	0.65	2.38
15	4: 2,3,3-TMP	(1)	0.670	1.981		
16	5: 3E,2M-TMP	(1)	0.509	2.155		
17	6: 3E,3M-TMP	(1)	1.034	1.837		
2	7: 1,1,3-TMCP	(2)	17.42	0.396		
3	8: 1,2,4-TMCP	(2)	9.27	0.557		
4	9: 1,1,2-TMCP	(2)	17.36	0.735	13.3	0.68
5	10: 1,2,3-TMCP	(2)	8.74	0.556		
6	11: 1E,1M-TMCP	(2)	9.82	0.984		
7	12: 1,1DM-CH	(3)	28.14	1.416		
8	13: 1,3DM-CH	(3)	65.58	2.804	57.3	2.31
9	14: 1,2DM-CH	(3)	69.03	2.480		

RESULTS

Principal components projection

A graphical projection of the overall data structure was obtained by an initial principal components analysis (PCA) of the whole data set scaled to unit variance for each variable. This PCA is equivalent to the factor analysis used by Rozett and Peterson [23], Duewer et al. [24], Williams et al. [25] and others. Evidently, the alkylpentane spectra are well separated from the two groups of cycloalkanes in Fig. 4. This indicates that the class specification is consistent with the data structure. It should be noted that this projection was obtained without specifying the class of the compound to the computer. In contrast to earlier studies, the obtained separation is not the result of supervised learning, and it is highly likely to be real.

SIMCA classification

Phase 1. Training. Separate class PC models were fitted to the two classes (1) alkylpentanes and (2) alkylcyclopentanes. There are too few alkylcyclohexanes in the present collection to allow stable SIMCA class modelling. The number of significant components estimated by cross-validation [26] was 2 for both the classes 1 and 2. Hence, there was a significant systematic variation around the average autocorrelated mass spectral information in each class.

In the two classes, 27 and 19 of the 35 variables, respectively, have high modelling power (more than 0.5), showing that most of them are well described by the class models.

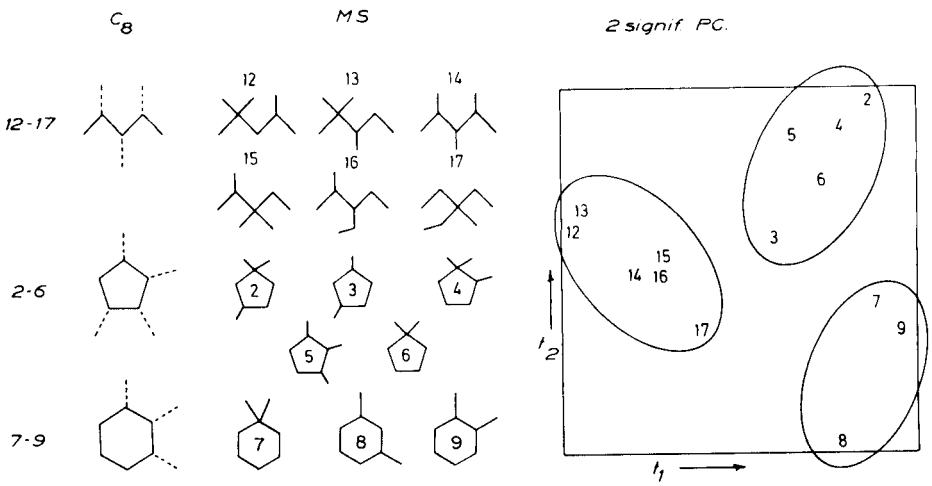

Fig. 4. The first two principal components of the autoscaled autocorrelation-transformed mass spectral data for fourteen C_8 alkanes: 12—17 are open chain, 2—6 are cyclopentanes, and 7—9 are cyclohexanes.

Phase 2. Classification. All the 21 autocorrelated mass spectra were then refitted to the two class models. The resulting distances are shown in Table 1. To show the information power in the approach, only the simplest class models with one component each and non-weighted residuals were used. An optimal SIMCA classification increases the separation further by a factor of about 4.

The separation of the classes in the present approach is very good. The class distances (1:2) = 3.69, (1:3) = 88.55, (2:3) = 3.42 are highly significant, according to approximated F-tests (F = 13.62, 7841.5, and 11.7; for p = 0.01, F = 10.7, 9.78, and 12.1, respectively). The distance between the alkylcyclohexanes (class 3) and class 1 is calculated as the pooled standard deviation of class 3 compounds fitted to class model 1 divided by the pooled standard deviation of class 1 compounds fitted to class 1. The analogous procedure was used for the class 3—class 2 distance.

The variables having the largest discrimination power were 5—7, 17—19, and 24—32 between classes 1 and (2, 3), i.e., straight-chain alkanes/alicyclic. These variables correspond to the mass shifts 11—13, 28—30, 41—47, and 55, 56. Between classes 2 and 3 (cyclopentane/cyclohexane), the variables with large discrimination power were 1, 2, 6—12, 23, 25, 31, and 33, corresponding to the mass shifts 1, 2, 12—18, 40, 42, 55, and 57.

CONCLUSION

The autocorrelation transform makes the information in mass spectra easily extractable by pattern recognition. It should be emphasized that the method of pattern recognition used must be able to handle many variables

even when the number of spectra is small. This makes methods based on principal components and factor analysis, such as the SIMCA method, suitable for this purpose. Methods like linear discriminant analysis and the closely related linear learning machine are not useful.

Much investigation is needed to elucidate the "natural class structure" of mass spectra. Simple projections of autocorrelation-transformed spectra should be helpful in such investigations. For larger data sets, cluster analytical methods may be advantageous. The methodology presented in this paper can, however, already be applied to well specified problems such as the alkylpentane/alkylcycloalkane problem used as an illustration above. It tells clearly which variables actually contribute to the separation of classes. Furthermore, it shows that there is a large class separation even between C_8 cyclohexanes and cyclopentanes.

The present study shows that mass spectra contain much structural information which can be extracted by appropriate methods. This may lead mass spectrometry a step further as a technique not only for structure identification but also for structural classification.

REFERENCES

1 S. R. Heller, W. L. Budde, D. P. Martinsen and G. W. A. Milne, in E. R. Schmid, K. Varmuza and I. Fogy (Eds.), Adv. Mass Spectrom., 1982, C. 313, Elsevier, Amsterdam, 1983.
2 G. M. Pesyna, R. Venkatarahgavan and F. W. McLafferty, Anal. Chem., 48 (1976) 1362.
3 H. Damen, D. Henneberg and B. Weimann, Anal. Chim. Acta, 103 (1978) 289.
4 P. Bruck and J. Tamas, 1981. In A. Quayle, Adv. Mass Spectrom., 8B (1981) 1535. Heyden, London.
5 D. P. Martinsen, Appl. Spect., 35 (1981) 255 (and references therein).
6 D. H. Smith, B. G. Buchanan, R. S. Engelmore, A. M. Duffield, A. Yeo, E. A. Feigenbaum, J. Lederberg and C. Djerassi, J. Am. Chem. Soc., 94 (1972) 5962.
7 D. H. Smith, L. M. Masinter and N. S. Shiradon, in W. T. Wipke, S. R. Heller, R. J. Feldmann and E. Hyde (Eds.), Computer Representation and Manipulation of Chemical Information, Wiley, New York, 1974, p. 287.
8 K.-S. Kwok, R. Venkatarahgavan and F. W. McLafferty, J. Am. Chem. Soc., 95 (1973) 4185.
9 D. Henneberg, in A. Quayle, Adv. Mass Spectrom., 8 (1981) 1511, Heyden, London.
10 K. Varmuza, Anal. Chim. Acta, 122 (1980) 227.
11 P. C. Jurs, Anal. Chem. 48 (1971) 1812.
12 B. R. Kowalski and C. F. Bender, Anal. Chem., 45 (1973).
13 J. R. McGill and B. R. Kowalski, J. Chem. Inf. Comput. Sci., 18 (1978) 52.
14 J. T. Clerc and G. Szekely, In E. Pungor, G. E. Veress and I. Buzas (Eds.), Pattern Recognition in Analytical Chemistry, Akad. Kiado, Budapest, 1984, p. 49.
15 J. R. Chapman, Computerized Mass Spectrometry, Academic Press, London, 1978.
16 R. G. Dromey, Anal. Chem., 48 (1976) 1464; 51 (1979) 133, 229.
17 N. A. B. Gray, Anal. Chem., 48 (1976) 2265.
18 S. Wold and W. J. Dunn, III, J. Chem. Inf. Comput. Sci., 83 (1983) 6.
19 S. Wold, Pattern Recognition, 8 (1976) 127.
20 S. Wold, C. Albano, W. J. Dunn, III, U. Edlund, K. Esbensen, P. Geladi, S. Hellberg, E. Johansson, W. Lindberg and M. Sjostrom, in B. R. Kowalski (Ed.), Proc. NATO Adv. Study Inst. Chemometrics, Cosenza, 1983, Reidel Publishing Co., 1984.

21 S. Wold, C. Albano, W. Dunn, III, K. Esbensen, S. Hellberg, E. Johansson and M. Sjostrom, in H. Martens and H. Russwurm (Eds.), Data Analysis in Food Research, Applied Science Publishers, London, 1983.
22 R. Annino and E. Grushka, J. Chromatogr. Sci., 14 (1976) 265.
23 R. W. Rozett and E. M. Peterson, Anal. Chem., 47 (1975) 1301, 2377; 48 (1976) 817.
24 D. L. Duewer, B. R. Kowalski and J. L. Fasching, Anal. Chem., 48 (1976) 2002.
25 S. S. Williams, R. B. Lam and T. L. Isenhour, Anal. Chem., 55 (1983) 1117.
26 S. Wold, Technometrics, 20 (1978) 397.

Analytica Chimica Acta, 165 (1984) 61—74
Elsevier Science Publishers B.V., Amsterdam — Printed in The Netherlands

COMPUTER-AIDED IDENTIFICATION OF COMPOUNDS BY COMPARISON OF MASS SPECTRA

L. DOMOKOS,*[,a] D. HENNEBERG and B. WEIMANN
Max-Planck Institut für Kohlenforschung, Mülheim/Ruhr (Federal Republic of Germany)
(Received 23rd January 1984)

SUMMARY

A new identity-orientated search procedure for mass spectral libraries (IDS) was developed by extending the similarity search system SISCOM. The aim of IDS is an exact identification of pure compounds and mixtures on the basis of their mass spectra. The concepts and methods applied, e.g., filtering, feature selection and optimization with pattern recognition, are described. Characteristics of IDS are summarized and demonstrated for several examples.

The SISCOM system for mass spectral library search [1, 2] has been used successfully for several years in routine laboratory practice. It searches for a set of compounds that are structurally similar or identical to a given pure unknown compound or to the components of a mixture. The input of the system is the mass spectrum of the unknown which is encoded and then compared with the encoded spectra of the reference libraries. The result, the similarity hit list, provides a list of reference compounds, selected and ranked by the search as the most similar ones. This hit list contains at most 150 spectra. The output usually offers only the first 16 best references, giving their names, formulae and comparison factors. These factors are derived from comparison of the encoded unknown spectrum with the corresponding reference spectra, and are used to rank these references according to a similarity measure. Considerable effort has been put into optimization of the encoding and of the similarity measure so that similarity in encoded spectra corresponds to similar chemical structures. The system is being continuously improved.

As an extension of the SISCOM technique which is mainly similarity-orientated, a new identity-orientated search procedure (IDS) has been developed. The goal of IDS is not to find the compounds that are similar in some way, but to identify exactly the unknown pure compound or mixture components. Thus, the aim is to find a reference compound identical with the

---

[a]Permanent address: Institute for General and Analytical Chemistry, Technical University Budapest, Gellért-tér 4, H-1521 Budapest, Hungary.

0003-2670/84/$03.00

unknown pure compound or with a component of a mixture, rather than to find spectra that are numerically identical.

The requirements of search systems orientated towards identity and similarity are different. A similarity search should result in a hit list of somehow similar compounds with the identical compound first in the list if its spectrum is the most similar one. An identity search, however, must decide clearly between two categories: a reference compound is or is not identical with the unknown. Instead of a continuous similarity criterion, a decision between two categories is necessary. Two difficulties are encountered. First, the reference library will almost certainly contain a set of compounds that are similar in some aspect but not necessarily an identical compound. This is particularly likely if the unknowns come from research work. Secondly, even if the identical reference compound is in the library, its spectrum may be fairly different from the unknown spectrum. Such differences, mainly with respect to the pattern but in some cases even to mass numbers, are due to different conditions of measurement. Differences or reduced quality are also caused by noise, impurities or bad recording. Another reason for differences is when the unknown is a mixture. To investigate and characterize the spectrum quality, a preliminary investigation has been done [3]. Other workers have also reported on this problem [4, 5].

Problems of existing methods

An identification is relatively easy if it is known that the unknown is a pure compound, if the identical reference is contained in the library and if the corresponding spectra are of good quality. Then, a similarity search ranks the identical reference most frequently in the first position. Difficulties arise if identification of mixture components is also required, if it is not known whether an identical reference exists, and if the spectra are distorted or of bad quality. The many existing systems and efforts reported in the literature, and the fact that the problem has not been satisfactorily solved yet, indicate the non-triviality of the problem.

Although a similarity search frequently ranks the identical reference first, the above-mentioned deviations between mass spectra of identical compounds often cause the correct reference to appear at lower positions of the hit list. For example, the spectra of chemically similar compounds measured under the same conditions may be more similar than the spectra of identical compounds measured under different conditions. If the identical reference is not included in the library, then the most similar spectrum cannot be the identical spectrum. In the case of mixtures, even if the first component is at the top of the similarity hit list, the other components are often relegated to low positions because references similar to the first component are ranked higher. Consequently, different factors and valuations must be applied, depending on whether the aim of the search is to retrieve similar or identical reference compounds. The general scheme of most of the existing library search systems is that the unknown spectrum or its reduced (encoded) form

is matched with the same form of reference spectra; those with the highest score are the candidates for being identical. Spectrum reduction very often selects, globally or locally, the most intense peaks. Such a method depends strongly on the intensity relations in the spectrum, i.e., on the most questionable part of the information contained in a mass spectrum.

DESCRIPTION OF THE IDS TECHNIQUE

The IDS method is based on the 150 members of the SISCOM hit list which are selected with respect to similarity, and by using a coding method where neither low intensity nor the number of selected peaks excludes possibly characteristic peaks. During this presearch, intensity ratios are not highly weighted. As a consequence, the choice of references is less sensitive to the mentioned sources of inaccuracy. To these 150 reference spectra, IDS applies a special treatment for identity: it first looks for the dissimilar spectra and excludes them before ranking the remaining ones by a special criterion of identity.

This principle corresponds to the way of thinking applied in statistical hypothesis testing [6]. Library searching is, of course, a series of hypothesis testing, to decide on the null hypothesis (H_0) that the reference is identical to the unknown. The problem is to decide if H_0 is true or not, or more exactly if H_0 is acceptable on the basis of the mass spectra or not. There are two types of error: in the type I error, H_0 is rejected but it is true; in the type II error, H_0 is accepted but it is false. Statistically, the acceptance of H_0 is not a proof of H_0, but gives only the possibility of validity. Usually, the probability of being strictly true is very low; this corresponds to reality, because two samples or spectra are never exactly the same in every detail. The question is, what a tolerance is allowed. In contrast, the statement that H_0 is not true, is a very firm one, and there is a high probability of its validity. When mass spectra are compared for retrieving identical compounds, certain types of differences are not tolerable, e.g., pronounced spectral characteristics of the reference spectrum missing in the unknown. This and other conditions enable the number of possible identical references to be reduced. Unfortunately, if one type of error is decreased, the other will increase unless the quality of spectra is improved.

The IDS system works as follows: (1) it starts after the similarity search, using the 150 references of the similarity hit list; (2) it searches for the significantly different references of the hit list and eliminates them by using a series of filters; (3) it ranks the remaining references according to an identity measure for spectra; (4) if the filtering leaves several references that are similar to each other, the most probable are selected as candidates for being identical. Only the 5 or 6 best, if any exist at all, are listed.

Filters

The filters are required to discover the significantly different references, which cannot be identical to the unknown, and remove them from further processing. The plan was to keep the more dangerous error of type I low, which of course is possible only at the expense of type II error. This means that the filters cannot be too strict. Despite careful filtering, the proper reference may be lost if certain errors occur in unknown or reference spectra and result in a type I error.

A thorough investigation of a large number of test runs was made to develop the filters and their threshold values. In order to distinguish the various kinds of deviations between spectra of identical compounds caused by mixture, impurities, noise, tilting, etc., from the real differences caused by different chemical structures, the tests were run with different data bases, thus involving a considerable number of existing duplicates measured at different places with different conditions and methods. The test set of unknowns consisted of 160 measured spectra from g.c./m.s. runs, including mixtures from unresolved components, and in addition a group of 40 spectra specially selected to represent typical difficulties such as skewed spectra, contaminations and even partly wrong spectra. The whole test set was combined to form a representative training set.

The filters are applied in a sequence which minimizes the computational requirements. The first filter is the similarity search itself, and the second uses only values already computed from the encoded spectra by the similarity search. The next two filters use the more complex unreduced spectra and the last filter uses not only the unknown spectrum but also several spectra adjacent to the unknown in the series of measured spectra.

Filter A is the similarity search itself, i.e., IDS is applied only to the 150 spectra of the similarity hit list. This is sufficient, because earlier experience with SISCOM proved that the identical references are almost always somewhere in this list. Filter B is based on the comparison factors determined from the encoded spectra by the similarity search. Besides the 15 spectra at the top of the similarity hit list, filter B passes spectra with the ten best scores of each comparison factor.

The similarity search and filters A and B require only the encoded spectra. The unreduced spectra are used for the further filters C, D and E and for deriving several additional features used in the identity measure described below. This use of full spectra is, of course, more time-consuming but it permits more thorough matching. Fortunately, the number of reference spectra to be processed at this stage usually does not exceed 50—60.

Filter C is an intensity filter. Reference spectra are excluded if they have a significant peak, at least of 20% of the base peak intensity, which is not present in the unknown; or if they have a significant summed intensity of (smaller) peaks not present in the unknown. The opposite (i.e., that the unknown contains significant peaks not present in the reference) must be allowed because the search also includes mixture components.

Filter D is based on the quotient spectrum developed by Henneberg and Weimann [7]. The "intensities" in the quotient spectrum are computed for each mass as the suitably normalized logarithm of the quotients of respective intensities in the reference and unknown. Basically, if the two spectra, reference and unknown, are of different compounds, the quotient spectrum will be very irregular, but if they are of the same compound and the spectral differences are caused only by measurement conditions (e.g., differently tilted spectra from g.c./m.s., then their quotient spectrum will follow a smooth, inclined curve and can be approximated by a parabola with low curvature. The same is approximately valid for the influence of instrumental conditions on spectra and is valid if the reference is a component of the unknown mixture. However, in the latter case, only those masses in the quotient spectrum are to be considered which are significant masses for the reference compound and do not overlap with the other component. This subset of lines is selected by an iterative method and a parabola is fitted only to them.

To characterize the degree of deviation of the quotient spectrum from a parabola, three parameters are derived: the variance of the residuals (*VA*), the curvature of the parabola (*DI*), and the sum of intensities of the quotient spectrum lying far above the fitted parabola (*IVO*). Filter D excludes reference spectra if one of these three parameters or their product is greater than a prescribed threshold value. Applications proved that the three parameters can be applied successfully for identification of compounds with differing spectra, and very often for recognizing components of a mixture. The reason is that quotient spectra are rather insensitive to typical deviations in the conditions of measurement but sensitive to different compounds, except for types of isomerism that result in identical mass spectra.

The parabola P can be fitted to the quotient spectrum Q, which is $Q = \log(R/U)$, where R is the reference and U the unknown, and a corrected reference spectrum R^* can be computed from the above equation after replacing Q by P, i.e., $R^* = U \times \exp(P)$. If the reference is identical to the unknown, then this correction removes the tilting and a numerical comparison of R^* and U is more exact than that of R and U. From this comparison two further parameters are computed denoted by *TU* and *TR*, respectively; *TU* is the percentage of the summed positive intensities in $U - R^*$ related to the sum of intensities in U and *TR* is the same with the negative intensities related to the sum of intensities in R^*. Thus *TU* is a measure correlated to impurity: it is zero for the spectrum of a pure unknown and relatively small for a main component. Because *TR* contains the part of R^* missing in U, it is a strong indication that a reference compound is not identical. Therefore references with large *TR* values are also filtered out.

Filter E is applicable only in cases where the unknown spectrum is taken from a series of measured spectra (as is usual when a data system is used for g.c./m.s. or fractional evaporation) and the spectra of this series are available.

If the unknown is a mixture, the reference spectrum of a component of a mixture must be part of the unknown spectrum. Unfortunately, there are references the spectra of which are also a part of the unknown spectrum without being a mixture component. This happens particularly with references exhibiting only few peaks, which gives a good chance to cover a small part of the unknown spectrum rather exactly. So far, there is no condition strong enough to exclude such "pseudo-component" references which are in the similarity hit list, and which are completely covered by the unknown spectrum, even if the reference compound itself is very different from the unknown. Filter E tries to recognize and exclude the reference spectra of such pseudo-components.

Up to this stage, only two spectra, reference and unknown, were used and their peaks were handled independently, without considering which peaks belong to one component. To discover which group of peaks of the unknown must be present together in the corresponding true reference, the time behaviour of the intensities is examined by using the unknown and its 6—12 neighbouring spectra from the series. The number of spectra to be used depends on the separating ability of the technique applied for measurement. In g.c./m.s., for instance, it corresponds to the g.c. peak width, and for fractional evaporation to the respective evaporation profile.

In the case of a pure component, the intensities of all masses correlate closely, i.e., their changes across the selected spectra of the measurement are synchronous. In such a case, the spectrum of an identical reference compound must include all these correlating peaks. If a mixture is present and the components are partly resolved, there is a chance to separate groups of masses with closely correlating intensities. Namely, the time behaviour of the intensities is different for the masses of each group, indicating again that they should be present together in the spectrum of the identical reference. In any case, the respective groups of masses may be used to exclude pseudo-components.

Filter E is applied after ranking has been done according to the identity measure to be described below. It calculates the correlations between the 40 most significant peaks of the unknown and determines groups of masses with strongly correlating intensities. Reference spectra which do not contain any of the resulting groups are discarded with the exception of references from the two best matches of the similarity list as well as the identity measure. This can prevent a possible type I error, i.e., incorrect elimination of true mixture components with unique ions which are not separated at all and therefore appear in the same group. A more detailed description of the correlation method is given in the next paper [8].

Measure of identity

After the application of the filters, usually 0—25 references remain as candidates for being identical to the unknown. For these spectra, the identity measure *ID* is calculated. According to their *ID* values, the five best references are printed.

The measure of identity, *ID*, is a function of different parameters, referred to here as features. They are derived from comparison of the encoded spectra and the unreduced spectra of the unknown and reference, respectively. Some features are identical with the comparison factors in the similarity search; others correspond to the parameters computed from the quotient spectrum and there are several features which are arithmetic functions of certain combinations of these. A large number of features, about 30–40, was originally considered as possibly useful, and after a feature selection process, eight of them were included in the final identity measure, These are *VA*, *NO*, *DI*, *VA* × *NO*, *TU*, and *TR* which make use of quotient spectra and have already been explained, and $NC/(NR + 2)$ and $NC/(IR + 3)$ where *NC* is the number of peaks common to the encoded unknown and reference; *NR* is the number of encoded reference peaks not present in the encoded unknown; *IR* is the percentage of intensities in *NR* (*NC*, *NR* and *IR* are three of the comparison factors from the similarity search).

The *ID* measure was sought in the form of a linear function of the selected features. The coefficients of this function were optimized. For the optimization, empirical and pattern recognition methods [9] were used. An earlier stage of this work has already been outlined [3]. The above-mentioned 200 "unknowns" of known composition were used for training and testing.

First, an attempt was made to determine the coefficients such that the *ID* value is positive for the correct references and negative for the incorrect ones. As expected, this condition turned out to be very restrictive and could not be generally satisfied. Therefore another weaker condition was used. The aim was to establish the parameters so that for each unknown the *ID* values of the correct references were greater than those of the incorrect ones. As described earlier [3], this required a transformation on the features, which made the maximization equivalent to a binary classification problem that could be treated by pattern recognition training algorithms.

Because of the convenient input/output and the dimension of the problem (ca. 2500 data vectors of dimension between 5 and 25), a special program was written for the pattern recognition training procedure using the error correction feedback method, combined with a type of a "one at a time" optimization algorithm. An algorithm based on the TLU (threshold logical unit) method was also used. This computer program proved to be very useful. It made possible quick and objective checking and optimization with different sets of features. The optimal *ID* delivered by the algorithm ranked 96–97% of the retrieved references correctly. The reasons for failures were erroneous references, difficulties with components of low concentration, and pseudo-components with high *ID* value. Filter E could not be used for the training because the spectra series of the unknowns no longer existed.

To check the stability of the coefficients, i.e., of the optimized *ID*, a kind of analysis for sensitivity was done. Different subsets were removed from the training set of the 200 unknowns, and the program was applied to each of these sub-training sets. The coefficient vectors given by the program were

fairly different for the different subsets, and also for the same subset when different starting values of features or different algorithms were used. However, the measures of identity corresponding to the different coefficient vectors obtained by the optimization process, gave about the same performance in the correct ranking of retrieved references, indicating a relative great freedom for choosing an *ID* function. A significantly larger training set, of course, would diminish this freedom.

To establish the final *ID* for ranking, the results of training, based on the whole training set and its subsets representing different types of measurements, were used and adjusted according to practical considerations regarding the physical meaning of features and experience gained in daily applications. Pattern recognition was used here as a tool; its results were not blindly accepted and applied without any criticism or understanding. But, as mentioned, it proved to be a useful tool for gaining more insight into the data structure and hints for new ideas.

The *ID* value is normalized so that it lies between 0 and 99. Practice has shown that in the case of pure unknowns, the *ID* value is helpful in judging the identity without looking at the spectra. Mixture components can have very different *ID* values.

EXAMPLES

The IDS technique was tested mainly by its application in daily laboratory work, but also with several simulated spectra. Series of spectra of mixtures were artificially generated by adding two library spectra in different ratios to simulate partly resolved components. To simulate noise and impurities, a different, randomly selected spectrum was added to each member of the series.

In the example shown in Fig. 1, diethylphenylboroxin and trimethylsilyl-1-dodecanol were selected as the two components C1 and C2 of a mixture. The 7. spectrum of the simulated series was taken as the "unknown" U_s, which was the sum of 80% C_1, 7% C_2 and 10% of the randomly selected 2,3-dibromoindan as noise C_n. The percentages correspond to the base peak-normalized spectra. The filters A to E left 150, 55, 22, 7 and 2 spectra, respectively. The retrieved two spectra were correctly C_1 and C_2 with *ID* values of 81 and 39. When the correlation filter was omitted, 7 spectra were retrieved; C_1 was ranked first, C_2 seventh and the noise spectrum C_n second. The other four spectra were pseudo-components. The similarity-orientated SISCOM also retrieved all the three spectra, C_1 ranking first, C_2 105th and C_n 17th.

This example shows the differences between the similarity and identity-orientated searches. Both searches found both components and ranked C_1 in the first position. The similarity search filled the top of the hit list with non-identical references similar to the main component C_1, shifting the second component C_2 of low concentration to the 105th position. The identity-orientated IDS filtered out these similar but non-identical references and placed C_2 in the second position.

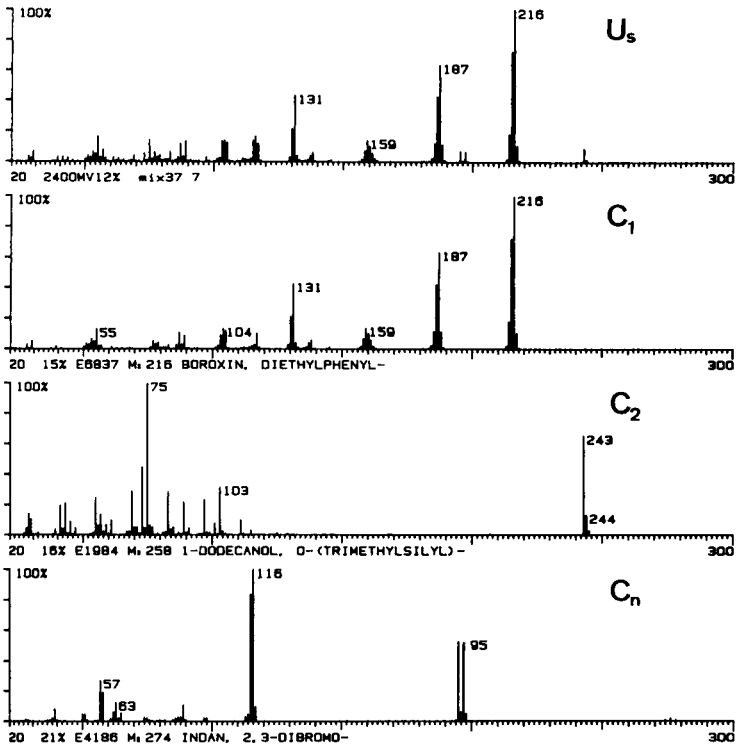

Fig. 1. Example of a 2-component mixture. U_s, simulated unknown; C_1, first component added with 80%; C_2, second component added with 7%; C_n, "noise" spectrum added with 10%. See text for detail.

The next example (Fig. 2) concerns a measured unknown with spectrum U_m. The filtering left 150, 48, 24, 7 and 2 spectra, respectively, as shown in Table 1. The IDS identified U_m correctly with R_1, giving the highest possible *ID* value 99. There was a second reference, R_2, which passed the filters, showing a type II error (i.e., R_2 is similar but not identical). Its *ID* value was only 54. Despite some remarkable differences in the spectra (e.g., at m/z 150, 164, 243) R_2 was retrieved because of the cautious filtering. Without the correlation filter E, spectrum R_p, which is a typical pseudo-component of the unknown, was ranked third with the same *ID* value as R_2. Other, structurally more similar references such as R_s were removed by other filters. Though R_s is similar, it cannot be a component of the unknown because of the high intensity at $m/z = 274$.

The similarity search also placed R_1 at the top of the hit list but the advantage of IDS is that it reduced the list of references to only two spectra. However, if R_1 had not been included in the reference library, the only candidate of IDS would have been R_2, which is false. In contrast, the similarity hit list shown in Fig. 3 is very informative even without the identical R_1,

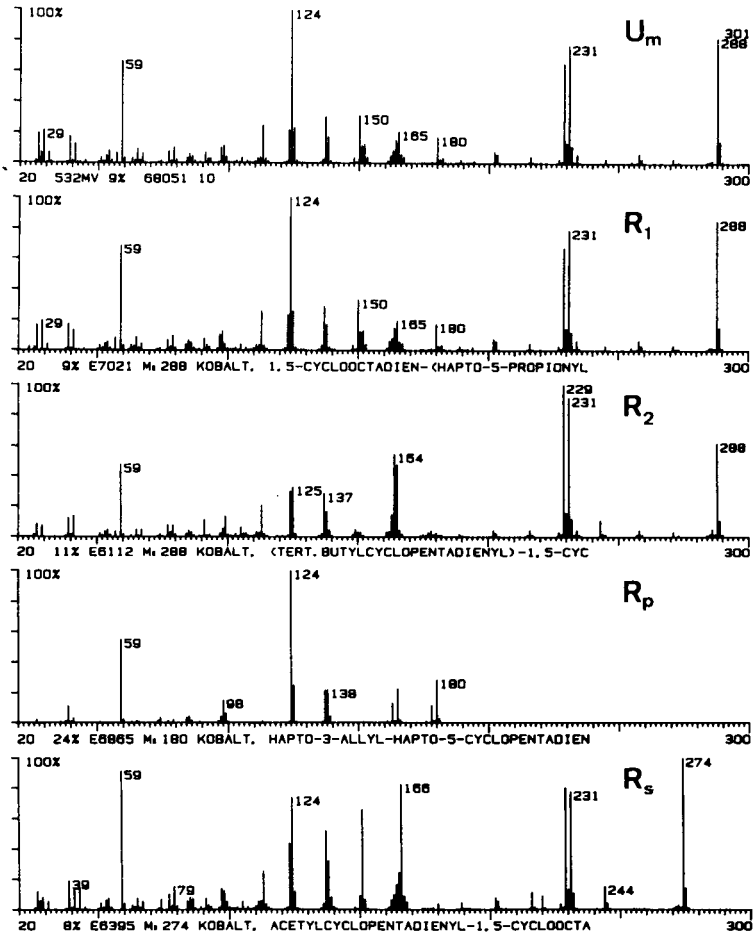

Fig. 2. Example of a measured unknown spectrum, U_m; R_1, identified reference spectrum; R_2, retrieved spectrum of a non-identical compound; R_p, spectrum of a pseudo-component; R_s, a similar but not retrieved spectrum, e.g. $m/z = 274$.

because all the references at the top contain cobalt and cyclopentadiene units, indicating a high probability for the presence of both partial structures in U_m. This example underlines the advantages of combined application of similarity- and identity-orientated searches.

For further testing, a series of 1620 spectra was used, resulting from a g.c./m.s. analysis of an artificially mixed sample of 120 typical components of wine aroma. A program which is regularly applied for the automatic selection of significant spectra from series, produced 165 spectra from the 1620 for library search and for further evaluation. From these 165 spectra, the identity of 119 could be confirmed by correlating the chromatogram and search results with knowledge about the composition of the mixture. All

TABLE 1

Output format of IDS: (a) with filter E; (b) without filter E

a. SPNUM	*SIP*	*ID*	*TU*	*TK*	*KF*	*MG*	Name
E 7021	1	99	0	0	60	288	Cobalt, 1,5-Cyclooctadien-(Hapto-5-
E 6112	2	54	27	32	29	288	Cobalt, (Tert butylcyclopentadienyl
Filters:	48	24	7	2	spectra		MU = 41
Date:	1/9/1983				** Version 2 ** 29.7.83		
Unknown:	532MV 9% 68051 10						

b. SPNUM	*SIP*	*ID*	*TU*	*TK*	*KF*	*MG*	Name
E 7021	1	99	0	0	0	288	Cobalt, 1,5-Cyclooctadien-(Hapto-5-
E 6112	2	54	27	32	0	288	Cobalt, (Tert butylcyclopentadienyl
E 6865	3	54	60	16	0	180	Cobalt, Hapto-3-allyl-hapto-5-cyclo
E 6910	6	51	74	31	0	180	Cobalt, Dicarbonyl-cyclopentadienyl
E 6309	9	47	70	23	0	180	Cobalt, Cyclopentadienyl-bis(ethyl
Filters:	48	24	7	7	spectra		MU = 41
Date:	1/9/1983				** Version 2 ** 29.7.83		
Unknown:	532MV 9% 68051 +10						

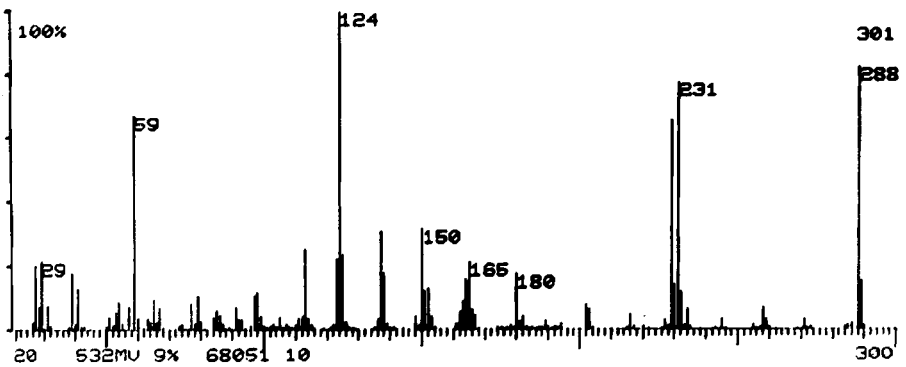


```
E 7021   0 32   0· 4 98 C16H2101CO1   12 16 KOBALT, 1,5-CYCLOOCTADIEN-(HAPT
E 6112   3 27   9·16 43 C17H25CO1      7 15 KOBALT, (TERT.BUTYLCYCLOPENTADI
E 6865   3 14   5·56 82 C9H13CO1      12 38 KOBALT, HAPTO-3-ALLYL-HAPTO-5-C
E 6395  10 22  37·33 78 C15H19O1CO1   11 17 KOBALT, ACETYLCYCLOPENTADIENYL-
E 5035   7 19  14·49  9 C13H15O1CO1    7 28 KOBALT, CYCLOPENTADIENYL-(2,7-D
E 6910   3 10   4·65 76 C7H5O2CO1     12 55 KOBALT, DICARBONYL-CYCLOPENTADI
E 6743   2 11  12·62 76 C11H13CO1     12 31 KOBALT, (1,2,3,4-.ETA.)-1,3-CYC
E 2157  10 18  26·45 12 C13H17CO1     12 23 KOBALT, 1,5-CYCLOOCTADIEN-CYCLO
E 6309   2  9   6·66 56 C9H13CO1      12 66 KOBALT, CYCLOPENTADIENYL-BIS(ET
E 3155   8 12  10·69 38 C11H16S1      12 37 SULFID, BUTYL P-TOLYL
E 6200  13 13  16·74  9 C11H18O1       9 17 5,8,10-UNDECATRIEN-3-OL
E 4428   7 11  25·62 59 C10H13CO1     12 36 KOBALT, CYCLOPENTADIENYL-1,3-PE
E 2495  18 17  35·38 24 C19H28O2       8 16 4-ANDROSTEN-17B-OL-3-ON (TESTOS
E 1258   5  9   5·73  0 C11H17P1       1 33 PHOSPHAN, BENZYL-TERT.BUTYL-
E 4934   9 11  38·62 82 C12H13CO1     12 21 KOBALT, CYCLOPENTADIENYL-NORBOR
MU· 41 E    99 66 47 45 42 29  IS· 12 7 11 8 3 5 10 13 9 1 6 T 29
 E 7021 E 6112                      ID· 99 54          S·  1  2
```

Fig. 3. Output format of the similarity search. The condensed result of IDS is in the last row.

these compounds were contained in one of the reference libraries. The corresponding spectra belonged partly to well-resolved g.c. peaks and partly to overlapping g.c. peaks. A summary of the results obtained with the similarity search and IDS on the 119 identified peaks is shown in Table 2. The performance of the filters in the 165 searches is shown in Table 3.

The average CPU time required for one search was 8 s. About 65—70% of this time was used for the similarity search with two reference libraries of altogether ca. 45 000 spectra, and the rest for IDS. Because the time-consuming treatment of the unreduced spectra in IDS is applied only to the few spectra left by filter B, the additional identity hit list requires almost negligible computing time.

To obtain a simple overview of the results, the output of the IDS was kept as short as possible. A condensed result from IDS appears as one line added to the normal output of the similarity search. This last line (see Fig. 3) contains the library numbers, the *ID* values and the positions in the similarity hit list of the (at most five) best references retrieved by IDS. If necessary, a more detailed IDS list can be obtained, as in Table 1, which contains the five best references along with the reference having the smallest *TU* value if it is not already present among the first five. For each reference are given the library

TABLE 2

The positions of identical references[a]

Position	Similarity	IDS
1	88 (7)	101 (11)
2	13 (0)	4 (2)
3—5	9 (5)	8 (5)
6—10	2 (1)	1
16—30	4 (2)	—
31—150	3 (3)	—
not found	—	5

[a]The number of cases representing mixture components given in parentheses.

TABLE 3

Performance of the filters

Filter	A	B	C	D	E
Number of spectra	24750	10104	6300	2617	1406
% of spectra	100	41	25	11	6
Number of spectra left by the last filter		in cases			
0—3		40			
4—10		78			
11—20		38			
21—30		9			
Average no. of spectra left by the last filter:		8.5			

number, position in similarity ranking *SIP*, *ID* and *TU*. Items *TK* and *KF* in Table 1 are temporary output during a phase of development (*TK* is a value combined from *TU* and *TR*, and *KF* characterizes the number and size of correlation groups present in the reference). Molecular weight and chemical name (limited to 27 characters) are also given for each reference as well as the number of spectra left by filters B—E, the date and an identification text for the unknown.

Currently promising experiments are in progress to find groups of similar compounds among the candidates of the *ID* hit list and to include only the most probable one of each group in the printed list. This aims at favouring less dominant components which otherwise may be cut off by the limitation to five members.

DISCUSSION

Experience obtained during several months of application of IDS can be summarized as follows. If the unknown is a pure compound and an identical reference compound is present, then in almost all cases it appears at the top of the output list, indicating correct identification. Generally, the number of retrieved references is not greater than 5—8, because of effective filtering. Secondly, if the unknown is pure but an identical reference compound is not present, then frequently no reference is retrieved, all the similar but non-identical references being filtered out, which is the ideal case for an identity-orientated system. Otherwise, some similar compounds appear in the list (type II error). A low *ID* value of those references might indicate their non-identity. Finally, if the unknown is a mixture then one of its components is almost always retrieved, and quite often also further components of significant concentration. Quite generally, type I errors tend to be very low, 2—3%, in contrast to type II error. This means that ca. 90% of the searches also produce one or more non-identical (but similar) references in the list, though these are mostly not at the top and often have considerably lower *ID* values. This error could be diminished by tighter filtering, but then the undesirable type I error would be increased, i.e., the power of hypothesis testing is not high enough. There are cases in which IDS fails because of a type I error; these are caused by very poor references or by mixture components of low concentration, or by mixtures with unfavorably overlapping component spectra.

Although both the similarity search and IDS frequently rank an identical reference in the first place, IDS offers some advantages: (1) the shorter output list, often only 1—3 references, facilitates the final assessment; (2) there is better identification of mixture components, especially of the second or third components; (3) the absolute value of *ID* can be used to guess the probability of having retrieved references or not. The disadvantages of IDS are: (i) its results are necessarily disturbing if there are no identical references in the library unless the filters exclude all references; (ii) it has great sensitivity

to erroneous spectra. Accordingly, the most advantageous method is a combined evaluation of the results given by the two types of searches.

Data bases and programs

As in development and routine work with SISCOM, four larger mass spectra collections were used as reference libraries, labelled E, C, L and U. The collections are: E, in-house library of ca. 6000 spectra; C, EPA/NIH Mass Spectral Data Base of ca. 38800 spectra; L, Atlas of Mass Spectral Data, ca. 41400 spectra; U, in-house library of ca. 4000 significant but uncertified spectra which are not identified in every detail and/or may be contaminated.

The programs were written in Fortran and run on the VAX11/780 computer system [10] of the Institute. IDS is being made a part of SISCOM, which in turn is a part of the MARS program system, which incorporates all operations used for the evaluation of mass spectra.

The authors thank H. Damen, W. Joppek, W. Schmöller and E. Ziegler for helpful discussions and critical comments.

REFERENCES

1 D. Henneberg, in A. Quayle (Ed.), Advances in Mass Spectrometry, Vol. 8B, Heyden, London, p.1511.
2 H. Damen, D. Henneberg and B. Weimann, Anal. Chim. Acta, 103 (1978) 289.
3 L. Domokos, D. Henneberg and B. Weimann, Anal. Chim. Acta, 150 (1983) 37.
4 D. D. Speck, R. Vankataraghavan and F. W. McLafferty, Org. Mass Spectrom., 13 (1978) 209.
5 G. W. Milne, W. L. Budde, S. R. Heller, D. P. Martinsen and R. G. Oldham, Org. Mass Spectrom., 11 (1982) 547.
6 J. R. Green and D. Margerison, Statistical Treatment of Experimental Data, Elsevier, Amsterdam, 1978.
7 D. Henneberg and B. Weimann, 31st Annual Conference on Mass Spectrometry and Allied Topics, 1983, Boston, MA, p. 185.
8 L. Domokos and D. Henneberg, Anal. Chim. Acta, 165 (1984) 75.
9 K. Varmuza, Pattern Recognition in Chemistry, Springer Verlag, Berlin, 1980.
10 E. Ziegler, Anal. Chim. Acta, 147 (1983) 77.

Analytica Chimica Acta, 165 (1984) 75—86
Elsevier Science Publishers B.V., Amsterdam — Printed in The Netherlands

A CORRELATION METHOD IN LIBRARY SEARCH

L. DOMOKOS*,[a] and D. HENNEBERG
Max-Planck Institut für Kohlenforschung, Mülheim/Ruhr (Federal Republic of Germany)
(Received 23rd January 1984)

SUMMARY

The identification of unknown pure compounds or mixtures by means of mass spectral library search can be improved by partly resolving the spectra of the individual components within the spectrum of the measured unknown. This is accomplished by investigating sequential spectra in series of spectra; masses with highly correlating sequential intensities are clustered into individual groups. On the assumption that correlated masses belong to the same component spectrum, a filtering algorithm is developed to exclude spectra of non-identical compounds. The basic ideas, methods, examples and experiences gained with applications are reported.

A regular problem in analytical laboratories is to identify the components of a mixture on the basis of measured data, e.g., spectra, that in fact comprise the superposed data of the single components and of noise. This happens in chromatography and in many types of spectroscopy. Library search techniques are of growing importance in solving this problem. This paper is concerned with mass spectral library search, but the methodology is applicable to other types of library searches. In general, the spectrum of the unknown substance is compared with the spectra of the reference library and a hit list of references is presented containing those references which are probably identical or which are in some respect similar to the unknown. This hit list is used to make the final assessment. Depending on the spectral features and on the measure of similarity applied in the comparison, there are many search systems. One of the mass spectral search systems is SISCOM [1], which searches first for similar references and is followed by a secondary identity-orientated search which tries to reduce the retrieved list of references most similar to the unknown to the identical references [2, 3].

The components of an unknown mixture can be identified by library search in two basically different ways. In one, the unknown spectrum is decomposed to its component spectra which are then identified separately with or without library search; in the other, a library search which is efficient in identifying the components of a mixture without previously decomposing it,

---

[a]Permanent address: Institute for General and Analytical Chemistry, Technical University Budapest, Gellért-tér 4, H-1521 Budapest, Hungary.

0003-2670/84/$03.00

is applied directly. The first way seems to be very reasonable but the existing algorithms for spectrum decomposition are limited. The best ones are several recently developed approaches based on factor analysis or related methods like principal components analysis [4, 5]. They have the advantage that they do not require a priori knowledge either about the number of components or about the mathematical form of the spectra. The disadvantage of this is that they use not only one but more spectra belonging to the same components mixed in different ratios, as in spectra of g.c./m.s. series. Difficulties arise with these methods if the number of components is erroneously estimated by the algorithm, or if the spectra of the components change within the several spectra that are used because of increasing or falling of relative concentration along a g.c. peak resulting in differently tilted spectra; or if, because of bad separation, the ratio of the concentrations of the components does not change with the spectra; or if the number of components exceeds 2 or 3; or if there are not enough spectra.

A major objection to uncontrolled routine preliminary decomposition is that some numerical results are always produced even if the premises are not satisfactorily fulfilled (e.g., number of components, unchanging component spectra, impurities, etc.), and these probably unreliable data must be used in the further steps. An erroneous decomposition, not rare in practice, can lead to a completely misleading identification with library search.

In direct application of a library search to an unknown, a search algorithm is needed to retrieve those reference spectra which correspond to the pure unknown or to its components in mixtures. The reference spectra to be retrieved must then be either very similar to the whole unknown spectrum (for a pure unknown) or to part of the unknown (for a mixed unknown). Mathematically, the only condition imposed is that the retrieved references should be a part of the unknown. The search thus corresponds to a search technique, where references having significant peaks not present in the unknown are discarded. References remaining after this selection are ranked according to some measure based on the intensities common to both referene and unknown spectra. Unfortunately, there are usually a great number of references that satisfy the condition of being part of the unknown spectrum without the corresponding reference substance actually being a component of the unknown mixture. Such undesirable references are called pseudo-components.

METHOD

In this paper, a correlation method is described that was developed to help to overcome the above-mentioned difficulties in the identification of components of a mixture by a library search. The correlation method was developed, tested and applied in mass spectral library searches. It helps to recognize and exclude the unwanted pseudo-components. In contrast to the unreliable decomposition algorithms, the correlation method does not try to

establish the number of components or to decompose the whole spectrum; rather, it tries to give some firm assessment, if possible, of the relation of peaks in the spectrum. In practice, the unknown spectrum is taken very often from a series of spectra, e.g., measured with fractional evaporation or g.c./m.s.; the use of several successive spectra of the series can provide additional information on behaviour with time. Information such as which subset of peaks must be present together or which peaks must not occur together in a component spectrum, can be very helpful in recognizing irrelevant reference spectra. Such information cannot be obtained from a single unknown spectrum, but is available by using several spectra of a series if the mixture components are partly separated. The aim of the correlation method is to discover such relationships by trying to determine which mass intensities are running together in the spectra adjacent to the unknown spectrum. The correlation method computes the correlation between the intensities of significant peaks at different *m/z* values along several spectra of the series. In this aspect, it resembles factor analysis or principal components analysis, which also investigate more than one spectrum and the correlation or covariance matrix. On the basis of these correlations, the correlation method clusters the masses, if possible, into groups of highly correlated mass intensities. Intensities clustered in the same group are considered to belong to the same component. Negatively correlated groups of masses indicate mixtures. It is important to emphasize here that the philosophy of this correlation method is to grasp only firm relationships and not force the use of dubious information. A result is used only if significantly correlated large groups are found.

The algorithm for the correlation method is as follows

(1) From the mass spectrum S of the unknown, peaks having more than 3% relative intensity are selected. If there are more than 40 peaks above this threshold, then the 40 most intense ones are taken. Included are 2 or 3 peaks from the highest *m/z* (later referred to simply as "mass") range, even if they are of lower intensity.

(2) The corresponding intensities of the selected masses in a window of ± 6 spectra around S of the spectrum series are taken (in cases of rapidly changing spectra series, only ± 3 neighbouring spectra are used). Thus, for each of the selected ca. 40 masses, a vector of 13 (or 7) intensities is taken from the 13 spectra. If S is near the beginning or the end of the spectrum series, then less than 6 spectra are taken, so that the vectors are less than 13-dimensional; however, a lower limit is 5, if it is less than 5, the algorithm ends.

(3) The correlation matrix of the intensity vectors is computed.

(4) A clustering algorithm sets up groups of highly correlated masses. A combination of the agglomerative clustering algorithms known as single-linkage and complete-linkage methods [6, 7] are used. At the start, each mass is a group itself. The "greatest similarity" of two different groups is defined as the highest correlation between the intensity vectors of these groups, and the "smallest similarity" is defined as the lowest correlation between their

intensity vectors. Both similarity values lie between −1 and 1. At each step, two different groups having the highest "greatest similarity" are merged if this value is at least 0.97 and the "smallest similarity" of the groups is not less than 0.94. If the size of one of the two groups is greater than 10, then both thresholds will be set higher to 0.98. Thus large groups must contain very strongly correlated masses. After two groups have been merged, the "smallest" and "greatest" similarities between the groups are updated and the merging process continues until no further merging is possible. Finally, a secondary merging of groups is possible after the matching with the reference spectra has been evaluated (see below).

(5) The "smallest" and "greatest" similarities between the different groups are stored for further use.

(6) Matching with the reference spectra, and the exclusion of the irrelevant references are the final steps.

The basic idea for the application of this correlation method is that masses belonging to the same group are considered to belong to the same component. Conversely, of course, it is not necessarily true that masses belonging to different groups do not belong to different compounds. However, if these groups are very poorly or negatively correlated, then they usually really belong to different components. Masses of a strongly correlated group are considered to be unique for a component, or overlapped only with another component of very low concentration. Difficulties arise, leading to false interpretation, if the concentration ratio of two different components is about the same along the selected 13 spectra, i.e. if the components are not separated enough by g.c. or by the evaporation. In this case, non-unique masses from different components can be clustered in the same group, which makes the identification of S more troublesome or erroneous. In general, overlapping masses of different components produce small groups or are not included in any of the groups.

The exclusion of irrelevant references is based on the correlation groups. Three conditions are used: (a) the masses of at least one group must be contained in the reference spectrum; (b) if 3 masses of a group are contained in a reference, then the whole group must be contained; (c) a reference spectrum must not contain significant peaks belonging to different groups that are very negatively correlated. With large groups, of at least 8 masses, some tolerance is allowed in the above conditions.

In the presence of small groups condition (a) is easily met. Therefore, to enhance the filtering capability of the correlation method, a secondary merging of the groups is done. Small groups of only 2 or 3 masses are merged with larger ones if three conditions are satisfied: (i) the larger group has at least five masses; (ii) the "smallest similarity" between the small and large groups is above 0.8; (iii) there is at least one retrieved reference which contains all masses of both groups.

If only small groups of 2—3 masses, or only a few of the selected ca. 40 masses are included in one of the groups, then the correlation method does

not impose any condition on the search, but remains inactive. However, if there are bigger groups of five or more masses, then the correlation method can result in a very effective filtering of pseudo-components or in recognition of mixture components. The fact that one or more groups of masses are completely included in a reference, can be used for building up an effective matching criterion as well.

EXAMPLES

Three examples are given to demonstrate the use of the correlation method in mass spectral library search. The correlation method was tested with several simulated mixtures, and with a large number of real measurements.

Simulated series of spectra from two-component mixtures were constructed by adding two spectra in different ratios. Additional noise (impurities) was generated by adding to each spectrum of the series a third randomly selected spectrum. This "noise" spectrum is different for each member of the series. In the examples below, the noise spectra were added to a level of 10%. A spectrum series consisted of 32 spectra. Several spectra were selected from the series and were taken as "unknown" spectra for the SISCOM identity search algorithm [2, 3] with the correlation method as a filter to exclude the pseudo-components.

Example 1

Figure 1 shows the tenth spectrum, denoted by **S1**, of a simulated series, where the first component **C1** is diethylphenylboroxin, the second component **C2** is ethylphenylboroxin; **S1** is the sum of 100% **C1**, 30% **C2** and 10% of the noise spectrum **N1**. The percentages given refer to the base-peak normalized spectra. Spectrum **S1** was taken as the "unknown" for the library search. The selected significant masses and their clustering into highly correlated groups are shown in Table 1(a). Table 1(b) gives the similarity values, i.e., correlations, (multiplied by 100) between the six groups. The first value is the "smallest similarity", and the second one is the "greatest similarity" between the two corresponding groups. The fact that the two significant groups 5 and 6 are negatively correlated indicates that the unknown is a mixture of at least two components, and that the masses of these groups are characteristic of these components. The four small groups (1—4) with only two masses consist of overlapping masses or of the masses of noise.

The search algorithm used [3] for identifying **S1** produced only six library spectra as candidates for being a component of the mixture. The library code numbers of the six references and the numbers of masses of the groups not present (or only at negligible intensity) in the references are listed in Table 1(c).

According to Table 1(b, c), the conditions for merging small groups with larger ones are met, thus groups 1, 2, and 3 can be merged with groups 5 and 6, respectively. This leads to exclusion of reference E1231. The last column

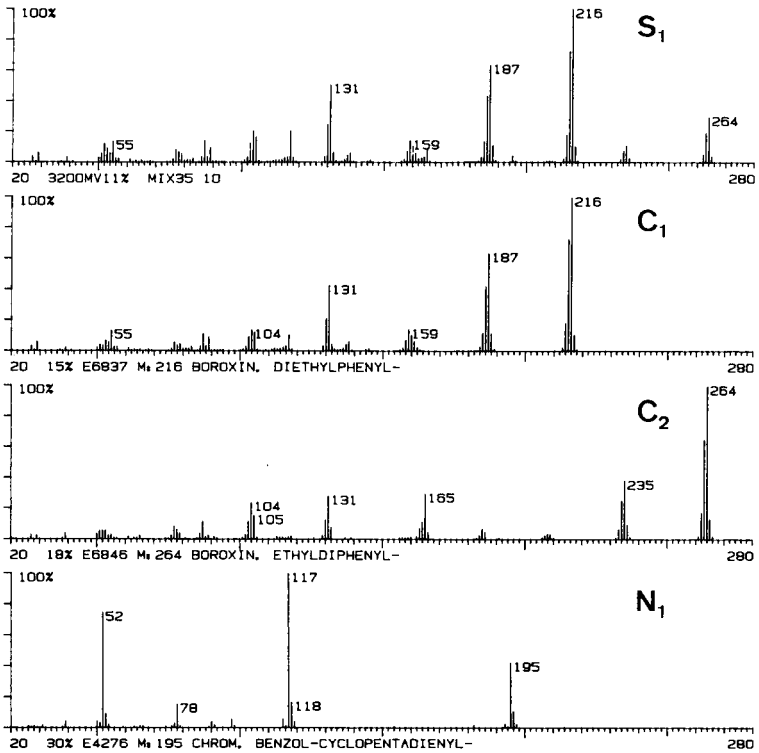

Fig. 1. Example of library search. S_1, simulated unknown; C_1, first component added with 100%; C_2, second component added with 30%; N_1, "noise" spectrum added with 10%. For details, see text.

of Table 1(c) contains the minimum number of masses not present in any of the groups, except for the small merged groups, in this example in groups 4, 5 and 6. If this minimum value is larger than zero, then according to condition (a), the corresponding reference will be excluded from the final ranking of references. In order to avoid false exclusion, the threshold for the minimum number of missing masses can be larger than zero in the case of large groups, of at least eight masses. For the same reason, references having the highest matching value are not excluded either, but only marked in the output list of the library search. In this example, only the two correct references **C1** and **C2** are left. The fact that **C1** coincides with group 7, and **C2** with group 8, indicates that they relate to two different components of the unknown. Though not all the incorrect references can be excluded with this correlation method of filtering, the number of masses of groups completely present in the references can be used successfully as a parameter for the ranking function.

When 30% noise spectra were added instead of 10%, the result was about the same, only the two correct references being kept. However, the clustering

TABLE 1

Data treatment for the example shown in Fig. 1

(a) Significant masses and their clustering

Group	Sum of intensities	Masses
1	1266	29, 54
2	2493	55, 160
3	3532	87, 104
4	3885	130, 185
5	31956	137, 138, 186, 187, 214, 215, 216, 217
6	8674	165, 234, 235, 262, 263, 264, 265
In no group		51, 52, 77, 78, 79, 89, 103, 105, 117 131, 132, 158, 159, 161, 188

(b) Matrix of smallest and greatest similarities

Group	1	2	3	4	5	6
1	97 97					
2	86 96	97 97				
3	69 86	37 64	98 98			
4	93 97	74 86	86 94	98 98		
5	81 94	92 97	24 65	67 85	95 99	
6	41 50	5 20	86 94	64 97	−9 10	99 100

(c) Number of masses not present in the references

Ref. spectra	Group						
	1	2	3	4	5	6	Minimum
E1231	0	2	1	2	8	7	2
E6837 * C1	0	0	0	0	0	7	0
E1616	2	2	1	2	8	7	2
E6846 * C2	0	0	1	0	7	0	0
E5139	2	2	1	2	8	7	2
E5887	2	2	2	1	6	7	1

was somewhat different. Instead of six, there were only four groups of masses 54, 130; 87, 104; 186, 187, 214, 215, 216, 217; and 165, 234, 235, 262, 263, 264, 265. The lowest correlation between groups 3 and 4 was 28. The search retrieved only five instead of six reference spectra.

Example 2

In general, the correlation method does not produce such straightforward filtering as in the above example, which gave only the correct references. However, as the next example shows, even with less performance in filtering, the correlation method can be helpful.

For the two components, *cis*-stilbene (spectrum K1), and ethyldiphenylboroxin (spectrum K2) were selected (Fig. 2). Spectrum 18, denoted by S2,

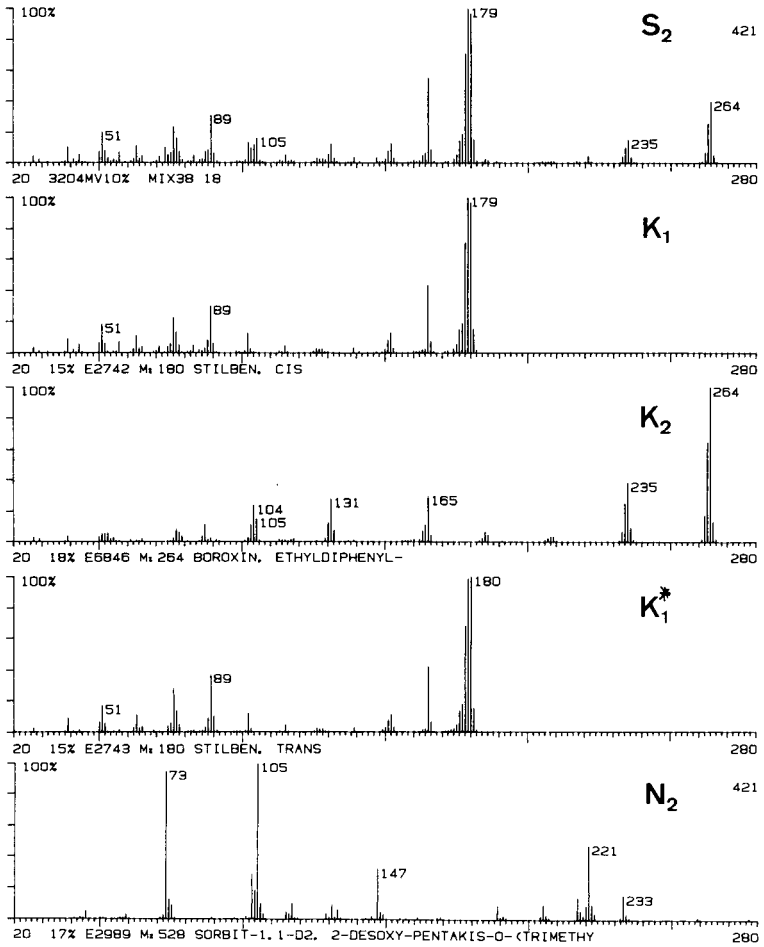

Fig. 2. Example of library search. S_2, simulated unknown; K_1, first component added with 40%; K_2, second component added with 100%; K_1^*, similar to the first component; N_2, noise spectra added with 10%. For details, see text.

was considered as the "unknown", which is the sum of 40% K2, 100% K1 and 10% "noise" spectrum, N2. The selected masses and their clustering, the correlation matrix, and the number of missing masses in the retrieved 20 references are listed in Table 2.

The strong negative correlations between the two large groups 1 and 3 in Table 2(b) indicate the presence of at least two components. The search program retrieved twenty reference spectra. Groups 1 and 2 were merged. On using the correlation method filtering, eight of them were left. The final matching ranked K1 first and K2 seventh; without the correlation method, K2 were ranked tenth. Moreover, K2 was the only spectrum among the retrieved twenty references that contained all masses of group 3, suggesting

TABLE 2

Data treatment for the example shown in Fig. 2

(a) Significant masses and their clustering

Group	Sum of intensities	Masses
1	39329	57, 63, 76, 89, 90, 152, 176, 177, 178, 179, 180
2	2190	88, 102
3	14468	103, 104, 130, 131, 164, 234, 235, 262, 263, 264
4	6393	165, 166
In no group		39, 50, 51, 52, 73, 75, 77, 78, 87, 105, 151, 181

(b) Matrix of smallest and greatest similarities

Group	1	2	3	4
1	96 99			
2	94 98	99 99		
3	−62−36	−44−23	98 99	
4	45 73	63 82	23 51	98 98

(c) Number of masses not present in the references

Ref. spectra	Group				Minimum
	1	2	3	4	
E933	1	1	8	0	0
E1428	1	1	8	0	0
E1706	4	2	9	1	1
E2742 * **K1**	0	0	8	0	0
E2743 **K1**	0	0	8	0	0
E3310	1	1	8	0	0
E2681	9	2	10	2	2
E4304	1	1	9	0	0
E6237	10	2	10	2	2
E6846 * **K2**	11	0	0	0	0
E2908	9	2	8	2	2
E2763	7	2	8	2	2
E3050	6	2	10	2	2
E3363	1	1	9	0	0
E5235	3	1	9	0	0
E1922	3	1	10	2	2
E1962	2	1	10	2	2
E2765	3	0	10	2	2
E5262	3	1	7	2	2
E5762	3	1	10	1	1

that it was the only candidate for the second component. This recognition can be useful for interpretation; the ranking could not place it higher because of the presence of several spectra very similar to **K1**, e.g., **K1*** in the second place. Other references placed before **K2** contained only the small group 4 completely. As it was possible to merge groups 4 and 1, then only the three references **K1**, **K1*** and **K2** were left.

Example 3

This example comes from a measured series of spectra. The 23. spectrum of the series, denoted by S3, was taken as unknown (Fig. 3). The groups of masses, their correlation and the number of missing masses with the retrieved eleven references are shown in Table 3. Because of the low correlations

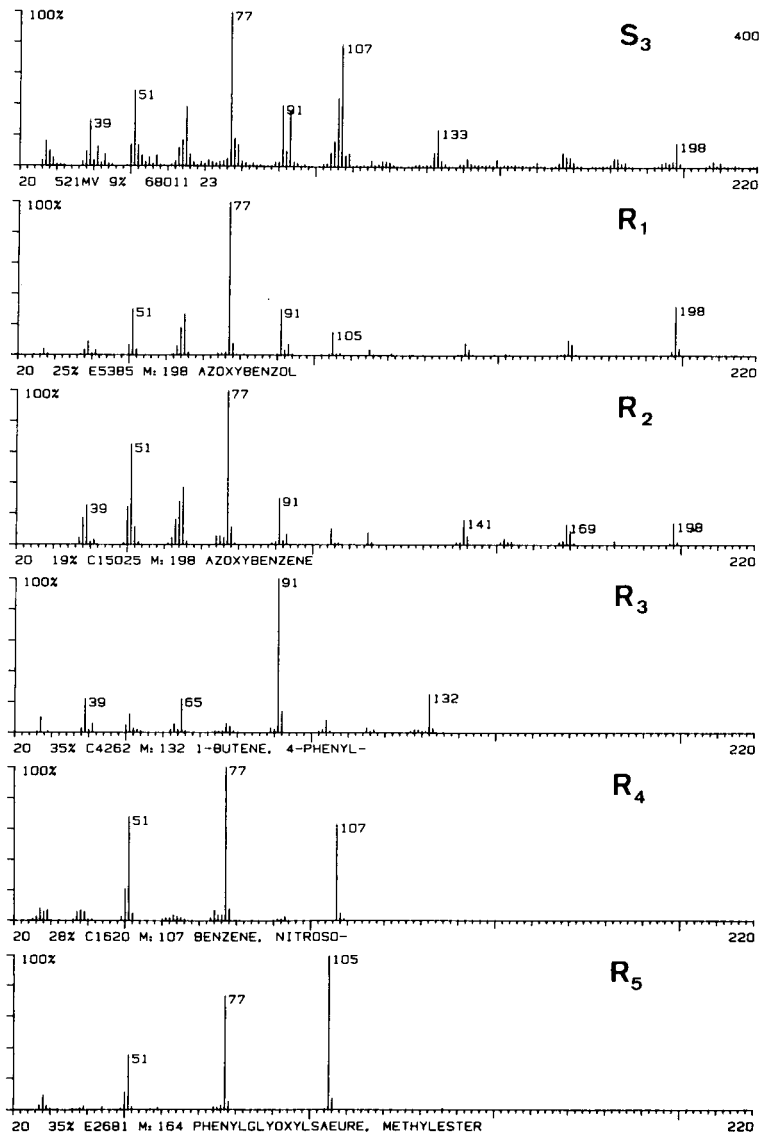

Fig. 3. Example of library search. S_3, measured unknown; R_1, R_2, correctly retrieved references; R_3, R_4, R_5, pseudo-components excluded by the correlation method. For details, see text.

TABLE 3

Data treatment for the example shown in Fig. 3

(a) Significant masses and their clustering

Group	Sum of intensities	Masses
1	2212	38, 63
2	3232	43, 57, 269, 270
3	28139	50, 51, 64, 65, 77, 91, 169, 198
4	3883	53, 79, 226
5	1932	104, 132
6	13966	106, 107, 108, 240
7	2761	133, 399
In no group		39, 41, 52, 66, 78, 92, 93, 105, 109, 167, 168

(b) Matrix of smallest and greatest similarities

Group	1	2	3	4	5	6	7
1	97 97						
2	13 23	94 99					
3	86 98	−19 10	95 99				
4	−50−18	28 49	−70−37	96 99			
5	−84−73	−10 −3	−84−75	32 55	99 99		
6	−60−37	−2 26	−74−52	84 98	43 56	97 99	
7	−79−73	−29−22	−75−63	1 21	91 96	17 26	99 99

(c) Number of masses not present in the references

Ref. spectra	Group							Minimum
	1	2	3	4	5	6	7	
C5385 * R1	0	4	0	3	1	4	2	0
C2681	1	4	5	3	2	3	2	2
C2195	0	4	5	2	1	3	2	1
C20370	0	3	3	1	1	1	2	1
C1601	0	4	5	2	1	3	2	1
C15025 * R2	0	4	0	2	2	4	2	0
C1620 R4	0	4	4	3	2	2	2	2
C4262 R3	0	4	4	2	0	4	2	0
C15023	0	3	1	3	2	4	2	1
C6865	1	3	5	3	2	3	2	2
C9676	1	4	5	3	2	3	2	2

between several groups, S3 must be a mixture. Groups 1 and 3, 4 and 6, and 5 and 7 might belong together. According to Table 3(b, c), groups 1 and 3 can be merged. Therefore, as the last column in Table 3(c) shows, eight of the eleven references can be excluded. From the remaining three references, R3 can be also removed, because of condition (b), i.e., R3 contains six masses (50, 51, 64, 65, 77 and 91) of the eight masses in group 3. But group 3 is a strongly correlated group, indicating that its masses are characteristic of one

of the components, and not overlapped. Thus a correct reference cannot contain only six masses of that group. The two references **R1** and **R2** left by the correlation filtering represent the same compound with spectra from two different data bases. Both are correct for one of the components. The other component or components were not found by the search. However, it can be seen that characteristic, not overlapped, masses of further components are in groups 4—7. Without the use of the correlation method, reference **R4** was ranked first, because of its good agreement with masses 50, 51, 77, 107, which is due to the identical substructure in **S3** and **R4**. Anything other than the correlation filtering used in the identity search could not exclude the pseudo-component **R4** from the list of the possible components of mixture **S3**.

DISCUSSION

The correlation method has been applied for several months with the above-mentioned SISCOM mass spectral search system in the secondary identity-orientated search developed for the exact identification of pure compounds or mixtures [2, 3]. The correlation method helps to recognize and exclude those incorrect references which are only pseudo-components of the unknown *S*, which means that the reference spectrum is part of *S*, but the corresponding reference compound is not a component of the unknown.

Experience with applications has shown that the correlation method is very effective in some cases but gives little benefit in other cases. In general, it reduces the list of reference spectra retrieved for final ranking by 50—60%. A very important point is that only rarely does it give a false result, i.e., no correct references are filtered out. Another advantage is its simplicity. The correlation method gives a lot of additional information, and the main problem is how to use it reliably in the algorithm.

Data bases and programs

Three large mass spectra collections were used as reference libraries: E, an in-house library of ca. 6000 spectra; C, EPA/NIH Mass Spectral Data Base of ca. 38800 spectra; L, Atlas of Mass Spectral Data, ca. 41400 spectra with duplicates.

The programs were written in Fortran and run on the VAX11/780 computer system [8] of the Institute.

The authors thank H. Damen, W. Joppek, W. Schmöller, B. Weimann and E. Ziegler for helpful discussions and critical comments.

REFERENCES

1 H. Damen, D. Henneberg and B. Weimann, Anal. Chim. Acta, 103 (1978) **289**.
2 L. Domokos, D. Henneberg and B. Weimann, Anal. Chim. Acta, 150 (**1983**) **37**.
3 L. Domokos, D. Henneberg and B. Weimann, Anal. Chim. Acta, 165 (**1984**) **61**.
4 W. H. Lawton and E. A. Sylvestre, Technometrics, 13 (1971) 617.
5 Jie-Hsung Chen and Lian-Pin Hwang, Anal. Chim. Acta, 133 (1981) 271.
6 K. Varmuza, Pattern Recognition in Chemistry, Springer-Verlag, Berlin, **1980**.
7 D. L. Massart and L. Kaufmann, The Interpretation of Analytical Chemical Data by the Use of Cluster Analysis, Wiley, New York, 1983.
8 E. Ziegler, Anal. Chim. Acta, 147 (1983) 77.

Analytica Chimica Acta, 165 (1984) 87—96
Elsevier Science Publishers B.V., Amsterdam — Printed in The Netherlands

SPECTRAL INTERFERENCES AND BACKGROUND OVERCOMPENSATION IN ZEEMAN-CORRECTED ATOMIC ABSORPTION SPECTROMETRY
Part 1. The Effect of Iron on 30 Elements and 49 Element Lines

G. WIBETOE* and F. J. LANGMYHR

Department of Chemistry, University of Oslo, P.O. Box 1033, Blindern, 0315 Oslo 3 (Norway)

(Received 4th June 1984)

SUMMARY

The background compensation performance of a Zeeman corrector with the magnetic field acting on the graphite atomization cell was assessed for 30 elements and 49 element lines in an iron matrix. Two of the elements studied, gallium and zinc, are influenced by background overcompensation which introduces serious negative systematic errors. The overcompensation is due to the presence of iron lines close to the 287.4-nm gallium line and the 213.9-nm zinc line; when the magnetic field is on, the σ-components of the adjacent iron lines overlap at the position of the analyte line and a background, which is not present when the magnetic field is off, is recorded. When gallium and zinc are measured under the same conditions but with deuterium arc background correction, the adjacent iron lines cause positive systematic errors. These spectral interferences for gallium in the presence of iron can be avoided by doing the measurements at the 294.4-nm gallium line; the two lines have about the same sensitivity. When zinc is to be measured at the 213.9-nm line, with either type of background correction, the spectral interferences from iron can be avoided by careful selection of the graphite-furnace parameters. In addition to spectral interferences, iron also affects the sensitivity for both gallium and zinc.

Compared to the conventional continuum-source background correctors used in atomic absorption spectrometry (a.a.s.), the Zeeman system of background correction offers definite advantages [1—7]. According to Fernandez and Giddings [6], two types of spectral interferences are encountered when continuum-source correctors are employed. First, when absorbing lines of a matrix element are situated so close to the analyte emission line that they fall within the spectral bandwidth of the optical system, these lines absorb radiation from the continuum source but not from the analyte source, and the absorption signal is overcorrected. In the second type, when broad-band background signals have fine structures, the background measured by the continuum source may be different from the background measured by the analyte radiation source, resulting in an inaccurate background correction. These types of interferences are avoided with most Zeeman instruments which measure the background exactly at or very close to the analyte emission line.

0003-2670/84/$03.00

Fernandez and Beaty [7] stated that Zeeman effect background correction is virtually free of any spectral interference problems. As shown previously by Stephens and Murphy [13] for a Zeeman source-modulated spectrometer, and as demonstrated here for an atomizer-modulated instrument, spectral interferences do occur in Zeeman background-correction systems.

There are several possible design approaches for Zeeman-effect a.a.s. The present paper reports on experiences with the Perkin-Elmer (P-E) model 5000/Zeeman instrument. This equipment has a transverse alternating current magnetic field across the atomization cell and a fixed linear polarizer. The instrument measures the analyte and background absorption when the field is off, and the background alone when the field is on. During the latter operation the polarizer removes the π-components and lets the σ-components pass.

When a complex material is heated in an atomization cell, many different atoms are formed, resulting in a complex absorption spectrum. The strong magnetic field applied to the atom vapour ($\approx$8 kgauss) splits the absorption lines into a very large number of π- and σ-components. According to the Perkin-Elmer literature, in a magnetic field of 8 kgauss, a normal Zeeman splitting moves the σ-components approximately 0.01 nm apart from the position of the fixed π-component. From this, it may be assumed that matrix atoms having an absorption line about $\pm$0.01 nm or closer from the analyte line may cause a background overcompensation effect because of overlap of one of the σ-components from the matrix element with the emission line from the analyte source lamp. Depending on the volatility of the analyte element compared to that of the interfering element, this spectral interference will be demonstrated by a reduced absorption signal or a negative signal appearing before or after the analyte absorption signal.

It was considered of interest to study the occurrence of this type of spectral interference with the present type of Zeeman instrumentation, and iron was selected as the possible interfering element. In addition to exhibiting an extremely line-rich spectrum, iron is a very common major or minor element in many types of materials in which trace elements have to be determined. A preliminary search through some wavelength tables [8—10] showed that several elements have resonance lines $\leqslant$0.01 nm apart from adjacent iron lines. As these tables did not give a complete list of lines, it was decided to investigate all the elements listed in Table 1 (see below).

EXPERIMENTAL

Instruments and apparatus

Two spectrometer/furnace systems were used. For measurements with Zeeman-effect background correction, a P-E model 5000/Zeeman atomic absorption spectrometer was used with a HGA-400 graphite furnace. Time-resolved absorbance data were collected and displayed with the P-E Data System 10 and the P-E 660 Printer, respectively.

TABLE 1

Elements tested for background overcompensation effect with a 0.1% iron solution (the furnace parameters are given in Table 2, except where mentioned, hollow-cathode lamps were used)

Element	Wavelength (nm)	Slit width (nm)	Element	Wavelength (nm)	Slit width (nm)
Ag	328.1	0.7	In	303.9	0.7
	338.3	0.7	Mg	285.2	0.7
Al	309.3	0.7	Mn	279.5	0.2
	237.3	0.2		279.8	0.2
As[a]	193.7	0.7	Mo	313.3	0.7
	189.0	0.7	Ni	232.0	0.2
	197.2	0.7	P[a]	213.6	0.2
Au	242.8	0.7		214.9	0.2
	267.6	0.7	Pb	283.3	0.7
B	249.7	0.7	Pt	265.9	0.7
	249.8	0.7	Sb[a]	217.6	0.2
Bi	222.8	0.2		206.8	0.2
	223.1	0.2		231.2	0.2
	306.8	0.7	Se[a]	196.0	2.0
Cd[a]	228.8	0.7		204.0	0.7
Co	240.7	0.2	Si	251.6	0.2
Cr	357.9	0.7	Sn[a]	286.3	0.7
Cu	324.8	0.7		224.6	0.2
	327.4	0.7		235.5	0.7
Ga	287.4	0.7	Te[a]	214.3	0.2
	294.4	0.7	Ti	365.3	0.2
Ge[a]	265.1	0.2	Tl	276.8	0.7
	259.2	0.2	V	318.4	0.7
	271.0	0.2	Zn	213.9	0.7
Hg	253.7	0.7			

[a]Electrodeless discharge lamp used.

The measurements with a continuum-source background corrector were made with the P-E 5000 spectrometer equipped with a deuterium background-corrector lamp, a P-E HGA-500 graphite furnace and a P-E AS-40 automatic sampler. The absorbance data were collected and displayed with the P-E 3600 Data Station and the P-E PR-100 Printer.

The graphite tubes were of the standard or pyrolytically-coated type; the atomization cells were purged with argon (<99.9% by volume). Solutions were introduced into the HGA-400 furnace with plastic micropipettes.

Reagents and standard solutions

Stock solutions (1 mg ml^{-1}) of iron(III), gallium and zinc were prepared from high-purity metals dissolved in minimum volumes of nitric acid (Suprapur, Merck). Nitric acid was also added to the dilute standard solutions to obtain the same concentration as in the 0.1% (w/v) iron(III) solution, i.e., approximately 1.0%.

Measurements

The effect of iron on the 30 elements and 49 element lines listed in Table 1 was studied with the model 5000/Zeeman instrument. Once the actual element lamp had been installed, the power and slit width adjusted, and the wavelength selected, 5 μl of the 0.1% iron solution was pipetted into the graphite tube and the element was atomized according to the furnace parameters given in Table 2.

At two of the wavelengths tested, the resonance lines of gallium and zinc, large negative signals appeared when iron was atomized. For these two elements the measurements were repeated using the optimal parameters listed in Tables 3 and 4. As is apparent from Table 4, two furnace programs were used for zinc. Gallium and zinc were atomized in the absence and presence of iron.

For comparison some measurements were made with both the Zeeman and the continuum-source background correction systems. The furnace parameters listed in Tables 3 and 5 were used during measurements at the 287.4-nm gallium and the 213.9-nm zinc line, respectively.

TABLE 2

Furnace parameters for studying the effect of iron on the elements listed in Table 1. The Zeeman-effect background corrector was used.
Keyboard entries are shown (pyrolytically-coated graphite tube; 5-μl samples)

Step	1	2	3	4[a]
Temp. (°C)	120	600	2200	2600
Ramp (s)	10	10	0	1
Hold (s)	20	20	5	4
Read (s)		29	—[b]	
Int. flow (ml min^{-1})			gas stop	

[a]Clean step. [b]Read step.

TABLE 3

Furnace and other parameters for determining gallium. The program was used with both the Zeeman-effect and the deuterium-arc background correctors (wavelength, 287.4 nm and 294.4 nm; light source, gallium hollow-cathode lamp; lamp current, 20 mA; graphite tube, standard or pyrolytically-coated; sample volume, 5 μl)

Step	1	2	3	4[a]
Temp. (°C)	120	800	2300	2600
Ramp (s)	10	10	0	1
Hold (s)	20	20	5	4
Read (s)		29	—[b]	
Int. flow (ml min^{-1})			gas stop	

[a,b]As in Table 2.

TABLE 4

Furnace and other parameters for determining zinc. Two furnace programs were used, one with maximum power heating and the other with ramp time in the atomization step. The Zeeman-effect background corrector was used (Wavelength, 213.9 nm; light source, zinc hallow-cathode lamp; lamp current, 20 mA; graphite tube, pyrolytically-coated; sample volume, 5 μl)

Program (a)					Program (b)				
Step	1	2	3	4[a]	Step	1	2	3	4[a]
Temp. (°C)	120	400	1200	2600	Temp. (°C)	120	400	1800	2600
Ramp (s)	10	10	0	1	Ramp (s)	10	10	1	1
Hold (s)	20	20	5	4	Hold (s)	20	20	4	4
Read (s)		29	—[b]		Read (s)		29	—[b]	
Int. flow			gas		Int. flow			gas	
(ml min^{-1})			stop		(ml min^{-1})			stop	

[a]Clean step. [b]Read step.

TABLE 5

A furnace program with two atomization steps (step 3 and 5) applicable for the determination of zinc and iron in the same sample portion with the Zeeman-effect or the deuterium-arc background corrector (Wavelength, 213.9 nm; light source, zinc hollow-cathode lamp; lamp current, 20 mA; graphite tube, pyrolytically-coated; sample volume, 5 μl)

Step	1	2	3	4	5
Temp. (°C)	120	400	1200	800	2600
Ramp (s)	10	10	0	10	1
Hold (s)	20	20	5	20	4
Read (s)		29	—[a]	29	—[a]
Int. flow (ml min^{-1})			300		300

[a]Read step.

RESULTS AND DISCUSSION

Among the 30 elements and the 49 element lines studied, iron was found to give a negative absorbance signal at the 287.424-nm gallium line and the 213.856-nm zinc line. These two lines both have adjacent iron lines, the 287.417-nm and the 213.859-nm iron lines which are 0.007 nm and 0.003 nm apart from the gallium and the zinc line, respectively [10]. These gallium and zinc lines are the main resonance lines recommended for a.a.s. determination of the elements; consequently, in the presence of iron, both elements will be subject to spectral interference which will introduce serious negative systematic errors, as discussed in more detail below.

Gallium

Figure 1(a, b) shows the absorption signals obtained by atomizing gallium and iron solutions separately and together with measurements at the 287.4-nm

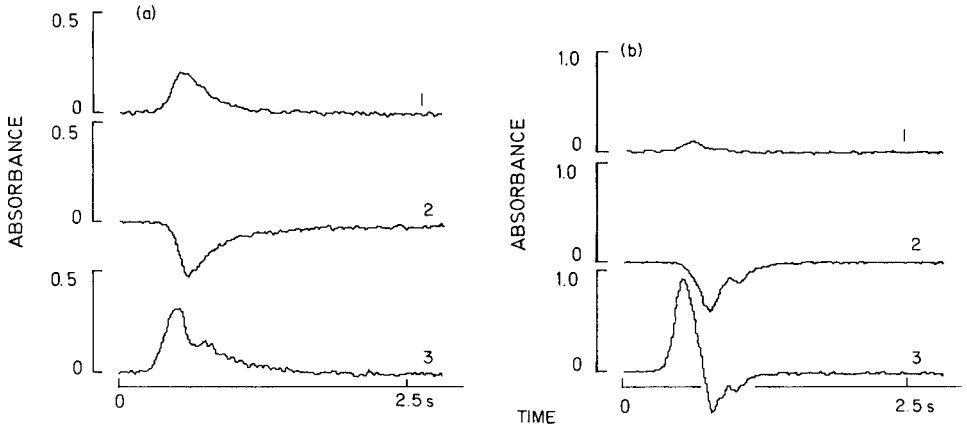

Fig. 1. Absorbance profiles showing the influence of iron on the 287.4-nm gallium line with the Zeeman background corrector. Profiles: (1) 0.5 μg ml^{-1} Ga; (2) 0.1% (w/v) Fe; (3) 0.5 μg ml^{-1} Ga in 0.1% Fe. (a) Standard graphite tube; (b) pyrolytically-coated graphite tube. For experimental conditions, see Table 3.

line. Standard graphite and pyrolytically-coated tubes were used. As can be seen from Fig. 1, iron solution alone gives large negative signals in both tubes. The signals from the mixture of the two elements reveal the negative interference of iron, but another effect complicates the signals; the presence of iron also increases the sensitivity of gallium (see also Figs. 2 and 3 below). The sensitivity and shape of the gallium signals are different in the two tubes and thus the signals from atomization of the mixture of the two elements are also different; in the standard graphite tube, the double-peaked signal only indicates the negative interference of iron, whereas in the pyrolytically-coated tube the signal of gallium in the presence of iron exhibits negative absorbances.

When measurements are made at the 287.4-nm line with the program given in Table 3, concentrations of iron as low as 20 μg ml^{-1} will cause background overcompensation. Because the gallium and iron signals overlap in time, and cannot be separated in time by careful program setting, the best way to avoid the systematic negative error is to measure at another wavelength. The 294.4-nm gallium line, which has about the same sensitivity as the 287.4-nm line, can be used instead.

In Fig. 2, the effects of iron, ashing temperature and type of graphite on the gallium sensitivity, at the 294.4-nm wavelength, are shown. The increased gallium sensitivity in the presence of iron is particularly evident at this wavelength at which the overcompensation effect of iron is not present. At this line, there is a slight background overcompensation when the deuterium arc background corrector is used. This interference is avoided by decreasing the slit width from 0.7 nm to 0.2 nm.

Figure 3 shows the signals obtained at the 287.4-nm gallium line with a pyrolytically-coated tube and a deuterium-arc background corrector. Iron

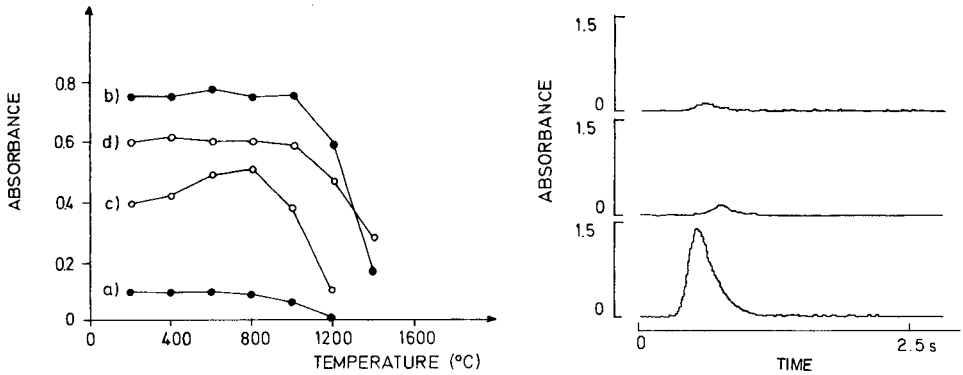

Fig. 2. The effects of ashing temperature, the presence of 0.1% iron and the tube type on the absorbance of 0.5 μg ml^{-1} gallium at the 294.4-nm line: (a) in a pyrolytically-coated graphite tube; (b) in a pyrolytically-coated graphite tube with 0.1% iron added; (c) in a standard graphite tube; (d) in a standard graphite tube with 0.1% iron added. The experimental parameters are given in Table 3.

Fig. 3. Absorbance profiles showing the effect of iron on the 287.4-nm gallium line with a pyrolytically graphite tube and the deuterium-arc background corrector. Profiles 1—3 as in Fig. 1. For experimental conditions, see Table 3.

alone gives a positive signal that appears somewhat later than the gallium signal and is not affected by a change of the slit width. The signal is probably caused by an overlap between the iron and gallium lines which are only 0.007 nm apart. The present results are in accordance with those of Frank et al. [11] who suggested that gallium could be determined by using an iron hollow-cathode lamp and the 287.4-nm line.

As can be seen from Fig. 4, the positive spectral interference is much smaller than the negative spectral interference present when the Zeeman background corrector is used; the iron line is probably overlapping at the wing of the gallium line, and the σ-component of the iron line is overlapping closer to the maximum of the gallium emission peak.

Zinc

Atomization temperature curves for zinc at the wavelength 213.9 nm are shown in Fig. 5; the experimental conditions are given in Table 4. In the two different furnace programs used, maximum power heating and a 1-s ramp time were used, respectively, in the atomization step. The negative signal from 0.1% iron solution, measured at the 213.9-nm zinc line, first appears at atomization temperatures of about 1400° C. Consequently, in most cases, it should not be difficult to select furnace parameters that provide time-separated zinc and iron signals.

As shown in Fig. 5, the sensitivity for zinc reaches a maximum at an atomization temperature of 1800° C and 1-s ramp time. The signal reproduced in Fig. 6 was obtained with these experimental conditions, and it shows a

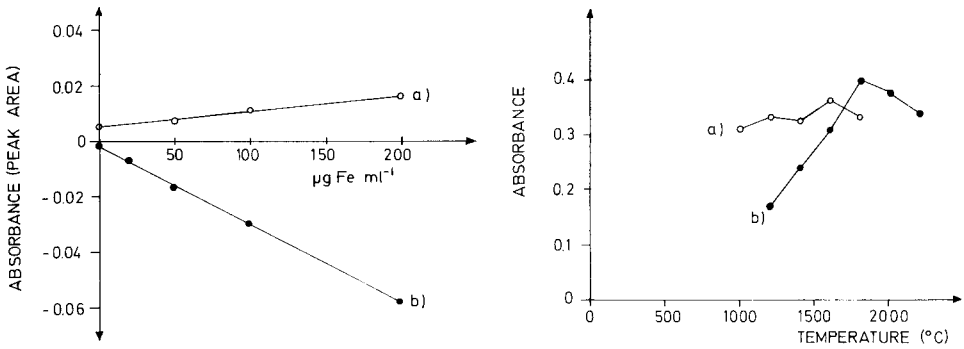

Fig. 4. Peak-area absorbances for iron at the 287.4-nm gallium line with (a) the deuterium-arc background corrector and (b) the Zeeman background corrector. For experimental conditions, see Table 3. Pyrolytically-coated tubes are used.

Fig. 5. Atomization temperature curves for 5 µl of 4 ng ml^{-1} zinc at the 213.9-nm line. The Zeeman background corrector is used. For experimental conditions, see Table 4. (a) Program a, Table 4 (maximum power); (b) program b, Table 4 (1-s ramp time).

time-separated zinc and iron signal. The overcompensation effect of iron will not influence the peak height of zinc, but when the zinc determination is based on peak-area measurements, it is important to select an integration time that ensures no contribution from the negative iron signal.

With the same furnace settings as used for the signal in Fig. 6, an integration time of 3 s will be suitable. In other matrices, where zinc does not evaporate so easily, it may be impossible to select furnace parameters that prevent time-overlap of the zinc and iron signals. When 0.1% iron solution was atomized at the 213.9-nm zinc line with the deuterium-arc background corrector, a positive signal was obtained. This result is in accordance with those of Kelly and More [12] who, using an air/acetylene flame, found that zinc is subject to a spectral interference from iron. By ensuring a time-separation of the zinc and iron signals in graphite-furnace a.a.s., as in the case of the overcompensation effect, this spectral interference will also not present any serious problem. As can be seen from Fig. 7, the positive spectral interference is much smaller than the negative interference obtained with the Zeeman background corrector; the iron absorbing line is probably again at a wing of the zinc emission line, and the σ-component of the iron line overlaps the maximum of the zinc line more closely.

If zinc and iron are present at suitable concentration ratios, the overcompensation effect or the positive spectral interference of iron can be utilized to determine zinc and iron simultaneously in the same sample portion. A suitable furnace program with two atomization steps is given in Table 5; in the first step, zinc is atomized at 1200° C without any loss of iron, and in the second step iron is atomized at 2600° C. The resulting zinc and iron signals with Zeeman background correction are reproduced in Fig. 8. As is apparent

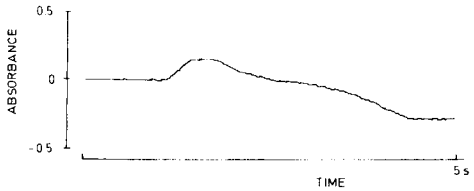

Fig. 6. Absorbance profile for 5 μl of 2 ng ml^{-1} zinc in the presence of 0.1% iron at the 213.9-nm line. The Zeeman background corrector is used. For experimental conditions see Table 4, program b.

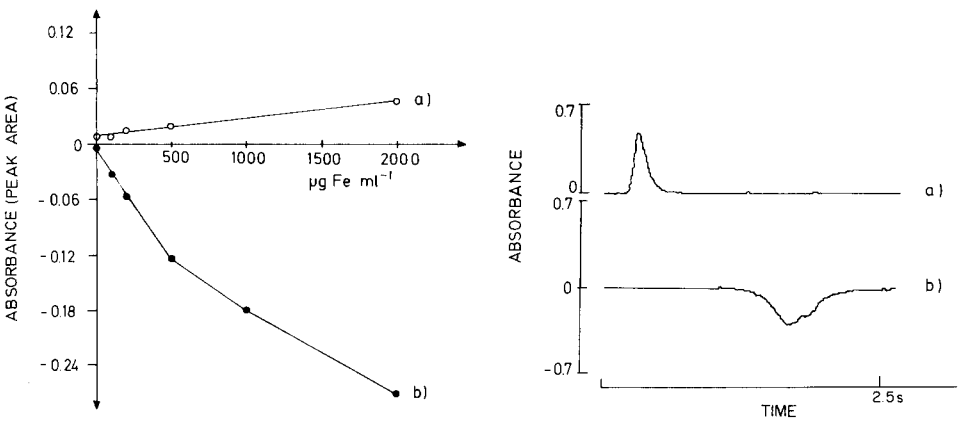

Fig. 7. Peak-area absorbances for iron at the 213.9-nm zinc line with (a) the deuterium-arc background corrector and (b) the Zeeman background corrector. For experimental conditions, see Table 5. The peak areas of the second atomization step (step 5) are plotted.

Fig. 8. Absorbance profiles of 5 μl of 20 ng ml^{-1} zinc in 0.1% iron atomized with the experimental conditions listed in Table 5 and with the Zeeman background corrector. Profiles: (a) atomization peak of zinc (step 3); (b) atomization signal of iron (step 5). The program can be used to determine zinc and iron simultaneously.

from Fig. 7, iron concentrations up to about 500 μl ml^{-1} and 0.2% with use of the Zeeman and deuterium arc background corrector, respectively, can be determined in the second atomization step. Iron also seems to influence the atomization processes of zinc; in the presence of iron, the zinc peak appears later, and both the peak height and area are altered.

Conclusions

The two cases of background overcompensation found in this work are assumed to be caused by overlapping of σ-components of matrix atomic lines with the analyte emission line. They are probably only two out of other cases occurring in Zeeman-corrected instruments of the same or similar design as that of the P-E 5000/Zeeman instrument. When the magnetic field is applied to the analyte source, this type of interference will not be

encountered. However, with these instruments the background is not measured exactly at the analytical wavelength; consequently, spectral interferences leading to incorrect background measurements may occur.

It is important to be aware of the cases where the background overcompensation effect is likely to happen. In many instances, especially when the signals from the analyte and the interfering element overlap in time, the background overcompensation effect is not always obvious and may be overlooked. This work on spectral interferences and overcompensation in Zeeman-corrected a.a.s. will be continued with studies of other combinations of elements.

REFERENCES

1 F. J. Fernandez, W. Bohler, M. M. Beaty and W. B. Barnett, At. Spectrosc., 2 (1981) 73.
2 W. Slavin, G. R. Carnrick, D. C. Manning and E. Pruszkowska, At. Spectrosc., 4 (1983) 69.
3 E. Pruszkowska, D. C. Manning, G. R. Carnrick and W. Slavin, At. Spectrosc., 4 (1983) 87.
4 G. R. Carnrick, D. C. Manning and W. Slavin, Analyst (London), 108 (1983) 1297.
5 U. Völlkopf, Z. Grobenski and B. Welz, At. Spectrosc., 4 (1983) 165.
6 F. J. Fernandez and R. Giddings, At. Spectrosc., 3 (1982) 61.
7 F. J. Fernandez and M. M. Beaty, Spectrochim. Acta, Part B, 39 (1984) 519.
8 P. W. J. M. Boumans, Line Coincidence Tables for Inductively Coupled Plasma Atomic Emission Spectroscopy, Pergamon Press, Oxford, 1980.
9 J. Reader, C. H. Corliss, W. L. Wiese and G. A. Martin, Wavelengths and Transition Probabilities for Atoms and Atomic Ions, U.S. Department of Commerce/National Bureau of Standards, NSRDS-NBS68.
10 E. Michaud and J. M. Mermet, Spectrochim. Acta, Part B, 37 (1982) 145.
11 C. W. Frank, W. G. Schrenk and C. E. Meloan, Anal. Chem., 38 (1966) 1005.
12 W. R. Kelly and C. B. More, Anal. Chem., 45 (1973) 1274.
13 R. Stephens and G. F. Murphy, Talanta, 25 (1978) 441.

Analytica Chimica Acta, 165 (1984) 97—103
Elsevier Science Publishers B.V., Amsterdam — Printed in The Netherlands

SELECTIVE SEPARATION AND DETERMINATION OF DISSOLVED CHROMIUM SPECIES IN NATURAL WATERS BY ATOMIC ABSORPTION SPECTROMETRY

T. L. MULLINS

School of Chemical and Earth Sciences, N.S.W. Institute of Technology, P.O. Box 123, Broadway 2007, Sydney, N.S.W. (Australia)

(Received 6th December 1983)

SUMMARY

A procedure for determining the concentrations of dissolved chromium species in natural waters is described. Chromium(III) and chromium(VI), separated by co-precipitation with hydrated iron(III) oxide, and total dissolved chromium are determined separately by conversion to chromium(VI), extraction with APDC into MIBK and determination by a.a.s. The detection limit is 40 ng l^{-1} Cr. The dissolved chromium not amenable to separation and direct extraction is calculated by difference. In the waters investigated, total concentrations were relatively high (1—5 $\mu g\ l^{-1}$) with Cr(VI) the predominant species in all areas sampled with one exception, where organically bound chromium was the major species.

Chromium is one of the trace metals that has been used in recent years to assist in the understanding of the geochemistry of the marine environment. This has primarily been due to its unusual ability to co-exist in analytical concentrations in two, soluble, stable oxidation states. Thus, numerous analytical procedures have been applied to determine dissolved chromium and the relative concentrations of these two states. These analyses have generally entailed the separation and determination of the soluble concentrations of total chromium and of one of the oxidation states. The concentration of the other oxidation state was calculated by difference. The methods employed were usually based on such separation and preconcentration procedures as co-precipitation [1—8], liquid—liquid extraction [9—11], ion exchange [12] and electrodeposition [13].

The calculation of one oxidation state by difference presupposes that the two oxidation states in question were statistically the only contributors to the total concentration. Because of this, contributions from other possible species such as organic complexes were generally not considered. It has recently been suggested [14], however, that this presumption may not be warranted and that contributions from organically bound chromium should be considered. This arises from the reported presence of dissolved organic species in natural waters which form stable soluble complexes with chromium

0003-2670/84/$03.00

and which may not readily be amenable to determination by the above procedures.

Two procedures have been developed which enable the concentration of the bound species to be calculated [6, 13]. Both methods, however, require the calculation by difference of two of the species sought, i.e., chromium(VI) and the organically bound chromium, respectively. In one [6], separation is achieved by a series of co-precipitations, while in the other [13] preconcentration and separation are achieved by electrodeposition of the chromium with mercury onto pyrolytic graphite-coated tubular furnaces.

This paper describes a simplified procedure to assess the contribution of the bound species by use of a single initial separation by co-precipitation, from which both chromium(III) and chromium(VI) concentrations are determined independently. The organic contribution is then calculated by difference from a determination of the total dissolved concentration.

EXPERIMENTAL

Reagents and instrumentation

All chemicals used were of analytical reagent grade. Distilled-deionized water was used throughout. Chromium(III) and chromium(VI) stock solutions (100 mg l^{-1}) were prepared by dissolving chromium(III) chloride and potassium dichromate in water. These solutions were acid-stabilized for at least 1 week. Subsequent working solutions were prepared as required by dilution of the stock solution with pure water for chromium(VI) standards or artificial sea water [15] for accuracy and precision studies. Hydrated iron(III) oxide suspensions were prepared by neutralizing an appropriate volume of an aqueous acidic solution of iron(III) chloride (100 mg Fe l^{-1}), to pH 7—8 with sodium hydroxide solution. Aqueous 1% solutions of ammonium pyrrolidinedithiocarbamate (APDC) were extracted with methyl isobutyl ketone (MIBK) at least 3 times immediately prior to use to decrease the impurity content to a minimum.

Atomic absorption measurements were made with a Varian Techtron AA5 spectrometer, modified by incorporation of integration and scale-expansion facilities, and an external printer. The chromium hollow-cathode lamp was operated with a fuel-rich air—acetylene reducing flame and absorbances were measured at 357.9 nm. To give the most precise results, the burner height was 7 mm below grazing incidence, and the nebulizer uptake was 6 ml min^{-1}.

Sampling

Samples of water were collected in acid-leached and solvent extracted 5-l high-density nylon Niskin-type bottles with rubber tubing closures. These bottles were constructed at the N.S.W. Institute of Technology specifically for trace metal samples. They were hung on a stainless steel wire and the closing mechanisms tripped by brass messengers. The water samples were filtered through a 0.45-μm HA Millipore filters within 2 h of sampling, and subsequent procedures were begun immediately.

Species separation

Chromium(III). To a 500-ml aliquot of filtered water sample, add a freshly prepared suspension of hydrated iron(III) oxide, pH 7—8, containing ca. 5 mg of iron(III). Stir moderately for 80 min, and allow the precipitate to settle for 3 h. Filter through an acid-washed 0.1-μm MF Millipore filter (47 mm diameter, type VCWP 04700). This precipitate contains all the chromium(III) species in the sample which are amenable to co-precipitation.

Dissolve the precipitate in the minimum volume of 1 M hydrochloric acid, dilute to 100 ml with water and adjust the pH with aqueous ammonia to incipient precipitation of the hydrated iron(III) oxide. To this solution, add 1 ml of 0.1 M ammonium peroxodisulphate solution and oxidize the chromium(III) recovered to chromium(VI) by heating on a water bath to 80°C for at least 30 min. After this time, increase the temperature until the solution boils gently. Continue boiling for 10 min to remove excess of oxidant by decomposition. Remove the solution from the water bath and allow it to cool to room temperature. At this stage the chromium should all be present as chromium(VI) and readily amenable to the subsequent extraction procedure. Separate the iron from solution by adjusting the pH to 6—8 to reprecipitate the hydrated iron(III) oxide and filter. Extract the chromium(VI) from the filtrate at pH 2 with 5 ml of 1% APDC into 10 ml of MIBK, aspirate into the flame and measure the absorbance at 357.9 nm.

Chromium(VI). The filtrate from the initial separation above should contain chromium(VI) and any chromium(III) species not amenable to co-precipitation with the hydrated iron(III) oxide. Extract the chromium(VI) directly from the filtrate at pH 2 with 5 ml of 1% APDC into 10 ml of MIBK, aspirate into the flame as soon as possible, and measure the chromium absorbance as above.

Total dissolved chromium. Acidify a 500-ml aliquot of the original filtered water sample with 0.1 M hydrochloric acid and add 3 ml of 0.1 M ammonium peroxodisulphate. Heat on a water bath to ca. 80°C for at least 30 min. Increase the temperature and boil the solution gently for 10 min to remove excess of oxidant. Remove the solution from the water bath and allow it to cool to room temperature. At this stage all the chromium present in the sample should be present as chromium(VI). Extract from the solution at pH 2 as described above for chromium(VI).

RESULTS AND DISCUSSION

Chromium(III) contact time

The quantitative separation of chromium(III) by co-precipitation with hydrated iron(III) oxide is a well-proven procedure and forms the basis of numerous analyses [1—7]. In many cases, however, the contact time between the precipitating and co-precipitating species seems to be arbitrary. Table 1 contains the results of an investigation to determine the minimum contact time to ensure a reproducible separation. After the addition of the hydrated

TABLE 1

Effect of time on chromium(III) separation from spiked artificial sea water containing 5.00 $\mu g\ l^{-1}$ each of Cr(III) and Cr(VI)

Time (min)	Cr(III)[a] found ($\mu g\ l^{-1}$)	S.d.[b]	R.s.d. (%)
120	4.38	0.74	16.9
180	4.81	0.30	6.2
240	4.93	0.10	2.0
300	4.96	0.06	1.2

[a]Mean of 3 determinations. [b]Standard deviation calculated as 0.59 × range [17].

iron(III) oxide to 500 ml of spiked artificial sea water, the mixture was stirred for one third of the total contact time followed by settling for the remainder of this time.

Quantitative separations were statistically complete after 2 and 3 h, but in each case the uncertainty was relatively high. After 4 h, however, the precision was remarkably improved. On this basis, a standard contact time of 4 h was chosen for the procedure.

Accuracy and precision

To determine the accuracy and precision of the procedure, known amounts of chromium(III) and chromium(VI) were added to samples of artificial sea water and the analysis was conducted as described. Each section of the analysis, i.e., total dissolved chromium, chromium(III) and chromium(VI), was assessed individually.

The quantitative oxidation of chromium(III) in solution to chromium(VI) followed by liquid—liquid extraction is an accepted procedure which produces accurate and reproducible results [9, 16]. Table 2 contains the results of the analyses of 9 sets of triplicate determinations of various mixtures of dissolved chromium(III) and chromium(VI). From these it was concluded that chromium(III) was quantitatively oxidized to chromium(VI), which was subsequently quantitatively extracted. The major source of error was in the extraction procedure and absorbance measurement. Except for the blank determination, the relative standard deviation (r.s.d.) for all mixtures was less than 1.0%. The detection limit, defined as twice the standard deviation of the blank, was 40 ng l^{-1}.

Tables 3 and 4 contain the results of triplicate determinations of chromium(III) and chromium(VI), respectively. Chromium(III) was quantitatively oxidized and extracted from all mixtures. The r.s.d. for all determinations was $<2.5\%$, and the detection limit was again 40 ng l^{-1}. Chromium(VI) was also quantitatively extracted from all mixtures. The r.s.d. for all determinations was $<1.0\%$, and the detection limit was once again 40 ng l^{-1}.

TABLE 2

Precision and accuracy for total dissolved chromium determinations in spiked artificial sea water

Cr(III) added[a]	Cr(VI) added[a]	Cr found[a]	Variance for oxidation ($\times 10^4$)	Variance for extraction ($\times 10^4$)	Total variance ($\times 10^4$)	R.s.d. (%)
0.00	10.00	9.99	4.63	12.7	12.7	0.4
2.00	8.00	9.98	15.4	24.5	31.2	0.6
3.50	6.50	10.00	9.63	23.4	24.6	0.5
5.0	5.00	10.01	7.25	11.9	14.5	0.4
10.0	0.00	9.98	21.5	23.1	31.8	0.6

[a]All concentrations are expressed in $\mu g\ l^{-1}$; each data analysis carried out on nine sets of triplicate measurements. The degrees of freedom for the data analyses are: oxidation = 8; extraction = 18; total = 26.

TABLE 3

Precision and accuracy for chromium(III) determinations in spiked artificial sea water

Cr(III) added[a]	Cr(VI) added[a]	Cr(III) found[a]	S.d.[a,b]	R.s.d. (%)
0.00	10.00	0.02	0.02	
2.00	8.00	1.97	0.04	2.0
3.50	6.50	3.55	0.08	2.3
5.00	5.00	4.96	0.09	1.8
10.00	0.00	9.87	0.11	1.1

[a]All concentrations are expressed in $\mu g\ l^{-1}$. [b]Standard deviation calculated as in Table 1; each analysis done in triplicate.

TABLE 4

Precision and accuracy for chromium(VI) determinations in spiked artificial sea water

Cr(III) added[a]	Cr(VI) added[a]	Cr(VI) found[a]	S.d.[a,b]	R.s.d. (%)
0.00	10.0	9.95	0.08	0.8
2.00	8.00	7.97	0.05	0.6
3.50	6.50	6.55	0.05	0.8
5.00	5.00	5.03	0.03	0.6
10.00	0.00	0.03	0.02	—

[a,b]As in Table 3.

Application to natural waters

The results of triplicate determinations of samples taken from six locations in the Sydney area, and analysed by the method described, are listed in Table 5. The r.s.d. values for the determinations of chromium(III), chromium(VI) and total dissolved chromium were generally <10.0%, 5.0% and 5.0%, respectively. From these results, the r.s.d. for the calculated concentration of the bound species was <20%.

The relatively high chromium concentrations found reflect in part the use of most of the waterways as industrial carriers. Lower levels found in Port Hacking reflect the primary use of the bay as a recreational area devoted particularly to the use of power and sail boats. In Port Hacking, the distribution of species was found to be in the order: organically bound > chromium(VI) > chromium(III), which was unique for the areas sampled. In the other areas, chromium(VI) predominated.

Because of the unknown character of the bonding species present in the various waterways, it was not possible to assess the efficiency of the oxidation of these species to extractable chromium(VI) directly from standard solutions. However, a comparison with values determined previously [13] for one of

TABLE 5

Determination of dissolved chromium species in some natural waters

Location	Chromium found[a] ($\mu g\ l^{-1}$)			
	Cr(III)	Cr(VI)	Cr bound	Cr total
Port Hacking	0.27 ± 0.02	0.49 ± 0.03	0.56 ± 0.07	1.32 ± 0.05
Georges River	0.42 ± 0.04	0.89 ± 0.04	0.42 ± 0.08	1.72 ± 0.06
Drummoyne Bay	0.32 ± 0.03	0.95 ± 0.04	0.69 ± 0.10	1.96 ± 0.07
Botany Bay	0.45 ± 0.04	1.26 ± 0.06	0.71 ± 0.03	2.41 ± 0.09
Cooks River	0.51 ± 0.04	2.98 ± 0.11	0.88 ± 0.10	4.37 ± 0.06
Parramatta River	0.88 ± 0.02	3.17 ± 0.06	0.82 ± 0.09	4.87 ± 0.11

[a]All results are the mean (± s.d.) of 3 measurements; s.d. calculated as in Table 1.

TABLE 6

Comparison of results for Georges River

	Chromium found ($\mu g\ l^{-1}$)			
	Cr(III)	Cr(VI)	Cr bound	Cr total
This paper	0.42	0.89	0.42	1.72
Previous workers[a]	0.22	0.68	0.35	1.25

[a]Electrochemical separation and preconcentration [13].

the waterways, (Table 6) indicates that the present results are in reasonably good agreement.

Throughout these analyses, the advantage of determining all fractions by the measurement of a single entity (chromium(VI)) was apparent. In addition, the procedure was easy to manipulate and allowed ready control of possible contamination and handling errors.

REFERENCES

1 R. Fukai and D. Vas, J. Oceanol. Soc. Jpn., 23 (1967) 298.
2 H. Elderfield, Earth Planet. Sci. Lett., 9 (1970) 10.
3 D. Grimaud and G. Michard, Mar. Chem., 2 (1974) 229.
4 R. E. Cranston and J. W. Murray, Anal. Chim. Acta, 99 (1978) 275.
5 E. Nakayama, T. Kuwamoto, H. Tokoro and T. Fujinaga, Anal. Chim. Acta, 131 (1981) 247.
6 E. Nakayama, T. Kuwamoto, H. Tokoro and T. Fujinaga, Nature, 290 (1981) 768.
7 A. J. Pik, J. M. Eckert and K. L. Williams, Anal. Chim. Acta, 124 (1981) 351.
8 H. F. Zhang, J. Holzbecher and D. E. Ryan, Anal. Chim. Acta, 149 (1983) 385.
9 G. J. de Jong and U. A. Th. Brinkman, Anal. Chim. Acta, 98 (1978) 243.
10 T. Matsuo, J. Shida, M. Abiko and K. Konno, Bunseki Kagaku, 24 (1975) 723.
11 H. Bergman and K. Hardt, Fresenius Z. Anal. Chem., 297 (1979) 381.
12 J. F. Pankow and G. E. Janauer, Anal. Chim. Acta, 69 (1974) 97.
13 G. E. Batley and J. P. Matousek, Anal. Chem., 52 (1980) 1570.
14 E. Nakayama, T. Kuwamoto, H. Tokoro, S. Tsurubo and T. Fujinaga, Anal. Chim. Acta, 130 (1981) 289.
15 J. Lyman and R. H. Fleming, J. Mar. Res., 3 (1940) 134.
16 T. R. Gilbert and A. M. Clay, Anal. Chim. Acta, 67 (1973) 289.
17 K. Eckschlager, in R. A. Chalmers (Ed.), Errors, Measurements and Results in Chemical Analysis, Van Nostrand-Reinhold, London, 1969, p. 89.

Analytica Chimica Acta, 165 (1984) 105—111
Elsevier Science Publishers B.V., Amsterdam — Printed in The Netherlands

CHARACTERIZATION AND ELIMINATION OF THE INTERFERING EFFECTS OF FOREIGN SPECIES IN THE ATOMIC ABSORPTION SPECTROMETRY OF CHROMIUM

A. M. ABDALLAH, M. M. EL-DEFRAWY* and M. A. MOSTAFA
Department of Chemistry, Faculty of Science, University of Mansoura (Egypt)
(Received 22nd June 1983)

SUMMARY

In the atomic absorption spectrometric determination of chromium(III), the interfering effects of different complexing agents can be completely eliminated by addition of excess of cyanide, boric acid or sulphosalicyclic acid. The effect of some complexing agents on the production of chromium atoms is discussed, and the mechanism of cyanide interaction is investigated in detail.

Although the sensitivity for chromium by atomic absorption spectrometry is greatest in a fuel-rich flame, interferences are also greater [1]. The origin of many interferences is still speculative. A fundamental understanding of interfering effects in atomic absorption spectrometry depends largely on a knowledge of the mechanisms which control atomization processes in flames [2—5].

The object of this paper is to investigate the feasibility of using a continuous titration technique [6—8] for studying the interfering effects of foreign species on the atomic absorption signal of chromium and thus establishing the possibility of using a simple method for eliminating such interferences.

EXPERIMENTAL

A Unicam SP-90A series 2 atomic absorption spectrometer was used with a Unicam chromium hollow-cathode lamp and a conventional 10-cm slot burner head for an air—acetylene flame. A continuous titration device [6] was attached to the instrument to conduct all the absorption and emission experiments; the titration plots were recorded with a Philips PM-8251 single-pen recorder at a chart speed of 30 cm min^{-1}. The evaluation of the titration plots was done by means of a Casio FX-502 type programmable pocket calculator.

The instrumental parameters used were as follows: lamp current, 12 mA; wavelength, 357.9 nm; slit-width, 0.1 mm (monochromator dispersion 2.9 nm min^{-1} at 370 nm); air flow rate, 5 l min^{-1}; fuel flow rate, 1.8 l min^{-1};

height in the flame, 6 mm. The emission study was done with the same equipment. All chemicals were of analytical-reagent grade.

RESULTS AND DISCUSSION

Effect of anions

The effect of four anionic species as sodium or potassium salts on the absorbance from a chromium(III) chloride solution is presented in Fig. 1. Each anion has a depressive effect, and at a definite stoichiometric ratio an inflection is observed, at mole ratios of interfering anion to chromium of 1:1 for phosphate and 3:1 for iodide, nitrite and nitrate, corresponding to the formation of $CrPO_4$, CrI_3, $Cr(NO_2)_3$ and $Cr(NO_3)_3$. The general trend is that the absorbance decreases during the first stages of the titration and after the stoichiometric ratio has been attained, the absorbance becomes constant, except for iodide. In this case, the absorbance is restored almost to its normal value at a ratio of 5:1. This phenomenon was exploited by Juhai et al. [9] who devised a procedure for the determination of chromium in steel, using iodide as a releasing agent for chromium.

Effect of complexing agents

The changes in the absorbance of 1.0 mM chromium(III) caused by various ligands are shown in Fig. 2. There is an initial suppressive effect from sulphosalicyclic acid (SSA) which has a maximum effect at a mole ratio of 1:1. This is followed by a sharp enhancement by higher concentration of SSA, finally doubling the absorbance at a ratio of 5:1. The inflection at 1:1 corresponds to the formation of a 1:1 complex. To prove the formation of this complex, spectrophotometric measurements were conducted. Figure 3

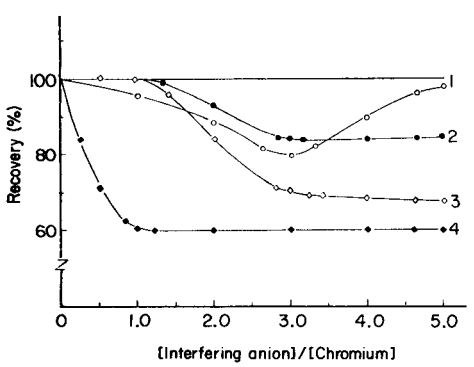

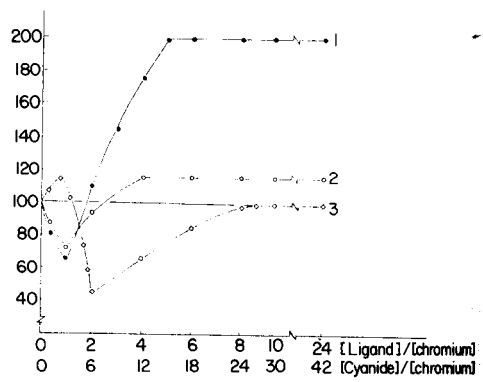

Fig. 1. Changes in the absorption signal of 1.0 mM chromium as a function of interfering anion:chromium ratio: (1) I^-; (2) NO_3^-; (3) NO_2^-; (4) PO_4^{3-}.

Fig. 2. Changes of chromium (1.0 mM) absorption signal as a function of ligand:chromium ratio: (1) sulphosalicyclic acid; (2) 4-aminosalicyclic acid; (3) potassium cyanide.

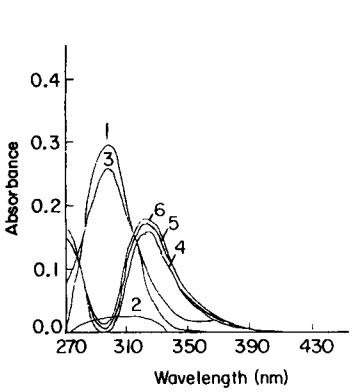

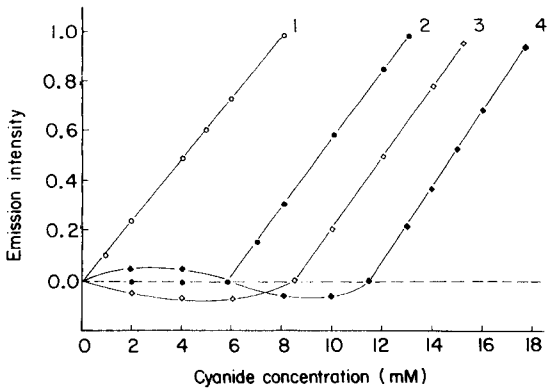

Fig. 3. Conventional absorption spectra for Cr-SSA mixtures: (1) SSA; (2) Cr^{3+}; (3) 1:1 at 60°C; (4) 1:1 after boiling; (5) 1:2 after boiling; (6) 1:3 after boiling.

Fig. 4. Changes of cyanide band emission intensity as a function of cyanide concentration in Cr solutions of the following concentrations: (1) 0.0; (2) 1.0; (3) 1.5; (4) 2.0 mM.

shows that the mole ratio is 1:1 irrespective of any increase in SSA concentration. Heating was required to speed up complex formation, and it seems probable that the required heating would occur during solvent evaporation in the flame. The marked increase in chromium absorbance is attributed to the efficiency of SSA in providing a reducing environment leading to increase in the chromium atom population in the area of measurement. Figure 2 shows that 4-aminosalicylic acid has a similar but smaller effect.

Cyanide forms stable complexes with chromium(III) [10]. Figure 2 indicates that the chromium absorbance generally decreases with increasing cyanide ion concentration, with a minimum at a ratio of 6:1; after which the absorbance increases and returns to the normal value at $\geqslant 25$ mM. At such high cyanide concentrations, the reducing action of the excess of cyanide compensates for the effect of complex formation. The behaviour of cyanide towards chromium in the flame can be discussed on the basis that three main steps take place during a continuous increase in ligand concentration. Vaporization of the solid complex particles causes their decomposition and release of chromium atoms which react instantly with oxidising species in the flame to form chromium compounds, mainly oxides [11]. After a particular stoichiometric ratio has been attained, the excess of the reducing species (CN radicals when potassium cyanide is used) in the flame reacts with chromium oxides

$$Cr_nO_m + m\ CN \rightarrow n\ Cr + 1/2m\ N_2 + m\ CO$$

to increase the chromium atom population. The continuous increase in concentration of the reducing species in the flame overcomes the effect of the oxidising species and causes the complete restoration of the chromium atom concentration.

The behaviour of organic additives in the flame is quite diverse, because such agents are not decomposed equally in the flame; their oxidising and reducing properties differ under different flame conditions. In order to obtain more information on the reducing action of the ligands in the flames, the effect of potassium cyanide solution has been given particular attention because its decomposition products are only CN and K. The emission intensity of CN in the flame can easily be measured. Work is in progress to obtain and measure the emission signals of some of the decomposition products of sulphosalicylic acid and related compounds.

The presence of cyanide radicals in the flame can be detected by measuring the emission intensity at 358 nm, no signal was detected when attempting to measure the absorbance of the cyanide radical at 358 nm, and the emission intensity of the cyanide band at the same wavelength does not effect the intensity of the line from a chromium hollow-cathode lamp. Moreover, the cyanide intensity at 358 nm is unaffected by the presence of chromium. Figure 4 indicates the initial existence of cyanide radicals in the flame at the start of the titration and in the absence of chromium. When the titration is conducted in the presence of 1.0, 1.5 and 2.0 mM chromium, Fig. 4 shows that the cyanide emission intensity is zero at the start of the titration and remains zero until the cyanide:chromium ratio reaches 6:1. After this, the cyanide emission resumes its original trend of continuously increasing with increasing cyanide ion concentration. Thus the delay in appearance of the cyanide band emission is due to the complexing action of the cyanide ion on chromium.

The reaction given above indicates that the reaction between chromium oxides and cyanide produces chromium, nitrogen and carbon monoxide. Figure 5 shows a progressive increase in the emission intensity of the carbon monoxide band when measured at 219 nm in solutions containing 1.0 mM chromium plus increasing amounts of cyanide. The increase is directly related to the concentration of the cyanide radical in the flame, after reaching the stoichiometric 6:1 ratio. Such a result indicates that the excess of cyanide radicals removes from the flame volume under measurement unwanted oxidising species and restores the chromium signal to its original value.

Interference of cations

Metal-metal interactions in the flame are complicated. Figure 6 shows that the chromium signal is considerably enhanced when aluminium, calcium or strontium is added to a chromium solution. Such metals may compete with chromium either for flame oxidizing species or for constituents of the nebulized solution so as to form metal monoxides. Dissociation energies D_0, in kcal mol^{-1}, for AlO, CaO, FeO, NiO, SrO and CrO are 106, 100, 99, 97, 97 and 101, respectively [12]. In addition, monohydroxides of calcium (D_0 = 104 kcal mol^{-1}) and strontium (D_0 = 103 kcal mol^{-1}) are likely to be present in air—acetylene flames. These hydroxides and monoxides have very similar stabilities, and an appreciable proportion of each metal is present in these forms in the flame, particularly in the measurement zone.

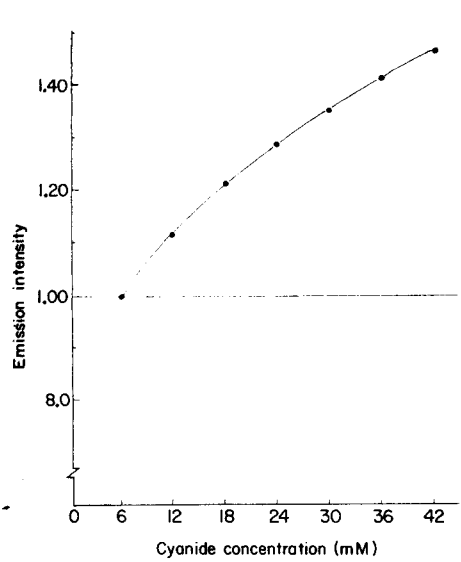

Fig. 5. Effect of potassium cyanide in the presence of 1.0 mM chromium on the CO band emission intensity at 219 nm.

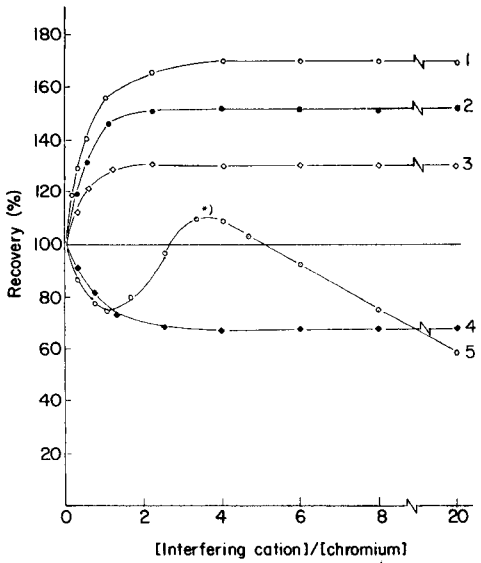

Fig. 6. Change in the absorption signal of 1.0 mM chromium as a function of interfering metal ion:chromium ratio: (1) Al^{3+}; (2) Ca^{2+}; (3) Sr^{2+}; (4) Fe^{3+}; (5) Ni^{2+}. (May be due to formation of $CrNi_3$ with low melting point and high volatility [15].)

When iron or nickel is present in aspirated solution of chromium, the experimental observations are in agreement with the theory that relatively non-volatile compounds are formed between chromium and iron or nickel. These compounds dissociate only slowly in the measurement zone. The severity of the depressive effect is decreased when the measurements are made in the higher regions of the flame, and has disappeared 1.2 cm above the flame base.

Control of interferences

The action of boron in an air–acetylene flame as a promising universal flame buffer was discussed in earlier papers [13, 14]. Its action in the flame, when present in excess, is to interact with the matrix components to form relatively stable, unreactive species, leaving the analyte atoms free. Table 1 indicates that boric acid is a powerful releasing agent and acts very effectively on oxidising species such as nitrate or chlorate and possible reducing species such as nitrite. Moreover, it removes from the area of measurement interfering distintegration products of organic chelating agents. In addition, formation of metal borides of the interferents leads to release of chromium without affecting the atomization process. However, the data in Table 1 help to reach the conclusion that boron can efficiently level the flame conditions to obtain signals identical to samples to which boron but no interferent has been added.

TABLE 1

Interference of various species on the absorbance of 1.0×10^{-3} M chromium(III) and the effect of different releasing agents

Addes substance(s) (200 mg l^{-1} each)	Chromium recovery (%)[a]			
	No releasing agent	Boric acid (1.85×10^{-2} M)	SSA (2.0×10^{-2} M)	KCN (5.0×10^{-2} M)
PO_4^{3-}	60	98	100	99
NO_3^-	83	100	100	100
NO_2^-	68	98	99	99
I^-	93	100	100	100
SO_4^{2-}	85	100	100	100
ClO_4^-	138	100	100	100
$PO_4^{3-} + NO_3^-$	33	100	100	105
$PO_4^{3-} + NO_3^- + Br^-$	88	100	100	100
$PO_4^{3-} + SO_4^{2-}$	69	100	100	100
EDTA	82	100	100	100
CDTA	80	100	99	99
NTA	82	100	100	100
EDTA + PO_4^{3-}	122	100	102	105
EDTA + PO_4^{3-} + Br^-	100	100	100	105
Al^{3+}	170	100	100	[b]
Ca^{2+}	154	100	100	[b]
Sr^{2+}	130	100	100	[b]
Fe^{3+}	68	98	99	[b]
Ni^{2+}	110	100	100	[b]
$Al^{3+} + Cu^{2+} + Pb^{2+}$	150	100	100	[b]
$Ca^{2+} + Mn^{2+}$ + EDTA	150	100	100	[b]
$Sr^{2+} + Cd^{2+} + Fe^{3+}$	94	100	95	[b]
$Sr^{2+} + Ba^{2+} + In^{3+} + NO_3^-$	83	100	95	[b]

[a]Recovery with respect to the chromium absorbance signal in the presence of the releasing agent alone (= 100%). [b]Precipitation of the metal cyanide.

While boric acid acts upon the interferents and their disintegration products, it does not enhance the absorption signals of the analytes. Sulphosalicylic acid (SSA), however, plays a unique role in reacting with the analyte to cause simultaneous enhancement and normalization of the recovered signal, when it is present in large amounts in both samples and standards. Differences in chromium from samples containing diverse ions completely disappear in the presence of 0.02 M SSA. Moreover, SSA doubles chromium signals compared to a chromium chloride solution.

The general usefulness of cyanide addition to chromium solutions of samples and standards is quite clear; its precipitating action on a variety of cations can be exploited by filtering off interfering species and the filtrate can be nebulized directly in order to determine chromium.

REFERENCES

1 J. C. Van Loon, Analytical Atomic Absorption Spectroscopy, Selected Methods, Academic Press, New York, 1980.
2 I. Rubeska and B. Moldan, Anal. Chim. Acta, 37 (1967) 421.
3 I. Rubeska, Can. J. Spectrosc., 20 (1975) 156.
4 J. Y. Marks and G. G. Welcher, Anal. Chem., 42 (1970) 1033.
5 C. B. Boss and G. M. Hieftje, Anal. Chem., 51 (1979) 895.
6 D. Stojanovic, J. Bradshaw and J. D. Winefordner, Anal. Chim. Acta, 96 (1978) 45.
7 J. Posta and J. Lakatos, Magy. Kém. Foly., 86 (1980) 284.
8 M. M. El-Defrawy, J. Posta and M. T. Beck, Anal. Chim. Acta, 115 (1980) 155.
9 E. Juhai, K. Szivos, V. Izekov, T. Kantor and E. Pungor, Magy. Kém. Foly., 86 (1980) 650.
10 A. G. Sharpe, The Chemistry of Cyano-Complexes of Transition Metals, Academic Press, London, 1976.
11 H. Remy, Treatise on Inorganic Chemistry, Vol. 2, Elsevier, Amsterdam, 1956.
12 A. G. Gaydon, Dissociation Energies and Spectra of Diatomic Molecules, 3rd edn., Chapman and Hall, London, 1968.
13 A. M. Abdallah and M. A. Mostafa, Ind. J. Chem., 19A (1980) 1112; Annali di Chimica, 70 (1980) 1.
14 A. M. Abdallah, M. M. El-Defrawy, M. A. Mostafa and A. B. Sakla, Paper presented at the 9th Int. Symp. Microchemical Techniques and Trace-Analysis, Amsterdam, 1983.
15 P. M. Hansen, Constitution of Binary Alloys, 2nd edn., McGraw-Hill, London, 1958.

Analytica Chimica Acta, 165 (1984) 113—119
Elsevier Science Publishers B.V., Amsterdam — Printed in The Netherlands

SIGNAL-LEVELLING AGENTS FOR ELIMINATING THE INTERFERENCES OF IRON, ALUMINIUM, BARIUM AND CALCIUM IN THE DETERMINATION OF LEAD BY FLAME ATOMIC ABSORPTION SPECTROMETRY

A. B. EL-SAYED*, N. E. AMINE, S. H. ABD EL-HALEEM and M. F. EL-SHAHAT

Department of Chemistry, Faculty of Science, Ain Shams University, Abbassia, Cairo (Egypt)

(Received 20th October 1983)

SUMMARY

The interferences of iron, aluminium, barium and calcium on the determination of lead by flame atomic absorption spectrometry are discussed; a titration procedure was used. Ascorbic acid, citric acid, EDTA and nitric acid were used successfully for levelling the interfering effects from the cations.

Few serious cation interferences have been reported in the determination of lead by atomic absorption spectrometry (a.a.s.) in an air—acetylene flame [1—4]. However, in direct application of the method to soils, minerals and alloys, the nature and complexity of the sample matrix together with the methods employed in treating and dissolving the sample may drastically affect the lead absorbance. For example, Price [1] stated that the presence of 1 mg ml^{-1} of iron enhances the signal from 5 μg ml^{-1} lead by 35% in a fuel—lean air—acetylene flame. Jederzejewska and Malusecka [2] studied the interfering effects of 5 mg ml^{-1} lanthanum, zirconium and iron used as carriers in preconcentration by co-precipitation. Li Qiying [3] reported that iron, aluminium and alkali and alkaline earth metals interfere in an air—acetylene flame, but this interference can be avoided by liquid—liquid extraction. Nakahara and Musha [4] concluded that the presence of elements such as aluminium, boron or silicon in the aqueous sample solution depresses the atomic absorption signal of lead at 217 nm. However, additions of calcium, potassium or particularly magnesium, decrease the depressant effect. Thus the strong effect of aluminium (100 μg ml^{-1}) on the absorbance of lead (4 μg ml^{-1}) is completely eliminated by the addition of magnesium (1 mg ml^{-1}) as its chloride. It is not clear, therefore, why alkali and alkaline earth metals have depressive effects yet can be used as releasing agents.

The atomic absorption inhibition titration (a.a.i.t.) was introduced by Looyenga and Huber [5] and was developed for indirect determination of anions [6—8], but few recent reports have been published, probably because of inadequate reproducibility. However, the recent introduction of the

0003-2670/84/$03.00

reproducible continuous titration device by Posta and Lakatos [9] for the study of interference problems facilitates the study of interference of iron, aluminium, barium and calcium on the determination of lead, which is reported in this paper. In addition, suitable levelling agents and conditions have been sought in order to eliminate variable interference effects.

EXPERIMENTAL

Instrumentation

A Pye-Unicam SP-191 atomic absorption spectrometer and a Philips x—y recorder model PM 8131 were used. A Pye-Unicam lead hollow-cathode lamp operated at 3.5 mA and 217 nm together with a conventional 10-cm slit burner head for the air—acetylene flame were also used. For all measurements, the optimal experimental parameters were as follows: burner height 10 mm, monochromator slit width 0.8 nm, fuel and air flow rates of 1.0 and 5.5 l min^{-1}, respectively, and rate of delivery for both titration and aspiration constant at 4.0 ml min^{-1}.

The linear titration device adopted by Posta and Lakatos [9] was used with the slight modification of replacing the metal capillary which was fixed into the ground-glass stopper through an inserted rubber plug by a chromium-nickel steel micro-syringe (0.20 mm i.d.). This was directly fastened by an inert substance to a glass capillary tube (1.0 mm i.d.) which was centrally fixed through a ground-glass stopper. The tip in the titration mixing vessel was placed 2 cm above the bottom of the vessel in order to allow for free stirring and to be capable of handling volumes as small as 10 ml.

Reagents

All solutions were prepared from analytical-reagent grade chemicals and deionized water. Glassware was treated overnight with (1 + 1) nitric acid before use. A standard solution of lead (1000 μg ml^{-1}) was prepared from lead nitrate, and standardized by EDTA titration. All interfering cation solutions (10 mg ml^{-1}) were prepared from the corresponding nitrates. Standard solutions of levelling agents (10 mg ml^{-1}) were prepared from the dried substances, except for nitric acid which was prepared by appropriate dilution.

Procedure

In the linear titration device [9], the titrating vessel is filled with about 40 ml of 10 μg ml^{-1} lead (nitrate) solution. The delivery vessel is charged with 30 ml of a mixed solution containing the interfering cation and 10 μg ml^{-1} lead.

The system is arranged so that a hole in the ground-glass stopper is left open. After the spectrometer, recorder and magnetic stirring under the titration vessel have been turned on, the assembly is connected to the spectrometer and the solution is nebulized in the flame, so that only the absorp-

tion signal from lead nitrate alone is recorded. The aspiration process is allowed to continue until the volume in the titration mixing vessel has reached 35 ml. At this time, the system is closed by turning the ground-glass stopper 90° to block the hole and allow the titration process to proceed. The recorder thus shows the influence of the titrant on the absorption signal of the titrated lead solution.

In further experiments, the same sequence of steps was followed, but the solution of interfering cation was replaced by a solution of levelling agent mixed with the same solution of lead being titrated. Likewise, mixed solutions of interfering cation (50 μg ml^{-1}) and levelling agent (1000 μg ml^{-1}) together with the lead solution were added to the delivery vessel, in order to establish the effect of the levelling agent on that of the interfering cation.

RESULTS AND DISCUSSION

Numerous substances have commonly been used as releasing agents in atomic absorption spectrometry [1, 10]. Their main function is to eliminate the suppression of the analyte signal caused by the formation of non-atomized species. Releasing agents were formerly defined [10] as "those compounds which when added in sufficient quantity in the presence of interferents, will restore the absorption magnitude of the analyte signal to its original values without interferents". Experience has shown that it is not always possible to find substances which precisely fit this restrictive definition. Most probably, when these substances are added in excess, they remove the interfering effects of matrix components but themselves influence the analyte signal, so that the signal is not precisely restored to its original value. This combined effect provides an analyte absorbance of constant value, and levels off the interfering effects of matrix components. It is suggested here that it is more practical and realistic to define such substances as levelling agents rather than releasing agents.

Effects of cationic interferents

The titration curves shown in Fig. 1 indicate the individual interfering effects of solutions of iron, barium, aluminium and calcium ions used as nitrates on the absorbance obtained from a 10 μg Pb^{2+} ml^{-1} solution. Iron interferes most strongly, especially at high concentrations. At 250 μg Pb^{2+} ml^{-1}, the interference of iron has reached its maximum value at ca. 13 μg ml^{-1}, at which stage it has enhanced the absorbance of lead by nearly 50%. Such great enhancement of smaller concentrations of lead is not achieved by this concentration of iron, nor is a maximum enhancement achieved.

It is well established that cationic interferences occur as a result of the combination of many factors [3, 4], but the mechanism of these effects has generally been investigated in terms of interactions between the analyte and matrix components in the gas phase in the flame. Because all the other experimental parameters were kept constant throughout the investigation

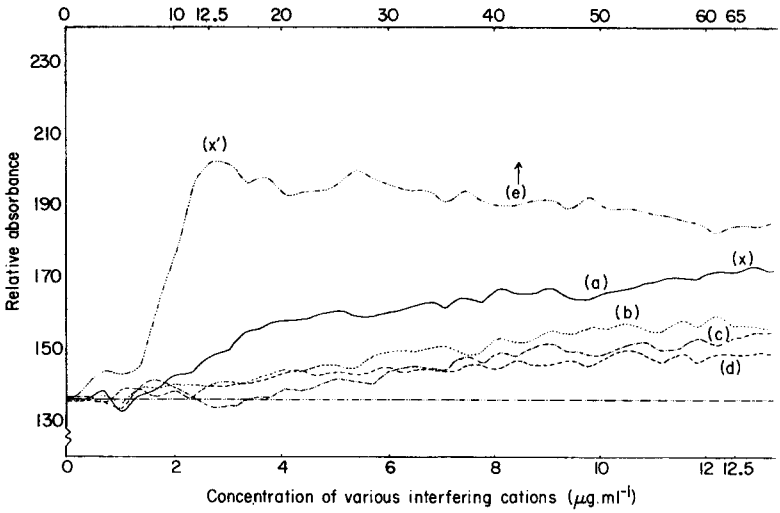

Fig. 1. Effect of 50 μg ml^{-1} solutions of (a) Fe^{3+}, (b) Ba^{2+}, (c) Al^{3+}, (d) Ca^{2+}, on the absorbance of 10 μg Pb^{2+} ml^{-1}. (e) Effect of Fe^{3+} on 250 μg Pb^{2+} ml^{-1}. (The horizontal line is the absorbance of Pb^{2+} alone.)

(i.e., rate of stirring, flame conditions and rates of delivery and aspiration), the different extent of enhancement observed for the two lead concentrations can only be explained on the basis of kinetic factors, such as the rate of interaction between lead and iron species in solution within the titrating vessel, and importantly, in the flame.

Effects of levelling agents

Figure 2 shows the titration profiles which indicate the characteristic effects of a number of levelling agents (1000 μg ml^{-1}) on the absorption signal from a 10 μg ml^{-1} solution of lead. Although the shape of the curves obtained near the beginning of the titration differs for each additive, beyond a certain concentration of each titrant, lead absorption becomes constant. Thus each additive may successfully be used as a levelling agent. The relative absorbance at the plateau regions is greater than those in Fig. 1 obtained with cationic interferents. There are two possible reasons for this. Firstly, the levelling agent may affect the lead signal because of some contaminants it possesses. Secondly, more favourable conditions for the formation of lead atoms occur in the flame in the presence of excess of these additives. Direct aspiration of the levelling agents into flame in the absence of the lead solution in the titrant gave no change in the lead signal. This rules out the first possibility.

Figure 2 shows that the titration curve for lead with nitric acid differs significantly in shape and degree of enhancement from those obtained with other levelling agents. This curve was repeated on different samples of A.R. nitric acid obtained from different reputable suppliers. They always

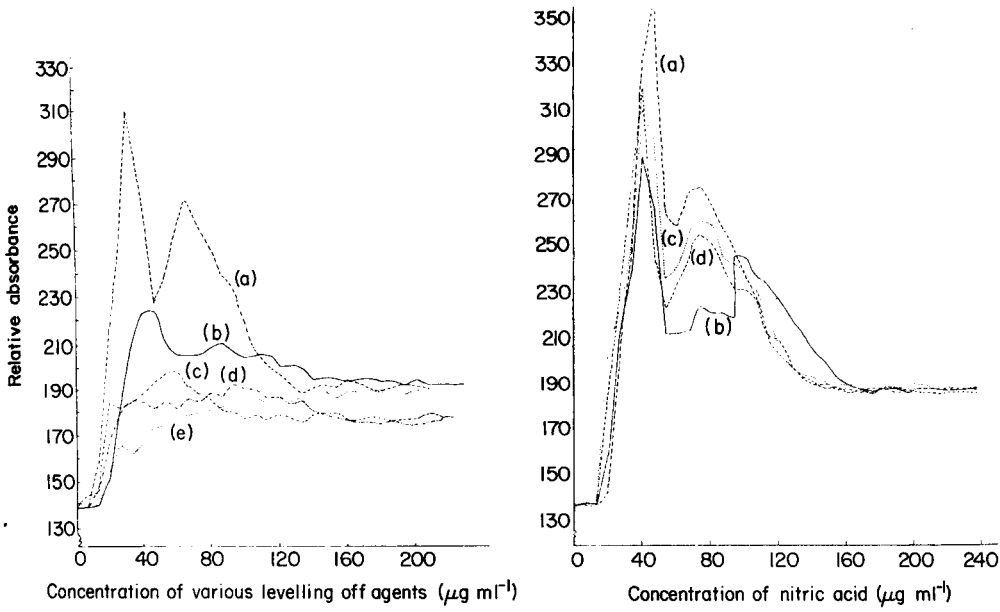

Fig. 2. Effects on absorbance of 10 μg Pb^{2+} ml^{-1} of 1000 μg ml^{-1} of: (a) nitric acid; (b) EDTA; (c) citric acid; (d) ascorbic acid; (e) potassium citrate.

Fig. 3. Effect of nitric acid on absorbance of 10 μg Pb^{2+} ml^{-1} in the presence of 10 μg ml^{-1} of: (a) Al^{3+}; (b) Fe^{3+}; (c) Ba^{2+}; (d) Ca^{2+}.

gave the same pattern of response as that shown in Fig. 2, with maxima always at 34 and 68 μg HNO_3 ml^{-1}.

Effect of levelling agents on interferents

Figure 3 shows the titration curves illustrating the effects of nitric acid on 10 μg ml^{-1} lead solution in the presence of various interferents. Figure 4

TABLE 1

Minimum concentrations of reagents required to level off the effects of interferents on 10 μg Pb^{2+} ml^{-1}

Levelling agent	Levelling agent conc. (μg ml^{-1}) needed[a]			
	Al^{3+}	Fe^{3+}	Ba^{2+}	Ca^{2+}
Nitric acid	150	170	165	165
EDTA	40	200	155	220
Citric acid	100	90	115	120
Ascorbic acid	30	40	30	50
K citrate	—	130	75	80

[a]Each interferent at 50 mg l^{-1}.

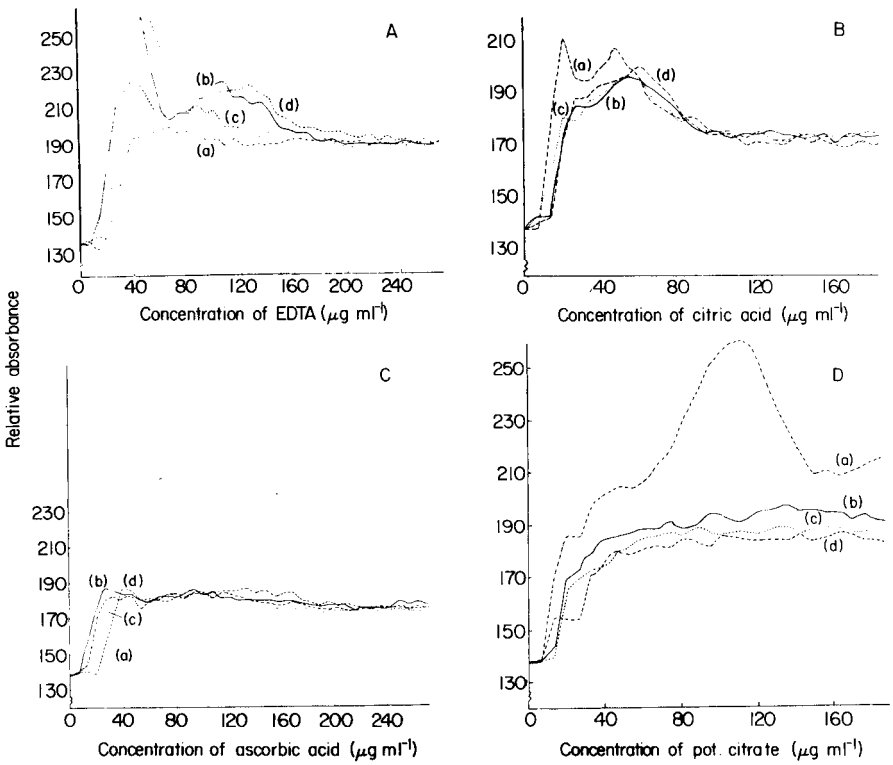

Fig. 4. Effects of other levelling agents on absorbance of 10 μg Pb^{2+} ml^{-1} in the presence of the metals specified in Fig. 3. Agent: (A) EDTA; (B) citric acid; (C) ascorbic acid; (D) potassium citrate.

shows similar curves for EDTA, citric acid, ascorbic acid and potassium citrate, respectively. These curves generally reflect the different capabilities of the various levelling to level off the lead absorbance in the presence of some interfering cations. Table 1 summarizes the minimum concentration of the reagents required for levelling the interfering effects of the different cations. Ascorbic acid can be considered to be the most effective levelling agent. It is interesting that compounds such as ascorbic acid and EDTA have also been found significantly to enhance lead atom production in carbon-furnace atomic absorption spectrometry [11]. Although nitric acid at low concentrations shows abnormal behaviour, it can be regarded as a good levelling agent at $\geqslant 150$ μg ml^{-1}. Figure 4D indicates that potassium citrate is not an effective levelling agent for aluminium interference. Citric acid and EDTA at higher concentrations also effectively stabilize the lead signal, in the presence of all the interferents investigated.

The authors express their appreciation for the valuable assistance offered by the National Center for Radiation Research and Technology.

REFERENCES

1 W. J. Price, Spectrochemical Analysis by Atomic Absorption, Heyden, London, 1979, p. 316.
2 H. Jederzejewska and M. Malusecka, Chem. Anal., 21 (1976) 585.
3 Li Qiying, Fenxi Huaxue, 9 (1981) 718.
4 T. Nakahara and S. Musha, Appl. Spectrosc., 29 (1975) 352.
5 R. W. Looyenga and C. O. Huber, Anal. Chem., 43 (1971) 498.
6 R. W. Looyenga and C. O. Huber, Anal. Chim. Acta, 55 (1971) 197.
7 C. I. Lin and C. O. Huber, Anal. Chem., 44 (1972) 2200.
8 W. E. Crawford, C. I. Lin and C. O. Huber, Anal. Chim. Acta, 64 (1973) 387.
9 J. Posta and J. Lakatos, Spectrochim. Acta, Part B, 35 (1980) 601.
10 J. A. Dean, Flame Emission and Atomic Absorption Spectroscopy, Vol. I (Theory), M. Dekker, New York, 1969.
11 F. Dolinsek and J. Stupar, Analyst (London), 98 (1973) 841.

Analytica Chimica Acta, 165 (1984) 121—130
Elsevier Science Publishers B.V., Amsterdam — Printed in The Netherlands

SUPPRESSION OF INTERFERENCES IN THE DETERMINATION OF LEAD IN NATURAL AND DRINKING WATERS BY GRAPHITE-FURNACE ATOMIC ABSORPTION SPECTROMETRY

PREM R. STHAPIT and JOHN M. OTTAWAY

Department of Pure and Applied Chemistry, University of Strathclyde, Glasgow G1 1XL (Great Britain)

DAVID J. HALLS* and GORDON S. FELL

Trace Metals Unit, Department of Biochemistry, Royal Infirmary, Glasgow G4 0SF (Great Britain)

(Received 15th May 1984)

SUMMARY

The problem of matrix interference encountered in the determination of lead in natural and drinking waters by graphite furnace atomic absorption spectrometry is examined by looking at the individual effects of various constituent salts (NaCl, KCl, $MgCl_2$ and $CaCl_2$, Na_2SO_4, KH_2PO_4 and $Mg(NO_3)_2$), of which $MgCl_2$ and Na_2SO_4 interfered most severely. The use of the L'vov platform decreased the sulphate interference, but was not successful in removing the other interferences. The mixture of 0.05% (w/v) lanthanum (as $LaCl_3$) and 1% (v/v) nitric acid previously proposed for wall atomisation was found to be effective in controlling the interferences. Nitric acid alone removed almost completely the effects of $MgCl_2$ and $CaCl_2$, but had little effect on the interference of sulphate, which required the addition of lanthanum for suppression. The removal of interferences in real water samples by the lanthanum/nitric acid mixture is demonstrated by comparison of results obtained by this approach with those obtained by atomic fluorescence spectrometry and by flame atomic absorption spectrometry after preconcentration by evaporation.

Its advantages make atomic absorption spectrometry (a.a.s.) an obvious choice for the determination of lead in waters. Flame a.a.s., however, is not sufficiently sensitive for direct determination, and requires the use of preconcentration techniques. Graphite furnace a.a.s. (g.f.a.a.s.) has much higher sensitivity which would allow direct determination, but the inorganic constituents of waters interfere with the atomisation of lead causing suppression of the signal [1—4]. The magnitude of the suppression appears to vary from sample to sample and with different designs of graphite furnace [4].

In 1979 the Water Research Centre [1] investigated several methods employing chemical releasing agents to overcome these suppressive interference effects. The releasing agents used, ascorbic acid and sucrose, oxalic acid, ammonium tetramethylenedithiocarbamate, diethylammonium diethyldithiocarbamate and ammonium nitrate, markedly decreased the suppressive effects but the interference was not completely eliminated. The L'vov

0003-2670/84/$03.00

platform [5] has also been used to overcome interferences in the determination of lead. Platform atomisation alone, however, is not successful in decreasing matrix interferences to an acceptable level for the determination of lead in natural waters [6, 7]. Graphite tubes coated with lanthanum or zirconium compounds also markedly decrease but do not eliminate the suppressive effects [1]. Thompson et al. [8] recommended the addition of lanthanum nitrate to standards and samples to overcome the interferences. This idea was taken further by Bertenshaw et al. [4] who found that lanthanum chloride in the presence of excess of nitric acid completely overcame the interferences.

In this paper the interference effects in the determination of lead in waters are examined comprehensively, both for wall atomisation and platform atomisation, by looking at the individual effects of the inorganic constituents of waters. Their suppression by the use of lanthanum chloride and nitric acid is examined and the effectiveness of the treatment assessed by comparison with the results obtained for the analysis by flame a.a.s. and flame atomic fluorescence spectrometry.

EXPERIMENTAL

Instrumentation

The work was carried out using a Perkin-Elmer 2280 spectrometer with an HGA 500 graphite furnace, an AS-1 autosampling system and a Model 56 recorder. Uncoated graphite tubes were used for wall atomisation. L'vov platforms of pyrolytic graphite were used with uncoated graphite tubes having machined retaining grooves, as supplied by Perkin-Elmer. Argon was used as the shield gas. Signal measurements were taken as recorder tracings of peak height. The furnace programs for wall and platform atomization are shown in Tables 1 and 2, respectively. The instrumental conditions were: slit width, 0.7 nm; lamp current, 10 mA; background correction, on; scale expansion, × 1; wavelength, 283.3 nm; sample volume, 20 μl, in all cases.

TABLE 1

Furnace program used for the determination of lead in natural waters, using wall atomization

No.	Step	Temperature (°C)	Time (s)	
			Ramp	Hold
1	Dry	120	2	15
2	Ash	750	10	10
3[a]	Atomise	2300	2	5
4	Clean	2700	2	1

[a] Also programmed in this step: 10 ml min^{-1} internal flow rate, auto zero, record at −2 s.

TABLE 2

Furnace program used for platform atomisation

No.	Step	Temperature (°C)	Time (s)	
			Ramp	Hold
1	Dry	250	10	15
2	Ash	800	10	15
3	Atomise	2300	2	5
4	Clean	2700	2	1

Reagents

The lead nitrate stock solution (1 mg ml^{-1} Pb) and lanthanum chloride (10% La w/v) were atomic spectroscopy grade (BDH), the nitric acid (s.g.1.42) was Aristar grade (BDH). All reagents used in preparing synthetic solutions and interference studies were AnalaR (BDH).

To simulate natural waters synthetic solutions were prepared containing 100 $\mu g\ l^{-1}$ Pb, with additions of the major inorganic constituents likely to be present in natural waters. The composition (g l^{-1}) of synthetic solution I used for optimisation of the furnace operating conditions was $MgCl_2$ (10), NaCl, KCl, $Al_2(SO_4)_3$, NH_4NO_3, $FeCl_3$ and KH_2PO_4 (all 2.5). Synthetic solution II used for optimisation of lanthanum and nitric acid concentrations and for the recovery test contained (mg l^{-1}) Ca^{2+}, Mg^{2+}, Na^+ and K^+ (all 500), Al^{3+} (250), PO_4^{3-} (200), NH_4^+ (250), Fe^{3+} (40), Cl^- (2740), SO_4^{2-} (1792) and NO_3^- (722).

Sample preparation and preservation

Water samples (30 ml) were collected in plastic containers (Universal Containers, Sterilin, England) and acidified with nitric acid (300 μl) to give a final acid concentration of 1% (v/v). The sample thus acidified when stored at 4—10°C did not show a change in lead concentration over four weeks. The required amount of lanthanum chloride was added immediately before analysis. Turbid samples were first centrifuged and the clear supernatant layer was removed and treated with nitric acid and lanthanum chloride.

Calibration was made with standard solutions in 1% nitric acid and 0.05% lanthanum for drinking water and in 5% nitric acid and 0.1% lanthanum for river water, borehole water and other waters containing large amounts of dissolved solids.

RESULTS AND DISCUSSION

Furnace program

The conditions for the furnace program were evaluated using three solutions, deionised water, a river water sample and synthetic solution I (see Experimental), each containing 100 $\mu g\ l^{-1}$ Pb with 0.05% lanthanum (w/v)

and 1% nitric acid (v/v). There was very little difference between the three solutions in terms of optimum furnace parameters; in each case the optimum ashing temperature was 750°C. The recommended furnace programs are presented in Table 1 for wall atomization and Table 2 for platform atomization.

Interferences

The effect of the total sample matrix is illustrated by the results in Table 3. A number of different water samples and synthetic solution II were analysed for apparent lead concentration by flame atomic fluorescence spectrometry and by g.f.a.a.s., with direct measurement against aqueous standards with no matrix modification. To the drinking waters, river waters and synthetic matrix, lead was added to ensure a measurable concentration. The atomic fluorescence method has been shown to be free of interferences [9—11], so the degree of suppression of the furnace measurements can be evaluated from the two sets of results. Signal suppression varied from 4 to 83%.

As in previous studies [4, 8, 13], a number of water samples were analysed for their major constituents and the degree of suppression of the lead signal was measured. The correlation between sample composition and suppression was not at all clear. Bertenshaw et al. [4] noted an apparent correlation between increasing hardness of the water and suppression. In a later paper [12] they found a better correlation with sulphate concentration and concluded that sulphate concentration was the dominant factor. The present results failed to show this correlation. For example, two samples containing 10 and 287 mg l^{-1} SO_4 showed similar suppressions of 58 and 61% respectively. Regan and Warren [13] found no simple correlation between any of

TABLE 3

Suppression of lead response by sample matrices for g.f.a.a.s. analysis compared with results obtained by atomic fluorescence spectrometry (a.f.s.)

Water type		Lead added ($\mu g\ l^{-1}$)	Total lead ($\mu g\ l^{-1}$)		Suppression (%)
			a.f.s.	g.f.a.a.s.	
Drinking	I	50	55	23	58
	II	50	78	59	24
	III	50	85	41	52
	IV	50	51	48	6
River	I	50	59	27	54
	II	50	98	38	61
	III	50	180	135	25
Waste	I	0	1.46×10^3	1.40×10^3	4
	II	0	81	28	65
	III	0	76	35	54
	IV	0	58×10^3	50×10^3	13
Synthetic		100	106	18	83

the matrix constituents of the waters examined and the degree of suppression.

Because of these difficulties in evaluating the effect of the complete matrix, it was thought to be better to look at some of the individual components of the matrix to investigate the degree of interference and how it could be suppressed. Figure 1 (A—G) shows respectively the interference effects of sodium, potassium, magnesium and calcium chlorides, sodium sulphate, potassium dihydrogenorthophosphate and magnesium nitrate. All the chlorides caused some suppression of the signal, the most severe being that of magnesium chloride with almost complete suppression at 10 g l^{-1} (Fig. 1C). Similarly large interference is shown by sodium sulphate (Fig. 1E), which causes significant suppression even at the 0.1 g l^{-1} level. Similar effects were given by aluminium sulphate (not shown) which is added to many Scottish water supplies to coagulate colloidal colouring matter. The interference of phosphate (Fig. 1F) becomes severe only at very high concentrations (above 1 g l^{-1}). Nitrate causes no interference, however, the effect of magnesium nitrate (Fig. 1G) contrasting quite markedly with the effect of magnesium chloride (Fig. 1C). From these results, it appears that the principal interference comes from chloride, especially as magnesium chloride, and from sulphate.

Magnesium chloride has been shown to cause vapour-phase interference [14, 15]. Manning and Slavin [7], however, have reported that magnesium chloride lowered the temperature at which lead could be lost and ascribed the interference in part to losses during the ashing stage. The interference of magnesium chloride at different ashing temperatures in the range 100—750°C was therefore investigated in this study, but no difference in the nature of the interference was observed.

The reason for the sulphate interference is not clear. Bertenshaw et al. [12] suggest that sodium sulphate, which is stable at relatively high temperatures, physically inhibits lead atomisation. According to Vollkopf et al. [16], sulphate causes a delay in the atomisation peak which is due to the great stability of lead sulphate, which is even more stable than lead phosphate. At an ashing temperature as high as 1000°C only minor losses of lead were seen in the presence of sulphate [16].

Suppression of interferences

The L'vov platform. The results (Fig. 1A—D) show that, under the conditions used, the platform alone is not effective in removing most of the interference from chlorides; in most cases, the interference curve parallels that found for wall atomisation. For potassium chloride, however, the interference was completely removed. No improvement was found for phosphate (Fig. 1F), but the platform is effective in decreasing interference from sulphate (Fig. 1E).

Slavin and Manning [5] showed that the platform was very effective in removing sulphate interference, moderately effective in decreasing the effect

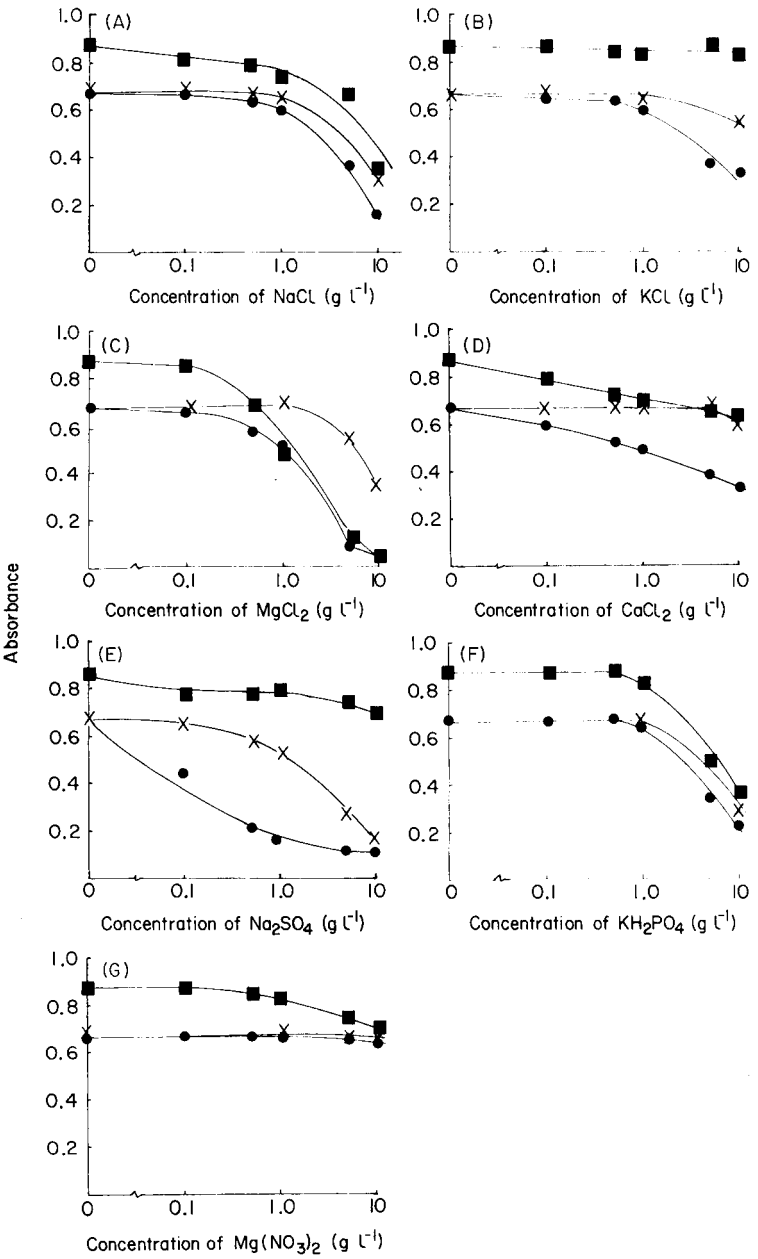

Fig. 1. The effect of: (A) NaCl; (B) KCl; (C) $MgCl_2$; (D) $CaCl_2$; (E) Na_2SO_4; (F) KH_2PO_4; (G) $Mg(NO_3)_2$, on the determination of lead (100 μg l^{-1}) using: (•) wall atomisation; (■) platform atomisation; (×) wall atomisation with added 0.05% La^{3+} and 1% HNO_3.

of chloride (as NaCl) and only slightly effective in removing the effect of phosphate. For practical water analysis, the additional use of a matrix modifier ($Mg(NO_3)_2$ + $NH_4H_2PO_4$) was recommended [7]. Chakrabarti et al. [17] have shown that for successful decrease of interferences in lead determination by use of the platform alone, isothermal conditions should be reached. This is achieved by a low ashing temperature, a fast wall heating rate and a low atomisation temperature.

Lanthanum and nitric acid. Bertenshaw et al. have demonstrated [4, 12] that a mixture of lanthanum chloride and nitric acid is effective in overcoming matrix interference from material in waters, even for those with high total hardness and high sulphate concentration. The effect of their mixture, 0.05% (w/v) lanthanum and 1% (v/v) nitric acid, on the individual interferences, using wall atomisation, is shown in Fig. 1. The treatment is effective in removing the interferences up to a concentration of 1 g l^{-1} in all cases except sulphate. The sulphate interference is much decreased by the lanthanum and nitric acid but only completely removed up to a concentration of 0.1 g l^{-1} sodium sulphate (Fig. 1E). With more concentrated suppressant, 0.1% lanthanum and 5% nitric acid, the interference is removed up to a concentration of 1 g l^{-1} (Fig. 3).

The contribution of nitric acid to the removal of the interference of magnesium chloride is seen in Fig. 2. Nitric acid completely removes the interference up to a concentration of 1 g l^{-1} $MgCl_2$. The addition of 0.05% lanthanum only slightly improves the situation at higher concentrations.

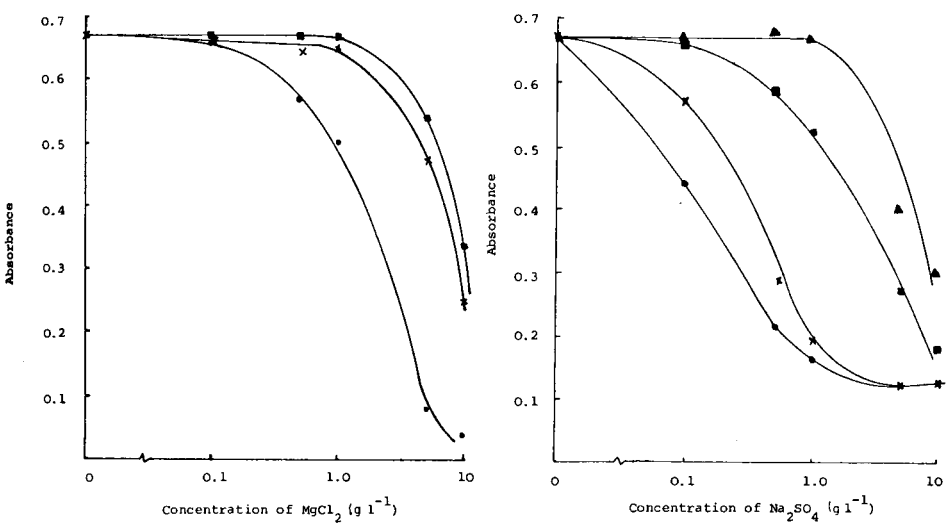

Fig. 2. The effect of $MgCl_2$ on the signal from 100 μg l^{-1} Pb^{2+}: (•) alone; (×) with 1% HNO_3 present; (▪) with 1% HNO_3 and 0.05% La^{3+} present.

Fig. 3. The effect of Na_2SO_4 on the signal from 100 μg l^{-1} Pb^{2+}: (•) alone; (×) with 1% HNO_3 present; (▪) with 1% HNO_3 and 0.05% La^{3+} present; (▲) with 5% HNO_3 and 0.1% La^{3+} present.

With a stronger acid concentration (5%) and 0.1% lanthanum, suppression of the interference is achieved up to 10 g l^{-1}. Nitric acid acts by converting magnesium chloride to magnesium nitrate allowing the chloride to be driven off as hydrogen chloride in the ashing step. As can be seen in Fig. 1G, magnesium nitrate causes no interference in lead determinations.

Bertenshaw et al. [12] claim that the interference from calcium chloride is different since it is not affected by nitric acid. The present results, however, showed that 1% nitric acid removed the interference exactly as for magnesium chloride.

Nitric acid makes only a small contribution to the suppression of interference of sulphate (Fig. 3), the principal effect being due to lanthanum. Thus the addition of both lanthanum and nitric acid is necessary to overcome interferences in water samples. The relative contributions of lanthanum and nitric acid to the suppression of interferences will depend on the relative contributions of the chloride and sulphate type of interference. For example, with synthetic solution II, the recovery of lead was improved from 15% to 92% by addition of nitric acid alone; presumably the chloride interference was dominant. Bertenshaw et al. [12] found that for 11 real samples the addition of nitric acid alone gave recoveries in the range 40—89%.

An exact interpretation of the magnitude of the suppression in terms of the matrix composition of a water sample is difficult for two reasons. Firstly, it is unlikely that the suppressive effects are completely reproducible. As others [5, 15] have found, the interference effects on lead can depend greatly on the condition of the graphite tube and its previous history. Secondly, as is seen in the effect of the different chlorides (Fig. 1A—D), the effect of chloride depends greatly on the cation with which it is associated. Sulphate interferences are likely to be similarly affected. Thus the interference should be determined not by a single ion, but the predominant combination of cation and anion.

Although there are still many unanswered questions about interferences in the determination of lead in water, it is clear from these studies that the combination of nitric acid and lanthanum as proposed previously [4] is a successful interference suppressor. For drinking waters of low to moderate hardness the combination of 0.05% lanthanum and 1% nitric acid is recommended, but for river, borehole and waste waters as well as drinking waters of high hardness, the more concentrated suppressant, 0.1% lanthanum and 5% nitric acid is advisable.

Comparison of results obtained by g.f.a.a.s. using the lanthanum—nitric acid mixture with other methods

The effectiveness of the g.f.a.a.s. method using lanthanum and nitric acid as interference suppressor was compared with two methods of proven reliability: flame a.a.s. after preconcentration by evaporation, the method widely used by water laboratories, and the flame atomic fluorescence method [9, 10]. Twenty-one drinking water samples (containing 0—500 $\mu g\ l^{-1}$ Pb)

analysed by the Strathclyde Regional Water Department using the flame a.a.s. procedure were analysed by g.f.a.a.s. after addition of 0.05% lanthanum and 1% nitric acid. A good correlation between the two sets of results was obtained, (r = 0.996, slope of line of best fit 0.96 ± 0.02, intercept on flame a.a.s. axis 3.0 ± 4.1 $\mu g\ l^{-1}$ Pb).

The atomic fluorescence method has been shown to be interference-free and, because of the minimal sample preparation, contamination can be kept to a minimum [11]. Results on the same samples obtained by this method correlated well with the g.f.a.a.s. method (r = 0.996, slope of line of best fit 1.02 ± 0.02, intercept on atomic fluorescence axis 0.4 ± 1.5 $\mu g\ l^{-1}$ Pb.) The comparisons confirm that the lanthanum/nitric acid mixture is successful in controlling interferences in the determination of lead in real water samples.

CONCLUSIONS

The interferences from natural waters in lead determination are confirmed to be principally from sulphate and chloride, of which the most important chloride is magnesium chloride. Although there remain problems in understanding completely the relationship between the complete matrix composition of a water sample and the degree of suppression of the lead signal, it is apparent that it is the combination of cations with chloride and sulphate that plays the critical role. The interference of sulphate on lead determination has not been satisfactorily explained. The suggestion of Bertenshaw et al. [12] that sodium sulphate physically inhibits lead atomisation does not seem consistent with the observed decrease in interference obtained by the use of the platform. This latter observation seems more consistent with a vapour phase interference, which nevertheless seems unlikely on a chemical basis.

Although the use of the platform was successful in decreasing sulphate interference, it did not control the other interferences and would require the use of a matrix modifier as Manning and Slavin [7] suggest. Since, however, the use of the matrix modifier, lanthanum and nitric acid, effectively controls interferences with wall atomisation, the use of the platform seems an unnecessary complication for a routine method.

It is shown that the nitric acid essentially controls the chloride interferences while the lanthanum removes the sulphate interference. The mode of action of the lanthanum is still unclear. According to Thompson et al. [8], the lanthanum may delay the atomisation of lead atoms in the sample so that they vaporise later than the interfering matrix components.

Comparison with two other methods, flame a.a.s. after preconcentration by evaporation and flame atomic fluorescence spectrometry prove that the lanthanum—nitric acid mixture effectively overcomes the interference effects in real samples, as Bertenshaw et al. have also shown [4]. The method proposed by them [4] is simple, straightforward and rapid and has proved a satisfactory replacement for a liquid—liquid extraction/g.f.a.a.s. method formerly used at the Royal Infirmary.

We are grateful to Mr. S. Davis of Strathclyde Regional Council Water Department, Glasgow, for providing analysed water samples, to Dr. P. I. Smith of the Regional Chemist and Analyst Department, Glasgow and Dr. G. Best of the Clyde River Purification Board, East Kilbride, for water samples, and to the Ministry of Overseas Development for financial support for PRS under the Colombo Plan.

REFERENCES

1 D. T. E. Hunt, R. L. Norton, B. Orpwood and D. A. Winnard, The determination of lead in drinking water by graphite furnace atomic absorption spectrometry, Water Research Centre, Technical Report ER 710, Medmenham, UK, 1979.
2 R. P. Mitcham, Analyst (London), 105 (1980) 43.
3 J. G. T. Regan and J. Warren, Analyst (London), 101 (1976) 220.
4 M. P. Bertenshaw, D. Gelsthorpe and K. C. Wheatstone, Analyst (London), 106 (1981) 23.
5 W. Slavin and D. C. Manning, Anal. Chem., 51 (1979) 261.
6 M. L. Kaiser, S. R. Koirtyohann and E. H. Hinderberger, Spectrochim. Acta, Part B, 36 (1981) 773.
7 D. C. Manning and W. Slavin, Appl. Spectrosc., 37 (1983) 1.
8 K. C. Thompson, K. Wagstaff and K. C. Wheatstone, Analyst (London), 102 (1977) 310.
9 P. R. Sthapit, J. M. Ottaway and G. S. Fell, Anal. Proc., 20 (1983) 599.
10 P. R. Sthapit, J. M. Ottaway and G. S. Fell, Analyst (London), 108 (1983) 235.
11 P. R. Sthapit, J. M. Ottaway and G. S. Fell, Analyst (London), 109 (1984) 1061.
12 M. P. Bertenshaw, D. Gelsthorpe and K. C. Wheatstone, Analyst (London), 107 (1982) 163.
13 J. G. T. Regan and J. Warren, Analyst (London), 103 (1978) 447.
14 J. M. Ottaway, Proc. Anal. Div. Chem. Soc., 13 (1976) 185.
15 C. W. Fuller, At. Absorpt. Newsl., 16 (1977) 106.
16 U. Vollkopf, Z. Grobenski, and B. Welz, At. Spectrosc., 4 (1983) 165.
17 C. L. Chakrabarti, S. Wu and P. C. Bertels, Spectrochim. Acta, Part B, 38 (1983) 1041.

Analytica Chimica Acta, 165 (1984) 131—140
Elsevier Science Publishers B.V., Amsterdam — Printed in The Netherlands

DETERMINATION OF SELENIUM IN HUMAN BODY FLUIDS BY HYDRIDE-GENERATION ATOMIC ABSORPTION SPECTROMETRY
Optimization of Sample Decomposition

BERNHARD WELZ* and MARIANNE MELCHER

Department of Applied Research, Bodenseewerk Perkin-Elmer & Co. GmbH, D-7770 Überlingen (German Federal Republic)

JEAN NÈVE

Laboratory of Analytical Chemistry and Toxicology, Free University of Brussels, Campus Plaine 205-1, B-1050 Brussels (Belgium)

(Received 1st May 1984)

SUMMARY

The accuracy of the determination of selenium in human body fluids by hydride-generation a.a.s. depends critically upon the sample decomposition-method used. Digestion with HNO_3 alone gave low selenium recoveries, but with nitric, sulfuric and perchloric acids at a final temperature of 310°C gave results that agreed with those obtained by other techniques. The recovery of selenomethionine added to whole blood and of trimethylselenonium iodide added to urine was 97—104%. The average selenium values found for 6 healthy individuals were 88 $\mu g\ l^{-1}$ in whole blood, 75 $\mu g\ l^{-1}$ in blood plasma and 307 μg (kg Hb)$^{-1}$ in erythrocytes. A detection limit of 5 $\mu g\ l^{-1}$ Se in body fluids was found under routine conditions.

Selenium has gained substantial interest as an essential trace element for several animals as well as for humans; its accurate determination, however, is still a major challenge for the analyst. Atomic absorption spectrometry (a.a.s.) with hydride generation offers the advantages of excellent sensitivity and relatively simple instrumentation. There is some doubt, however, about the accuracy of the results obtained. Recently we participated in an I.U.P.A.C. interlaboratory trial on the determination of selenium in two lyophilized human blood serum reference materials. The results that we obtained with hydride-generation a.a.s., 69 and 71 $\mu g\ l^{-1}$ [1] were considerably lower than the accepted average value of 91 ± 7 $\mu g\ l^{-1}$ for both serum samples [2]. The mean concentrations for the two samples found by the four laboratories using hydride-generation a.a.s., were 72 and 69 $\mu g\ l^{-1}$. These differ significantly from the overall mean for the remaining laboratories so that a systematic error cannot be excluded.

There are several reports that the sample decomposition technique applied is of great importance for the accuracy of the selenium values obtained in biological materials [3—10]. In the hydride-generation technique, sodium

0003-2670/84/$03.00

tetrahydroborate is added to the acidic sample solution, gaseous hydrogen selenide is formed, stripped from the solution and atomized in a heated quartz cell. For this reaction, it is essential that selenium is present as selenite. Organic selenium compounds must be decomposed completely for the successful application of this technique.

Many selenium compounds are volatile and can be lost during a poorly controlled destruction procedure. On the other hand, acid-resistant organoselenium compounds, such as selenomethionine, selenocysteine and the trimethylselenonium ion, are not fully decomposed, hence causing low results [3, 4]. A digestion with nitric acid alone is apparently insufficient, and is responsible for low selenium values found in some earlier work.

Kotz et al. [5] investigated the decomposition of biological materials, including blood, with nitric acid under pressure in a PTFE tube and found quantitative recoveries for selenium by a tracer method. This could not be confirmed by Verlinden [4], however, who reports only 60% recovery for selenium in blood after a pressure decomposition with nitric acid. Lloyd et al. [6] applied a digestion with nitric and sulfuric acids at 155° C for the determination of selenium in whole blood, plasma and erythrocytes. Brown et al. [7] analyzed whole blood, plasma and urine for selenium after a digestion with nitric and perchloric acids at temperatures up to 200° C. A mixture of nitric and perchloric acids at 210° C was also applied by Clinton [8] to decompose blood samples prior to the determination of selenium by hydride-generation a.a.s. A graded destruction with nitric and perchloric acids up to a final temperature of 210° C was also recommended by Verlinden [4]. This author found it necessary, however, to use digestion times of 15 to 30 h for complete decomposition of human blood and plasma. Robbins et al. [9] applied a mixture of nitric, sulfuric and perchloric acids (4 + 4 + 1) for the digestion of blood samples. The same acids but a more elaborate temperature program was proposed by Oster and Prellwitz [10]. Serum was heated to 180° C with a mixture of nitric and perchloric acids in an automatic digester. After the addition of sulfuric and nitric acids, the temperature was raised to 300° C and kept at this level until the solution was clear. Whenever perchloric acid is applied, selenium is partly oxidized to selenium(VI). A reduction step is therefore included after the digestion, and most authors simply heat the solution with 5—6 M hydrochloric acid for 15 to 30 min for this purpose.

In the present work we have investigated the influence of the sample decomposition technique on the accuracy of the selenium values obtained by hydride-generation a.a.s. A lyophilized human blood serum reference material was investigated as well as whole blood, plasma, erythrocyte and urine samples. A nitric acid digestion under normal and under elevated pressure and temperature was compared with a nitric, sulfuric and perchloric acid treatment applied successfully for the decomposition of marine biological tissue samples [11]. The recovery of selenomethionine added to whole blood and of trimethylselenonium iodide added to urine was tested. Some of

the samples were analyzed by an acid digestion/liquid—liquid extraction/graphite-furnace a.a.s. procedure described elsewhere [3, 12] to confirm the accuracy of the results.

EXPERIMENTAL

Apparatus

A Perkin-Elmer Model 4000 atomic absorption spectrometer, equipped with an electrodeless discharge lamp for selenium, operated from an external power supply at 6 W, was used throughout. A spectral slit-width of 2.0 nm was used to isolate the 196.0 nm resonance line. The signals were recorded with a Perkin-Elmer Model 56 strip chart recorder. A Perkin-Elmer Model MHS-20 Mercury/Hydride System was operated at a quartz cell temperature of 900° C. The time settings at the controller were 40 s PURGE I, 8 s REACT (during this time, sodium tetrahydroborate solution is injected into the sample solution continuously) and 30 s PURGE II.

A Perkin-Elmer Autoclave-3, heated on a hot plate with temperature control, was used for pressure decompositions. Nitric, sulfuric and perchloric acid digestions were carried out in graduated quartz flasks with a long neck and a nominal volume of 40 ml (Kürner Analysentechnik, Rosenheim, F.R.G.) which are described in detail elsewhere [13]. The flasks were heated in a home-made aluminum heating block for 6 digestion flasks. The temperature was controlled by a thermostat from a Perkin-Elmer Model F 20 gas chromatograph.

Reagents

Sodium tetrahydroborate(III) solution, 3% (w/v), was prepared by dissolving sodium tetrahydroborate powder (Riedel-de-Haen) in deionized water and stabilizing with 1% (w/v) sodium hydroxide. The solution was filtered before use and could be stored for only a few days. Hydrochloric acid (32% w/v), perchloric acid (70% w/v) and sulfuric acid (96% w/v) were of Suprapur quality (Merck). Nitric acid (65% w/v) was further purified by subboiling distillation (subboiling still, Kürner Analysentechnik, Rosenheim, F.R.G.).

Stock standard solution (1000 mg l^{-1}) for selenium(IV) was prepared from Titrisol concentrates (Merck) by diluting to volume with deionized water. Working standard solutions were obtained by further dilution with 0.5 M hydrochloric acid. Selenomethionine, $H_2NCH(COOH)CH_2CH_2SeCH_3$, 16.4 mg, was dissolved in 50 ml of (1 + 1) deionized water/methanol. This solution contained 132 mg l^{-1} Se and was diluted 1 + 99 with deionized water before use. Trimethylselenonium iodide, $(CH_3)_3SeI$, 35.0 mg, was dissolved in 100 ml of deionized water. This solution contained 110 mg l^{-1} Se, and was diluted 1 + 99 with deionized water before use. Selenomethionine and trimethylselenonium iodide were obtained as described previously [3].

Sample preparation

Lyophilized human blood serum reference material, Seronorm, Batch 103 (Nyegaard & Co., Oslo, Norway) was dissolved in deionized water according to the manufacturer's recommendations. Heparinized whole blood samples were obtained from healthy adult individuals by collecting the blood in heparinized 10-ml PS tubes (Greiner No. 160 151). To obtain blood plasma samples, the heparinized whole blood was centrifuged carefully for 10 min and the supernatant plasma removed with a Pasteur pipette. To obtain pure erythrocytes, the residue was washed by mixing with about 5 ml of isotonic saline; after centrifuging, the upper phase was discarded and the washing procedure repeated. After the last separation, the erythrocytes were diluted to the original 10 ml with isotonic saline and mixed well before analysis.

Nitric acid digestion

Serum or whole blood (0.5 ml) and 0.5 or 1.0 ml of nitric acid were placed in 10-ml volumetric flasks and heated in a boiling water bath for 6 h. After cooling, the solution was diluted to volume with deionized water. For the determination of selenium, 50 ml of 0.5 M hydrochloric acid was placed into the reaction flask of the hydride system and 0.5 ml of the diluted digestion solution (corresponding to 25 μl of serum or whole blood) added. It was not possible to use larger volumes of the digestion solution because of excessive foam formation during the reaction. Calibration solutions were prepared to contain 2, 5 and 10 ng of selenium, respectively, in the solution for measurement.

For some experiments, a nitric acid digestion was carried out under pressure. Whole blood (0.5 ml) and 1 ml of nitric acid were placed in the PTFE beaker of the Autoclave-3 and heated to 160° C for 1 h. After cooling, the solution was transferred to a 10-ml volumetric flask, diluted to volume with deionized water and further analyzed as described above.

Nitric, sulfuric and perchloric acids digestion

Serum, whole blood, plasma or erythrocytes (0.5 ml), or 1.0 ml of urine, and 1.0 ml of nitric acid were placed in the long-necked quartz digestion flasks, heated slowly to 140° C in an aluminum heating block and kept at this temperature for 30 min. After cooling to room temperature, 0.5 ml of sulfuric and 0.2 ml of perchloric acid were added. The temperature was slowly raised to 140° C, 200° C, 250° C and 310° C, and held at each of these temperatures for 15 min before the next increase. The final temperature of 310° C was held for at least 20 min so that most of the perchloric acid was removed and the volume of the digestion solution was decreased to about 0.5 ml. After cooling to room temperature, 20 ml of 5 M hydrochloric acid was added to the digestion solution, which was heated to 95° C and held at this temperature for 20 min to reduce all selenium(VI) to selenium(IV). The solution was allowed to cool to room temperature and diluted to volume (40 ml) with deionized water.

For the determination of selenium, 5 ml of the digestion solution and 15 ml of deionized water were placed in the reaction flask of the hydride system (corresponding to 62.5 μl of serum, whole blood, plasma or erythrocytes and 125 μl of urine). Calibration standards containing 2.5, 5 and 10 ng of selenium were prepared to contain approximately the same concentration of hydrochloric acid as the samples (0.5 M HCl in the solution for measurement). Larger aliquots or even the total volume of the digestion solution can be transferred to the reaction flask of the hydride system when higher sensitivity is required. Alternately, smaller sample volumes and correspondingly larger aliquots of the digestion solution can be applied if only limited amounts of sample are available. Foam formation is not a problem when this perchloric acid digestion procedure is used.

For some experiments, a nitric, sulfuric and perchloric acids digestion was applied at a maximum temperature of 260°C. All experimental conditions were as described above except that the temperature was raised slowly from 200 to 260°C, and held for 35 min at 260°C. This was followed by the reduction with hydrochloric acid as described above. In some experiments, the final reduction step with 5 M hydrochloric acid was omitted.

Determination of haemoglobin

The results for selenium in erythrocytes are expressed in μg of selenium per kg of haemoglobin (Hb). Haemoglobin concentrations were determined by the haemoglobin cyanide method (Merck No. 9405) using a Combur M 1000 photometer.

RESULTS AND DISCUSSION

In a first set of experiments the nitric acid digestion in a boiling water bath was compared with the nitric, sulfuric and perchloric acids digestion at 310°C for the lyophilized blood serum (Seronorm, Batch 103). In six independent digestions with nitric acid an average selenium content of 64 ± 3 $\mu g\ l^{-1}$ was found which is close to the 71 ± 9 $\mu g\ l^{-1}$ found for the material in earlier work [1]. Using the nitric, sulfuric and perchloric acids digestion, however, an average value of 89 ± 3 $\mu g\ l^{-1}$ was obtained which compares favorably with the accepted value of 91 ± 7 $\mu g\ l^{-1}$. This indicates that the low mean obtained in the interlaboratory comparison for this reference material with hydride-generation a.a.s. [2] is not due to systematic errors in the final determination of selenium with this technique, but to an improper acid digestion procedure.

Selenomethionine and the trimethylselenonium ion are among the most acid-resistant compounds found in human body fluids [3, 4]. To further elucidate the influence of the decomposition procedure used prior to the determination of selenium with hydride-generation a.a.s., the recovery of these organoselenium compounds from aqueous solutions was tested, as well as from spiked whole blood and urine. Figure 1 shows the signals obtained

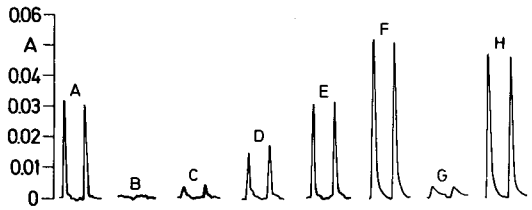

Fig. 1. Absorbance signals showing recovery of organoselenium compounds from aqueous solutions after different acid digestions: (A) reference solution, 8 ng Se(IV); (B—E) selenomethionine, 7.9 ng Se; (B) no digestion; (C) nitric acid in boiling water bath; (D) HNO_3 under pressure; (E) nitric, sulfuric and perchloric acids, 310° C; (F) reference solution, 15 ng Se(IV); (G, H) trimethylselenonium iodide, 13.2 ng Se; (G) no digestion; (H) as (E).

from aqueous solutions of these compounds after different acid digestions in comparison to reference solutions prepared from selenite.

Without digestion, no signal was obtained from selenomethionine. Using a nitric acid digestion, with 6 h on a boiling water bath, or 1 h at 160° C under pressure, the recoveries were 10% and 50%, respectively. Only after a nitric, sulfuric and perchloric acids digestion with a maximum temperature of 310° C was 100% recovery obtained for selenium from selenomethionine as well as from the trimethylselenonium ion. Essentially, the same behavior was found for these organoselenium compounds when added to whole blood or urine samples (Tables 1 and 2). The values found for selenium in a whole blood sample after a nitric acid digestion in a boiling water bath or under pressure were 10 to 15% lower than those obtained after a nitric, sulfuric and perchloric acids digestion. The recoveries of selenomethionine added to this blood sample, however, were only 35 and 77%, respectively, with the two nitric acids digestion procedures, whereas it was always near to 100% for selenomethionine and the trimethylselenonium ion after a nitric, sulfuric and perchloric acid digestion.

For the whole blood sample, with and without added selenomethionine, the need was investigated for a reduction step which is employed by most authors after a perchloric acid digestion to reduce selenium(VI). The results in Table 1 show a clear dependence on the maximum digestion temperature that was used. After a digestion at 260° C the values for selenium originally present in the blood sample and for added selenomethionine were both only 55—60% of the value obtained after reduction with 5 M hydrochloric acid. This indicates that 40 to 45% of the selenium was oxidized to selenium(VI) under these conditions and was not available for determination involving hydride-generation. A reduction step therefore is essential when lower digestion temperatures are applied with perchloric acid.

After digestion with the same acid mixture but at a maximum temperature of 310° C, there was no difference between the results with and without the reduction step. This can be explained by the thermal instability of selenate, which tend to split off oxygen at elevated temperatures to form selenite [14]. In addition, the perchloric acid was driven off almost completely at

TABLE 1

Recovery of selenomethionine (SeMe) added to heparinized whole blood after different acid digestion procedures

Digestion procedure	n[a]	SeMe added ($\mu g\ l^{-1}$ Se)	Se found ($\mu g\ l^{-1}$)[a]	Recovery ($\mu g\ l^{-1}$)	(%)
(1 + 1) HNO_3	6	0	90 ± 3		
95° C, 6 h	6	79	118 ± 4	28	35
(1 + 1) HNO_3	6	0	91 ± 5		
pressure, 160° C	4	79	152 ± 7	61	77
HNO_3, H_2SO_4, $HClO_4$	3	0	62 ± 2		
260° C, no reduction	3	79	106 ± 2	44	56
HNO_3, H_2SO_4, $HClO_4$	6	0	105 ± 1		
260° C, HCl reduction	6	79	182 ± 2	77	97
HNO_3, H_2SO_4, $HClO_4$	3	0	102 ± 1		
310° C, no reduction	3	79	179 ± 4	77	97
HNO_3, H_2SO_4, $HClO_4$	3	0	103 ± 1		
310° C, HCl reduction	3	79	184 ± 2	81	102

[a]Mean ± standard deviation of n digestions.

TABLE 2

Recovery of trimethylselenonium (TMSe) iodide from aqueous solutions, or added to urine, after digestion with nitric, sulfuric and perchloric acids at 310° C, followed by reduction with 5 M hydrochloric acid

Sample	TMSe added ($\mu g\ l^{-1}$ Se)	Se found ($\mu g\ l^{-1}$)[a]	Recovery ($\mu g\ l^{-1}$)	(%)
deionized water	110	111 ± 1	111	101
urine	0	19 ± 1	—	—
urine	110	134 ± 1	115	104

[a]Each result is mean ± standard deviation of 3 digestions.

this temperature so that the digestion solution loses its oxidizing power. A reduction step therefore appears not to be required after a perchloric acid digestion with a maximum temperature of 310° C, but nevertheless it was used in all further experiments as a precautionary measure.

To test the accuracy of the procedure further, the nitric, sulfuric and perchloric acids digestion at 310° C followed by hydride-generation a.a.s., was applied to a number of erythrocyte and urine samples that were prepared and analyzed independently using an acid digestion and liquid—liquid extraction procedure followed by graphite-furnace a.a.s., as described in detail elsewhere [3, 12]. The results are given in Table 3.

TABLE 3

Comparative results for selenium in erythrocytes (E) and urine (U) samples analyzed independently using acid digestion, hydride-generation a.a.s., and acid digestion, liquid–liquid extraction graphite-furnace a.a.s.

Sample	Selenium found[a] ($\mu g\ l^{-1}$)			
	n	hydride generation	*n*	graphite furnace
E-1	3	102 ± 2	5	98 ± 4
E-2	3	74 ± 1	4	70 ± 7
E-3	3	51 ± 1	4	56 ± 5
E-4	3	78 ± 2	2	74 ± 1
E-5	3	94 ± 2	4	87 ± 7
E-6	3	78 ± 2	5	82 ± 6
U-1	3	39 ± 1	3	44 ± 2
U-2	3	50 ± 1	3	49 ± 2
U-3	3	39 ± 1	3	39 ± 3
U-4	3	32 ± 1	3	36 ± 1
U-5	3	33 ± 1	3	36 ± 2

[a]Mean ± standard deviation of *n* digestions.

Finally, heparinized whole blood, plasma and erythrocytes of six healthy, adult individuals (4 male, 2 female) were analyzed using the recommended procedure (Table 4). All determinations, including the acid digestion procedure were run in duplicate and the results were typically in agreement to within 2 ng l^{-1}. The average results (range) for selenium were 88 (78—110) $\mu g\ l^{-1}$ in whole blood, 75 (69—91) $\mu g\ l^{-1}$ in plasma and 307 (265—382) $\mu g\ (kg\ Hb)^{-1}$ in erythrocytes. The average result for selenium in erythrocytes using the graphite-furnace procedure was 300 (225—392) $\mu g\ (kg\ Hb)^{-1}$. It may be of interest that the ratio of the selenium contents of whole blood, plasma and erythrocytes were essentially the same for all six individuals investigated.

Figure 2 shows the peaks obtained for the determination of selenium in six independent decompositions of a serum sample, each one analyzed in duplicate; the relative standard deviation was 2.6%. From these responses, a routine detection limit (2*s*) of 5 $\mu g\ l^{-1}$ Se in serum, whole blood, plasma, erythrocytes or urine samples can be calculated. This limit can be lowered to $<1\ \mu g\ l^{-1}$ in the original sample by applying larger aliquots or using all the digestion solution for the determination. No interferences were found from other constituents of human body fluids, such as iron or copper under the conditions used.

CONCLUSION

Accurate values for selenium in human body fluids can be obtained with hydride-generation a.a.s. when a suitable sample decomposition procedure is

TABLE 4

Selenium determined in whole blood, plasma and erythrocytes of six adult individuals

Subject	Selenium concentration[a]			
	Whole blood ($\mu g\ l^{-1}$)	Plasma ($\mu g\ l^{-1}$)	Erythrocytes (μg (kg Hb)$^{-1}$)	
			hydride generation	graphite furnace
BW (male)	94	75	353	345
GS (male)	82	70	279	275
MM (female)	110	91	382	392
SA (male)	78	71	277	267
SG (female)	82	69	287	297
WE (male)	82	71	265	225

[a]Each value is the mean of 2 determinations (3 or 4 for the graphite furnace procedure).

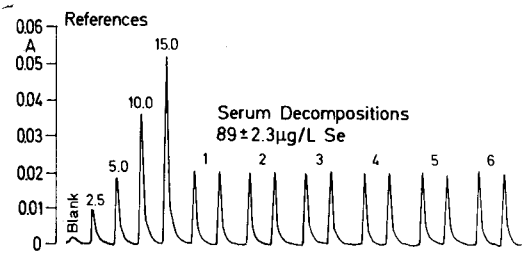

Fig. 2. Routine determination of selenium; (left to right) reagent blank, references with 2.5, 5.0, 10 and 15 ng of Se, and six independent digestions of a serum sample, each one analyzed in duplicate.

applied. The recommended procedure includes a digestion with a nitric, sulfuric and perchloric acids mixture at a maximum temperature of 310° C.

The authors are grateful to Dr. Bantle and his coworkers for taking the blood samples, preparing the plasma and erythrocyte samples and for the determination of the haemoglobin values.

REFERENCES

1 B. Welz, M. Melcher and G. Schlemmer, Fresenius Z. Anal. Chem., 316 (1983) 271.
2 M. Ihnat, M. Wolynetz, Y. Thomassen and M. Verlinden, Pure Appl. Chem., submitted.
3 J. Nève, M. Hanocq, L. Molle and G. Lefebvre, Analyst (London), 107 (1982) 934.
4 M. Verlinden, Talanta, 29 (1982) 875.
5 L. Kotz, G. Kaiser, P. Tschöpel and G. Tölg, Fresenius Z. Anal. Chem., 260 (1972) 207.
6 B. Lloyd, P. Holt and H. T. Delves, Analyst (London), 107 (1982) 927.
7 A. A. Brown, J. M. Ottaway and G. S. Fell, Anal. Proc., (1982) 321.
8 O. E. Clinton, Analyst (London), 102 (1977) 187.
9 W. B. Robbins, J. A. Caruso and F. L. Fricke, Analyst (London), 104 (1979) 35.

10 O. Oster and W. Prellwitz, Clin. Chim. Acta, 124 (1982) 277.
11 B. Welz and M. Melcher, Anal. Chem., in press.
12 J. Nève, M. Hanocq and L. Molle, Anal. Chim. Acta, 115 (1980) 133.
13 G. Kaiser, D. Goetz, G. Tölg, G. Knapp, B. Maichin and H. Spitzy, Fresenius Z. Anal. Chem., 291 (1978) 278.
14 A. F. Hollemann and E. Wiberg, Lehrbuch der Anorganischen Chemie, 71—80 edn., Walter de Gruyter, Berlin, 1971.

Analytica Chimica Acta, 165 (1984) 141—147
Elsevier Science Publishers B.V., Amsterdam — Printed in The Netherlands

A STUDY OF BACKGROUND SIGNALS IN GRAPHITE-FURNACE ATOMIC ABSORPTION SPECTROMETRY

P. ALLAIN* and Y. MAURAS

Laboratoire de Pharmacologie, Centre Hospitalier Universitaire, 49036 Angers Cedex (France)

(Received 4th January 1984)

SUMMARY

The non-specific absorption from inorganic and organic molecules between 190 and 400 nm are measured using a graphite furnace and an atomic absorption spectrometer with a deuterium source.

The molecular absorption spectra of NaCl, KCl, RbCl and CsCl are very similar, with two maxima at ca. 200 and 250 nm. That of LiCl is very weak, as is that of NaF. The spectra of NaBr, NaI, KBr, KI, $CaCl_2$, $MgCl_2$, $SrCl_2$, $BaCl_2$, $FeCl_3$, $LaCl_3$ are also reported.

The non-specific absorption spectrum arising from albumin decreases from 190 to 400 nm, and that for plasma is similar to albumin, although a contribution from inorganic salts can also be seen. To decrease the non-specific absorption from metal chlorides or biological samples of mainly inorganic composition such as urine, addition of HNO_3 is satisfactory. Oxygen introduction during low temperature charring is better for removing contribution from organic molecules.

Graphite furnace atomic absorption spectrometry (g.f.a.a.s.) is a very sensitive technique for the determination of many elements, but determinations in complex matrices such as biological samples are frequently hindered by background absorption problems. To a certain extent, this background can be corrected spectroscopically, or decreased by using a furnace with a capacitive discharge, by matrix modification, by increasing the char temperature, by using a L'vov platform or application of an alternative gas. All these problems have been reviewed in recent papers [1—6].

Molecular absorption spectra of many simple inorganic salts in the graphite furnace have been reported [7—12]. However, these spectra were obtained at various molecular concentrations. Such spectra of rubidium and caesium salts, however, have not been reported, nor have those of organic molecules.

It is the purpose of this paper to report the molecular absorption spectra of inorganic and organic molecules between 195 and 400 nm obtained in the graphite furnace, and to look for means to decrease this absorption for improving routine determinations of elements in biological samples.

0003-2670/84/$03.00

EXPERIMENTAL

The Perkin-Elmer HGA 500 graphite furnace was used with an AS 40 autosampler and a Varian 875 atomic absorption spectrometer with deuterium arc background correction. The absorption signals were recorded and displayed using a Hewlett-Packard model 85 microcomputer. The standard conditions for the graphite furnace were drying at 120°C for 30 s in the ramp mode, charring at 250°C for 25 s in the ramp mode, ashing at 500°C for 20 s and atomization at 2000°C with maximum power (0 ramp, 2 hold) with argon internal flow interrupted, and, finally, cleaning at 2500°C for 3 s. These conditions were modified for particular experiments as described in the text. The graphite tubes used were obtained from Perkin-Elmer (standard and pyrolytic tubes) and Carbone-Lorraine (pyrolytic tubes). The sample volume injected into the furnace was generally 10 μl. Each measurement was repeated three times. The background absorption was measured between 195 and 400 nm.

RESULTS

Molecular spectra of inorganic molecules

The molecular absorption spectra of NaCl, KCl, CsCl, LiCl and RbCl in Fig. 1a were obtained by measurements at different wavelengths during atomization at 2000°C after injection into the graphite furnace of 10 μl of 1.0×10^{-2} M aqueous solutions. The molecular absorbance of lithium with a maximum at 230 nm is less than 0.25. The maximum absorbance of the other species is observed between 195 and 200 nm but a second maximum, smaller than the first, except for sodium, is observed at about 250 nm.

The wavelength of maximum molecular absorption of 1.0×10^{-2} M NaF, NaCl, NaBr and NaI at 2000°C (Fig. 1b) increase with increasing molecular weight; $NaNO_3$ and $NaCH_3COO$ are hardly detectable at this concentration in contrast to Na_2SO_4 (Fig. 1c). The spectra of KCl, KBr and KI (Fig. 1d) show the same pattern as the sodium halides.

Figure 1e shows the molecular absorption spectra obtained from $MgCl_2$, $CaCl_2$, $SrCl_2$, $BaCl_2$, $LaCl_3$ and $FeCl_3$. Magnesium at this concentration has very little absorbance, strontium and calcium have a maximum at 220 and 240 nm respectively. The absorption spectrum obtained from lanthanum chloride gradually increases between 260 and 195 nm. The greatest absorbance is given by iron with maxima at 195 and 240 nm. The absorbance for these elements, however, was less than those given by the alkali metals.

The pattern and magnitude of the absorption spectra of these inorganic molecules are approximatively the same for normal and pyrolytic tubes.

Molecular spectra of organic molecules

The absorption spectra of organic molecules such as hexane and methyl isobutyl ketone, injected into the furnace without dilution, and of glycerol,

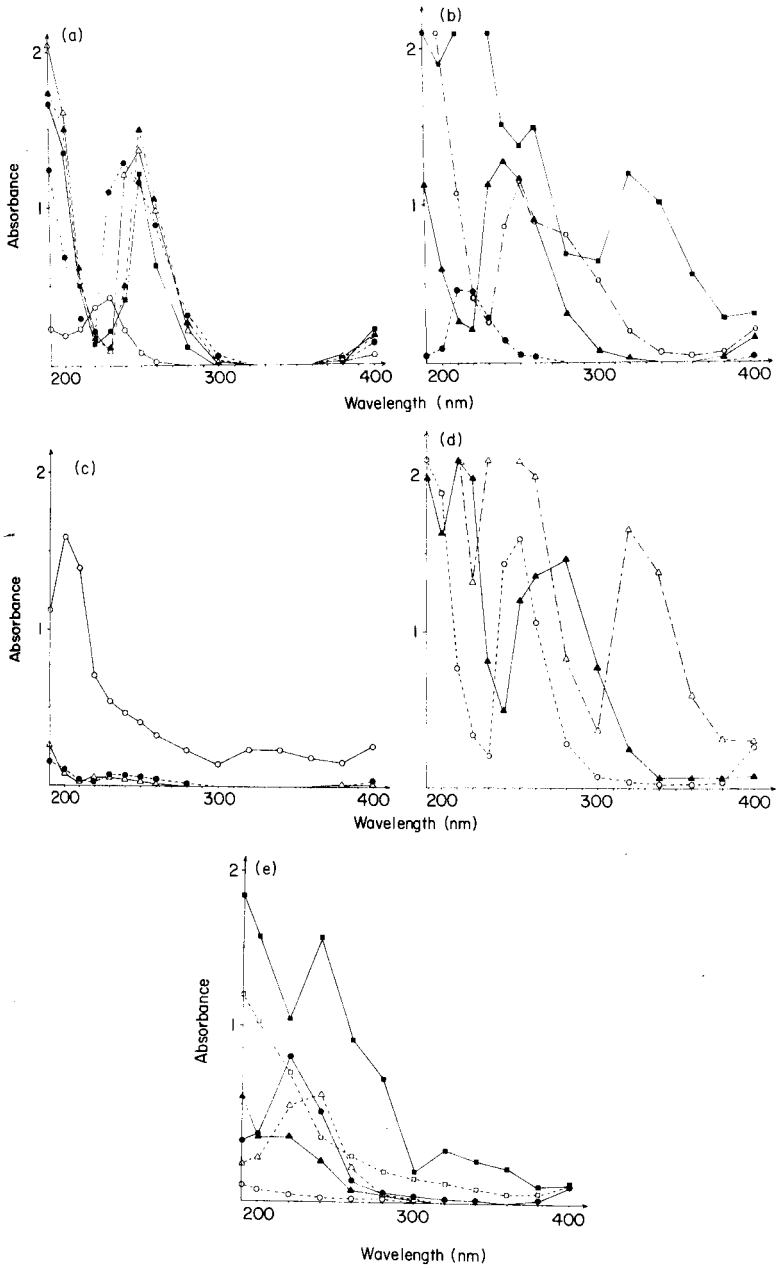

Fig. 1. Absorption spectra at 2000° C of 1.0×10^{-2} M solutions of: (a) (○) LiCl; (●) NaCl; (△) KCl; (▲) RbCl; (■) CsCl; (b) (●) NaF; (▲) NaCl; (○) NaBr; (■) NaI; (c) (○) Na_2SO_4; (●) Na acetate; (△) $NaNO_3$; (d) (○) KCl; (▲) KBr; (△) KI; (e) (○) $MgCl_2$; (△) $CaCl_2$; (●) $SrCl_2$; (▲) $BaCl_2$; (■) $FeCl_3$; (□) $LaCl_3$.

mannitol and Triton (1% in water) have been measured during the atomization step under the standard conditions. The absorbance was generally less than 0.1 and decreased from 200 nm to 400 nm. With organic solvents of low surface tension such as hexane and methyl iso butyl ketone, however, the important non-specific absorption sometimes observed arises because they spread out of the tube, and infiltrate between the tube and the electrical contacts, thus giving smoke during atomization. The phenomenon was minimized by using a grooved tube and a very slow increase in drying temperature.

The absorbance obtained from albumin (1%) and of two diluted blood plasmas (Fig. 2) decreased from 200 nm to 400 nm. These spectra could result from molecular absorption and light scattering by smoke. The similarity between the curve of albumin and plasma showed that the organic molecules played the main role in producing non-specific absorption from plasma. The absorbance was dependent on the quality of the graphite tubes and, for the same tube, could increase during use.

Decrease of background absorption

To improve the quality of determination of elements in complex matrices such as biological samples, it is often necessary to decrease the background absorbance. The effects of some procedures on the absorbance produced by inorganic and organic matrices have been investigated.

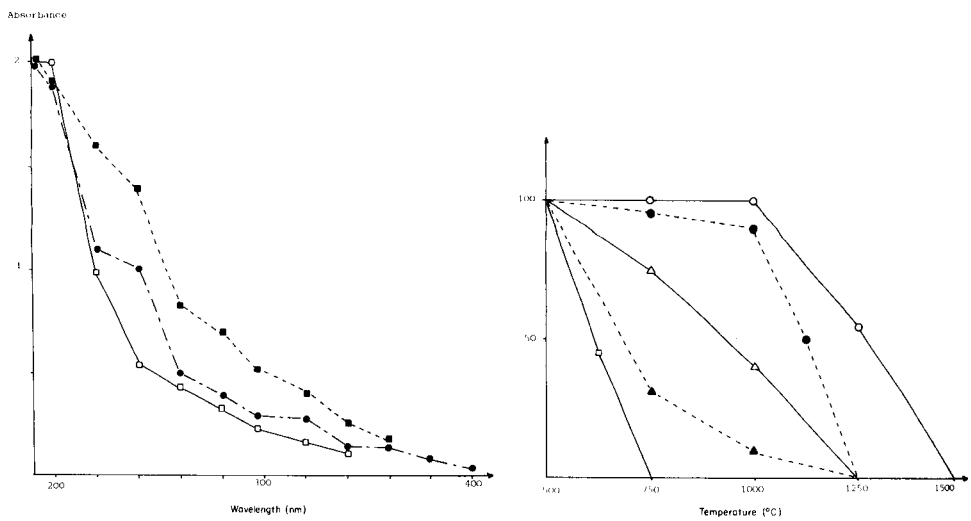

Fig. 2. Absorption spectra at 2000°C obtained from: (□) 1% albumin in water; (■, •) human plasma samples diluted 10 × with water (18 μl injected into the furnace).

Fig. 3. Effect of increasing charring temperature on non-specific absorption at 240 nm, expressed as % of signal observed after 500°C charring temperature for: (○) $CaCl_2$; (•) NaCl; (△) human plasma; (▲) whole blood; (□) albumin.

Increasing charring temperatures. Figure 3 compares the effect of increasing the charring temperature from 500 to 1500°C on the background absorbance for calcium and sodium chlorides, albumin, plasma and whole blood. For a mineral matrix, under the standard conditions, there was almost no decrease in absorbance until 1000°C was reached, in contrast to albumin whose background absorbance contribution was considerably decreased at 750°C. This decrease was also increased by increasing the ashing time at the maximum usable temperature. The non-specific absorption of plasma and whole blood decreased with increasing charring temperature intermediate between the behaviour of organic and inorganic matrices. But to obtain a significant decrease in background it is necessary to ash at 1000°C, at which temperature there is a loss of some analyte elements.

Matrix modification. Among the many substances that have been proposed for matrix modification, ammonium nitrate and nitric acid at concentrations between 1 and 5% in the final solution injected into the furnace have been investigated. Both compounds considerably decrease the non-atomic absorption of inorganic matrices such as NaCl, KCl, RbCl, $CaCl_2$, $FeCl_2$ and urine. However, better results are obtained with nitric acid than ammonium nitrate. Figure 4a shows the decrease of non-specific absorption of a synthetic mineral matrix similar to plasma by 2.5% nitric acid. In contrast, nitric acid injected into the furnace after albumin, to avoid precipitation, did not decrease the non-specific absorption and sometimes increased it (Fig. 4b). The maximum peaks for the mineral and organic matrices are after 0.4 and 0.2 s, respectively.

Effect of oxygen as an alternative gas. Oxygen has been used during the two first steps up to 500°C at a flow of 30 ml min^{-1}. During the third step, holding at 500°C, argon was used to eliminate oxygen before atomization. This procedure did not decrease the non-atomic absorption of the inorganic matrices, but it decreased the non-specific absorption from albumin, whole blood and plasma by more than 50%.

Oxygen has also the advantage of eliminating any residue in the graphite furnace after analysis of blood and plasma. Without oxygen, it is necessary to remove the graphite tube for cleaning, thus preventing automated analyses. When oxygen was used at high flow rates, it increased the diameter of the

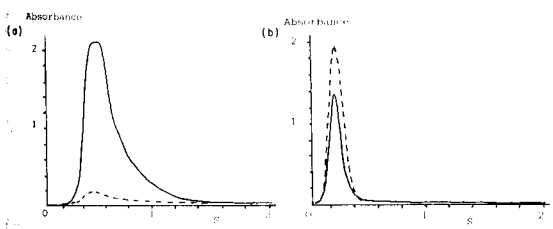

Fig. 4. Non-specific absorption at 240 nm vs. time for (a) synthetic mineral plasma diluted 1:1 with (—) water; (— —) 5% HNO_3; (b) albumin dissolved in: (—) water; (— —) 5% HNO_3.

graphite tube by which the gas escapes, but this disadvantage was eliminated when its flow was decreased to ca. 30 ml min^{-1}, without loosing efficiency.

Application to biological samples

For decreasing the background absorbance during the measurement of elements in urine, which is essentially an inorganic matrix, it is recommended that nitric acid or ammonium nitrate be used, at a final concentration of 2.5—5%.

For plasma, the organic and inorganic composition was demonstrated by recording at 240 nm the non-specific absorption peak vs. time, using a HP 85 microcomputer (Fig. 5). The first maximum occurred after 0.2 s atomization (albumin) and the second at 0.4 s (mineral mixture). A similar double peak was observed with whole blood. The addition of 10% nitric acid to plasma in the tube with the autosampler decreased the second peak without affecting the first. In contrast, the use of oxygen as an alternative gas essentially decreased the first peak. It is noteworthy, however, that the pattern of non-specific absorption vs. time is dependent on the quality of the graphite furnace and the atomization temperature ramp. As the organic component played a major role in the genesis of background absorption, oxygen dramatically decreased this background.

DISCUSSION

In this work, the spectra of inorganic salts injected in the furnace in the same molar concentration are in very good agreement with literature data [7—12]. Moreover, the absorption spectra of RbCl and CsCl, previously unreported, have the same pattern and intensity as those of NaCl and KCl. In contrast, the LiCl spectrum, also previously unreported, has less absorbance than that of the other alkali metal chlorides.

The absorption spectrum obtained from albumin showed an absorbance decrease from 200 to 400 nm. Because the spectral patterns of plasma and

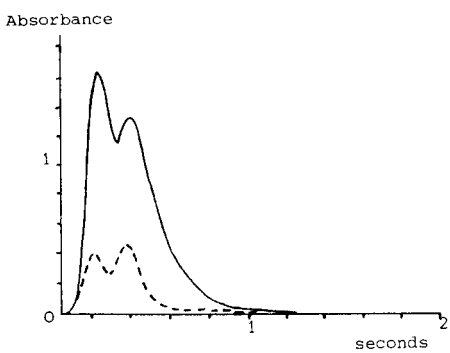

Fig. 5. Non-specific absorption 240 nm vs. time for plasma with atomization at 2000°C: (—) without oxygen; (— —) with oxygen.

whole blood were quite similar to that obtained from albumin, it can be concluded that the organic components played the major role in producing non-specific absorption from these samples.

The background absorption is approximatively the same for inorganic salts with every graphite tube tested, but for organic molecules the absorbance is more dependent on the quality of the tube.

To decrease background absorption from biological matrices having a predominantly mineral composition, such as urine or cerebrospinal fluid, addition of 2—5% nitric acid gives very good results. For blood and plasma, rich in organic molecules, the use of oxygen as an alternative gas at low flow rate during the two first steps had the best effect, chiefly when it is not possible to exceed an ashing temperature of 500—600° C without losing the analyte.

The authors are indebted to A. Kabli for his technical assistance, Mrs. Laisne for typing and Fondation Langlois for its support.

REFERENCES

1 C. L. Chakrabarti, C. C. Wan, H. A. Hamed and P. C. Bertels, Anal. Chem., 53 (1981) 444.
2 W. Slavin, D. C. Manning and G. R. Carnrick, Anal. Chem., 53 (1981) 1504.
3 W. Slavin, Anal. Chem., 54 (1982) 685.
4 S. R. Koirtyohann and M. L. Kaiser, Anal. Chem., 54 (1982) 1515.
5 J. J. Sotera, L. C. Cristiano, M. K. Conley and H. L. Kahn, Anal. Chem., 55 (1983) 204.
6 J. J. Sotera and H. L. Kahn, Int. Lab., 13(4) (1983) 24.
7 B. R. Culver and T. Surles, Anal. Chem., 47 (1975) 920.
8 M. J. Adams, G. F. Kirkbright and P. Rienvatana, At. Absorpt. Newsl., 14 (1975) 5, 105.
9 L. H. Sierstsema, Clin. Chim. Acta, 69 (1976) 533.
10 M. W. Pritchard and R. D. Reeves, Anal. Chim. Acta, 82 (1976) 103.
11 K. Saeed and Y. Thomassen, Anal. Chim. Acta, 130 (1981) 281.
12 J. P. Erspamer and T. M. Niemczyk, Anal. Chem., 54 (1982) 538.

Analytica Chimica Acta, 165 (1984) 149—157
Elsevier Science Publishers B.V., Amsterdam — Printed in The Netherlands

REDUCTION OF EFFECTS OF STRUCTURED NON-SPECIFIC ABSORPTION IN THE DETERMINATION OF ARSENIC AND SELENIUM BY ELECTROTHERMAL ATOMIC ABSORPTION SPECTROMETRY

J. BAUSLAUGH[a], B. RADZIUK[a], K. SAEED and Y. THOMASSEN*
Institute of Occupational Health, P.O. Box 8149 DEP, Oslo 1 (Norway)
(Received 3rd February 1984)

SUMMARY

The presence of iron and phosphates in biological matrices causes deuterium arc background-correction systems to overcompensate at several arsenic and selenium resonance lines. The addition of platinum as matrix modifier has a significant effect on both the absorbance/time profile of iron and the formation of gaseous phosphate decomposition products. A nickel/platinum matrix modifier is shown effectively to control the problems in the determination of selenium arising both from thermal instability and spectral interferences. The same combination eliminates the spectral interferences found at the arsenic resonance lines. Remaining problems are the thermal stabilization of organometallic arsenic compounds present in biological samples. When radioactively-labelled ^{74}As compounds prepared in vivo were applied, none of the tested matrix modifiers (Ni, Cu, Ag, Pd, Zr, Ce, Ce + magnesium nitrate) showed a significant influence on the volatility of arsenic in whole blood and urine from rats.

Various authors have described the determination of arsenic and selenium by electrothermal atomic absorption spectrometry (e.a.a.s.). The difficulties reported are spectral interferences, analyte volatilization problems and vapour phase interferences. As these volatile elements are subject to losses during the drying and charring steps, matrix modification techniques are recommended. Since 1970, when Storm discovered that selenium was thermally stabilized by a nickel matrix [1] in the determination of selenium by e.a.a.s., this and other matrix modifiers have been applied in the determination of arsenic and selenium in a variety of materials [2—13]. The results, even for similar e.a.a.s. studies, are often confusing and contradictory. This may be due to memory effects when the same graphite tube is used with several different modifying agents [11, 12], and to the fact that the estimation of analyte losses during drying and charring is based on the atomic absorption measured during atomization, which is itself subject to vaporization, vapour phase, spectral and non-specific absorption interferences. The influence of matrix modification on analyte volatility is most suitably studied by using

[a]On leave from Institut für Spectrochemie, Dortmund, Federal Republic of Germany.

0003-2670/84/$03.00

radioactive isotopes, as has been reported for As [9], Cr [14], Se [10, 11, 15] and Te [16]. This also makes it possible to monitor analytes in biological matrices by means of naturally occurring metallo-organic compounds prepared in vivo [10, 11, 16].

Selenium in body fluids may be determined by e.a.a.s. without sample pretreatment after thermal stabilization with either nickel or silver [10, 11]. Although the mechanism of the thermal stabilization of selenium compounds is unclear, the chemical form of selenium in the sample has generally been disregarded. Isotopic studies have shown that the behaviour of naturally occurring selenium compounds (present in whole blood, serum and urine) is different from that of inorganic selenium compounds. Although various metal compounds are able to stabilize inorganic selenium compounds at high charring temperatures, only nickel and silver have any substantial effect on the thermal stability of metabolized forms of selenium. This may explain the large discrepancies between the results of earlier in-vivo tracer studies [10, 11], in which a loss of selenium was measured in the presence of copper nitrate at temperatures higher than 400° C, and up to 75% loss was obtained at 700° C, and the results of Welz et al. [17], who claimed that selenium compounds present in serum were stabilized by copper nitrate, even though they were entirely unable to establish selenium recoveries for charring temperatures below 700° C (because of the high background absorption obtained when thermal pretreatment temperatures are too low).

With the exception of dimethylarsinic acid, little information is to be found regarding the volatility and thermal stabilization of organoarsenic compounds. Edgar and Lum [18] noted that nickel nitrate prevented the loss of dimethylarsinic acid at charring temperatures up to 1800° C in the analysis of human urine. Because arsenic in unexposed humans is present primarily in various methylated forms [19], in vivo tracer studies of the thermal stabilization of these compounds should be undertaken.

The presence of gaseous phosphate decomposition products and of iron atoms may cause deuterium arc background-correction systems to overcompensate at several arsenic and selenium resonance lines [20, 21]. There is also reported to be direct spectral overlap from P_2 molecular absorption at the 204.0-nm selenium resonance line [21].

In this work methods of decreasing the volatility of arsenic in whole blood and urine samples from rats were studied. The influence of noble metals on the volatilization of iron and on phosphate decomposition was investigated with the aid of time-resolved data acquisition, using both wall and platform atomization techniques. The direct determination of selenium in whole blood, urine and acid-digested biological samples, with deuterium arc background correction and platinum-nickel matrix modification, is described.

EXPERIMENTAL

Apparatus, reagents and standard solutions

A Perkin-Elmer model 5000 atomic absorption spectrometer equipped with deuterium arc background correction and arsenic and selenium electrodeless discharge lamps, an HGA-500 graphite furnace, an AS-40 automatic sampler and a model 56 recorder were used for all determinations. Time-resolved absorbance data collected either by a Perkin-Elmer 3600 Data Station or by an Apple II microcomputer were displayed using a PR-100 printer and an Omnigraphic 2000 X—Y recorder, respectively. The interface between the spectrometer and the Apple II has been described [22]. The optimal furnace conditions for the determination of selenium are summarized in Table 1. All the thermal stability and matrix modification studies were done with pyrolytically-coated graphite tubes and platforms which had not previously been in contact with other reagents [11, 23]. The furnace was purged with argon. γ-Radiation was measured by a Packard Auto-Gamma scintillation spectrometer.

Analytical-grade reagents were used throughout. The 1000 mg l^{-1} standard solutions of arsenic and selenium were obtained from BDH. Stock solutions of other reagents were obtained by making appropriate solutions of platinum(IV) chloride, rhodium(VI) oxide (in hydrochloric acid), palladium(II)

TABLE 1

Typical furnace programs for the determination of selenium in biological matrices by wall and L'vov platform atomization

a. Platform atomization (10-µl sample plus 10-µl matrix modifier (0.1% Ni, 2.5% Pt in 3M HNO_3))

Step	1	2	3	4	5	6	7	8
Temperature (°C)	180	220	450	1000	1300	1300	2600	20
Ramp time(s)	5	5	5	5	10	1	0	1
Hold time(s)	15	20	5	5	15	4	6	20
Recorder(s)							—5	
Read(s)							—1	
Baseline(s)					15			
Internal gas flow (ml min^{-1})	300	300	300	300	300	10	10	300

b. Wall atomization (15-µl sample plus 15-µl matrix modifier (as above))

Step	1	2	3	4	5	6
Temperature (°C)	120	300	500	1150	2100	2700
Ramp time(s)	5	5	5	15	0	1
Hold time(s)	35	5	5	20	6	3
Recorder(s)					—5	
Reads(s)					—1	
Baseline(s)				15		
Internal gas flow (ml min^{-1})	300	300	300	300	40	300

chloride (in hydrochloric acid), cerium(III) sulfate, zirconium nitrate, nickel nitrate and silver nitrate. A solution of ^{74}As as arsenic acid in 0.04 M hydrochloric acid was obtained from The Radiochemical Centre (Amersham, U.K.).

Preparation of in-vivo organoarsenic compounds labelled with ^{74}As

Wistar rats were injected intraperitoneally with an ^{74}As-labelled solution of suitable activity, and kept overnight in metabolism cages for urine collection. Whole blood was sampled from the vena cava after 24 h.

Acid digestion of biological samples

An appropriate amount of bovine liver, fish soluble matter or freeze-dried animal blood (0.2—0.5 g) was weighed into a pyrex test tube. After addition of 3 ml of concentrated nitric acid, each sample was kept overnight at room temperature to avoid foaming on warming. Each sample was heated at 110° C for 1 h, then the temperature was raised to 140° C and maintained until the volume was decreased to about 0.5 ml. Each solution was made up to 10 ml with distilled water.

RESULTS AND DISCUSSION

Thermal stabilization of arsenic compounds prepared in vivo

The thermal stabilization of arsenic was investigated by applying the same technique as described earlier [10, 11], with ^{74}As incorporated in vivo. The results are shown in Fig. 1. Platinum, copper and silver had only slight effects. In the absence of matrix modifiers, loss of arsenic was observed at as low as 200° C and was complete at 600° C. It is noteworthy that arsenic in such samples is more volatile than when inorganically bound. It may be supposed that this arises from a decrease in the stabilization of arsenic by graphite when oxidizing agents are present [9]. Matrix modifiers which have been shown to stabilize inorganic compounds were only partially effective. Nickel, which is used extensively, allowed retention of only 50% of the original activity at 800° C. None of the metal compounds tested significantly influenced the volatility of arsenic in whole blood and urine from rats. Further, in contrast to the results obtained for inorganic arsenic compounds [9], the volatility of arsenic in these samples was not decreased by the presence of oxidizing agents such as nitric acid and magnesium nitrate.

Arsenic compounds prepared in vivo in rats may not be entirely suitable for volatility studies because the rat has a unique arsenic metabolism in which arsenic is stored in haemoglobin and is released only when the red blood cells have been broken down. It has been suggested that rabbits or hamsters, for example, would provide better models for such studies [19]. The results presented here, however, emphasize that the chemical form of the element is of vital importance with regard to thermal behaviour. Further work is necessary to establish whether direct determination of arsenic in biological fluids by e.a.a.s. without prior acid digestion is feasible.

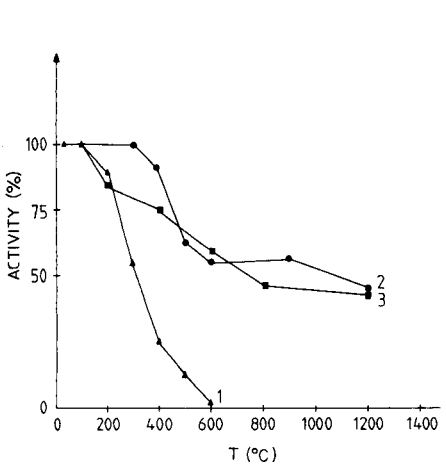

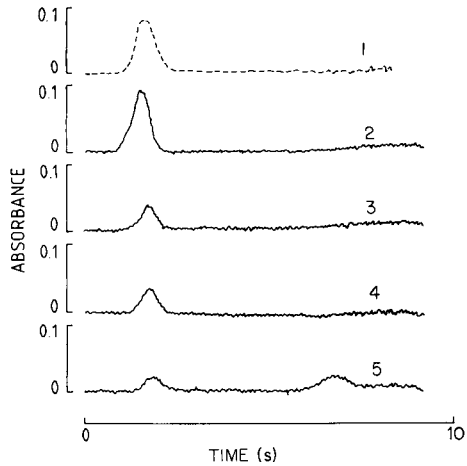

Fig. 1. Retention of activity as a function of charring temperature for in-vivo prepared whole rat blood and urine labelled with ^{74}As, with addition of: (1) no matrix modifier; (2), Zr, Ce, Pd or Ce + $Mg(NO_3)_2$; (3) Ni (1% of each metal, 5% $Mg(NO_3)_2$).

Fig. 2. Absorbance profiles showing the time overlap between the atomization of Fe and Se, under the conditions listed in Table 1 for platform atomization. Curves: (1) 0.2 μg Fe ml^{-1}; (2) 0.6 μg Se ml^{-1}; (3) 0.6 μg Se ml^{-1} + 0.05% Pt; (4) 0.6 μg Se ml^{-1} + 0.1% Pt; (5) 0.6 μg Se ml^{-1} + 1% Pt. Wavelength: (1) 248.3 nm; (2—5) 196.0 nm.

The influence of platinum on the volatilization of iron and selenium

The conventional method of background correction which is based on the use of a continuum source, is subject to spectral interference. At the 196.0-nm selenium resonance line, this can arise from the presence of a complex absorption spectrum consisting of iron lines and probably both line and narrow bands from phosphate decomposition products. Because background correction based on the Zeeman effect or the Smith—Hieftje system operates over a very narrow spectral range, the results are essentially free from this interference [13, 24—26]. Figure 2 shows that there is a direct time overlap between iron and selenium atomic absorption when the conditions described in Table 1 are used and nickel (0.1%) with different platinum concentrations is added as matrix modifier to the selenium solution. The addition of platinum only slightly delays the selenium peak, but decreases the selenium sensitivity even with platform atomization.

The addition of platinum has a significant influence on the absorbance/time profile of iron volatilized from a graphite surface (Fig. 3). Of several other noble metals tested, a similar though less marked effect was observed only on addition of rhodium or palladium. While the sensitivity for selenium is decreased by the addition of platinum (Fig. 2), there is little effect on the time profile, but the appearance temperature of iron is so increased that the absorption signal is completely separated in time from that of selenium. This

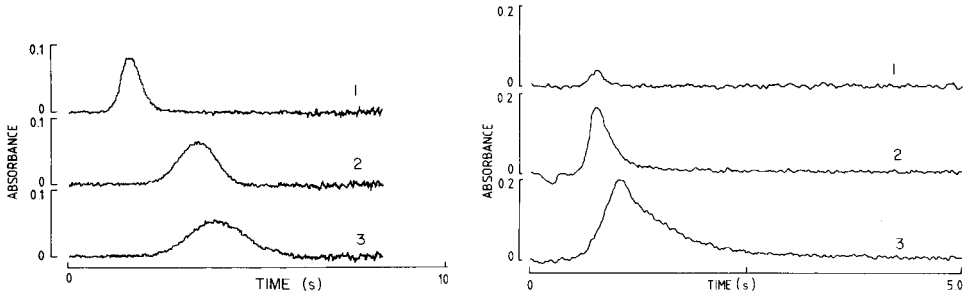

Fig. 3. The influence of the addition of platinum on the atomization of iron (0.2 μg ml^{-1}) measured at 248.3 nm with the experimental parameters given in Table 1 (for platform atomization). Platinum added: (1) 0; (2) 0.01%; (3) 0.05%.

Fig. 4. The effect of nickel or platinum on the platform atomization of urine, measured at the 213.6 -nm phosphorus line. Additions: (1) none; (2) 0.1% Ni; (3) 0.1% Pt.

effect offers an interesting possibility for removing the spectral interference of iron in the determination of selenium by e.a.a.s.

Frech et al. [27] have shown by means of both high-temperature equilibrium calculations and empirical observations that the formation of iron atoms can be described by

$$FeO(s) + C(s) \rightarrow CO(g) + Fe(s) \rightarrow Fe(g)$$

The decomposition of iron oxides to iron metal can occur above 1300°C. The fundamental processes involved in matrix modification, however, are not well understood. A mechanism consistent with the present observations is the formation of a Pt—Fe alloy from which iron volatilizes more slowly than selenium from a Pt—Se alloy or a selenide.

The role of carbon in these reactions must also be considered [9]. Even after clean-out steps, significant residual platinum is found on the atomizing surface (wall or platform). Tests with an electron microscope equipped with an energy-dispersive x-ray detector confirmed that after a very few atomization and clean-out sequences, the graphite surface was completely coated with tiny spherules of platinum, presumably in the elemental form.

Platinum not only has the benefit of decreasing the interference of iron, but also, as has been reported by Saeed and Thomassen [21], is among those elements which decrease the overcompensation effect of phosphorus. The effect of the addition of platinum to a urine matrix on the atomic absorption of phosphorus measured at 213.6 nm is shown in Fig. 4. It is apparent that phosphorus atom formation is enhanced, thereby decreasing the spectral interferences which are known to arise from molecules present in the gas phase. In our opinion, nickel is the only matrix modifier which is practical for use in the quantitative thermal stabilization of both organic and inorganic selenium compounds. Platinum has little or no stabilizing effect [11]. However, both elements must be added in order to achieve quantitative,

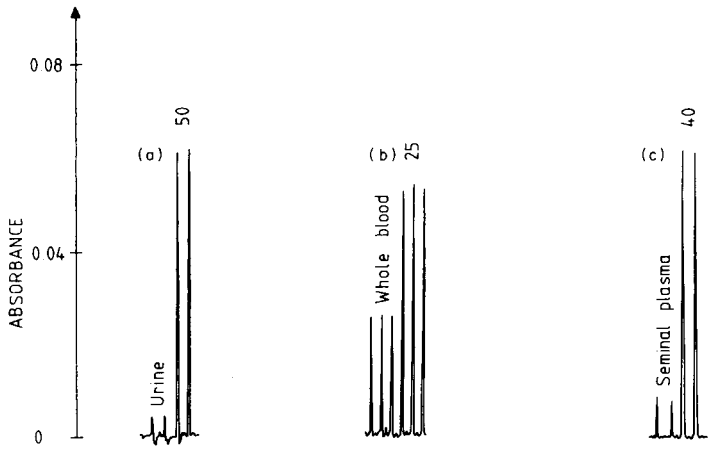

Fig. 5. Typical recorder traces obtained by the proposed matrix modification technique with wall atomization, applied to body fluids. (a) Undiluted urine from a patient with phenylketonuria; content is 4.2 μg Se l^{-1}; standard addition 50 μg Se l^{-1}. (b) Whole blood diluted 5× with 0.2% Triton X-100; content is 125 μg Se l^{-1}; standard addition 25 μg Se l^{-1}. (c) Seminal plasma diluted as in (b); content is 35 μg Se l^{-1}; standard addition 40 μg Se l^{-1}.

interference-free selenium determinations in samples containing iron and phosphorus.

Although the effect of spectral interferences in the determination of selenium has been clearly demonstrated, some authors have reported remarkably accurate results, using continuum-source background correction and adding only nickel, for samples such as whole blood, tissues, skim milk, bovine liver and marine biological specimens which contain high interferent/selenium ratios [28—30]. Julshamn et al. [30] have reported that the concentration of nickel required for accurate results was very dependent on the sample matrix and conversely that only one nickel concentration yielded values within the acceptable range of the certified selenium level for NBS Bovine Liver. The results obtained for such an analysis are strongly influenced by the previous history of the graphite tube, instrumental response limitations, performance of the background corrector and other details of experimental conditions. It is quite possible that the spectral interferences discussed above have sometimes been masked by a combination of these factors.

The determination of selenium and arsenic in body fluids

The findings of the above study were applied to the direct determination of selenium in several complex matrices such as whole blood, urine and seminal plasma. Figure 5 shows recorder traces obtained for such samples. The urine was chosen because of its very low selenium content (calculated to be 4.2 μg l^{-1}), from a patient on a selenium-free diet. Because reference values reported for selenium in urine from healthy humans with normal diets are

TABLE 2

Selenium determined in some reference materials (conditions as in Table 1, platform atomization)

Sample	*n*	Selenium conc. ($\mu g\ kg^{-1}$)	
		Range	Mean ± s.d.
NBS Bovine Liver[a]	4	1.07—1.26	1.16 ± 0.08
IAEA Dried Whole Animal Blood A-2	3	0.45—0.48	0.46 ± 0.02
IAEA Fish Solubles A-6	4	2.59—2.80	2.69 ± 0.09

[a]Certified value 1.1 ± 0.1 $\mu g\ kg^{-1}$.

typically 20—100 $\mu g\ l^{-1}$, the small residual overcompensation by phosphate which can be seen in this trace will not be significant.

Although the combination of nickel and platinum also markedly decreased the spectral interferences at the arsenic resonance line, the afore-mentioned difficulties with the thermal stabilization of arsenic compounds present in biological fluids are not removed. Acid digestion pretreatment of biological samples is still preferable to direct methods of determination which are of questionable accuracy.

Table 2 shows the results obtained for the determination of selenium in some biological materials dissolved in nitric acid.

CONCLUSIONS

The nickel-platinum matrix modifier offers a simple and effective means by which problems in the determination of selenium by e.a.a.s. arising from thermal instability and spectral interferences may be controlled. This is essential when instrumentation with a continuum-source background corrector is used. With regard to the effect on the spectral interferences from phosphate decomposition products at the wavelengths of arsenic resonance lines, the same combination works for arsenic and may be expected to work at the other resonance lines in this spectral region where such interferences have been reported. The application of platinum as an atomization rate modifier for other cases is being investigated.

B. Radziuk gratefully acknowledges financial support from the Alexander von Humboldt Stiftung, Bundesrepublik Deutschland.

REFERENCES

1 Å. Storm, Falconbridge Nikkelverk, Kristiansand, Norway, personal communication.
2 R. D. Ediger, At. Absorpt. Newsl., 14 (1975) 127.
3 E. L. Henn, Anal. Chem., 47 (1975) 428.
4 F. J. Szydlowski, At. Absorpt. Newsl., 16 (1977) 60.

5 M. Ihnat, Anal. Chim. Acta, 82 (1976) 293.
6 G. F. Kirkbright, S. Hsiao-Chuan and R. D. Snook, At. Spectrosc., 1 (1980) 85.
7 P. R. Walsh, J. L. Fasching and R. A. Duce, Anal. Chem., 48 (1976) 1014.
8 D. Chakraborti, W. De Jonghe and F. Adams, Anal. Chim. Acta, 119 (1980) 331.
9 J. Koreckovà, W. Frech, E. Lundberg, J.-Å. Persson and A. Cedergren, Anal. Chim. Acta, 130 (1981) 267.
10 K. Saeed, Y. Thomassen and F. J. Langmyhr, Anal. Chim. Acta, 110 (1979) 285.
11 J. Alexander, K. Saeed and Y. Thomassen, Anal. Chim. Acta, 120 (1980) 377.
12 K. Julshamn, O. Ringdal, K.-E. Slinning and O. R. Brækkan, Spectrochim. Acta, Part B, 37 (1982) 473.
13 G. R. Carnrick, D. C. Manning and W. Slavin, Analyst (London), 108 (1983) 1297.
14 C. Veillon, B. E. Guthrie and W. R. Wolf, Anal. Chem., 52(3) (1980) 457.
15 G. Norheim, K. Saeed and Y. Thomassen, At. Spectrosc., 4 (1983) 99.
16 G. Weibust, F. J. Langmyhr and Y. Thomassen, Anal. Chim. Acta, 128 (1981) 23.
17 B. Welz, M. Melcher and G. Schlemmer, Fresenius Z. Anal. Chem., 316 (1983) 271.
18 D. G. Edgar and K. R. Lum, Int. J. Environ. Anal. Chem., 16 (1983) 219.
19 Committee on Medical and Biological Effects of Environmental Pollutants: Arsenic, National Academy of Sciences, Washington, DC, 1977.
20 D. C. Manning, At. Absorpt. Newsl., 17 (1978) 107.
21 K. Saeed and Y. Thomassen, Anal. Chim. Acta, 130 (1981) 281.
22 K. Lum, D. Naranjit, B. Radziuk and Y. Thomassen, Anal. Chim. Acta, 155 (1983) 183.
23 B. Welz, G. Schlemmer and V. Voellkopf, Spectrochim. Acta, Part B, 39(2/3) (1984) 501.
24 F. J. Fernandez and R. Giddings, At. Spectrosc., 3 (1982) 311.
25 P. A. Pleban, A. Munyani and J. Beachum, J. Clin. Chem., 28 (1982) 311.
26 J. J. Sotera and H. L. Kahn, Int. Lab., 13(4) (1983) 24.
27 W. Frech, J.-A. Persson and A. Cedergren, Prog. Anal. At. Spectrosc., 3 (1980) 279.
28 C. D. Rail, D. E. Kidd and W. M. Hadley, Int. J. Environ. Anal. Chem., 8 (1980) 79.
29 G. T. C. Shum, H. C. Freeman and J. F. Uthe, JAOAC, 60(5) (1977) 1010.
30 K. Julshamn, O. Ringdal, K.-E. Slinning and O. R. Braekkan, Spectrochim. Acta, Part B, 37(6) (1982) 473.

Analytica Chimica Acta, 165 (1984) 159—169
Elsevier Science Publishers B.V., Amsterdam — Printed in The Netherlands

SPECTROFLUORIMETRIC DETERMINATION OF NIOBIUM WITH MORIN ENHANCED BY CETYLTRIMETHYLAMMONIUM BROMIDE MICELLES

A. SANZ-MEDEL* and J. I. GARCIA ALONSO

Department of Analytical Chemistry, Faculty of Chemistry, University of Oviedo, Oviedo (Spain)

(Received 20th May 1984)

SUMMARY

The effect of surfactants on the fluorescence of the niobium—morin system is described. Cationic surfactants strongly enhance the intensity (e.g., cetyltrimethylammonium bromide (CTAB) gives an 80-fold increase), while anionic and non-ionic surfactants are without effect. The formation of 1:1 and 1:3 (Nb:morin) complexes is demonstrated spectrophotometrically. The conditional stability constants for these complexes in CTAB micelles are $\beta_1 = (1.14 \pm 0.01) \times 10^4$ l mol^{-1} and $\beta_3 = (5.66 \pm 0.02) \times 10^{10}$ l^3 mol^{-3}. The micellar-enhanced fluorimetric method has a 1 μg l^{-1} detection limit, and is highly selective. The r.s.d. for the determination of 50 μg l^{-1} Nb is 3.5%.

Interest on the study of micellar solutions using fluorescent probes has increased over the last few years. However, little work has been done on the application of micellar systems to improve the fluorescent determinations of metals. Early work by Ishibashi and Kina [1, 2] described how addition of non-ionic surfactants to the fluorescent aluminum and gallium lumogallion complexes increases the intensity of the fluorescence. Kina et al. [3] also reported a similar effect on adding the cationic surfactant zephiramine to the fluorescent complex of zinc with 8-quinolinol-5-sulfonic acid; non-ionic surfactants had no effect. Pilipenko et al. [4] reported on the fluorescence enhancement effect of the addition of 1,2-ethylene-bis(carbodecyloxymethyl)dimethylammonium chloride to the complexes of aluminum, gallium and indium with lumogallion. This effect was attributed to the formation of a more rigid ion-association complex.

Other fluorescent aluminum chelates have been studied in the presence of surfactants of several types: the complex of aluminum with calcon [5], the fluorescence of which is greatly enhanced by cationic surfactants, and the aluminum—morin complex [6], which is made more sensitive by a non-ionic surfactant (Genapol PF-20) whereas its fluorescence is quenched by the presence of other non-ionic or cationic surfactants. Finally, the use of non-ionic surfactants as solubilizing agents to improve the fluorimetric determination of lanthanides with β-diketones and tri-n-octylphosphine oxide must be mentioned. Apart from the simplicity of the procedures

0003-2670/84/$03.00

derived from avoiding the customary extraction step, a great increase in the fluorimetric sensitivity attainable was also reported [7, 8].

At present, there are no general rules about which type of surfactant will enhance the fluorescence of a particular binary complex. Problems of fluorescence quenching usually arise [9, 10] and a search of an appropriate surfactant, if any, is difficult and tedious. In this context, Sanz-Medel et al. [9] reported on the characteristics of the fluorescence of some niobium chelates in the presence of cationic and non-ionic micelles. Curiously, the fluorimetric reagents tested possessing a negatively charged sulfonyl group in their molecule suitable for interacting with cationic micelles (8-quinolinol-5-sulfonic acid and lumogallion) gave rise to binary niobium complexes, but their fluorescence was not enhanced by the addition of cationic surfactants. In fact, for 8-quinolinol-5-sulfonic acid, the molar absorptivity of the niobium complex was enhanced while its fluorescence was quenched [10]. Non-ionic surfactants, such as Triton X-100, had a negligible effect on the above complex, but when added to the niobium-lumogallion system an 11-fold increase in the fluorescence intensity was observed at surfactant concentrations well above its critical micelle concentration (c.m.c.). In contrast, morin (a fluorimetric reagent lacking an easily ionized negative group in its molecule) in acidic medium forms a complex with niobium, the fluorescence of which is strongly affected by cationic surfactants. Non-ionic surfactants do not affect the fluorescence. In 1 M sulfuric acid the ternary system niobium/morin/cetyltrimethylammonium bromide (CTAB) showed a very intense fluorescence; an extremely sensitive, and selective, method for determination of niobium was reported [9].

While this work was being completed, a paper by Pilipenko et al. [11] on this fluorescent reaction of niobium with morin in micellar and in aqueous ethanol (or acetone) solutions was published. Their findings agree in general terms with our results. As this paper will show, however, the optimum experimental conditions found below differ from those recommended by Pilipenko et al. [11]. At the same time, the influence of important factors such as temperature, and time stability, not previously reported, are discussed. The composition of the species in the acidic micellar medium, and their stability constants are given. Experiments to elucidate the mechanism of this very interesting fluorescent reaction are discussed.

EXPERIMENTAL

Apparatus and reagents

Fluorescence intensity measurements were made, and corrected excitation and emission spectra recorded, on a Perkin-Elmer LS-5 spectrofluorimeter equipped with a Model 3600 data station; 5-nm slits were used for excitation and emission measurements in 1-cm quartz cells. The temperature of the sample cell was held constant by using a Julabo (Paratherm III) thermostat, which controls temperature to ±0.2°C. Absorbance measurements were

made on a Perkin-Elmer 124 spectrophotometer. A conventional stalagmometer was used for surface tension measurements. Distilled-deionized water was used throughout. All reagents used were of analytical grade. A 200 μg ml^{-1} niobium stock solution was prepared as described elsewhere [12]. All less concentrated niobium solutions were freshly prepared by appropriate dilution of the stock solution with 5 M sulfuric acid. The fluorimetric reagent was prepared by dissolving 0.1 g of morin and 5 g of cetyltrimethylammonium bromide (CTAB) in water (with warming) and diluting to 500 ml. Morin solutions without surfactant were obtained by dissolving 0.1 g of the reagent in 50 ml of absolute ethanol and diluting to 100 ml with water.

General procedure

Transfer an aliquot of standard niobium solution ($\leqslant 1$ μg Nb) into a 10-ml volumetric flask containing 2 ml of 5 M sulfuric acid. Add 5 ml of the fluorimetric reagent, mix thoroughly and dilute to the mark with water. Let the solution stand for 2 h and measure the fluorescence intensity at 503 nm with excitation of 433 nm. Prepare and measure in the same way a reagent blank, without niobium.

RESULTS AND DISCUSSION

Reaction conditions

Figure 1 shows the corrected excitation and fluorescence spectra (corrected for source and detector) of the systems niobium/morin and niobium/morin/CTAB in 1 M sulfuric acid (in all cases after subtracting the corresponding blank spectra). The addition of 0.5% CTAB causes a great increase in the fluorescence intensity (greater than 80-fold) and a bathochromic shift in the excitation maximum from 410 to 433 nm. Maximum fluorescence intensity occurs at 503 nm in both instances.

The influence of sulfuric acid concentration on the fluorescence of the ternary system is shown in Fig. 2. The intensity reaches a maximum in 1 M sulfuric acid, decreasing gradually as the sulfuric acid concentration increases further. Hydrochloric acid gave appreciably less intensity than sulfuric acid.

The fluorescence intensity depends strongly on the order of addition of reagents. The best order is niobium followed by sulfuric acid, then the mixed reagents solution. When morin and CTAB are added separately, the morin solution should be added before the surfactant. These kinetic effects are also indicated by the effect of standing time on the intensity. The emission decreases by ca. 30% over the first 30 min, after which it remains stable for at least 3 days.

The effect of temperature on the fluorescence intensity is critical. When the temperature is increased from 5 to 30°C the intensity decreases gradually (ca. -2.5% °C^{-1}). When the thermostat is used, which controls the cuvet

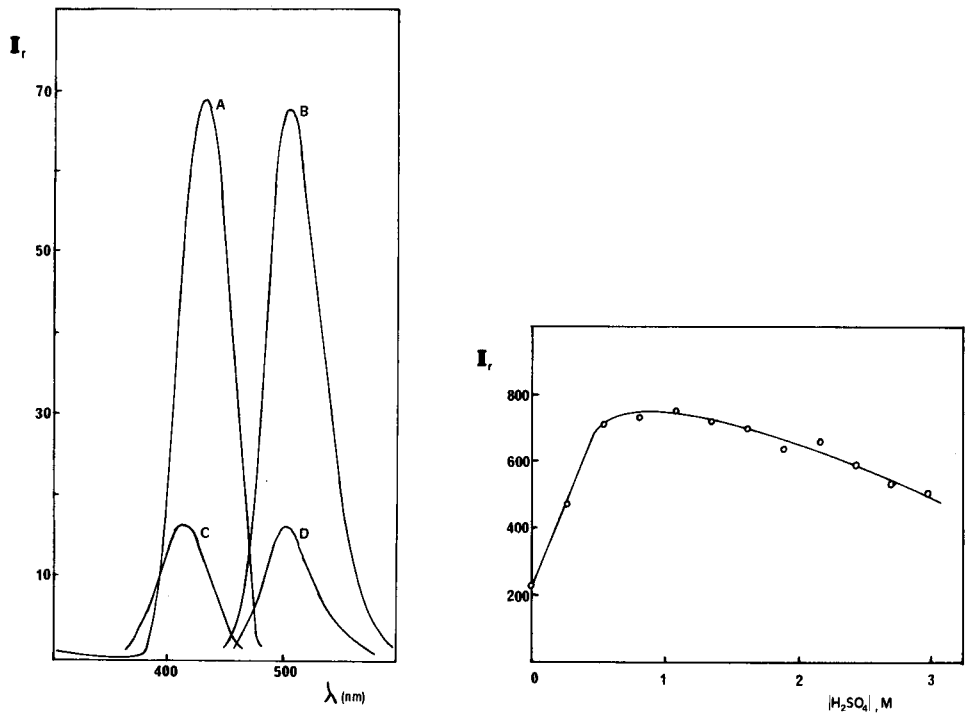

Fig. 1. Excitation and fluorescence spectra: (A, B) ternary system (scale: × 1); (C, D) binary system (scale: × 20). (5.35 × 10^{-7} M Nb, 1 M H_2SO_4, 0.5% (1.37 × 10^{-2} M) CTAB, 2.96 × 10^{-4} M morin.)

Fig. 2. Effect of sulfuric acid concentration on fluorescence intensity. (1.07 × 10^{-5} M Nb, 0.25% (6.8 × 10^{-3} M) CTAB, 2.96 × 10^{-4} M morin.)

temperature to ±0.2°C, the error from temperature variation is less than 1%. A temperature of 20 ± 0.2°C was used throughout.

The effect of CTAB concentration is shown in Fig. 3. The enhancement starts only after the c.m.c. has been reached (3.1 × 10^{-4} M, determined by surface tension measurements in 1 M sulfuric acid). The plateau occurs well above the c.m.c., indicating clearly the micellar nature of the fluorescence enhancement.

The addition of other cationic surfactants (cetylpyridinium bromide, cetylpyridinium chloride) produced similar effects although precipitation occurred after a time, thus these surfactants were discarded. Anionic (sodium lauryl sulfate) and non-ionic (Triton X-100) surfactants showed no effect on the excitation or fluorescence spectra of the niobium—morin complex.

Initially, the morin was dissolved in 50% ethanol; Fig. 4 shows the effect of morin concentration in this solution. The intensity reached a maximum at 1.8 × 10^{-4} M morin. The decrease in fluorescence intensity at greater

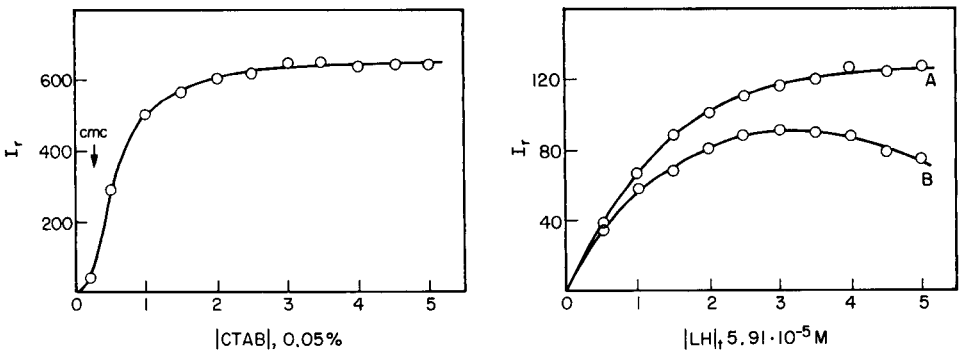

Fig. 3. Effect of CTAB concentration (1.07×10^{-5} M Nb, 1 M H_2SO_4, 2.96×10^{-4} M morin.)

Fig. 4. Effect of morin concentration: (A) morin in CTAB solution, (B) morin in 50% ethanol. (5.35×10^{-7} M Nb, 1 M H_2SO_4, 0.25% (6.8×10^{-3} M) CTAB.)

morin concentrations was found to be due to the increasing ethanol concentration (which destroyed the micelles). When the presence of ethanol was avoided by dissolving morin in the surfactant solution (as used in the recommended procedure) the intensity increased with morin concentration up to a constant value; 5 ml of the fluorimetric reagent solution (5.91×10^{-4} M morin in 1% CTAB) was selected for further use.

Pilipenko et al. [11] noticed the decrease in the fluorescence intensity in micellar solutions above a 15-fold excess of morin with respect to niobium. They attributed this effect to "formation of non-fluorescent niobium complexes of a different composition". According to the present results, by avoiding the addition of ethanol, excesses of morin of over 500 times with respect to 5.35×10^{-7} M niobium do not decrease the fluorescence intensity. As will be discussed later, the nature of the different niobium complexes formed at large morin concentrations has been elucidated. A 1:3 complex seems to be the predominant species under these conditions, but it is highly fluorescent, too.

Some complexing agents commonly used for dissolution and stabilization of niobium solutions may form ternary complexes with special fluorescent characteristics [13]. Therefore, hydrogen peroxide, oxalic acid, tartaric acid and fluoride were tested for their influence on the fluorescence emission of the niobium/morin/CTAB complex. In 1 M sulfuric acid containing 0.05 mg l^{-1} niobium, hydrogen peroxide almost completely destroyed the fluorescence of the complex even in only a 10-fold molar excess. Oxalic acid was tolerated up to a 10-fold molar excess. Fluoride and tartaric acid did not affect the fluorescence up to a 100-fold molar excess (the mole ratio Nb:tartaric acid in the stock solution is 1:65); larger amounts quenched it.

Analytical parameters

The calibration graph was linear up to 0.1 mg l^{-1} niobium. A detection limit (2 σ) of 1 μg l^{-1} niobium was obtained. The relative standard deviation, evaluated from ten independent determinations of 0.05 mg l^{-1} niobium, was 3.5%.

Interferences. The effect of twenty metals, which are often associated with niobium in samples, was studied. The results are summarized in Table 1. They show that most metals which accompany niobium in its minerals and ores do not interfere at the maximum assayed concentration level. Only tin and tungsten increased the fluorescence of niobium, and were tolerated only to a limited extent (5- and 2-fold weight excesses, respectively). Molybdenum decreased the fluorescence signal, the decrease increasing with increasing molybdenum concentration, probably because of the formation of a non-fluorescent complex with morin, thus displacing niobium. The reaction of niobium with morin in CTAB micelles, therefore, is exceptionally selective. It is straightforward to remove the few interferences observed. Molybdenum and tungsten can be pre-separated [14] and tin is masked with EDTA (Table 1).

Nature of the enhanced fluorescence

In the absence of surfactants, niobium is precipitated by morin (LH) from sulfuric acid [15] as a red-brown complex, which has been proposed for use in the gravimetric determination of the metal [15]. We have shown that the same precipitate is obtained from 1 M hydrochloric acid in the absence of sulfate. Elemental analysis of the dried product indicated a

TABLE 1

Effect of some foreign metals (M) on the determination of 0.05 mg l^{-1} niobium

Metal[a]	Ratio (M: Nb) (w/w)	Niobium recovery (%)
Na	10^6	101
Sn(IV)	5	106
	10	109
	50	138 (99[b])
Mo(VI)	2	101
	10	97
	100	55
W(VI)	2	107
	5	110
	10	127

[a]Ca, Mn, Ni, Cd, Bi, Hg, Zn, Pb, Al, Cu, Fe(III), Co, V(V), U(VI), Ti and Ta (5 mg l^{-1}) all gave recoveries of 100 ± 4%. [b]Masking with 5 × 10^{-3} M EDTA.

stoichiometry (Nb:L) of 1:1. The solid compound is not fluorescent, but it dissolves slowly in ethanol, acetone or aqueous 0.5% CTAB yielding fluorescent solutions with spectral characteristics clearly different from those of morin.

Three different saturated solutions of such a precipitate were prepared in 0.2 M hydrochloric acid in 50% acetone, 50% ethonol, and 0.5% CTAB. To each solution potassium sulfate was added in order to increase their final sulfate concentration from 10^{-4} to 10^{-1} M. In all three solutions, a sharp increase in the fluorescence intensity was observed in the presence of enough sulfate (e.g., in the acetone solution the fluorescence intensity was enhanced 40-fold when the sulfate concentration was higher than 4×10^{-2} M). Pilipenko et al. [11] stated that the niobium—morin complex formed by mixing niobium and an excess of morin in the micellar solution did not fluoresce in the absence of sulfate ions. This effect was attributed to the formation of a negative ternary complex $(NbO(OH)SO_4 \cdot H_4R)^-$ because it fluoresced only in micellar solutions of cationic surfactants. As explained above, fluorescence (much weaker) was observed here in the absence of sulfate. Thus the possibility exists that the bromide counterions of CTAB (which may act as fluorescence quenchers) could be replaced by the non-quenching sulfate in the Stern layer of the micelles. It is known that sulfate ions have a stronger affinity than bromide for adsorption on the CTAB micelles [16], and this could explain the observed enhancement of fluorescence on addition of sulfate. However, such a possibility had eventually to be ruled out in the light of the following experimental facts. Replacement of cetylpyridinium bromide by the corresponding chloride had very little, if any, effect on fluorescence intensity. Addition of sulfate to 1 mg l^{-1} niobium in 0.2 M hydrochloric acid (and in an excess of morin) caused in all cases (50% acetone, 50% ethanol and aqueous 0.5% CTAB) a decrease in the absorbance at the 426 nm maximum (up to a 35% decrease in the acetone solution). At the same time, a clear shift of the excitation maximum from 426 to 432 nm was observed. In the case of ethanol or acetone, no bromide ions were present but sulfate addition enhanced the fluorescence in both cases.

Therefore, the present results strongly support the formation in the acidic medium of a real ternary complex between niobium, morin and sulfate, as proposed by Pilipenko et al. [11] who found a 1:1 Nb:sulfate mole ratio. Moreover, such a complex seems to build up and fluoresce only in structured solubilizing solutions (surfactant, ethanol or acetone solutions) otherwise the insoluble red-brown compound of niobium and morin precipitates.

Composition and stability of the niobium/morin complex in micelles

According to Pilipenko et al. [11], the niobium/morin ratio in the fluorescent complex is 1:1. The present results, based on Job's method with measurements of the fluorescence intensity of the isomolar series prepared

in the analytical conditions of the general procedure, indicated a stoichiometric ratio Nb:morin of greater than 1:1 (a mixture of complexes seems likely from such plots). Mole ratio methods were inconclusive because of the high dissociation observed. Therefore, the "corresponding solutions" method [17] was used, with spectrophotometric, instead of fluorimetric, determinations, in order to clear up the stoichiometry and measure the conditional stability constants of the complex between niobium and morin in CTAB micelles. A CTAB concentration of 0.5% and 1 M sulfuric acid were fixed in all solutions. Forty data points were obtained by testing each of four different niobium concentrations (1.07×10^{-5}—1.07×10^{-4} M) with ten morin concentrations (5.91×10^{-6}—2.96×10^{-4} M). Absorbances were measured at 426 nm after 2 h equilibration in a thermostat at 20°C.

Formation of two different complexes with stoichiometry Nb:morin of 1:1 and 1:3, having overall conditional stability constants $\beta_1 = (1.14 \pm 0.01) \times 10^4$ l mol^{-1} and $\beta_3 = (5.66 \pm 0.02) \times 10^{10}$ l^3 mol^{-3}, was the best fit with the results obtained. The corresponding equilibria can be simply depicted by

$$Nb_{ac} + LH(S^+)_m \overset{\beta_1}{\rightleftharpoons} Nb'L(S^+)_m + H_2O$$

$$Nb_{ac} + 3LH(S^+)_m \overset{\beta_3}{\rightleftharpoons} Nb''L_3(S^+)_m + 3H_2O$$

where Nb_{ac} is probably the complex $Nb(OH)_4SO_4^-$, which has lost one OH^- in Nb′ and two more OH^- in Nb″ on complexation with morin; LH is the molecular form of morin, completely protonated in the 1 M sulfuric acid medium; $(S^+)_m$ represents the micelles of CTAB.

Owing to the limited solubility of morin in the surfactant medium, only the first part of the formation curve could be obtained (see Fig. 5), from which the composition and stability constants were calculated. The fit between the theoretical and experimental curves, however, is very good, as shown in Fig. 5. The best fit was worked out by minimizing the expression $\Sigma(\bar{n}_{exp} - \bar{n}_{cal})^2$ with the aid of a Simplex microcomputer program and by further graphic treatment of the $\bar{n}$, [LH] data.

The β_1 value was also evaluated from fluorimetric mole ratio data. For such a purpose, different experimental curves of intensity vs. total morin concentration $[LH]_t$, were obtained at four different niobium concentrations, and the function Φ was calculated ($\Phi = (I_s - I_b)/[Nb(V)]_t$, where I_s and I_b are the fluorescence intensities of the sample and blank, respectively, normalized by referring them to the fluorescence of a 1 mg l^{-1} quinine sulfate standard). Figure 6 shows the results for different niobium concentrations. Because of the large excess of morin used, the same curve is obtained for every niobium concentration tested.

In this case, at low morin concentrations, where the 1:1 complex is formed, the plot of $\log \Phi_i/(\Phi_{max} - \Phi_i)$ vs. $\log [LH]_t$ is a straight line with slope 1.0, and $\log \beta_1 = -\log [LH]_t$ at the point $\log \Phi_i/(\Phi_{max} - \Phi_i) = 0$. The β_1 value obtained is 1.13×10^4 l mol^{-1}, which is in very good agreement with the value obtained by the corresponding solutions method.

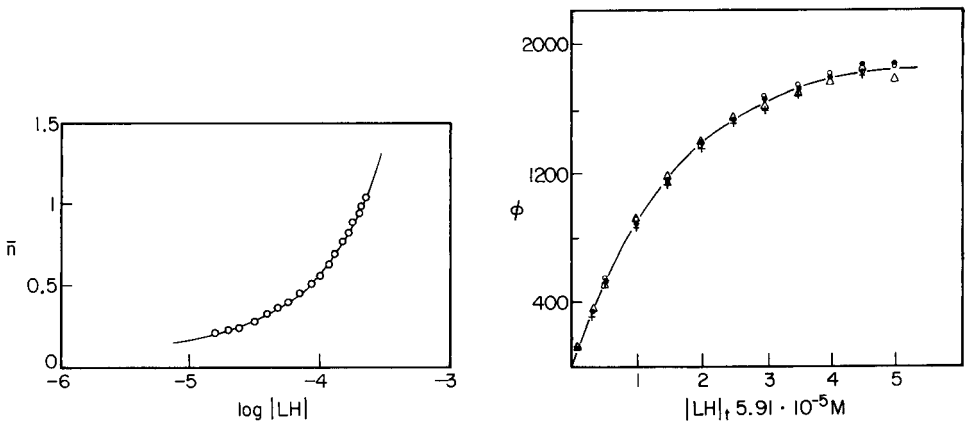

Fig. 5. Formation curve for the morin—niobium complex in CTAB—sulfuric acid. The points are experimental values; the line is the calculated values. ([LH] = free morin, not bound to Nb.)

Fig. 6. Effect of total morin concentration on Φ for different niobium concentrations: (+) 40; (△) 60; (○) 80; (•) 100 μg l^{-1}. (1 M H_2SO_4, 0.5% (1.37 × 10^{-2} M) CTAB.)

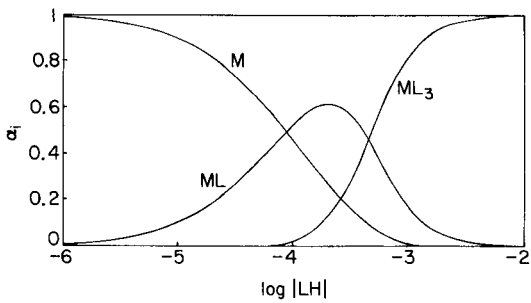

Fig. 7. Degree of formation of the various complexes (LH is free morin).

Figure 7 shows the degree of formation curves for the various niobium complexes, which allow the computation of the molar absorptivities of the two complexes detected by the corresponding solutions method. The best fit corresponded to the values $\epsilon_1 = (8.96 \pm 0.01) \times 10^3$ and $\epsilon_3 = (3.56 \times 0.01) \times 10^4$ l mol^{-1} cm^{-1}.

The role of the surfactant and micellar effects

The power of cationic surfactants to enhance spectroscopic properties of organic dyes or metal chelates may be ascribed to two effects. The first is the formation of unusual [10] ion-association complexes. The spectral changes observed occur well below the c.m.c. of the surfactant, and stoichiometric ratios of metal to surfactant are observed [10, 12, 18]. The second is the formation of micelles able to solubilize or organize molecules in their

amphiphilic regions, and thus alter the microenvironment experienced by a given chromophore or luminophore in the bulk solution. Formation of such microscopically organized aggregates (micelles) takes place at concentrations of surfactant above the c.m.c. and, therefore, a stoichiometric ratio of metal to surfactant would be meaningless. From Fig. 3 and the fact that the niobium—morin complex precipitates in bulk aqueous solution (in the absence of micelles), it seems clear that such a complex is solubilized and "organized" into or onto the micelles and, in this way, its lowest excited singlet state is stabilized and protected.

The reaction of niobium with morin in micelles in 1 M sulfuric acid (the analytical conditions) is quite involved: only cationic surfactants seem to enhance the fluorescence and, above all, it is sulfate ions that cause a dramatic increase of fluorescence. Sulfuric acid is known to enhance the colour of some niobium complexes by replacement of hydroxide ions in the cation by sulfate or hydrogensulfate ligands [19]. However, niobium very often forms fluorescent coordination-unsaturated ternary complexes, which are responsible for the improved selectivity of fluorimetric methods based thereon [13]. In the light of this information [11], it appears that negatively charged ternary complexes of the coordination-unsaturated type are built up by niobium, morin and sulfate in the analytical reaction medium.

The micellar medium seems to favour, as usual, elimination of water (or hydroxide ligands) from the chelate, giving rise to an increase in the coordination number of the cation (formation of a 1:3 complex at the analytical morin concentrations). Experience shows that ethanol or acetone provides a solubilizing organized media in which the microenvironment experienced by the luminophore is quite similar to that in the CTAB micelles. As acetone or ethanol would never form micelles in the aqueous solution (no hydrophobic cores present), the fluorescent probe in the CTAB solution should reside at the micelle-water boundary, away from the highly hydrophobic centre of the CTAB micelles.

The authors thank the Comision Asesora de Investigacion Cientifica y Tecnica for financial support, and Dr. M. E. Díaz García for her assistance with some of the early experimental work.

REFERENCES

1 N. Ishibashi and K. Kina, Anal. Lett., 5 (1972) 637.
2 K. Kina and N. Ishibashi, Microchem. J., 19 (1974) 26.
3 K. Kina, K. Tamura and N. Ishibashi, Japan Analyst, 23 (1974) 1404.
4 A. T. Pilipenko, A. I. Volkova, G. N. Pshenko and V. P. Deniseerku, Ukr. Khim. Zh., 46 (1980) 200.
5 A. T. Pilipenko, G. N. Pshenko and A. I. Volkova, Ukr. Khim. Zh., 48 (1982) 957.
6 J. Medina Escriche, M. de la Guardia Cirugeda and F. Hernández Hernández, Analyst (London), 108 (1983) 1386.
7 T. Taketatsu and A. Sato, Anal. Chim. Acta, 108 (1979) 429.
8 T. Taketatsu, Talanta, 29 (1982) 397.

9 A. Sanz-Medel, M. E. Díaz García and J. I. García Alonso, Spectrochim. Acta Part B, Suppl., 38 (1983) 289.
10 J. I. García Alonso and A. Sanz-Medel, Talanta, 31 (1984) 361.
11 A. T. Pilipenko, T. A. Vasil'chuk and A. I. Volkova, Zh. Anal. Khim., 38 (1983) 855.
12 A. Sanz-Medel, C. Cámara Rica and J. A. Pérez-Bustamante, Anal. Chem., 52 (1980) 1035.
13 P. R. Haddad, Talanta, 24 (1977) 1.
14 A. Sanz-Medel and M. E. Díaz García, Analyst (London), 106 (1981) 1268.
15 O. Tomiček, K. Spurny, L. Jerman and V. Holeček, Collect. Czech. Chem. Commun., 18 (1953) 757.
16 M. Grätzel and J. K. Thomas, J. Am. Chem. Soc., 95 (1973) 6885.
17 F. J. C. Rossotti and H. Rossotti, The Determination of Stability Constants, McGraw-Hill, New York, 1961, p. 282.
18 S. B. Savvin, R. K. Chernova and I. V. Lobacheva, Zh. Anal. Khim., 36 (1981) 9.
19 H. A. Flaschka and A. J. Barnard, Jr., Chelates in Analytical Chemistry, Vol. 2, M. Dekker, New York, 1969, p. 231.

Analytica Chimica Acta, 165 (1984) 171—176
Elsevier Science Publishers B.V., Amsterdam — Printed in The Netherlands

SPECTROFLUORIMETRIC DETERMINATION OF CATECHOLAMINES WITH 1,2-DIPHENYLETHYLENEDIAMINE

HITOSHI NOHTA, AKANE MITSUI and YOSUKE OHKURA*

Faculty of Pharmaceutical Sciences, Kyushu University 62, Maidashi, Higashi-ku, Fukuoka 812 (Japan)

(Received 16th January 1984)

SUMMARY

A sensitive spectrofluorimetric method for the determination of catecholamines with 1,2-diphenylethylenediamine is described. The method is based on the reaction of catechol compounds in neutral medium with 1,2-diphenylethylenediamine in the presence of hexacyanoferrate(III) and glycine at ambient temperature. The fluorescence produced shows excitation and emission maxima around 345 and 480 nm, respectively. The method is simple, selective for catechol compounds and very sensitive. Catecholamines can be determined at concentrations as low as 15—20 pmol ml^{-1}.

Many fluorimetric methods have been reported for the determination of catecholamines. They can be classified into three groups based on native fluorescence [1], trihydroxyindole [2—4] and ethylenediamine condensation [5, 6]. The native fluorescence method is not sensitive. The trihydroxyindole methods, which have been most widely used, are selective for catecholamines and sensitive for L-norepinephrine and L-epinephrine, but do not have sufficient sensitivity for the determination of dopamine. The ethylenediamine condensation methods require complication procedures though they are fairly sensitive.

1,2-Diphenylethylenediamine (DPE) has recently been found to react in a neutral medium with catecholamines and other catechol compounds in the presence of hexacyanoferrate(III) to give a compound which fluoresces intensely. The reaction is accelerated by amino acids such as glycine. Catecholamines (norepinephrine, epinephrine and dopamine) and D,L-isoproterenol were used to establish suitable reaction conditions for a general analytical method.

EXPERIMENTAL

Reagents, solutions and apparatus

Norepinephrine hydrogen tartrate, dopamine hydrochloride and bicine (Wako, Osaka), isoproterenol hydrochloride (Nakarai, Kyoto) and epinephrine hydrogen tartrate (Sigma, St. Louis) were used. Bicine was recrystal-

0003-2670/84/$03.00

lized from aqueous ethanol (50%, v/v) to remove fluorescent impurities. All other chemicals were of reagent grade. Deionized and distilled water was used. The DPE was synthesized by the method of Irving and Parkins [7] and recrystallized successively from petroleum ether and water to give colorless leaflets (m.p. 121°C).

For the DPE solution, 212 mg of the compound was dissolved in 10 ml of ethanol (0.1 M DPE). The solution was stable for at least one week when stored at room temperature, even in daylight.

Uncorrected fluorescence excitation and emission spectra, and intensities were measured with a Hitachi MPF-4 spectrofluorimeter in 10 × 10-mm quartz cells: spectral bandwidths of 5 nm were used in both the excitation and emission monochromators.

Procedure

To 1.0 ml of aqueous test solution in a test tube, 2.0 ml of 50 mM bicine buffer (pH 7.0) containing 0.5 M glycine, and 0.1 ml each of the DPE solution and 2.4 mM potassium hexacyanoferrate(III) were added successively. The mixture was incubated at 37°C for 30 min. To prepare the blank, the same procedure was followed except that the 1.0 ml of test solution was replaced with 1.0 ml of water. The fluorescence intensities of the test and blank were measured at the wavelength of maximum emission with irradiation at the excitation maximum (see Table 1).

RESULTS AND DISCUSSION

Determination of the catecholamines and isoproterenol

The excitation and emission maxima for the product from norepinephrine occur at 340 and 480 nm, respectively (Fig. 1). On irradiation at 340 nm, a very weak fluorescence of the reagent blank is observed (Fig. 1); the intensity is 1% of that given by 1 nmol ml^{-1} norepinephrine. The fluorescence of the blank is due to the impurities in bicine that remained even after recrystallization. 1,2-Diphenylethylenediamine (DPE) does not fluoresce over the pH range 1—13. The products from epinephrine, dopamine and isoproterenol show almost identical excitation and emission spectra with those from norepinephrine; the maxima are not really characteristic of the individual amines (Table 1).

Effect of reactant concentrations. With the catecholamines and isoproterenol, DPE gives a fluorescence in the presence of potassium hexacyanoferrate(III) and glycine in neutral medium. Concentrations of DPE ranging from 0.1 to 0.2 M in the DPE solution give almost maximum and constant fluorescence intensity for each amine (Fig. 2); 0.1 M was selected as optimum. The DPE was dissolved in ethanol. Ethanol does not affect the fluorescence development over the concentration range of 1—30% (v/v) in the reaction mixture; 3.1% (v/v), i.e., 0.1 ml as DPE solution in the final volume of 3.2 ml, was used.

TABLE 1

Excitation and emission maxima of the fluorescences from catechol compounds, their relative fluorescence intensities and limits of detection (LD)

	Excitation maximum[a] (nm)	Emission maximum[a] (nm)	Relative fluorescence intensity[b]	LD[c] (pmol ml^{-1})
Catechol	345	480	14	100
Pyrogallol	330	475	3	500
3,4-Dihydroxybenzylamine	340	470	32	50
3,4-Dihydroxybenzoic acid	330	480	3	500
Norepinephrine	340	480	100	15
Epinephrine	350	496	64	20
Dopamine	347	470	84	20
Isoproterenol	356	497	104	10
1-DOPA	348	480	19	80
3,4-Dihydroxyphenylacetic acid	345	477	72	20
3,4-Dihydroxymandelic acid	350	470	9	150
3,4-Dihydroxyphenylethyleneglycol	347	478	95	15
2-Hydroxyestrone	350	475	6	300
4-Hydroxyestrone	350	475	1	1800

[a]Portions (1.0 ml) of 1 nmol ml^{-1} solutions of catechol compounds were treated as in the procedure. [b]The fluorescence intensity from norepinephrine was taken as 100. [c]Defined as the concentration in the sample solution which gives a fluorescence intensity twice the blank fluorescence.

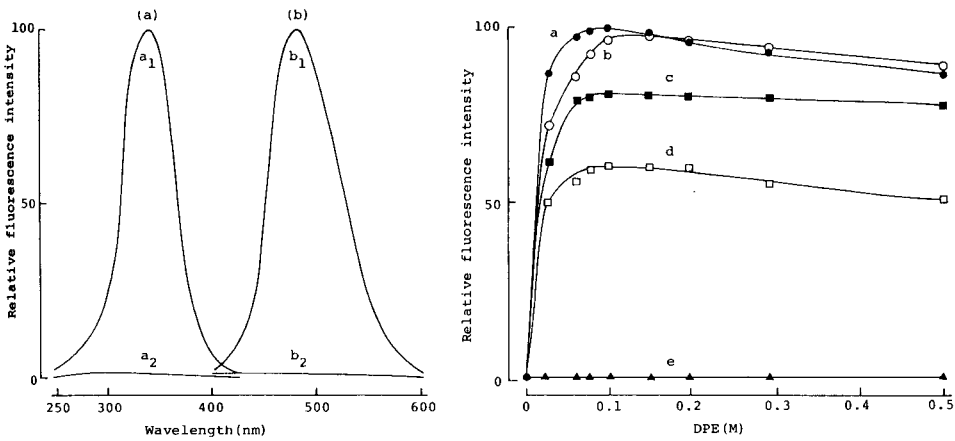

Fig. 1. (a) Excitation (340 nm) and (b) emission (480 nm) spectra of the reaction mixture of norepinephrine (a_1, b_1) and the reagent blank (a_2, b_2). Portions (1.0 ml) of 1 nmol ml^{-1} norepinephrine solution, and of water for the reagent blank, were treated as in the procedure.

Fig. 2. Effect of the concentration of DPE on the fluorescence development. Portions (1.0 ml) of 1 nmol ml^{-1} solutions of the amines, and of water for the reagent blank, were treated as recommended with various concentrations of DPE. (●) Isoproterenol; (○) norepinephrine; (■) dopamine; (□) epinephrine; (▲) reagent blank.

The concentration of potassium hexacyanoferrate(III) has an effect on the fluorescence development (Fig. 3A); in its absence, the fluorescence reaction occurs only slightly, probably because of oxygen dissolved in the reaction mixture. This suggests that oxidation is concerned with the reaction. Concentrations of hexacyanoferrate(III) in the reagent solution ranging from 1.8 to 3.0 mM provide maximum intensity; a concentration higher than 3.0 mM causes inhibition of the fluorescence development in proportion to the concentrations of hexacyanoferrate(III). This inhibition is due to the inner-filter effect (absorption of the fluorescence by hexacyanoferrate(III)), because such inhibition was not observed when the hexacyanoferrate(III) was decomposed by adding a reducing reagent such as ascorbic acid, β-mercaptoethanol or sodium hydrogen sulfite to the final reaction mixture. A hexacyanoferrate-(III) concentration of 2.4 mM was selected as optimum.

Glycine, lysine, ornithine and ω-amino acids, such as β-alanine, 4-amino-n-butyric acid, 6-amino-n-caproic acid and 8-amino-n-caprylic acid, accelerate the fluorescence reaction. Of these amino acids, glycine is most effective. Maximum and constant fluorescence intensity is attained at concentrations of glycine in bicine buffer in the range 0.375—0.625 M for norepinephrine, epinephrine and isoproterenol, whereas the fluorescence from dopamine increases with increasing concentrations of glycine up to 0.75 M (Fig. 3B); 0.5 M was selected tentatively.

Effect of pH. The optimum pH for the fluorescence reaction of norepinephrine is 6.0—7.2 (Fig. 4), and those for the reaction of the other compounds of interest are almost identical. Acetate and bicine buffers give almost the same fluorescence intensity for norepinephrine (Fig. 5) and the other amines examined, and their concentrations in the buffer solutions do

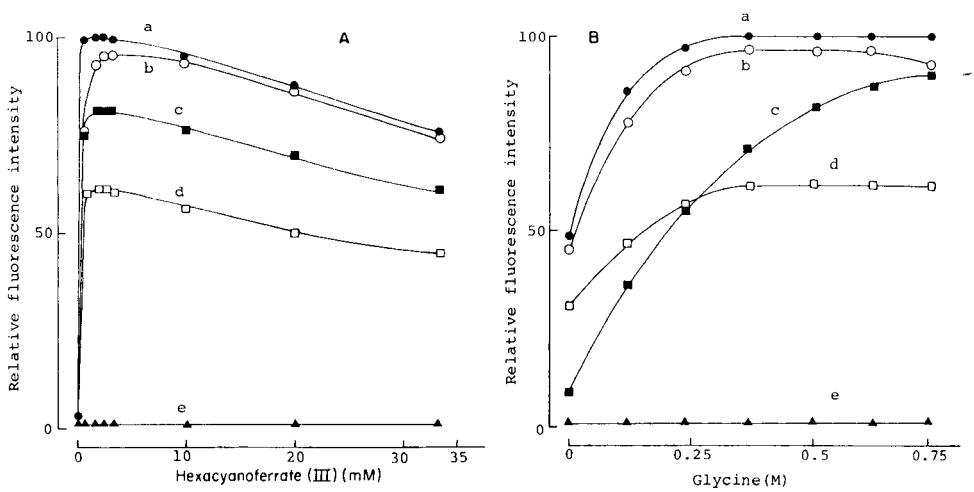

Fig. 3. Effect of the concentrations of (A) hexacyanoferrate(III) and (B) glycine on the fluorescence development. Portions (1.0 ml) of 1 nmol ml^{-1} solutions of the amines, and of water for the reagent blank, were treated as recommended with various concentrations of hexacyanoferrate(III) or glycine, the other concentration being as described in the procedure. Symbols as in Fig. 2.

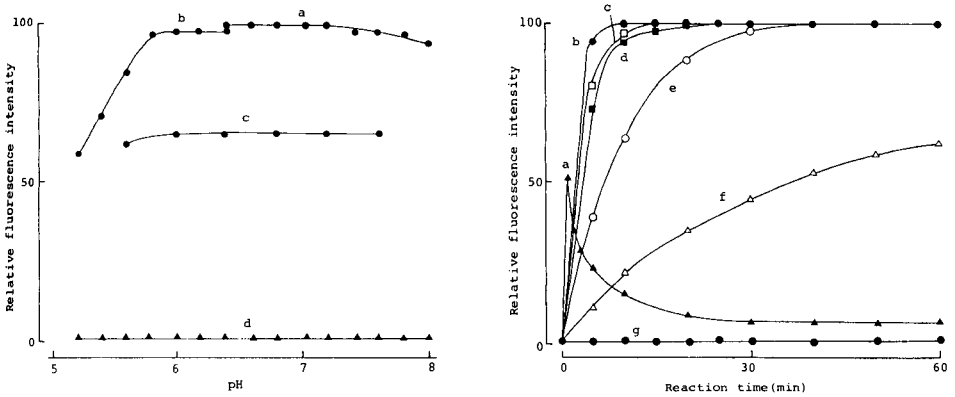

Fig. 4. Effect of pH on the fluorescence development from norepinephrine. Portions (1.0 ml) of 1 nmol ml^{-1} norepinephrine solutions, and of water for the reagent blank, were treated as recommended with buffers of various pH: (a) 0.05 M bicine buffer; (b) 0.05 M acetate buffer; (c) 0.05 M phosphate buffer; (d) reagent blank corresponding to (a—c).

Fig. 5. Effect of reaction temperature and time on the fluorescence development from norepinephrine. Portions (1.0 ml) of 1 nmol ml^{-1} norepinephrine solutions (and water) were treated as recommended for various times at different reaction temperatures: (a) 100; (b) 70; (c) 50; (d) 37; (e) 25; (f) 0°C. Curve (g) is the reagent blank corresponding to (a—f).

not affect matters over the ranges 0.01—0.5 M and 0.01—0.1 M, respectively; 0.05 M bicine buffer of pH 7.0 was used tentatively. The phosphate buffer inhibits the reaction (Fig. 4); the reason for this is unknown.

Effect of reaction temperature and time. The fluorescence reaction for norepinephrine occurs even at 0°C; at higher temperature the fluorescence develops more rapidly (Fig. 5). However, a temperature of 100°C causes marked reduction of the fluorescence, probably because of decomposition of the fluorescent compound. The fluorescence intensities at 37—70°C reach a maximum after heating for at least 25 min. A temperature of 37°C and a reaction time of 30 min were selected for reproducible results. The effect of the reaction temperature and time on the fluorescence development for the other compounds of interest are closely similar to those for norepinephrine.

Stability of fluorescence and precision of procedure. The fluorescences developed from the amines under the prescribed conditions do not change on irradiation for 10 min at their excitation maxima, and are stable for at least 2 h in daylight. The calibration graph is linear for each amine over concentrations ranging from 20 pmol ml^{-1} to 20 nmol ml^{-1}. The precision of the procedures for norepinephrine, epinephrine, dopamine and isoproterenol was established by running 20 determinations on 1 nmol ml^{-1} solutions. The relative standard deviations were 1.2, 0.8, 2.3 and 1.2%, respectively.

Fluorescence from other catechol compounds

All other catechol compounds tested also fluoresce under the conditions recommended. The excitation and emission maxima, the relative fluorescence

intensities and the limits of detection for all the compounds examined are summarized in Table 1. The proposed method is particularly sensitive for the catecholamines, isoproterenol and their metabolites in mammals, 3,4-dihydroxyphenylethyleneglycol and 3,4-dihydroxyphenylacetic acid. The limits of detection are in the range 10—20 pmol ml^{-1}. The excitation and emission spectra of the fluorescences from those compounds are fairly similar in shape and maxima to those of the fluorescence from norepinephrine and are not particularly characteristic of individual compounds.

Reaction of other substances

Other biologically important substances examined did not fluoresce at a concentration of 10 nmol ml^{-1}. The compounds tested were 17 different L-α-amino acids, tyramine, histamine, serotonin, octopamine, creatine, creatinine, uric acid, putrescine, spermidine, spermine, acetone, formaldehyde, acetaldehyde, *p*-hydroxybenzaldehyde, lactic acid, pyruvic acid, α-ketoglutaric acid, phenylpyruvic acid, oxalic acid, homovanillic acid, acetic acid, D-glucose, D-fructose, D-galactose, D-ribose, D-glucosamine, maltose, sucrose, L-ascorbic acid, uracil, thymine, cytosine, adenine, guanine, cholesterol, cortison, EDTA and sodium citrate. They also did not affect the fluorescence development from the catecholamines and isoproterenol. This suggests that the proposed method is selective for catechol compounds. Large amounts of reducing agents such as L-ascorbic acid and cysteine inhibit the reaction, because they consume the hexacyanoferrate(III) needed in the fluorescence reaction.

Studies on the mechanism of the fluorescence reaction are in progress. The reaction between ethylenediamine and catechol compounds gives a fluorescent quinoxaline derivative [8] so that the reaction used here probably yields 2,3-diphenylquinoxaline derivatives. The role of glycine is unknown.

The proposed method is simple and is approximately 10 times more sensitive for norepinephrine and epinephrine and about 500 times more sensitive for dopamine than the THI method [3]. It is also about 10 times more sensitive for all the catecholamines than the ethylenediamine condensation method [5]. Therefore, this method should be useful for the determination of traces of catecholamines in biological samples after their chromatographic separation.

A generous gift of 2- and 4-hydroxyestrones from Prof. T. Nambara and Ass. Prof. K. Shimada of Tohoku University are gratefully acknowledged.

REFERENCES

1 O. H. Lowry, J. Biol. Chem., 173 (1948) 677.
2 A. Lund, Acta Pharmacol. Toxicol., 6 (1950) 137.
3 U. S. von Euler and I. Floding, Acta Physiol. Scand. 33, Suppl., 118 (1955) 45.
4 R. J. Merrills, Nature, 193 (1962) 988.
5 H. Weil-Malherbe and A. D. Bone, Biochem. J., 51 (1952) 311.
6 T. Seki, J. Chromatogr., 155 (1978) 415.
7 M. N. H. Irving and R. M. Parkins, J. Inorg. Nucl. Chem., 27 (1965) 271.
8 J. Harley-Mason and A. H. Laird, Tetrahedron, 7 (1959) 70.

Analytica Chimica Acta, 165 (1984) 177—185
Elsevier Science Publishers B.V., Amsterdam — Printed in The Netherlands

STOPPED-FLOW INJECTION DETERMINATION OF COPPER(II) AT THE ng ml^{-1} LEVEL

F. LÁZARO, M. D. LUQUE DE CASTRO and M. VALCÁRCEL*

Department of Analytical Chemistry, Faculty of Sciences, University of Córdoba, Córdoba (Spain)

(Received 11th July 1983)

SUMMARY

A stopped-flow injection method for the determination of copper(II) in the range 0.2—300 ng ml^{-1} is proposed, based on the catalytic effect of this ion on the 2,2′-dipyridylketone hydrazone/hydrogen peroxide reaction. The oxidation product shows an intense blue fluorescence that is monitored at λ_{ex} = 350 nm, λ_{em} = 427 nm. The sampling rate (72 h^{-1}), r.s.d. (1.4%) and the lack of interference from most foreign ions, allowed application of the method to the determination of copper in foods and blood serum.

Stopped-flow techniques have been applied in traditional kinetic methods based on fast reactions; in general, they need complex instrumentation [1, 2]. Flow injection analysis (f.i.a.) makes it possible to develop stopped-flow techniques using simple instrumentation, but they cannot be used for very fast reactions. To stop the reaction zone in the detector, two flow-injection manifolds have been described. One involves intermittent pumping, by which sulphur dioxide in wine [3], ethanol in blood [4], lactate dehydrogenase [5] and glucose [6] have been determined. In the other, an additional valve diverts the flow before its arrival at the detector; polyphosphates and EDTA have been determined in this way [7]. The variation of the signal over a fixed time is measured. A third approach is also possible. It consists of stopping the flow before the reaction zone has reached the detector, so that the "stop time" is not used for measurement but for incubation. An increase in sensitivity is thus achieved because the residence time is lengthened without an increase in dispersion. With this technique, traces of cobalt have been determined [8] and a merging-zones system for fluoro-immunoassay has been proposed [9].

In this paper, the use of the first type of stopped-flow mode is described for the spectrofluorimetric determination of copper(II) based on its catalytic action on the 2,2′-dipyridylketone hydrazone(DPKH)/hydrogen peroxide system. The solutions of DPKH are very slowly oxidized by atmospheric oxygen, forming a product that gives a strong blue fluorescence (λ_{ex} = 350 nm, λ_{em} = 427 nm) in a strongly acidic medium. The presence of some cations [10, 11] accelerates the appearance of this fluorescence, copper(II)

0003-2670/84/$03.00

being the most effective. The oxidation takes place only in alkaline media, its rate increasing exponentially with hydroxide concentration. The fluorescence, however, is greatest in very acidic media (pH 0.7), decreasing with increase in pH until it disappears at pH 7.0.

This reaction has been used in three methods for the determination of copper, conventional equilibrium [10] and kinetic [11] methods, and f.i.a. [12]. In the equilibrium procedure two steps for developing maximum fluorescence are necessary; the oxidation product is generated slowly (90 min) in a neutral medium followed by acidification to allow fluorescence. The kinetic method requires only one step, but the intermediate pH (6.3) necessary neither produces the oxidation product rapidly, nor provides maximum fluorescence. The equilibrium method is highly sensitive (0.4—1.0 ng ml^{-1}), but is slow and the relative standard deviation (r.s.d.) is 4.5%. The kinetic method is less sensitive (0.1—1.0 $\mu g\ ml^{-1}$), but faster (4 min per sample) and the r.s.d. is 2.0%. In the flow-injection method [12], the oxidation is done in alkaline solution at optimum pH, and then an acidic stream is introduced to allow optimum fluorescence measurement. The method is very sensitive (8—300 ng ml^{-1}) and fast (100 samples h^{-1}) and the r.s.d. is 2%. Nevertheless, the interference of many cations and anions made the method inapplicable to the determination of copper in real samples. The use of the stopped-flow mode gives a better detection limit, smaller r.s.d. and the almost complete elimination of interferences, without sacrificing the advantages of the f.i.a. approach.

EXPERIMENTAL

Equipment and solutions

A Tecator 5020 flow injection analyzer was used; it has two peristaltic pumps connected to a microprocessor which can stop and start them individually, and synchronize them with the injection system. The microprocessor also displays the increase of fluorescence that occurs when the flow has stopped and prints it out. The injection valve (Tecator L-100-1) has a variable volume. All the reactor coils were made of teflon tubing, as were the sample loops which were calibrated spectrophotometrically using a dye. The flow cell was a Hellma 176.52-QS with 25-μl inner volume. A Perkin-Elmer MPF-43 A spectrofluorimeter was used, connected to a Perkin-Elmer 56 chart recorder. The printer was an Alphacom 40. Other instruments used were a Beckman 3500 pH meter, a thermostat bath and a Selecta S-382 thermostat.

Stock solutions used included an aqueous solution (1.0000 g l^{-1}) of DPKH and a copper(II) nitrate solution containing 1.0236 g l^{-1} of copper(II) standardized iodometrically.

The manifold used is described in Fig. 1. A 60-μl sample (0.25 M $NaClO_4$, 0.5 M H_2O_2 and Cu^{2+} at pH 4.4) was injected into a reagent stream (1×10^{-4} M DPKH and 0.1 M KNO_3 at pH 4.2). The reagent flow-rate was 1.0 ml min^{-1}

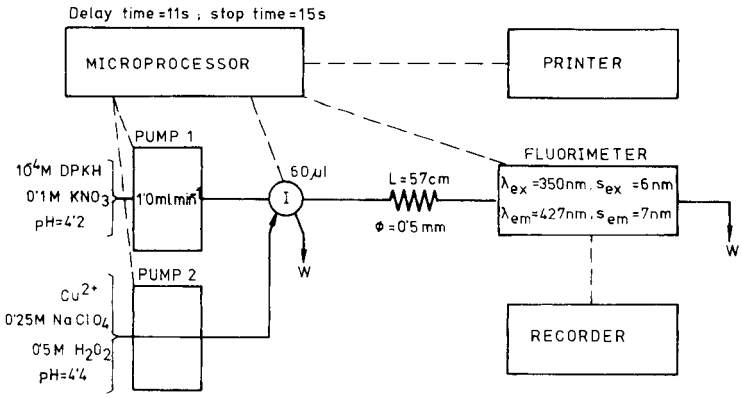

Fig. 1. Schematic diagram of the manifold used.

and the reactor length was 57 cm (0.5 mm i.d.). The spectrofluorimeter parameters were: λ_{ex} = 350 nm, λ_{em} = 427 nm, slit S_{ex} = 6 nm, S_{em} = 7 nm. The delay time (time between injection and reaching the detector) was 11 s; the stop time (the time the stopped solution remained in the detector) was 15 s.

Sample pretreatment

Foods. The samples (5 g, 12 g and 23 g for rice, banana and pear, respectively) should be treated according to the IUPAC-recommended procedure [13] as follows. In a beaker, gently warm the accurately measured mass or volume of the food sample with 10—20 ml of (1 + 1) sulphuric—nitric acid. In order to destroy the organic matter completely, add several drops of 30% hydrogen peroxide. Collect the remaining solution in a 100-ml volumetric flask and dilute to volume with distilled water to give the stock solution from which the samples for analysis are prepared, as described below.

Deproteinization of serum. To 1 ml of serum add 0.7 ml of 2 M hydrochloric acid, and allow to react for 10 min. Add 1 ml of 20%(w/v) trichloroacetic acid, stir and allow to stand for 10 min. Centrifuge, and transfer exactly 0.1 ml of the supernatant solution to a 25-ml volumetric flask. Add the necessary reagents (see below) and dilute to volume with distilled water.

RESULTS AND DISCUSSION

Study of variables for the flow-injection manifold

The variables studied were sample volume, length and inner diameter of the reactor, flow rate and delay time. The concentrations used in these experiments were as follows: carrier solution, 5×10^{-4} M DPKH/0.1 M KNO_3/pH 4.5; sample solution, 102.4 ng Cu ml^{-1}/0.400 M H_2O_2/pH 4.5. The manifold parameters used in the optimization procedure were a reactor length of 64.5 cm, inner diameter 0.5 mm, a stop time of 20 s and a mode (FIA 5020) of 9. The spectrofluorimeter parameters were as described above.

The sample volume was varied between 29.3 and 229.5 μl. The increase in fluorescence intensity, ΔI_f, plotted vs. sample volume (Fig. 2A) was almost linear up to ca. 120 μl. As a compromise between the higher sensitivity achieved with larger sample volumes and economy of reagent and faster analysis achieved with smaller volumes, a sample volume of 59.5 μl was chosen for further experiments.

The influence of the reactor length on the analytical signal is shown in Fig. 2B. An exponential decrease of the signal on increasing the tube length is obtained. Therefore the optimum value of this variable is the minimal length that permits the connection of the injection system to the flow cell. This will provide maximum signals and sampling rates and in this case was 57 cm. The tube diameters studied were 0.35, 0.50 and 0.70 mm. A decrease of signal was observed when the diameter was increased, as a consequence of the lower concentration of the sample plug on arrival in the detector cell. The delay time increased with tube diameter (at the same flow rate) because of the increased volume of solution that needs to be displaced before the sample reaches the detector.

Increasing flow rates produced an exponential decrease in the signal (Fig. 2C), because of a corresponding increase in the dispersion. A flow rate

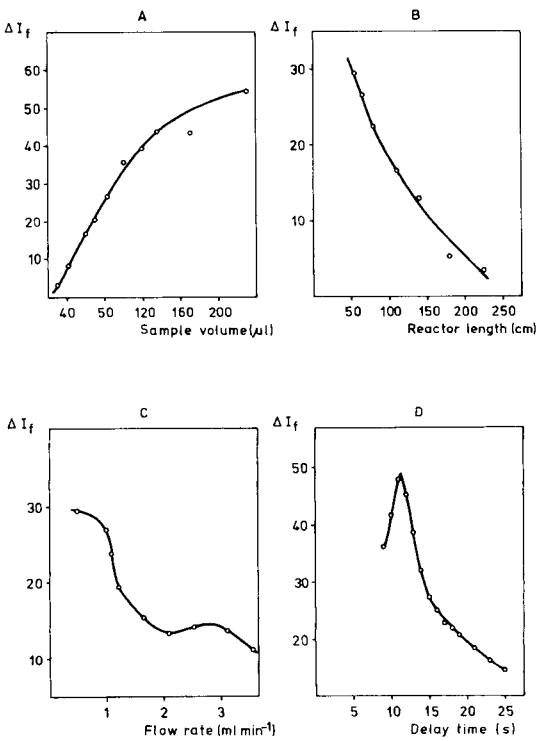

Fig. 2. Influence of flow variables on the increase in fluorescence intensity, ΔI_f: (A) sample volume; (B) reactor length; (C) flow rate; (D) delay time (for conditions see text).

of 1.0 ml min^{-1} was chosen as a compromise between the sampling frequency and sensitivity. Figure 2D shows that, when the optimum conditions established above were used, a delay time of 11 s gave the greatest signal. The reason for this is shown in detail in Fig. 3.

Study of reagent concentrations

Variables such as pH (sample solution and reagent-carrier solution), ionic strength (sample and reagent), temperature, concentration of DPKH and hydrogen peroxide were optimized. The pH has an important effect on the development of the analytical signal because of its very different effects on DPKH oxidation and fluorescence production. The influence of the pH of the carrier solution was studied by adding sodium hydroxide or hydrochloric acid until the desired pH was reached and adding potassium nitrate to give an ionic strength of 0.1 M. Figure 4A shows that the pH which gives the greatest signal is 4.2, intermediate between the maximum oxidation rate of DPKH (alkaline) and the maximum fluorescence (very acidic). With regard to the sample pH Fig. 4A shows that the signal is constant for pH values between 4 and 6. In subsequent experiments, pH 4.4 was used.

The ionic strength of the reagent solution has a great influence on the analytical signal. For 0.0—0.1 M potassium nitrate there is a marked decrease in signal with increasing ionic strength. The decrease was less marked for 0.1—0.5 M solutions. Thus 0.1 M was selected for further experiments. The effect of the ionic strength of the sample is different. The analytical signal

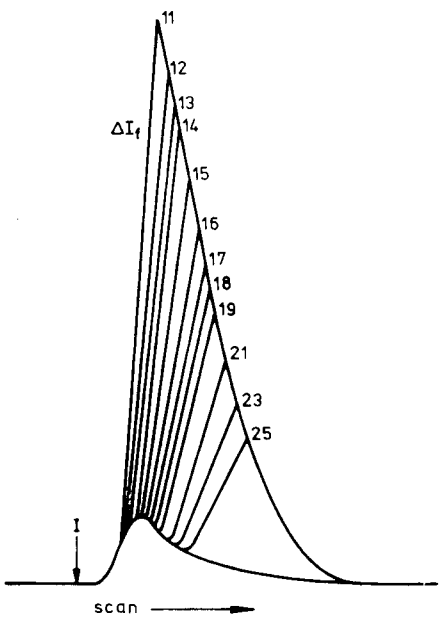

Fig. 3. Influence of delay time on the slope of the stopped-flow responses.

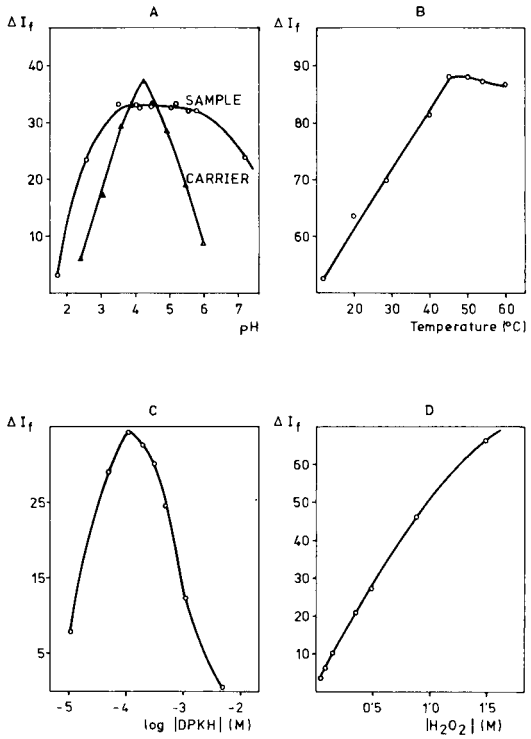

Fig. 4. Influence on the fluorescence intensity of: (A) pH; (B) temperature; (C) DPKH concentration; (D) H_2O_2 concentration.

increases enormously with increasing potassium nitrate concentration. Other salts were also tested. Sodium chloride decreased the signal with increasing salt concentration because of complexation of copper by chloride. Sodium perchlorate (up to 0.3 M) caused a slight increase in signal with increasing concentration. Further experiments were performed in 0.25 M sodium perchlorate.

The effect of temperature is shown in Fig. 4B. Up to ca. 45° C the signal increases linearly with temperature; it is constant between 45 and 50° C and decreases slightly at higher temperatures because of the rapid decomposition of hydrogen peroxide. Therefore 45° C is recommended. The effect of DPKH concentration was studied between 10^{-2} and 10^{-5} M (Fig. 4C). The maximum signal was obtained for 1.0×10^{-4} M DPKH. The effect of hydrogen peroxide concentration is shown in Fig. 4D; obviously a high peroxide concentration is necessary to achieve sensitive responses.

Determination of traces of copper

Calibration graphs for copper(II) obtained under the optimal conditions specified above were linear for 0.2—2.0 and 2.0—10.0 ng Cu ml^{-1} for different

values of stop time, as shown in Table 1. The table also shows how the stop time affects the sampling rate and the sensitivity. The intermediate value (15 s) is recommended as a compromise between sensitivity, sampling rate and reproducibility. These straight segments are part of a calibration curve that extends from 0 to 300 ng ml^{-1}. This curve could be fitted to a 4th-order polynomial by using a least-squares method.

The reproducibilities of determination of copper within each linear range, and in the curved region, are shown in Table 2. The precision is greater with this stopped-flow technique than that obtained with normal f.i.a. [12].

Interferences were studied by injecting samples containing 1.0 ng Cu ml^{-1} and up to a maximum of 100 ng ml^{-1} of foreign ions. Some of the results obtained are shown in Fig. 5. EDTA interferes at the same concentration as the catalyst. Some species interfere positively [Au(III), Fe(III), Hg(II), Sn(II), Co(II), Ni(II) and I^-], while others show a negative interference. Figure 5 also shows that the present method has a substantially improved selectivity compared with the conventional f.i.a. technique. For example species that, in the normal mode, interfered at the same level as copper, such as Al(III), Cr(III), Be(II) and Sn(II), did not affect the signal in the new method even in a 100:1 ratio to copper [Sn(II) 60:1]. Only dihydrogenphosphate shows greater interference in the stopped-flow mode in which a 80:1 ratio cannot be tolerated. Especially interesting is the absence of interference from

TABLE 1

Calibration data

Stop time (s)	Sampling frequency (h^{-1})	Correlation coefficient[a]	
		0.2—2.0 ng Cu ml^{-1}	2.0—10.0 ng Cu ml^{-1}
20	60	0.993	0.991
15	72	0.997	0.995
8	90	0.980	0.994

[a]5 points for each graph.

TABLE 2

Statistical study of the method[a]

Cu conc. (ng ml^{-1})	1.0	6.1	73.7
$\bar{x}$	1.01	6.11	73.9
s[b]	0.0809	0.2937	3.088
$s_m = s/n^{1/2}$	0.0244	0.0885	0.939
$s_r = s_m\ 100/\bar{x}$ (%)	1.74	0.92	1.73
$\%E = s_r t$ (%)[c]	3.15	1.66	3.14

[a]For 11 measurements at each concentration level. [b]Standard deviation. [c]t relates to Student's t-test.

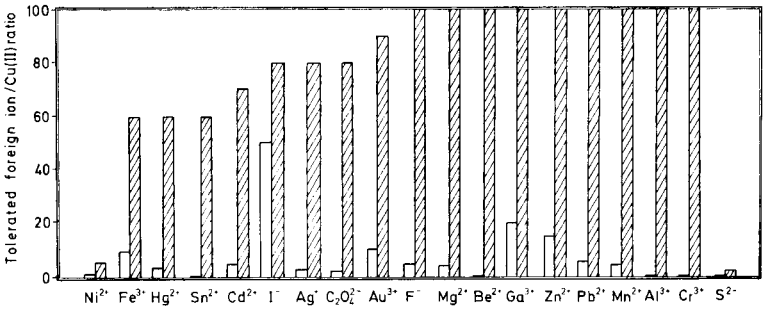

Fig. 5. Comparison of the tolerance to foreign ion/Cu(II) ratios between the normal flow injection method [12] (open columns) and the proposed stopped-flow method (dashed columns.).

TABLE 3

Determination of copper in real samples

Sample	Cu found (μg ml^{-1})		Sera No.	Cu found (μg ml^{-1})	
	Stopped-flow	A.a.s.		Stopped-flow	A.a.s.
Rice	2.07	2.13	1	1.54	1.57
Banana	0.33	0.33	2	1.28	1.21
Pear	0.43	0.44	3	1.21	1.30
			4	1.11	1.16
			5	1.25	1.31
			6	1.08	1.04

magnesium at a ratio of 100:1, because this permits the determination of copper in blood, where the maximum ratio of magnesium to copper is ca. 80:1. This determination was impossible in the normal mode.

Determination of copper in real samples

The stopped-flow method was used for the determination of copper in foods (rice, banana and pear) and blood serum. The results were checked by liquid—liquid extraction, with detection by atomic absorption spectrometry [14]. The results obtained by both techniques are in good agreement (Table 3).

REFERENCES

1 J. W. Moore, W. K. Hicks, R. G. Williams, K. Gehring, S. Pittinger, J. R. Vidolich and S. Schubbe, Trends Anal. Chem., 2(4) (1983) 74.
2 H. V. Malmstadt, C. J. Delaney and E. A. Cordos, Crit. Rev. Anal. Chem., 2 (1972) 559.
3 E. H. Hansen and J. Růžička, Anal. Chim. Acta, 114 (1980) 19.
4 P. J. Worsfold, J. Růžička and E. H. Hansen, Analyst (London), 106 (1981) 1309.
5 S. Olsen, J. Růžička and E. H. Hansen, Anal. Chim. Acta, 136 (1982) 101.

6 J. Růžička and E. H. Hansen, Anal. Chim. Acta, 106 (1979) 207.
7 N. Yoza, Y. Kurokawa, Y. Hirai and S. Ohashi, Anal. Chim. Acta, 121 (1980) 281.
8 T. Yamane, Anal. Chim. Acta, 130 (1981) 65.
9 C. S. Lim and J. N. Miller, Anal. Chim. Acta, 114 (1980) 183.
10 F. Grases, F. García-Sánchez and M. Valcárcel, Anal. Chim. Acta, 119 (1980) 359.
11 F. Grases, J. M. Estela, F. García-Sánchez and M. Valcárcel, Anal. Chim. Acta, 125 (1981) 21.
12 F. Lázaro, M. D. Luque de Castro and M. Valcárcel, Analyst (London), 109 (1984) 333.
13 P. L. Schuller and L. E. Coles, IUPAC, Applied Chemistry Division, Comission on Food Contaminants, Pure Appl. Chem., 51 (1979) 385.
14 M. Silva and M. Valcárcel, Analyst (London), 107 (1982) 511.

Analytica Chimica Acta, 165 (1984) 187—194
Elsevier Science Publishers B.V., Amsterdam — Printed in The Netherlands

A MICROMETHOD FOR THE DETERMINATION OF SELENIUM IN TISSUES AND BIOLOGICAL FLUIDS BY SINGLE-TEST-TUBE FLUORIMETRY

GEORG ALFTHAN
National Public Health Institute, Mannerheimintie 166, SF-00280 Helsinki 28 (Finland)

(Received 21st February 1984)

SUMMARY

A sensitive single-test-tube procedure for the fluorimetric determination of ng quantities of selenium with diaminonaphthalene, from small samples of animal origin is described. Several parameters related to the nitric/perchloric/sulphuric acid digestion, subsequent reduction and piazselenol formation are studied using blood as the matrix. The detection limit is 0.45 ng Se. The within-series precision for blood and heart tissue is 4.2% and 2.3% and between series is 5.0% and 3.6%, respectively. Recovery of added selenite and selenomethionine to blood, heart tissue and urine ranges from 98—101%. The correlation coefficient between the proposed and an electrothermal atomic absorption spectrometric method for serum samples is 0.997. This procedure is especially suitable for serial operation with a daily (8-h) throughput of 25 samples in duplicate.

Assessment of the selenium status of humans requires analysis of several different types of samples [1]. Samples low in selenium and of limited size such as biopsy samples may also be encountered. Fluorimetry is often the method of choice owing to its virtual freedom of matrix interferences, its sensitivity and the relatively inexpensive equipment used. The classical methods were developed mainly for plant materials [2, 3] but some have also been applied to other biological materials [4—9] and some have been semiautomated [10, 11].

Fluorimetric methods, however, require in general a rather tedious sample digestion with complexation and extraction, including transfer of the solution, which is impractical with large numbers of samples. A method suitable for routine assays coupled with increased sensitivity was required. This paper reports a single test tube modification based on the proposed method of the Analytical Methods Committee [5]. It is shown to be precise and accurate for blood, urine and muscle tissue. Several parameters related to sample digestion and subsequent complex formation with 2,3-diaminonaphthalene (DAN) have been studied. The whole procedure is carried out in the same test tube thus minimizing sample transfer, glassware and possible contamination.

0003-2670/84/$03.00

EXPERIMENTAL

Apparatus

A Perkin-Elmer Model LS-5 fluorospectrometer, a Liebisch aluminium heating block with 60 holes (diameter 18 mm, depth 65 mm), an Orion Research Model 701 A pH meter with a glass electrode having an outer diameter of 5 mm, and glass-stoppered test tubes (16 × 125 mm) were used. All glassware except disposable Pasteur pipettes was of borosilicate glass and was acid-washed.

Solutions

The reagents were at least of analytical grade unless otherwise stated. Deionized water was further purified by passing through a Millipore Super Q system.

Technical grade DAN was purified by crystallizing once from boiling water [4, 9]. DAN solution [5] was made by dissolving 0.1 g of DAN in 100 ml of 0.1 M hydrochloric acid. Remaining impurities were removed by extracting this solution 3—4 times with 10 ml of cyclohexane. The aqueous solution was filtered through a prewashed (0.1 M HCl) filter paper and stored in the dark at 4° C, covered with a cyclohexane layer. The reagent is stable for at least 2 weeks.

EDTA masking reagent was prepared by dissolving 5 g of $Na_2H_2EDTA \cdot 2H_2O$ and 25 g of hydroxylammonium chloride in 1 l of water. The used cyclohexane could be reused after a simple purification procedure. It was extracted successively with sulphuric acid, water and sodium hydrogencarbonate solution. After fractional crystallization (5—10% discarded) it was treated with activated charcoal and filtered. This purified cyclohexane gave slightly lower fluorescence readings than commercial HPLC-grade cyclohexane.

A 1.000-g l^{-1} selenium standard was prepared from selenium dioxide in 0.1 M hydrochloric acid or from elemental selenium [5]. This was further diluted to 1 mg l^{-1}, from which appropriate amounts were pipetted into the test tubes.

Procedure

Tissue samples of 10—100 mg dry weight (or the equivalent weight of fresh tissue), 0.25—0.5 ml of serum, whole blood or urine, standards and blanks were transferred to the test tubes. A 1-ml portion of nitric acid was added to each and the tubes were left at room temperature until the samples had dissolved (usually overnight). A few antibumping granules were added to each tube followed by 0.4 ml of 1:20 sulphuric: perchloric acids (v/v) and the tubes were transferred to the heating block at ambient temperature in a fume hood. The temperature of the block was set to 120° C, which was reached in 40 min, and maintained for 20 min. The temperature was next set to 150° C for 1 h followed by 180° C for 1.5 h. Aluminium foil around the

test tubes during heating at 180° C was used to avoid condensation of vapours [10, 12]. At the end of the digestion the digest was colourless or slightly yellow.

A few drops of 30% hydrogen peroxide were added to each cooled tube and heated for 10 min at 150° C (instead of 180° C to avoid excessive frothing, which can result in loss of selenium [10]). This step was repeated if fumes of nitrogen dioxide were observed. To each cooled tube 1 ml of 6 M hydrochloric acid was added and the tubes heated at 110° C for 10 min. The tubes were removed from the heating block, 1 ml of 6 M formic acid as buffer [5] and 1.5 ml of the EDTA reagent were added to each and the contents mixed well. The pH was adjusted to 1.5—2.0 using the pH meter with (ca. 1.5 ml) 4 M ammonia. The tubes were protected from direct light hereafter. A 1-ml portion of the DAN reagent was added, mixed well and the tubes placed in a water bath at 50° C for 30 min [13]. The test tubes were cooled briefly in cold water to facilitate better separation of the phases, 2.5 ml of cyclohexane was added, the tubes were stoppered and extracted vigorously, manually, for 30 s. The cyclohexane layer was transferred to a 1-cm cuvette with a Pasteur pipette and the fluorescence was measured (cyclohexane blank) at excitation and absorption wavelengths of 369 and 518 nm, respectively.

RESULTS AND DISCUSSION

Sample digestion

The amount of digestion mixture used was sufficient for samples up to a dry weight of about 150 mg (fat content under 20%). The digestion of biological materials has been studied intensively [4, 9, 12, 14, 15] and it seems that losses of selenium through volatilization are generally overemphasized, except when samples are charred [9]. Decreased recovery is generally due to the incomplete digestion of the organic forms of selenium and/or subsequent reduction of the total selenium to selenite [12, 14, 15]. The digestion mixture consisting of nitric, perchloric and sulphuric acids [3, 5, 9] has been shown to result in nearly complete recovery of resistant selenium species present in biological samples [14]. In the present study this digestion mixture was preferred over a nitric/perchloric acid mixture [2, 4] because sulphuric acid prevents the tubes from accidentally drying. The use of sulphuric acid, however, increases the risk of charring, which, as mentioned, may result in losses of selenium [9]. Using the present procedure samples having a high (25—30%) fat content, e.g. lyophilized milk, tended to char during the last stages of the digestion. Charring of such samples could be prevented by adding 0.5 ml of nitric acid after the first heating stage (120° C) or alternatively by increasing the amount of perchloric acid [9] initially by 0.2 ml.

Digestion for 30 min at the highest temperature, 180° C, resulted in complete destruction of the resistant organic selenium species present in blood and urine, and extending the digestion time from 30 to 105 min (at 180° C)

did not alter the selenium content (Table 1). The cessation of boiling and the evolution of perchloric acid fumes were taken as signs of complete digestion, which occurred between 60 and 90 min.

Reduction of selenium

The formation of the piazselenol requires that the selenium is present as selenium(IV). Residual nitric acid [10] in the digest, because of the moderate digestion temperature, has to be expelled because it can unspecifically enhance the fluorescence [5] or interfere with the reduction of selenate to selenite [1]. Complete reduction has to be ensured as Watkinson [2] reports that extended boiling of selenite in perchloric acid may convert up to 60% of selenite to selenate.

Nitric acid can conveniently be expelled by treatment with hydrogen peroxide [3, 5, 9]. This will also result in the reduction of selenate to selenite, but as discussed by Bye [16] reduction in a sulphuric acid medium is incomplete (see below). Thus to ensure complete reduction, hydrochloric acid is generally preferred [2, 4, 5, 9] as it is effective in both sulphuric and perchloric acid media [16]. Using the present procedure it was found that only 85% of the selenium in digested blood was in the required oxidation state when reduction by hydrochloric acid was omitted. To achieve quantitative recovery the minimum concentration for the hydrochloric acid solution was found to be 4 M (giving a final concentration of 2.5 M). The reduction step is critical as boiling of selenium in a hydrochloric acid medium exceeding 6 M (final) may result in losses due to formation of volatile selenium species [5].

Interferences

Watkinson [10] reported that 0.1 M sulphate in the digest decreased the recovery of selenium by about 10%. Hence to investigate the possible interference from sulphuric acid in the present digestion mixture blood was digested in duplicate with different amounts of sulphuric acid. No interference was found for the concentration range studied (0.04—0.2 M final concentration in the aqueous phase) except for a slight precipitation in the

TABLE 1

Effect of digestion time at the highest temperature setting (180°C) on the measured selenium content (ng)

Time (min)	30	45	60	75	90	105	120
Blood[a] (0.25 ml)	30.0	30.7	31.3	30.1	30.2	30.6	—
Urine[b] (0.5 ml)	17.3	—	17.4	—	16.3	—	16.3

[a]Mean of 3 replicates. [b]Mean of 2 replicates.

cyclohexane layer at the highest concentration. The contribution of sulphate from a 100-mg sample of hair, which is the tissue richest in sulphur, increases the final sulphate concentration from 0.08 to 0.11 M.

In order to test the effect of the addition of perchloric acid to the digest in cases of fatty samples (see the discussion of digestion) blood was digested in duplicate with increasing amounts of perchloric acid in the digestion mixture (0.2—1.0 ml, final concentration 0.85—4.2 M). The perchloric acid did not affect the results although a white precipitate was formed in the aqueous phase at the highest concentration used.

Blood iron is the most likely metal in animal samples to interfere with piazselenol formation [17]. The masking of iron was studied experimentally by digesting blood and varying the EDTA: iron mole ratio from 0.0 to 9.0. Adequate masking was achieved by a ratio of about 1:1, and the ratio (4.4) used in the recommended procedure was sufficient to complex the iron in 2 ml of blood.

Other variables

The maximum formation of the piazselenol from selenium standards has been shown to occur at pH 2.0 [18] and from digested bovine liver at pH 1.8 [11]. Many authors, however use pH 1—2 [4, 6, 7] or a certain value between 1 and 2 [2, 5, 10, 11, 13, 19, 20]. The dependence of the fluorescence on the pH was studied by using digested blood. The fluorescence slightly increased with increasing pH between pH 1.0 to 2.4. Under the conditions in the procedure a distinct pH maximum could not be demonstrated.

The final concentration of DAN used in most published methods falls within the range 0.005—0.036% [2, 4—6, 8, 9, 19]. In order to optimize the concentration of DAN, blood selenium was determined in duplicate and the concentration of DAN varied between 0.003—0.046% (final concentration in aqueous phase). Maximum intensity was obtained between 0.0076 and 0.046% DAN. The slight precipitation in the cyclohexane layer seen in the tubes at the highest DAN concentration was without effect. A final concentration of 0.018% was chosen based on the low blank value which typically was 1—2 ng of selenium.

The extraction of the piazselenol into cyclohexane was studied. A complete extraction from blood digests was achieved by vigorous manual shaking in 30 s. This is in accordance with the results of Chan [19]. Washing of the cyclohexane phase with 0.1 M hydrochloric acid as suggested by some authors [1, 4, 5] offered no improvement.

Precision, recovery and accuracy

The precision of the method was tested by analyzing different materials (Table 2). The coefficient of variation (c.v.) varied from 2.3 to 4.3%. The precision between series of results for blood, heart tissue and urine is shown in Table 3. The c.v. varied from 3.6 to 5.7%.

The recovery of added selenite to blood and heart tissue is presented in Table 4. The additions were quantitatively recovered from both materials

TABLE 2

The within-series precision of the method for different types of sample

Sample	*n*	Mean ± s.d.	c.v. (%)
Blood (0.5 ml)	8	125 ± 5.2[a]	4.2
Heart muscle, fresh tissue (90—230 mg)	8	224 ± 5.0[b]	2.3
Milk powder (45—55 mg)	6	82 ± 3.5[b]	4.3

[a] $\mu g\ l^{-1}$. [b] $\mu g\ kg^{-1}$.

TABLE 3

The precision of the method between series for blood, heart tissue and urine

Sample	No. of series	No. of determinations	Mean ± s.d.	c.v. (%)
Blood	6	21	129 ± 6.4[a]	5.0
Heart muscle (lyophilized)	9	32	1025 ± 37[b]	3.6
Urine	4	12	49.4 ± 2.8[a]	5.7

[a] $\mu g\ l^{-1}$. [b] $\mu g\ kg^{-1}$.

TABLE 4

Recovery of added selenite to blood and heart tissue

Sample	Se added (ng)	Mean[c] sample weight (mg)	Mean Se recovered (ng)	Recovery (%)
Blood[a]	—	48.5	18.7	—
(lyophilized)	25	46.4	43.1	101
Heart[b] tissue	—	24.8	25.2	—
(lyophilized)	20	22.3	42.9	101

Range of the amount of sample weighed into test tube: [a] 40—63 mg, [b] 18—30 mg, [c] mean of 5 measurements.

indicating that there was no appreciable matrix effect. A second recovery test was conducted by adding selenomethionine, a form occurring in biological samples and difficult to decompose [12, 14]. The quantitative recovery of selenomethionine proved the digestion to be complete, as presented in Table 5.

TABLE 5

Recovery of added selenomethionine to blood and urine

Sample	Se added (ng)	Mean sample amount	Mean Se recovered (ng)	Recovery (%)
Blood[a]	—	49.5 mg	18.5	—
(lyophilized)	20	49.5 mg	38.0	97
Urine	—	0.5 ml	10.2	—
	20	0.5 ml	30.2	100

[a]35—57 mg of sample weighed into test tubes.

The determination of selenium in the certified reference material Bovine Liver (NBS no. 1577, certified at 1.1 ± 0.1 mg Se kg^{-1}) gave the result 1.12 ± 0.02 mg kg^{-1} (n = 6). For Animal Muscle (International Atomic Energy Agency H-4, certified at 0.28 mg kg^{-1}, 95% confidence interval = 0.25—0.32 mg kg^{-1}) the results were 0.30 ± 0.01 mg kg^{-1} (n = 6). Verification of the accuracy of the method for blood and serum was obtained in an interlaboratory comparison study in which 14 laboratories in Finland participated [21]. The results obtained by the present method were within 5% of the overall mean. The accuracy of the method for serum was further studied by analyzing 4 serum samples by the present method and by direct electrothermal atomic absorption spectrometry [22]. The two methods agreed well between 30 and 290 μg Se l^{-1} with a correlation coefficient of 0.997.

The detection limit (defined as three times the standard deviation of the mean blank) of the method was 0.45 ng of selenium. By analyzing digested standards (n = 5) on 5 different days, the calibration graph was linear (r = 0.999) for 5—75 ng of selenium.

CONCLUSIONS

The acid digestion employed in this study is capable of decomposing resistant organic selenium species. Incomplete reduction rather than losses due to the volatilization of selenium was shown to be the cause of low recoveries. Under the conditions used the fluorescence was insensitive to moderate variations in the concentration of the reagents. The high sensitivity of the method together with the low detection limit enables the determination of selenium from very small (10-mg) tissue samples. Further, the procedure allows convenient operation in series of sixty tubes per day.

The author wishes to thank Mrs. Eeva Ehrstedt for technical assistance.

REFERENCES

1 C. D. Thomson and M. F. Robinson, Am. J. Clin. Nutr., 33 (1980) 303.
2 J. H. Watkinson, Anal. Chem., 38 (1966) 92.
3 I. Hoffmann, R. J. Westerby and M. Hidiroglou, J. Assoc. Off. Anal. Chem., 51 (1968) 1039.
4 O. E. Olson, I. S. Palmer and E. E. Cary, J. Assoc. Off. Anal. Chem., 58 (1975) 117.
5 Analytical Methods Committee, Analyst (London), 104 (1979) 778.
6 A. Geahchan and P. Chambon, Clin. Chem., 26 (1980) 1272.
7 S. Y. Chen, P. J. Collip, L. H. Boasi, D. S. Isenschmid, R. J. Verolla, G. A. San Roman and J. K. Yeh, Ann. Nutr. Metab., 26 (1982) 186.
8 R. Hasunama, T. Ogava and Y. Kawanishi, Anal. Biochem., 126 (1982) 242.
9 M. Ihnat, J. Assoc. Off. Anal. Chem., 57 (1974) 368.
10 J. H. Watkinson, Anal. Chim. Acta, 105 (1979) 319.
11 F. J. Szydlowski and D. L. Dunmire, Anal. Chim. Acta, 105 (1979) 445.
12 M. Verlinden, Talanta, 29 (1982) 875.
13 P. R. Haddad and L. E. Smythe, Talanta, 21 (1974) 859.
14 J. Nève, M. Hanocq, L. Molle and G. Lefebre, Analyst (London), 107 (1982) 934.
15 H. J. Robberecht, R. E. Van Grieken, P. A. Van Den Bosch, H. Deelstra and D. Van Den Berghe, Talanta, 29 (1982) 1025.
16 R. Bye, Talanta, 30 (1983) 993.
17 M. W. Brown and J. H. Watkinson, Anal. Chim. Acta, 89 (1977) 29.
18 P. F. Lott, P. Cukor and J. Solga, Anal. Chem., 35 (1963) 1159.
19 C. C. Y. Chan, Anal. Chim. Acta, 82 (1976) 213.
20 J. E. Spallholz, G. F. Collins and K. Schwarz, Bioinorg. Chem., 9 (1978) 453.
21 G. Alfthan, J. Lehto and J. Kumpulainen, submitted for publication.
22 G. Alfthan and J. Kumpulainen, Anal. Chim. Acta, 140 (1982) 221.

Analytica Chimica Acta, 165 (1984) 195—200
Elsevier Science Publishers B.V., Amsterdam — Printed in The Netherlands

APPLICATION OF THE OPAL-GLASS METHOD FOR ION-EXCHANGER SPECTROPHOTOMETRY

YUKIO TAKAGI and MINORU YOSHIDA*

Department of Chemistry, Faculty of Science, Tokyo Institute of Technology, Meguro-ku, Tokyo (Japan)

(Received 1st December 1983)

SUMMARY

A simple and precise method for the measurement of the net absorbance of colored species sorbed on ion-exchange resins is reported. Identical opal-glass plates are inserted on the transmission sides of both the sample-cell and blank-cell compartments of the spectrophotometer. Absorbances of sample-resin layers are measured against a blank-resin layer as reference. Scattering effects caused by resin particles are almost eliminated by using opal glass. For the determination of chromium(VI) with diphenylcarbazide reproducible calibration lines were obtained without tedious compensation methods.

Ion-exchanger spectrophotometry, devised by Yoshimura et al. [1—3], is based on direct measurement of the absorbance of an ion-exchange resin phase which has sorbed the colored species to be determined. The resin concentrates the species, providing remarkable enhancement of sensitivity. In the usual method, the resin slurry is poured into a 1-mm cell. The light beam falls on a settled resin layer and the absorbance is measured against a neutral density filter. Most of the incident light hits the translucent resin beads and is absorbed by the colored species but, of course, there is marked scattering and little of the transmitted light is caught by the photodetector in the usual optical arrangement of a spectrophotometer. The light that passes through the interstitial aqueous phase (colorless) mostly reaches the detector, thus leading to deformed absorption curves. Moreover, as the packing state of the resin beads is not very reproducible, the measured absorbances will also show poor reproducibility.

To avoid these disadvantages, Yoshimura et al. calculated the net absorbance of the colored species on the resin (A_{RC}) from

$$A_{RC} = A_s(\lambda_{max}) - A_{bl}(\lambda_{max}) - \{A_s(\lambda_0) - A_{bl}(\lambda_0)\}$$

where A_s is the observed absorbance of the sample resin layer at the indicated wavelength, A_{bl} that of the blank-resin layer, λ_{max} the wavelength corresponding to the absorption maximum of the colored species and λ_0 a definite wavelength in a region where the species absorbs practically no light. The

0003-2670/84/$03.00

effect of the packing condition is mostly compensated and the A_{RC} value is fairly reproducible. However, four measurements are needed to obtain one A_{RC} value.

Shibata et al. [4] devised the opal glass method for the measurement of absorption spectra of suspensions of micro-organisms. In this method, the sample and blank cell compartments in the spectrophotometer are both provided, on the light-transmission side, with identical opalescent plates. These plates diffuse uniformly both the scattered and the passing light as they leave the cells and an average portion of the total transmitted light reaches the detector. Thus, the use of the opalescent plate may provide a very simple means of removing the effect of the packing conditions in ion-exchanger spectrophotometry. The determination of chromium(VI) with *s*-diphenylcarbazide (1,5-diphenylcarbohydrazide) was used as an example for testing the opal-glass method in comparison with the A_{RC} calculation method [1, 2]. Satisfactory reproducibility was obtained by a single absorbance measurement of the sample-resin against the blank-resin as reference.

EXPERIMENTAL

Apparatus

A Hirama model 6B spectrophotometer was used with some modifications in the cell compartments (Fig. 1). First, cells 20-mm wide were used in appropriate cell holders to increase the available light diffused by the opalescent plates. Secondly, the cell holder was placed in the photometer in the

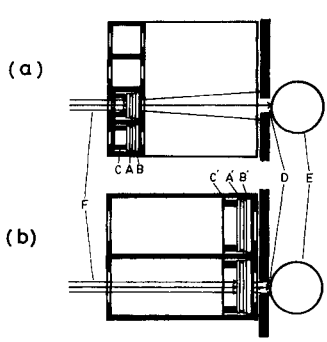

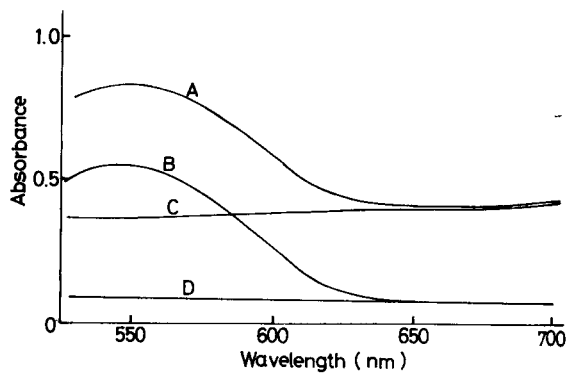

Fig. 1. Schematic diagram showing the arrangement of original (a) and modified (b) cell compartments. A, 10-mm wide cell; A′, 20-mm wide cell; B and B′, opal-glass plate; C and C′, spring; D, window; E, phototube; F, incident light.

Fig. 2. Effect of opal glass on the apparent absorption curves of the blank and colored ion-exchange resin. Chromium-diphenylcarbazide sorbed resin (8.32 μg Cr/200 ml) measured (A) without and (B) with opal glass; blank resin measured (C) without and (D) with opal glass. Conditions: water as reference; 0.380 g of Dowex 50W-X2 (100—200 mesh); 2.5-mm × 20-mm cell; Ag—Cs phototube.

opposite direction from normal in order to shorten the distance from the cell to the detector; the shorter the distance, the more diffused light will reach the detector. Opal glass (3.2-mm thick; Schott Glaswerke, Mainz) was cut to suitably sized plates, which were inserted into the cell holder with the flashed side towards the transmission sides of the sample and the reference cells. Glass cells of 1-mm pathlength (20-mm wide) were mainly used, although some data were obtained with 2.5-mm cells. The photometer was equipped with two phototubes, an Sb—Cs tube for 360—630 nm and Ag—Cs tube for 630—1000 nm. The latter can be used, however, in the range 520—1000 nm.

Reagents

Ion-exchange resins used were Dowex 50W-X2 (50—100, 100—200 and 200—400 mesh) and 50W-X4 (200—400 mesh) in the H^+-form. They were conditioned as usual, air-dried and stored in a hygrostat over saturated sodium chloride solution (relative humidity 75%).

Standard chromium(VI) solution (0.02 M) was prepared from powdered potassium dichromate (99.98%; a standard reference material for titration) which had been dried at 110° C for 3 h. Working standards were prepared by suitable dilution.

s-Diphenylcarbazide solution (0.25% w/v) was prepared in acetone immediately before use.

All the chemicals were of analytical grade unless otherwise stated.

Procedure

To 200 ml of sample solution containing 0.2—10.4 μg of Cr(VI) in a 300-ml beaker, add 0.300 g of the cation-exchange resin (Dowex 50W-X2, 100—200 or 200—400 mesh), 2 ml of 2.5 M sulfuric acid and 5 ml of 0.25% diphenylcarbazide solution. Stir the mixture for 30 min, and then leave for 3 min to allow the resin beads to settle. Transfer the resin slurry to the 1-mm × 20-mm cell with a 10-ml or 15-ml transfer pipette. Measure the absorbance of the resin layer at 548 nm.

RESULTS AND DISCUSSION

Optimization of conditions

The conditions for the color development and the sorption of the chromium-diphenylcarbazide complex recommended by Yoshimura et al. [1] were adopted with slight modifications. In this study, 0.300 g of the resin (0.380 g in case of 2.5-mm cell) was used for 200 ml of the sample solution to increase the sensitivity. About 20 min was required for full development of the color on the resin (50W-X2, 100—200 mesh). Because of the smaller amount of resin, a longer time was needed than in Yoshimura's procedures. Stirring for 30 min was adopted. The use of the 50—100-mesh resin was unsuitable, because it required more time to sorb the complex.

The color of the complex on the resin fades slowly on standing. The absorbance should be measured within 15 min after the color development.

Absorption spectra

The absorption curves of the blank and colored resin were constructed by using water as a reference with and without the opal glass (Fig. 2). Without opal glass, the absorbances for the blank and for the colored resin were very high and the curves did not coincide in the region where the complex absorbed no light (⩾660 nm). Three kinds of resin were used to examine the effect of the opal glass on the absorbance measurements for the blank resin. The observed absorbances against water at 548 nm (see below) and absorbance differences are shown in Table 1. Without the opal glass, the observed absorbances were high and poorly reproducible. Further the values obtained with the Sb—Cs tube were much higher than those with the Ag—Cs tube even at the same wavelength (548 nm). This discrepancy may be caused by small differences in the geometry of the photosensitive parts of the phototubes exposed to the non-uniformly scattered light. The absorbance differences are fairly reproducible under the same measuring conditions; this gives the basis for the A_{RC} calculation method [1, 2]. In contrast, the absorbances measured with opal glass were much lower, highly reproducible and independent of the kind of phototube used. The change in absorbance with wavelength was also small.

These results show that scattering rather than absorption of the incident light is largely responsible for the apparent absorbance of the blank-resin layer without the opal glass. The scattering effects can be almost eliminated by using opal glass; the net absorbance of the sorbed colored species can then be measured directly with the blank resin as reference. The absorption curve of the chromium-diphenylcarbazide complex on the resin thus obtained has its maximum (548 nm) shifted slightly to a longer wavelength than that in solution (540 nm).

TABLE 1

Effect of use of opal glass on the observed absorbance of the blank resin[a]

Resin (mesh)	Opal glass	Sb—Cs phototube		Ag—Cs phototube	
		Absorbance A_{548} [b]	Absorbance difference $A_{548}-A_{630}$ [b]	Absorbance A_{548} [b]	Absorbance difference $A_{548}-A_{700}$ [b]
50W-X2	without	0.512 ± 0.010	0.048 ± 0.002	0.143 ± 0.012	−0.034 ± 0.002
(100—200)	with	0.041 ± 0.001	0.003 ± 0.001	0.041 ± 0.001	0.000 ± 0.001
50W-X2	without	0.796 ± 0.012	0.083 ± 0.003	0.362 ± 0.007	−0.063 ± 0.002
(200—400)	with	0.073 ± 0.002	0.005 ± 0.002	0.072 ± 0.002	−0.003 ± 0.001
50W-X4	without	1.214 ± 0.022	0.106 ± 0.006	0.694 ± 0.018	−0.046 ± 0.007
(200—400)	with	0.159 ± 0.006	0.012 ± 0.004	0.159 ± 0.005	−0.007 ± 0.005

[a] 1 mm × 20 mm cell, water as reference. [b] With standard deviation on 10 determinations.

Calibration lines and precision

The apparent absorbances of the sample resins (two particle sizes of 50W-X2, and 200—400 mesh 50W-X4) were measured against water for a series of working standard solutions (0—4.16 μg Cr/200 ml) with and without the opal glass. The absorbances against the blank resins and A_{RC} were calculated from these data and sets of four calibration graphs were constructed for each of the six combinations of resins and phototubes. These plots were all linear through the origin; the equations obtained by the least-squares method are listed in Table 2.

Measurements of absorbances against the blank resin with the opal glass were at least as precise as those given by A_{RC} without the opal glass and were usually more precise; the blank-resin reference method without opal glass led to large errors. The A_{RC} calculation with the opal glass did not improve the precision further. The limit of detection (c_l) in Table 2 is defined as the concentration giving an absorbance three times the standard deviation of the blank (see Table 1).

When the Sb—Cs tube was used, the sensitivity (represented by the regression coefficient) obtained by the A_{RC} method was lower than that by the blank-resin reference method, or when the Ag—Cs tube was used whether or not the opal glass was in position. This is caused by the slight light absorption by the complex at 630 nm. However, the regression equations obtained by

TABLE 2

Calibration lines for determination of Cr(VI) by the recommended procedure as regression equation ($A = (k \pm s_k)c \pm s_0$, with A = absorbance, c = mg l^{-1} Cr(VI), k = slope with standard deviation s_k; s_0 is standard deviation of intercept, n = 20)

Resin (mesh)	Measuring method[a]	Sb—Cs phototube				Ag—Cs phototube			
		k (l mg^{-1})	s_k (l mg^{-1})	s_0	c_l[b]	k (l mg^{-1})	s_k (l mg^{-1})	s_0	c_l[b]
50W-X2 (100—200)	BR — N	6.90	0.16	0.013	4.4	6.31	0.19	0.013	5.7
	BR — O	7.15	0.02	0.002	0.3	6.98	0.03	0.002	0.3
	A_{RC} — N	6.50	0.04	0.004	1.1	6.81	0.06	0.003	0.9
	A_{RC} — O	6.60	0.02	0.002	0.4	6.94	0.04	0.002	0.4
50W-X2 (200—400)	BR — N	9.86	0.27	0.018	3.8	8.35	0.19	0.013	2.3
	BR — O	9.19	0.08	0.005	0.9	8.93	0.07	0.005	0.6
	A_{RC} — N	7.81	0.17	0.010	1.0	8.13	0.06	0.004	1.1
	A_{RC} — O	8.15	0.06	0.004	0.6	8.71	0.05	0.003	0.5
50W-X4 (200—400)	BR — N	12.10	0.44	0.031	5.4	10.94	0.52	0.036	4.9
	BR — O	13.78	0.17	0.013	1.2	13.65	0.17	0.011	1.2
	A_{RC} — N	10.81	0.25	0.017	1.7	11.38	0.25	0.018	1.9
	A_{RC} — O	12.58	0.13	0.009	1.0	13.67	0.13	0.010	1.1

[a]BR: blank-resin reference method; A_{RC}: A_{RC}-calculation method; N: without opal glass; O: with opal glass. [b]c_l is limit of detection in μg l^{-1}, see text.

the blank-resin reference method with the opal glass practically coincided with each other regardless of the kind of phototube. Precision was good for both the mesh sizes of 50W-X2 resin tested. Higher sensitivity was obtained by the use of 50W-X4 resin (200—400 mesh), but the precision was poorer.

A linear calibration plot was obtained by direct measurements of absorbance of the colored resin against the blank resin with the opal glass in the concentration range 1—52 $\mu g\ l^{-1}$ Cr(VI) with 200-ml sample solutions.

REFERENCES

1 K. Yoshimura, H. Waki and S. Ohashi, Talanta, 23 (1976) 449.
2 K. Yoshimura and S. Ohashi, Talanta, 25 (1978) 103.
3 K. Yoshimura, S. Nigo and T. Tarutani, Talanta, 29 (1982) 173 (and references therein).
4 K. Shibata, A. A. Benson and M. Calvin, Biochem. Biophys. Acta, 15 (1954) 461.

Analytica Chimica Acta, 165 (1984) 201—207
Elsevier Science Publishers B.V., Amsterdam — Printed in The Netherlands

THE DETERMINATION OF CHROMIUM(VI) IN WASTE WATER AND INDUSTRIAL EFFLUENTS BY DIFFERENTIAL PULSE POLAROGRAPHY

C. HARZDORF* and G. JANSER

Analytisches Laboratorium, Sparte Anorganische Chemikalien, Bayer AG, D-5090 Leverkusen (Federal Republic of Germany)

(Received 16th January 1984)

SUMMARY

A method for the determination of chromium(VI) in water and waste water is described. Interfering cations are separated by co-precipitation with aluminium from the phosphate-buffered solution. Differential-pulse polarographic measurement of chromium(VI) in the same background solution at pH 10 or 12 provides a lower limit of determination of 30 $\mu g\ l^{-1}$ Cr(VI). No significant losses of chromium(VI) occur in the precipitation step; chromium(VI) is not susceptible to reduction by waste-water constituents at the moderate pH maintained throughout the procedure. The polarographic characteristics of chromium(VI) in phosphate-buffered solution are discussed.

The determination of chromium(VI) in waste water and industrial effluents presents intricacies because of the complex nature of the samples, the susceptibility of quantitative reactions of chromium(VI) to interference, and the instability of the oxidation states of chromium. Potential interferences are primarily heavy metal ions as well as oxidants and reductants. In particular, organic constituents, which are most often unspecified for waste water, cause most of the established analytical methods to fail because they introduce the risk of chromium(VI) reduction, especially in acidic solutions. In contrast, chromium(III) is remarkably susceptible to oxidation in alkaline medium. Only in neutral solution are the different chromium species comparatively resistant to redox reactions, partly because of slow kinetics and partly because of the oxidation potential of the Cr(III)/Cr(VI) couple in such solutions. Consequently, a procedure for the determination of chromium(VI) in complex samples should be designed to operate at medium pH. This condition is not met by common methods for the determination of chromium(VI) such as spectrophotometry or valence-selective extraction because these procedures require acidic solution. Polarography, however, is promising because chromium(VI) is electrochemically active over the entire pH range so that viable operating conditions should be possible.

There are various methods for the polarographic determination of chromium(VI) in different supporting electrolytes. The commonly used electro-

0003-2670/84/$03.00

lytes recommended by instrument manufacturers are ammonium chloride/ammonia buffer, ammonium tartrate and sodium hydroxide solutions; ammonium acetate/acetic acid buffer [1], sodium fluoride solution [2] and sodium sulphate solution [3] have also been suggested. These electrolytes may be suitable for the determination of chromium(VI), but are inadequate in the analysis of waste waters either because the pH range is inappropriate or because interferences from the various metal ions likely to be encountered in waste waters are not suppressed. These ions may cause direct interference if they are polarographically active in the potential range of interest, as well as indirect interference by co-precipitation of chromium(VI) with the hydroxides of polyvalent cations, formed at medium pH.

These difficulties can be overcome if a phosphate buffer is used. In such solutions, many polyvalent cations are removed as sparingly soluble phosphates. To capture interferences, even if present at only very small concentrations, aluminium chloride is added as auxiliary agent. With this procedure, losses of chromium(VI) by co-precipitation are negligible. After separation of the precipitate, chromium(VI) can readily be determined in the same background solution. Two polarographic peaks are obtained in the pH range 9—12, the characteristics of which depend strongly on the actual pH. Both peaks reflect the reduction of Cr(VI) to Cr(III). This is an anomaly and is discussed in detail later. The peaks appear at about —0.3 and —0.9 V vs. silver/silver chloride, thus providing the option of measuring at different potentials. By this means, interference from polarographically active organic constituents can be detected and optimum conditions of measurement may be selected for different types of sample.

EXPERIMENTAL

Apparatus and reagents

A PAR model 384 polarographic analyzer was used with the static mercury dropping electrode (model 303). A silver/silver chloride electrode served as reference electrode and a platinum wire as counter electrode. Argon purified by passing through an Oxisorb cartridge was used for purging.

Sodium phosphate buffer (0.2 M) was prepared from phosphoric acid (Suprapur; Merck) and sodium hydroxide (Suprapur) by neutralization and adjustment of the final pH to 8.0. Aluminium chloride hexahydrate solution (10 g l^{-1} Al) was made from the analytical-grade salt.

An artificial inorganic waste water containing 50 mg l^{-1} Fe^{3+} with 20 mg l^{-1} each of Cr^{3+}, Al^{3+}, Cd^{2+}, Pb^{2+}, Cu^{2+}, Ni^{2+}, Zn^{2+} and Mn^{2+} was prepared from the analytical-grade metal chlorides.

Procedures

Sample treatment. The sample solution (10 ml) and 10 ml of the phosphate buffer solution were mixed and the pH was adjusted to 8.0 with 1 M sodium hydroxide. A portion (1 ml) of the aluminium chloride solution was

added slowly with continuous stirring. The resulting pH was 7.0—7.4 depending on the composition of the sample. The solution was then stirred for 30 min and left for a further 30 min. Subsequently, the precipitate was separated by centrifugation or filtration on a membrane filter (0.2-μm pore size). If strong oxidants were suspected, sodium sulphite (15 mg) was added immediately after the pH was re-adjusted to 8.0. Thus, oxidation of chromium(III) compounds at the pH of operation was prevented.

Polarographic measurement at pH 10. A 10-ml aliquot of the clear solution was transferred to the polarographic cell, adjusted to pH 10.0 with 10 M sodium hydroxide, and purged for 15 min with argon. Polarographic measurements were done with the following instrumental settings: initial potential —0.2 V, final potential —0.6 V, scan increment 6 mV, pulse height 0.05 V, drop time 0.5 s. The polarographic curves were evaluated by multiple additions of a potassium chromate standard solution of appropriate concentration.

Polarographic measurement at pH 12. A 10-ml portion of the filtrate or supernatant solution was transferred to the polarographic cell, 90 mg of disodium-EDTA was added and the pH was adjusted to 12.0 with 10 M sodium hydroxide. The method was then the same as described above, except that the potential scan was selected between —0.6 to —1.2 V.

All results were corrected for changes in volume caused by the addition of the aluminium chloride and sodium hydroxide solutions and by the increments of standard solution added.

RESULTS AND DISCUSSION

Representative current-voltage curves for chromium(VI) in phosphate buffer solutions of different pH are shown in Fig. 1. The curves recorded in the sampled d.c. mode (Fig. 1A) show that the half-wave potential and the limiting current of the first wave depend strongly on the pH, whereas the parameters of the second wave remain almost unaffected by changes in pH within the range 9—12. It can further be seen that the first polarographic wave exhibits anomalous behaviour in that no constant limiting current is achieved with the normal scan towards negative potentials. Quantitative treatment of the corresponding polarographic curves obtained with the dropping mercury electrode in the original d.c. mode indicated that the second wave corresponds to a three-electron reaction whereas fractional values of less than three were calculated for the first wave, depending on the pH and on the chromate concentration. This anomaly may be interpreted in terms of surface passivation by reduction products of chromium(VI), formed at the potential of the first wave. This interpretation was first given by Kolthoff and Lingane [4] who observed similar phenomena for chromate reduction in unbuffered, neutral solution and in ammoniacal buffer, pH 8.9. The appearance of two waves for the reduction of chromium(VI) to chromium(III) in neutral or slightly alkaline medium was reported for a variety of supporting electrolytes by Tondeur et al. [5].

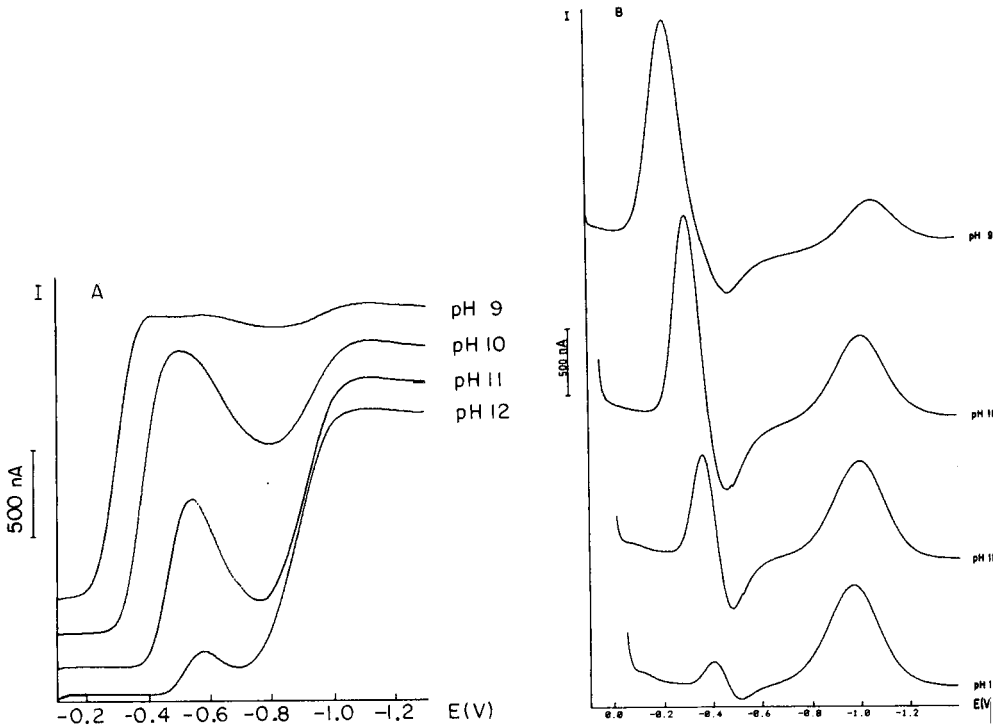

Fig. 1. Polarographic curves for 10 mg l^{-1} chromium(VI) in phosphate buffer solutions of different pH: (A) sampled direct-current; (B) differential pulse. Waves offset for clarity.

Corresponding to the d.c. polarographic curves, which were used exclusively for the characterization of the polarographic behaviour of chromium(VI), the differential-pulse polarographic curves exhibit two well-separated peaks, with the shape and peak potential of the first peak depending remarkably on pH (Fig. 1B). For routine analysis, the optimum pH proved to be 10 for the first peak and 12 for the second peak. The relationship between peak height and chromium(VI) concentration was found to be almost linear for the second peak over the entire range studied up to 500 mg l^{-1} Cr(VI). The linear range for the first peak is comparatively short and limited to about 50 mg l^{-1} Cr(VI) which is, however, sufficient for most practical analyses. The lower limit of the method was evaluated as 0.03 mg l^{-1} Cr(VI).

For verification of the accuracy of the procedure, model tests were done with the synthetic inorganic waste water containing no chromium(VI). These artificial samples were subjected to the precipitation step and the filtrate was used to record the polarographic background curves. The curves (Fig. 2) clearly indicate that there is no interference in the potential range of interest. Minor interference was observed only at pH 12 when EDTA was not added before the polarographic measurement. This effect can be attributed to small residual concentrations of other ions still present after precipitation.

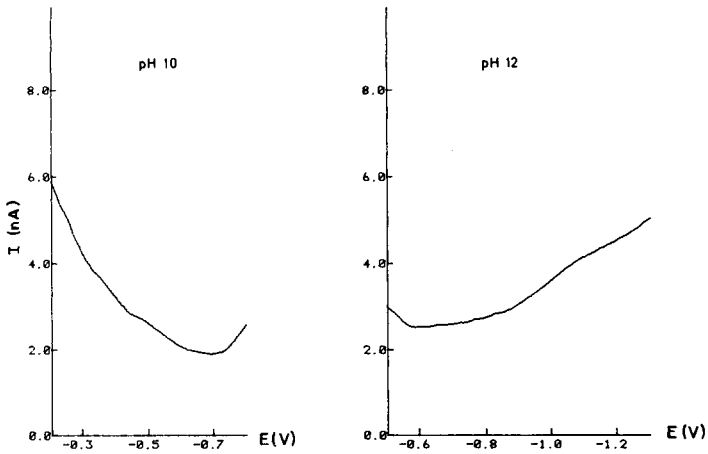

Fig. 2. Differential-pulse polarographic background current of synthetic inorganic waste water in phosphate buffer solution at pH 10 and 12.

Further tests were then conducted with the synthetic waste water containing known amounts of chromium(VI), and the recovery after precipitation was determined. The results (Table 1) indicate that there are no substantial losses of chromium(VI) in the precipitation step. Typical curves for the detection of chromium(VI) in the artificial inorganic waste water are shown in Fig. 3.

Additional tests dealt with potential interference caused by oxidation of chromium(III), which may still be present at trace concentrations after precipitation. This residual chromium(III) concentration was found, by atomic absorption spectrometry, to be $15 \pm 2\ \mu g\ l^{-1}$ for the artificial waste water and $50 \pm 4\ \mu g\ l^{-1}$ for a pure chromium(III) solution containing 20 mg l^{-1} as the initial concentration. The latter solution was allowed to stand after the precipitation step open to the air for 3 h. Subsequently, the chromium(VI) concentration was determined by spectrophotometry and found to be less than $10\ \mu g\ l^{-1}$ which was the detection limit of the method. This indicates that

TABLE 1

Recovery tests with artificial waste water

Cr(VI) added (mg l^{-1})	Cr(VI) found (mg l^{-1})	
	At pH 10	At pH 12
0.2	0.19, 0.18	0.16, 0.18
1.0	0.97, 0.90	0.99, 0.92
2.0	1.89, 2.17	1.96
5.0	5.07, 4.89	4.92, 4.82
20.0	20.8, 20.8	19.7

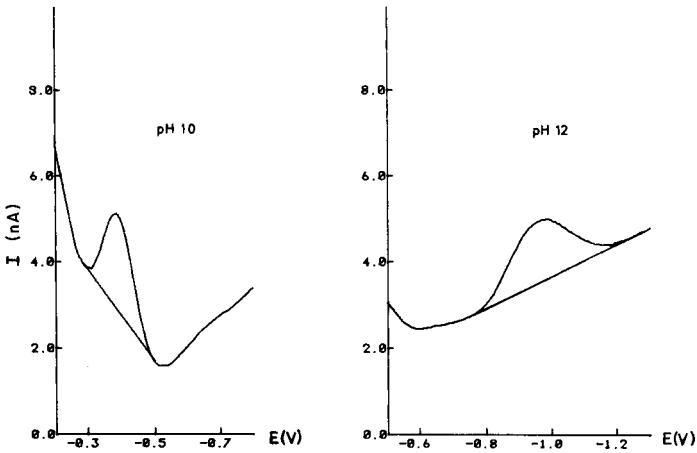

Fig. 3. Differential-pulse polarographic curves for 0.2 mg l^{-1} chromium(VI) in synthetic inorganic waste water.

interference from chromium(III) may be neglected as far as normal samples are concerned and provided that samples are not stored for a prolonged time prior to measurement. However, if it is suspected or indicated that the original samples contain strong oxidants, it is advisable to stabilize the samples

TABLE 2

Recovery tests with samples of waste water and natural water

Sample	COD (mg l^{-1})	Initial Cr(VI) content (mg l^{-1})	Cr(VI) added (mg l^{-1})	Total Cr(VI) found (mg l^{-1})	
				At pH 10	At pH 12
Waste water	21	n.d.[a]	0.50	0.49, 0.49	0.48, 0.48
	25	n.d.	1.00	1.05	0.92
	18	0.06	0.50	0.55	0.54
	30	n.d.	0.50	0.49	0.51, 0.46
River water	67	n.d.	0.10		0.10, 0.11
			0.40		0.35, 0.40
	27	n.d.	0.10		0.10, 0.09
			0.40		0.40, 0.38
	25	n.d.	0.50	0.48, 0.44	0.46, 0.43
			1.00	1.03	0.91
Natural water (lake)	20	n.d.	0.10		0.10, 0.10
			0.40		0.39, 0.40
Natural water (gravel pit)	15	n.d.	0.10		0.10, 0.09
			0.40		0.39, 0.40

[a]Not detectable.

with sodium sulphite, as described above, to avoid oxidation of chromium-(III) species at the working pH of this method.

For final validation, waste-water samples and natural waters with different values for the chemical oxygen demand (COD) were examined. These samples, after their initial chromium(VI) contents, had been determined, were spiked with known volumes of potassium chromate standard solution and processed again, following the entire procedure. The results (Table 2) indicate that satisfactory recovery of the chromium(VI) added was achieved throughout.

Despite the good results obtained in the presence of organic matter, it should be noted that there are possible components that can reduce chromium(VI) even in the moderate pH range applied in this method. Obviously, there can be samples in which the lifetime of chromium(VI) is short whatever the treatment. However, this is a property of individual samples rather than an analytical problem.

The authors are indebted to members of the DIN working group on the determination of chromium in water for suggestions and valuable discussion.

REFERENCES

1 S. T. Crosmuin and Th. R. Mueller, Anal. Chim. Acta, 75 (1975) 199.
2 P. W. West, J. F. Dean and E. J. Breda, Collect. Czech. Chem. Commun., 13 (1948) 1.
3 R. M. Bhatnagar and A. K. Roy, Technology, 3 (1966) 131.
4 I. M. Kolthoff and J. J. Lingane, J. Am. Chem. Soc., 62 (1940) 852.
5 J. J. Tondeur, A. Dombret and L. Gierst, J. Electroanal. Chem., 3 (1962) 225.

Analytica Chimica Acta, 165 (1984) 209—216
Elsevier Science Publishers B.V., Amsterdam — Printed in The Netherlands

DEVELOPMENT OF A MICROPROCESSOR-BASED ELECTROCHEMICAL INSTRUMENT INTERFACED TO A MICROCOMPUTER SYSTEM FOR DIFFERENTIAL-PULSE STRIPPING VOLTAMMETRY IN DIFFERENT TIME DOMAINS

A. M. BOND*, H. B. GREENHILL, I. D. HERITAGE and J. B. REUST[a]

Division of Chemical and Physical Sciences, Deakin University, Waurn Ponds, Victoria 3217 (Australia)

(Received 13th June 1984)

SUMMARY

An inexpensive, compact microprocessor-based instrument for polarographic and voltammetric analysis has been developed for use in chemically hazardous laboratories, radiation laboratories or clean laboratories. This low-cost unit controls the experiment, collects the data and can be regarded as expendable. The microprocessor-based instrumentation is interfaced to a microcomputer system, which is external to the laboratory and has all the required peripherals associated with larger laboratory computers. In this institution, four laboratories having the inexpensive microprocessor systems are linked to the larger microcomputer which is housed in an air-conditioned room better suited for computers. A new approach to data collection and evaluation using different time domains in differential-pulse stripping voltammetry is presented as an example of the use of such instrumentation.

In modern analytical chemistry, the use of microcomputer-based instrumentation can be regarded as routine [1]. Frequently, this instrumentation has to be used in the same laboratory where the experiment is carried out. Unfortunately, many analytical laboratories offer harsh environments which are not ideally suited for computer-based instrumentation because computers and their peripherals require a dust- and corrosion-free air-conditioned environment for optimal performance and minimal maintenance. A new but distinctly different problem now being encountered with the advent of clean laboratories for trace analysis is the contamination introduced by the presence of the instrument in the laboratory.

Microprocessor-based technology in an appropriate configuration can still offer the best compromise in the above dilemmas. The cost of a microprocessor-based system dedicated solely to experiment control and data collection can be sufficiently low to be regarded as expendable. Thus, on economic grounds the use of this kind of device in high-risk areas can be

[a]Present address: Analytical Research and Development, Sandoz Ltd., CH-4002, Basle, Switzerland.

0003-2670/84/$03.00

justified. Furthermore, in the absence of peripherals the size can be reduced to a minimum. Consequently, hermetic sealing is possible which is ideal for use in clean laboratories [2].

A frequent problem in this university is the difficulty of employing stripping voltammetric techniques in clean laboratories where conventional instrumentation itself is a contamination problem when trace concentrations of metals are determined. On other occasions, toxic chemicals need to be examined under far from ideal atmospheres (e.g., organic solvents in the hazards laboratory). Radiation laboratories present an obviously related problem. Confronted with the need to undertake substantial numbers of experiments in clean laboratories or in chemically hazardous situations, we have constructed a very inexpensive microprocessor-based system for actual use in the laboratory. This microprocessor is interfaced to a more expensive master microcomputer system, which is equipped with the peripheral devices and programming aids traditionally required and is housed in a dust-free air-conditioned laboratory. The relatively inexpensive system is used near the potentiostat (in electrochemical applications) so that noise pick-up is minimal, and transmits data in digital form to the master computer which is responsible for all data manipulation, display, etc. The master computer provides extensive access to computing power and can be housed in an environment appropriate for the care and protection of expensive instrumentation. Currently, four laboratories with inexpensive systems interfaced to the master computer are operational and a distributed system of computers has proved most advantageous. This hierarchical approach is similar to that adopted between laboratory and mainframe computers in many laboratories or in some cases even with microcomputers [3—6]. In individual laboratories, microprocessor-based electrochemical instruments have been developed extensively (e.g. [3, 6—14]). The new aspect is that one of the computer-based systems is regarded as expendable.

In this paper, application of this microcomputer system for differential-pulse anodic stripping voltammetry (d.p.a.s.v.) is described. Stripping voltammetry is a relatively lengthy experimental procedure typically requiring 30 min for a determination by conventional standard additions techniques. Many forms of interferences are possible and the technique is frequently applied to complex environmental samples [15, 16]. Computer-based electrochemistry systems commercially available produce results for determinations based on stripping voltammetry without comment on their validity. Although they have diagnostic criteria (hardware) to detect and warn of electrode malfunction, tests for chemical interference phenomena are not included. Pattern recognition techniques and related learning programs have been examined in some laboratories [7, 17, 18] and may be used to detect interferences. As a far simpler alternative, a multi-time domain approach in which certain criteria of acceptability must be met before an answer is regarded as valid is described here. All data are obtained from a single experiment.

EXPERIMENTAL

Reagents and procedure

Analytical-grade reagents were used throughout. The water used for preparing the samples was distilled tap water treated by a Nanopure system (Barnstead Sybron, Boston, MA), leading to ultrapure water of quality similar to that indicated by Reust and Meyer [19]. All potentials were measured against a saturated calomel electrode. The working electrode was a previously-plated rotating mercury-film glassy carbon electrode (EA-628, Metrohm, Herisau, Switzerland); the mercury film was deposited from a plating solution containing 10^{-4} M mercury(II) nitrate by applying a controlled potential of −400 mV for 600 s. Co-deposited impurities, such as copper, were removed from the film by applying a potential of +20 mV for a further 600 s under rotating electrode conditions. The film was generated daily. The sample size was 25 ml and the experiments were done at (20 ± 2)°C. A more detailed description of the experimental set-up used has been given elsewhere [20].

Instrumentation

For all experiments a VA-611 Detector (Metrohm) was used in the $I(t)$ mode as a potentiostat and current-measuring device. Waveform generation of the differential-pulse components was done by the computerized part of the instrumentation.

Block diagrams of the microprocessor-based system used are presented in Figs. 1 and 2.

Hardware. The instrumentation can be divided into two parts: A (master) system and B (slave) system. Part B is located in the laboratory where the experiment is done and part A is in the remote computer room. In Fig. 1, Part B is shown for the special case of d.p.a.s.v. experiments; implementation of other techniques needs only software changes.

Part B consists essentially of the cell, the potentiostat and the slave, a modified Motorola MEK-6800-D2 kit (Motorola Semiconductor Products, Phoenix, AZ) microprocessor system. The 6800 system essentially contains 16 kbyte of RAM and an input-output board containing a 12-bit DAC and ADC. In addition, some external control lines are available, e.g., for rotating the electrode, and opening and closing the nitrogen valve. Additionally, all programs are designed to be used with controllable mercury drop electrodes. A detailed description of the 8-bit version of the 6800 system on which the present work is based has been given elsewhere [10]. The compact instrumental arrangement enables the analog lines to be short, minimizing noise pick-up.

The master system (part A) is located in an air-conditioned room. It comprises a Sphere 6809 microprocessor system (Paris Electronics, Sydney, Australia) running Flex 9.0 (Technical Systems Consultants, West Lafayette, IN) as an operating system. There is 256 kbyte of dynamic memory of which

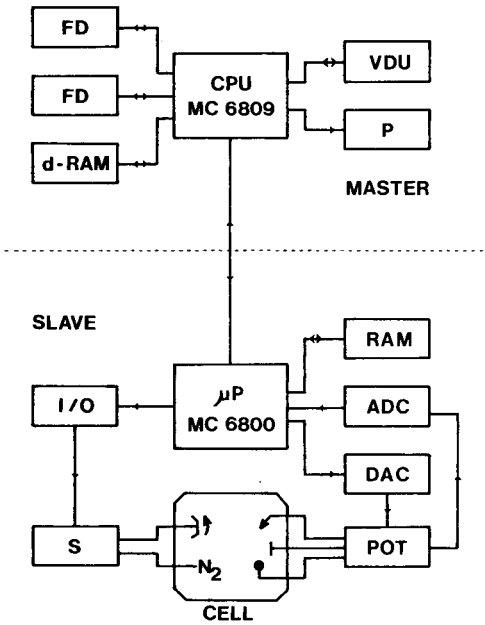

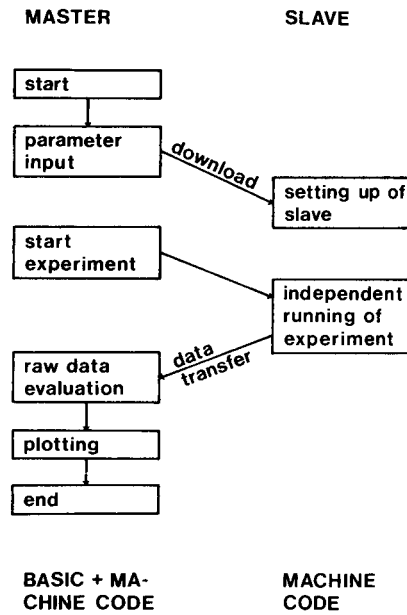

Fig. 1. Block diagram of the distributed microprocessor system and cell. Master system: CPU, central processing unit MC 6809; VDU, visual display unit; P, printer; FD, floppy disk; d-RAM, dynamic RAM. Slave system: μP, central processing unit MC 6800; I/O, input/output board; S, control devices for nitrogen purge and stirrer; POT, potentiostat; ADC, analog to digital converter; DAC, digital to analog converter.

Fig. 2. Flow chart describing operation of master and slave computer.

approximately 192 kbytes are incorporated as a virtual disk. Two DT/8 (1.2 Mbyte) floppy disk drives (Qume, San Jose, CA), a video terminal (Esprit; Hazeltine, Greenlawn, NJ) and a matrix printer (Epson MX-100-III; Shinshu Seiki Co., Nagano, Japan) are connected as peripherals. The master system is linked by RS232 interfaces to each slave system. The cost of the complete 6800 slave system is about a tenth of the cost of the 6809 master system.

Software. Machine language is used in part B and for communication to part A. At the master computer, both machine and high-level languages are used. Presently, programs involved with the input of parameters for experiments are written in BASIC. The required program for any particular experiment can be downline loaded from the master computer. In d.p.a.s.v. all the experimental parameters, such as deposition time, purging, etc., can be entered on the master computer and the whole experiment controlled from the computer room.

A flow chart for an experiment controlled by this distributed microprocessor system is shown in Fig. 2. The technique, such as voltammetry or polarography in differential-pulse or normal-pulse modes, is selected by

choosing the appropriate program on the master system. Almost any electrochemical method can be used but only d.p.a.s.v. is discussed here. The program then requests from the operator all experimental parameters required. The waveform for multi-time domain d.p.a.s.v. with timing parameters is shown in Fig. 3.

The direct current component of d.p.a.s.v. is collected just before applying the pulse and subsequently pulse currents are measured at 20-ms intervals during the pulse life. A 20-ms interval was chosen so that line synchronization was possible (line frequency in Australia is 50 Hz).

The experiment is commenced at the master system. The slave once initiated runs the whole program independently and the master system can then be used for any other task. Because the slave has its own memory, it can store the data indefinitely until transmission is requested by the master computer. The fact that the inexpensive microprocessor system can operate independently makes it possible to use several slave systems simultaneously. This would be impossible if the master system directly controlled both the experiment and the data acquisition. One set of raw data is stored in a file on a floppy disk and a second set is generated and converted to a format suitable for plotting. These data are plotted on the printer (resolution 660 × 560 dots) or any other graphic unit. Details of the hardware and software are available on request from the authors.

RESULTS AND DISCUSSION

The instrumental approach described is applicable to most analytical methods. Results for d.p.a.s.v. in which the slave system is in a clean laboratory are presented to show how the multi-time domain approach may be used to detect interferences. All results are for the determination of lead (lower $\mu g\ l^{-1}$ range) in 0.01 M hydrochloric acid in ultrapure water. In a typical experiment with conventional instrumentation, only one curve would be

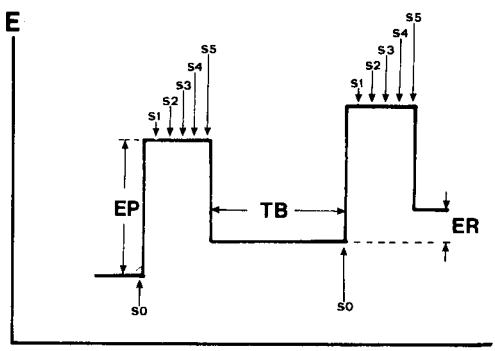

Fig. 3. Waveform and timing parameters used in multi-time domain d.p.a.s.v.: EP, pulse amplitude; TB, time between pulses; ER, ramp step; S_0, time of direct current measurement, just prior to application of pulse; S_{1-5}, time of current measurement on top of pulse, where S_5 is the effective pulse width.

generated from a single experiment. With the instrumentation described above, a series of curves can be obtained from the same experiment, as shown in Fig. 4A for stripping of lead. It is essential that the total time constant of the measuring system be much shorter than 20 ms, the shortest pulse width used, otherwise substantial instrumental distortion will be incurred as shown in Fig. 4B. Care must be exercised in the use and/or choice of an appropriate potentiostat to avoid substantial distortion of data.

In a conventional experiment, the peak height measured at one time domain is the sole parameter used for calculation of results. With the conventional method, no reliable conclusions can be drawn with respect to accuracy, even when standard addition techniques are applied. In contrast, with the multi-time domain method presented here, the possibility of interferences can be examined by determining the time dependence of the peak current for each family of curves. The peak position is not a very good criterion when the rotating mercury-film glassy carbon electrode is used, as the peak position is strongly dependent on the electrode surface. For d.p.a.s.v. of lead at the mercury-film electrode, the data in Table 1 give the current/time dependence in the presence and absence of the surfactant Triton X-100. Figure 5 shows the dependence of the peak stripping current on time (t) and $t^{-1/2}$. Clearly, the presence of a surfactant alters the current/time relation that might be predicted for the reversible case ($t^{-1/2}$ dependence). The current ratio given in Table 1 is the diagnostic criterion recommended for determining if a measurement is interference-free or not. Unknown solutions must produce the

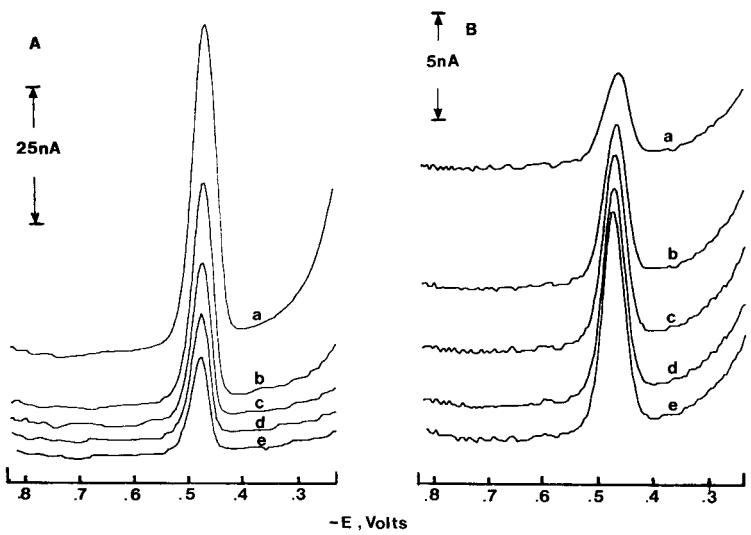

Fig. 4. Multi-time domain d.p.a.s.v. of 20 μg l^{-1} lead in 0.01 M HCl. Conditions: E(dep) = —0.85 V vs. SCE; E(final) = —0.25 V vs. SCE; E(pulse) = 50 mV; Scan rate = 5 mV s^{-1}; t(dep) = 60 s; t(rest) = 20 s; t(pulse) = 100 ms; rotation speed = 1500 rpm. Curves a, b, c, d, e correspond to 20, 40, 60, 80, 100 ms, respectively (S_{1-5}). Time constant: (A) <1 ms; (B) 300 ms.

TABLE 1

Data for a multi-time domain d.p.a.s.v. determination of lead in 0.01 M HCl in absence and presence of Triton X-100[a]

Pulse width (ms)	20 μg l^{-1} lead			20 μg l^{-1} lead + 1 mg l^{-1} Triton X-100		
	I_p (nA)	E_p (mV)	$I_p(x)/I_p(20)$	I_p (nA)	E_p (mV)	$I_p(x)/I_p(20)$
20	49.6	−470	1.00	7.3	−449	1.00
40	30.4	−475	1.62	7.5	−451	0.98
60	22.5	−477	2.21	7.3	−450	1.01
80	17.5	−481	2.84	7.5	−454	0.98
100	14.3	−481	3.47	6.7	−456	1.10

[a]Widths at half-height values, $W_{1/2}$, in both the presence and absence of Triton X-100 lie in the range 42 ± 3 mV. Reproducibility is much lower in presence of Triton X-100. I_p, peak current; E_p, peak potential vs. SCE; $[I_p(x)/I_p(20)]$, is the ratio of peak current at pulse width x ms (x = 20, 40, 60, 80 or 100) to peak current at pulse width 20 ms.

same ratio (e.g., for 100 ms to 20 ms) as the standards (or standard addition) for an answer to be acceptable. This form of investigation would not be practicable with standard instrumentation because of operator time constraints and technical reasons. Although the peak current in the presence of the surfactant is considerably less than that for the pure system, this interference would probably go unnoticed in a conventional analysis because peak position and peak half-width are similar in magnitude in both cases.

In addition to enhancing the prospect of detecting interferences, the multi-time domain d.p.a.s.v. method has other advantages. For example, data for the optimization of the pulse width required to obtain maximum sensitivity can be gained from just one experiment. The optimal pulse width may not occur at the fixed pulse width offered in most commercial instruments (40—60 ms).

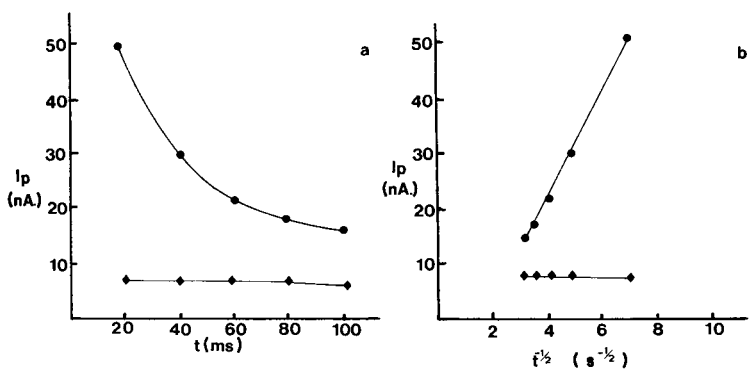

Fig. 5. Current/time response for d.p.a.s.v. of 20 μg l^{-1} lead in 0.01 M HCl in (•) absence and (♦) presence of 1 mg l^{-1} Triton X-100. (a) Peak current vs. t; (b) peak current vs. $t^{-1/2}$. Parameters as for Fig. 4A.

CONCLUSIONS

The distributed microprocessor system provides substantial computing power and is therefore appropriate for sophisticated analytical methodologies. At the same time, the ability to use a self-contained inexpensive microprocessor system in the laboratory provides advantages not available with any previously developed system. Whilst the present example is concerned with d.p.a.s.v., the conclusions should be equally valid for many other instrumental methods.

The equipment developed in this project was funded from a research grant provided by the Australian Research Grants Scheme (ARGS). The authors also gratefully acknowledge financial support to J. B. R. by the ARGS and the Swiss National Science Foundation and valuable discussions with T. Hooper and R. Sharp.

REFERENCES

1 E. B. James, Chem. Br., 18 (1982) 620.
2 J. B. Reust, Swiss Chem., 5 (1983) 33.
3 T. Wasa, H. Yamamoto and K. Akimoto, Bunseki Kagaku, 31 (1982) T95.
4 J. L. Hillburn and P. M. Julich, Microcomputers/Microprocessors: Hardware, Software and Applications, Prentice Hall, Englewood Cliffs, 1976.
5 G. A. Korn, Microprocessors and Small Digital Computer Systems, McGraw-Hill, New York, 1977.
6 P. Baecklund and R. Danielsson, Anal. Chim. Acta, 154 (1983) 61 and references cited therein.
7 M. Ichise, Denki Kagaku, 48 (1980) 150.
8 M. I. Cohen and P. A. Heimann, J. Res. NBS, 83 (1978) 429.
9 L. Kryger, Anal. Chim. Acta, 133 (1982) 592 and references cited therein.
10 J. E. Anderson, R. N. Bagchi, A. M. Bond, H. B. Greenhill, T. L. E. Henderson and F. L. Walter, Am. Lab., 13 (2) (1981) 21.
11 W. S. Woodward and C. N. Reilley, Pure Appl. Chem., 50 (1978) 785.
12 T. Ryan, Lab. Pract., 27 (1978) 189.
13 D. Gosden, M. Hayes, A. T. Kuhn and D. Whitehouse, J. Appl. Electrochem., 8 (1978) 437.
14 P. He, J. P. Avery and L. R. Faulkner, Anal. Chem., 54 (1982) 1313A.
15 A. Drescher, Chem. Tech., 26 (1974) 229.
16 T. R. Copeland, R. A. Osteryoung and R. K. Skogerboe, Anal. Chem., 46 (1974) 2093.
17 S. D. Schachterle and S. P. Perone, Anal. Chem., 53 (1981) 1672.
18 M. Ichise, Y. Nagayanagi and T. Kojima, J. Electroanal. Chem., 70 (1976) 245.
19 J. B. Reust and V. R. Meyer, Analyst (London), 107 (1982) 673.
20 J. B. Reust, Elektrochemische Schwermetallspurenanalytik und Reinraumtechnik, Inauguraldissertation, Universität Bern, Bern, 1982.

Analytica Chimica Acta, 165 (1984) 217—226
Elsevier Science Publishers B.V., Amsterdam — Printed in The Netherlands

A FLOW-INJECTION MANIFOLD BASED ON SPLITTING THE SAMPLE ZONE AND A CONFLUENCE POINT BEFORE A SINGLE DETECTOR UNIT

A. FERNÁNDEZ, M. A. GÓMEZ-NIETO, M. D. LUQUE DE CASTRO
and M. VALCÁRCEL*

Department of Analytical Chemistry, Faculty of Sciences, University of Córdoba, Córdoba (Spain)

(Received 8th September 1983)

SUMMARY

A configuration for flow injection analysis, which is suitable for simultaneous determinations, is proposed. It is based on division of the injected sample, with each sub-sample resulting from the division passing through reactors with different characteristics and the confluence of these channels before their arrival at the detector. A two-peak output is obtained as a consequence of the different residence times of the sub-samples. The behaviour of the new configuration is shown, for studies with dye solutions, to be in concordance with theoretical predictions. The geometric and hydrodynamic characteristics of the system are used in expressions that allow the splitting ratio of the injected sample to be predicted.

The simultaneous determination of several species can be especially important in areas such as clinical chemistry, industrial control and pollution analysis. For that reason, the design of automatic instruments for such purposes has been studied extensively. Flow injection analysis (f.i.a.) is a technique with versatility, simplicity and low cost, all of which make it very attractive for conducting simultaneous determinations, but this aspect has received relatively little attention [1]. Some of the simultaneous determinations that have been described are based on splitting the flow after the injection valve and using two detectors in parallel. In this manner, chloride and sulphate [2], alkali and alkaline earth metals [3], and nitrite and nitrate [4] have been determined simultaneously. With a proportional multi-injector, Bergamin and co-workers have reported several simultaneous determinations both by the zone-sampling mode with two detectors [5] and by sequential injection with a single detector [6].

The new configuration for simultaneous determinations described here is based on splitting the injected sample into two reactors with different characteristics and the subsequent confluence of these channels before their arrival at the detector. This results in two peaks caused by the different residence times of the two portions into which the injected volume is divided. The physical behaviour of this configuration was monitored spectrophoto-

0003-2670/84/$03.00

metrically with the aid of a dye. Predecessors of the configuration presented here for simultaneous determinations are those of Kagenow and Jensen [7], who used a double injection valve with confluence upstream from the detector, and Stewart and Růžička [8] who split the sample and passed each channel through identical photometric cells aligned in the same optical path. A similar configuration was used in an earlier paper by Růžička et al. [9] in the determination of chloride to allow the expansion of the analytical range without any loss of accuracy. In all cases two peaks were obtained.

EXPERIMENTAL

A Pye Unicam SP-500 spectrophotometer equipped with a Hellma 178.12 (inner volume 18 μl) flow cell was used. Ismatec S.840 peristaltic pumps, a Tecator L-100-1 injection valve, a Tecator TM-III Chemifold and a Hewlett-Packard HP-85 computer were also used.

The manifold is shown in Fig. 1. The values of the parameters used in the studies were: L_1 = 50 cm; ϕ_1 = 0.50 mm; L_2 = 75, 100, 150 or 200 cm; ϕ_2 = 0.35, 0.50 or 0.70 mm; q_1 = 1.1, 2.2, 3.1 or 4.0 ml min^{-1}; V_i = 40.8, 74.4, 91.1 or 127.0 μl; and temperature = 20, 30, 40, 50 or 60°C (where L is the tube length, ϕ the diameter, q the flow rate and V_i is the injected volume).

A bromocresol green stock solution was prepared by dissolving 0.400 g of the dye in 25 ml of 96% ethanol, making the final volume up to 100 ml with 1×10^{-2} M sodium borate solution. The working dye solution used was prepared by mixing 1 ml of the stock solution with 199 ml of 1×10^{-2} M sodium borate. The carrier stream solution was 1×10^{-2} M sodium borate.

RESULTS AND DISCUSSION

Hydrodynamic considerations

Laminar flow is a characteristic feature of f.i.a. Even under the most drastic experimental conditions in which this technique is used, the Reynolds number ($R_e < 400$) is much less than the value ($R_e < 2100$) established for

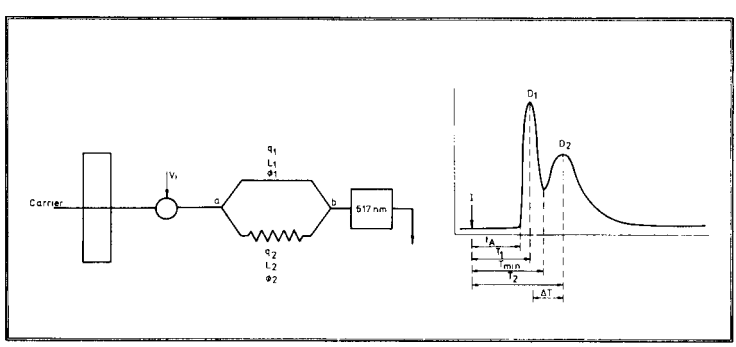

Fig. 1. Manifold used, and peaks obtained. For the meaning of the symbols, see text.

transition to the turbulent regime ($R_e > 3000$). Thus the loss of pressure, ΔP, can be calculated by the Hagen—Poiseuille and Fanning equations, when the friction factor, f, diameter and length of the tubing and the average linear flow velocity, $\bar{u}$, are known: $\Delta P = f(L/\phi)(\bar{u}^2/2g)$, where $f = 64/R_e$. This allows the flow at each point in the system to be calculated exactly. The flow is, of course, a variable of decisive importance in f.i.a.

The Bernouilli equation applied to a configuration such as that proposed here, taking into account that all the points in the system are at the same level, enables an equation for the flow distribution between the two channels to be deduced as a function of the diameter and length of the channels, i.e., as a relationship between the geometric and hydrodynamic characteristics of the manifold. The Bernouilli equation applied between points a and b of Fig. 1 for each channel, considering that $h_a = h_b$ and that the cross-section area of each channel is constant between a and b (thus $u_a = u_b$), gives $\Delta P_1 = (P_a - P_b)/\rho g$ and $\Delta P_2 = (P_a - P_b)/\rho g$, where P is the pressure at a given point in the system, ρ is the density of the liquid and g is the gravitational constant. Clearly, $\Delta P_1 \rightarrow \Delta P_2$.

From the Fanning equation, replacing the Reynolds number by its value $\rho\phi\bar{u}/u$ and simplifying gives $\bar{u}_1 L_1/\phi_1^2 = \bar{u}_2 L_2/\phi_2^2$, where u is the linear velocity of the fluid. The flow $\bar{u}$ may be replaced by $4q/\phi^2\pi$ to give the following expression

$$|\phi_2/\phi_1|^4 L_1/L_2 = q_2/q_1 \qquad (1)$$

which combines the geometric and hydrodynamic characteristics of the proposed configuration.

To show the influence of the lengths of the channels on the splitting of the flow, the flows were measured immediately before point b (Fig. 1). When the diameters of both channels are identical, Eqn. 1 becomes $L_1/L_2 = q_2/q_1$, hence $L_1/(L_1 + L_2) = q_2/q_t$ and $L_2/(L_1 + L_2) = q_1/q_t$. This ratio was proved by 15 experiments in which the tube lengths and flows were changed. The equation obtained and the correlation coefficient are given in Table 1.

To study the influence of a difference in temperature between the two channels, a series of systematic experiments was done; the geometry of the system was kept constant and the temperature in channel 2 was increased. A decrease of q_1/q_2 was observed as a consequence of the decrease in viscosity and the expansion of the tubing with increased temperature. The greater the value of L_2, the greater the effect of temperature (see Table 1).

Division of the injected volume of sample

This is the key aspect of the new configuration. The division is influenced by the geometry of the splitter. An arrow design ($\Rightarrow$) was used in these experiments. The manifold described was used with injection of dye and its detection at the ends of both channels (point b), and the absorbance of 10-ml aliquots of the fluid was measured in each channel (A_1 and A_2) for various injected volumes. The absorbance corresponding to the injected total

TABLE 1

Equations relating different variables

Conditions	Equations	Correlation coefficient (r)
$\phi_1 = \phi_2$	$L_1/L_2 = 0.065 + 0.899\, q_2/q_1$	0.970
	$q_1/q_t = -0.0419 + 1.005\, V_1/V_i$	0.996
	$q_2/q_t = -0.0518 + 0.953\, V_2/V_i$	0.997
$q_1 = 1.1$[a]	$T_1/T_2 = 0.0567 + 1.515\, \lvert L_1/L_2 \rvert^2$	0.999
$q_1 = 2.2$[a]	$T_1/T_2 = 0.0536 + 1.452\, \lvert L_1/L_2 \rvert^2$	0.998
$q_1 = 3.2$[a]	$T_1/T_2 = 0.0588 + 1.644\, \lvert L_1/L_2 \rvert^2$	0.998
$q_1 = 4.0$[a]	$T_1/T_2 = 0.0731 + 1.808\, \lvert L_1/L_2 \rvert^2$	0.997
$q_t = 1.65$[a]	$D_1 = 7.6240 + 0.153\, T$ (°C)	0.971
	$D_2 = 27.4720 + 0.258\, T$ (°C)	0.988
	$T_1 = 23.0000 + 0.099\, T$ (°C)	0.999
	$T_2 = 99.6000 - 0.230\, T$ (°C)	0.989
$q_t = 2.90$[a]	$D_1 = 6.0960 + 0.102\, T$ (°C)	0.972
	$D_2 = 38.9820 + 0.436\, T$ (°C)	0.998
	$T_1 = 8.8600 + 0.102\, T$ (°C)	0.995
	$T_2 = 54.1900 - 0.112\, T$ (°C)	0.985

[a] ml min^{-1}.

volume (A_t) was measured by diluting the particular injected volume of sample to 10 ml [$A_t = (A_1 + A_2)$].

The partial volumes (V_1 and V_2) into which the total sample volume is divided ($V_i = V_1 + V_2$) are directly related to the absorbance through Beer's law: $A_1/A_t = V_1/V_i$; $A_2/A_t = V_2/V_i$.

In these tests, L_1, ϕ_1 and q_t (50 cm, 0.50 mm and 4.4 ml min^{-1}, respectively) were kept constant but variations were made in L_2 (75, 100, 150, 200 cm) and ϕ_2 (0.35, 0.50, 0.70 mm). Consequently, q_1 and q_2 were changed. The data obtained from these experiments (Table 1) show that the ratio between flows and sample volumes that pass through each channel are given by the equations $V_i q_1/q_t = V_i L_2/(L_1 + L_2)$ and $V_i q_2/q_t = V_i L_1/(L_1 + L_2)$. From these expressions, the division of the injected volume as a function of the length of both channels can be calculated if the tube diameters are equal.

Influence of variables on the peaks obtained

Another important aspect that must be considered is the confluence of both channels before their arrival at the detector. The most significant theoretical equations proposed so far provide either peak-height or horizontal information. In the peak model of Růžička and Hansen [10],

$$D = 2\pi^{2/3} r^2 L^{1/2} \bar{u}^{1/2} \delta^{1/2}\ \bar{T}^{1/2} V_i^{-1}$$

where D is the dispersion, r the tube radius, $\bar{u}$ the mean velocity of the fluid, $\bar{T}$ the mean residence time, and δ the dispersion number [11]. In the horizontal scheme [12]:

$t_A = 109\, r^2 D^{0.025}/f\,|L/q|^{1.025}$

and $\Delta t_B = 35.4\, r^2 f/D^{0.36}\,|L/q|^{0.64}$

where t_A is the travel time, D the diffusivity of the measured substance, f the accommodation factor and Δt_B the dispersion time. Neither is very practical for directly predicting the peak shapes, because of the δ and f terms, respectively. A more versatile application of these equations is attempted here. For a theoretical study of the proposed configuration, the independent performance of each channel can be considered, and the lengths of the sections between the injection point and the split and between the confluence point and the detector are assumed to be negligible.

If the dispersions at the first and second peak maxima are D_1 and D_2, respectively, and taking into account the ratio between volumes of the subsample and flow deduced above, the following equation can be established from the one proposed by Růžička and Hansen [10]:

$$D_1/D_2 = 2\pi^{3/2} r_1^2 L_1^{1/2} \bar{u}_1^{1/2} \delta_1^{1/2} \bar{T}_1^{1/2} V_1^{-1} / 2\pi^{3/2} r_2^2 L_2^{1/2} \bar{u}_2^{1/2} \delta_2^{1/2} \bar{T}_2^{1/2} V_2^{-1}$$

$$= [r_l^2 L_1^{1/2} |q_1/\pi r_1^2|^{1/2} \delta_1^{1/2} |\pi r_1^2 L_1/q_1|^{1/2} |V_i q_1/q_t|^{-1}] / [r_2^2 L_2^{1/2} |q_2/\pi r_2^2|^{1/2} \delta_2^{1/2} |\pi r_2^2 L_2/q_2|^{1/2} |V_i q_2/q_t|^{-1}]$$

Simplifying yields

$$D_1/D_2 = (L_1 q_2/L_2 q_1)\, |r_1/r_2|^2 |\delta_1/\delta_2|^{1/2} \tag{2}$$

Considering the expression derived from the Bernouilli equation, that relates the diameters, length and flow of the configuration

$$D_1/D_2 = |L_1/L_2|^2 |r_1/r_2|^2 |\delta_1/\delta_2|^{1/2} \tag{3}$$

If the two channels have the same radius, the expression reduces to

$$D_1/D_2 = |L_1/L_2|^2 |\delta_1/\delta_2|^{1/2} \tag{4}$$

The expression of Vanderslice et al. [12] does not take into account the residence time (time to the peak maximum on the recording) but a time, τ, which can be defined as the time elapsed between the travel time, t_A, and the appearance of the maximum of the curve, T: $\tau = T - t_A$. If the sample behaves from the injection to the detector as a plug flow regime, $\tau = 0$ and therefore $T = t_A$. Under appropriate working conditions (high flow, short reactor lengths, etc.) this approximation can be introduced into the Vanderslice equation by replacing t_A by T. Hence

$$t_{A_1}/t_{A_2} \approx T_1/T_2 = [109(r_1^2 D^{0.025}/f_1)\, |L_1/q_1|^{1.025}] / [109 r_2^2 D^{0.025}/f_2 | - L_2/q_2|^{1.025}]$$

Simplifying gives

$$T_1/T_2 = (f_2/f_1)\, |r_1/r_2|^2 |L_1 q_2/L_2 q_1|^{1.025}$$

$$\text{or } T_1/T_2 = (f_2/f_1)\, |r_1/r_2|^2 |L_1/L_2|^{2.05} \tag{5}$$

Comparison of Eqns. 3 and 5, and making the approximation $|L_1/L_2|^{2.05} \approx$

$|L_1/L_2|^{2.00}$, the ratio between the parameters that define the coordinates of the flow-injection peaks is obtained

$$D_1T_1/D_2T_2 = (f_2/f_1)\,|\delta_1/\delta_2|^{1/2} \qquad (6)$$

The application of these expressions involves some difficulties. First, it is difficult to determine the travel time for the second peak, t_{A_2}. Therefore the value of f_2 for peak 2 cannot be experimentally calculated, although it can be calculated [14] from $f_2 = (t_{A_2})_{\text{theor.}}/(t_{A_2})_{\text{exp.}}$ or $f_2 = (\Delta t_{B_2})_{\text{exp.}}/(\Delta t_{B_2})_{\text{theor.}}$. It is, however, possible to determine the f_2/f_1 ratio from Eqn. 5. Secondly, the Levenspiel–Smith dispersion number depends on the variance ($\delta = 1/8|8\sigma^2 + 1)^{1/2} - 1|$), assuming a non-Gaussian behaviour of the recording; therefore, it will change with the characteristics of the flow-injection configuration, which in turn determines the shape of the curve. The ratio between the Levenspiel–Smith numbers can be found from Eqn. 5.

In order to establish the degree of agreement of these theoretical considerations with experimental reality, a systematic study was done. The manifold used is shown in the scheme in Fig. 1, and the different parameters were varied. A total of 177 experiments was done.

Effect of the ratio of tube lengths

Figure 2 shows the influence of the change of L_2 (constant ϕ_2) on the recordings when the geometric and hydrodynamic variables of channel 1 remain unaltered. Because q_1 is constant, the travel time of peak 1, (t_{A_1}), remains constant.

Figure 3 shows plots of the variation of several time parameters (residence time, T_1 and T_2, the travel time of the first peak, t_{A_1}, and time of appearance of the minimum between the two peaks, $T_{\min}$); the values of the dispersion coefficients (D_1 and D_2) and their ratio; and the flows (q_1, q_2 and q_t), all of

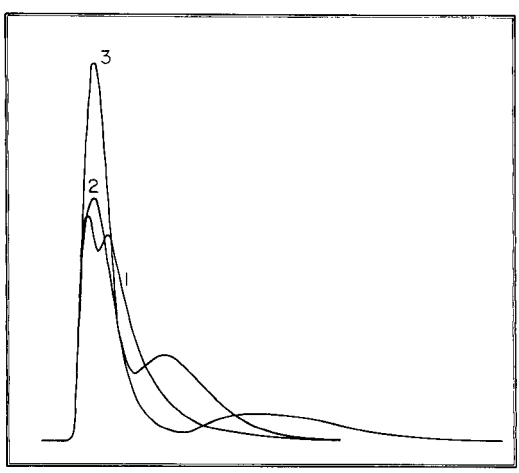

Fig. 2. Influence of the length of reactor 2 on the two-peak recording. L_2: (1) 75 cm; (2) 100 cm; (3) 150 cm. (q_1 = 1.16 ml min^{-1}, L_1 = 50 cm, V_t = 70.4 μl.)

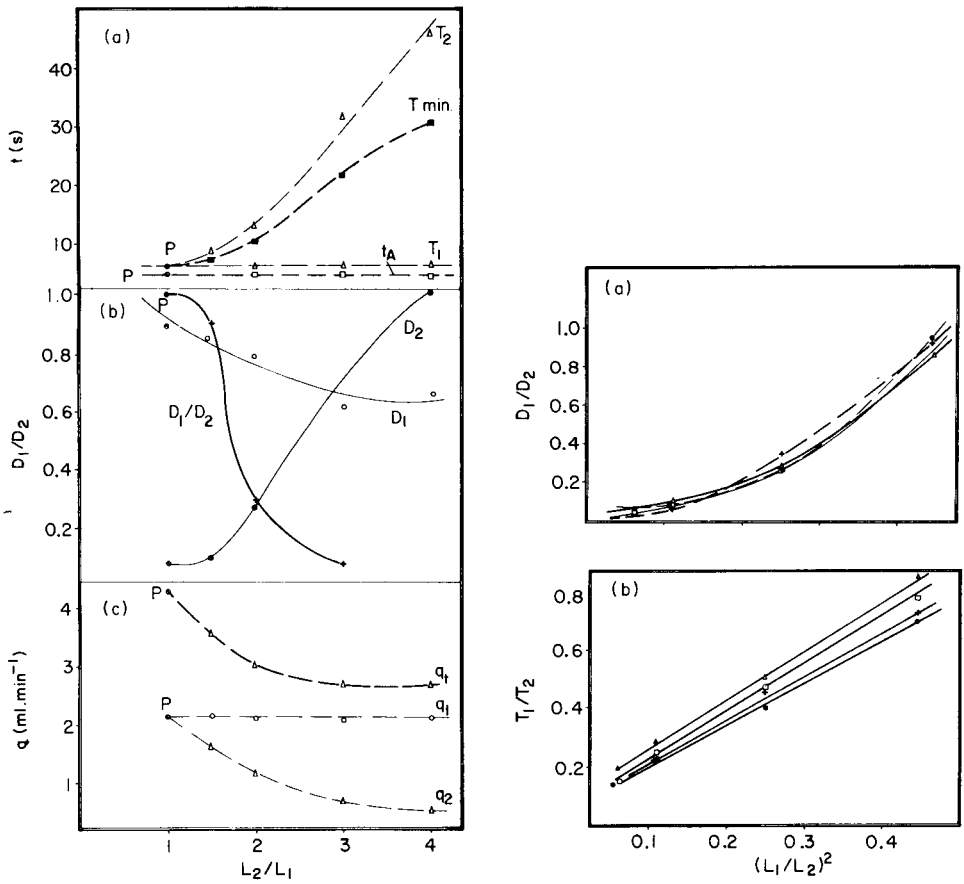

Fig. 3. Effect of the length ratio of the two channels on: (a) time parameters; (b) dispersion coefficients and their ratio; (c) partial and total flows. Symbols are experimental points; the lines are calculated.

Fig. 4. Influence of the square of the tube length ratio on: (a) dispersion coefficient ratio; (b) residence time ratio. Flow rate: (+) q_1 = 1.1 ml min^{-1}; (•) q_1 = 2.2 ml min^{-1}; (□) q_1 = 3.1 ml min^{-1}; (△) q_1 = 4.0 ml min^{-1}.

them as a function of the length ratio (L_2/L_1) for constant and equal ϕ_1 and ϕ_2. The plots of the theoretical point, P', corresponding to $L_1 = L_2 = 50$ cm, are included. The behaviour of the system meets the theoretical predictions in every case.

In order to verify Eqn. 5, as simplified by taking $a_1 = a_2$ and $T_1/T_2 = (f_2/f_1)(L_1/L_2)^2$, the data corresponding to a set of experiments for four different values of q_1 were processed and plotted (Fig. 4). From the corresponding equations summarized in Table 1, it can be inferred that: (a) the expression is verified for the set of experiments conducted; (b) the ratio between the accommodation factors is independent of the flow; (c) the ratio

between accommodation factors does not depend on the ratio of the channel lengths, which is predictable, considering that $L_1/L_2 = q_2/q_1$. The variation of D_1/D_2 vs $(L_1/L_2)^2$ is nonlinear (Fig. 4b) according to Eqn. 3. Because the Levenspiel–Smith number depends on the variance of each curve, $(\delta_1/\delta_2)^{1/2}$ is a variable factor for each length ratio. A change in q_1 has no significant influence on the behaviour of the system.

Effect of the flow

The influence of the flow was studied for different values of V_i and several ratios of channel lengths. The behaviour was similar in all cases. As an example, Figure 5 shows this behaviour for $V_i = 74.4$ µl and $L_2/L_1 = 2$. From this figure, it can be concluded that: (a) the residence times, T_1 and T_2 and travel time, t_{A_1}, decrease as the flow increases, their variation being exponential, as expected; (b) the dispersion coefficients also decrease with increasing flow; the flow has more influence on the value of D_2. As is logical, the D_1/D_2 ratio increases with q_1.

Influence of the injected volume

To define the influence of this variable, experiments were run at four V_i values (40.8, 74.4, 91.1 and 127 µl) in sets in which q_1 was kept constant (at four different values: 1.1, 2.2, 3.1 and 4.0 ml min^{-1}) and for four L_2 values (75, 100, 150 and 200 cm). As expected, the maximum absorbance of both peaks increased with increasing volume of dye injected and D_1 and D_2 decreased. The D_1/D_2 ratio was independent of the injected volume because V_i has the same influence on D_1 and D_2. The residence time T_1 increased slightly with V_i and was independent of L_2. The residence time T_2 also increased slightly with V_i, but its change with L_2 was more significant.

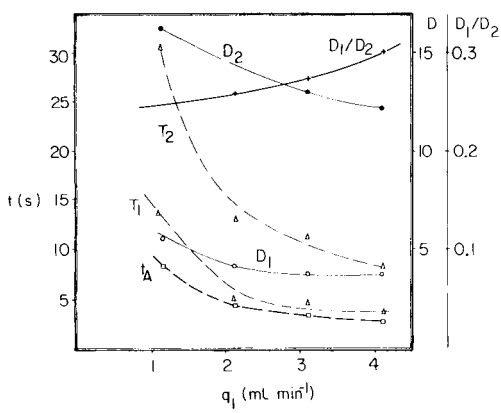

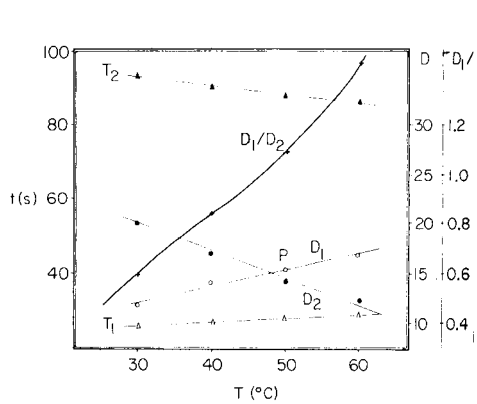

Fig. 5. Variation of time and dispersion parameters with the flow q_1, for $L_2/L_1 = 2$. Symbols are experimental points; the lines are calculated.

Fig. 6. Effect of temperature on the dispersion coefficient and residence times (q_t = 1.65 ml min^{-1}). Symbols are experimental points; the lines are calculated.

Effect of temperature

The manifold used to study the influence of this variable was similar to that in Fig. 1: V_i = 74.4 μl, q_t = 1.65 and 2.90 ml min^{-1}, L_1 = 30 cm, ϕ_1 = 0.35 mm, L_2 = 300 cm and ϕ_2 = 0.70 mm. The injector and channel 1 were kept at a constant temperature (25°C). Channel 2 was immersed in a thermostated bath at different temperatures (30°, 40°, 50° and 60°C). Figure 6 shows the variation of the residence times, dispersion coefficients and their ratio as a function of the temperature set for channel 2. The temperature has an important effect on the dispersion coefficients; D_2 decrease linearly as the temperature increases (by —0.6/°C). The dispersion coefficient of the first peak increases linearly, but less significantly, with the temperature of channel 2 (0.3/°C). The representative straight lines intercept at a point P'', the "inversion point" at which $D_1 = D_2$. This point divides the influence of the temperature into two parts: to the left (lower temperatures) $D_2 > D_1$ and peak 1 reaches a greater height; to the right (higher temperatures), $D_1 > D_2$.

The influence of an increase in temperature of channel 2 on the residence times is not very significant. In all cases, the relationship was linear with a very gentle slope; T_1 increased slightly (0.08 s/°C) and T_2 decreased (—0.12 s/°C). For another set of experiments, run at q_t = 2.90 ml min^{-1}, the behaviour of the system was analogous to that above. The slower the overall flow, the lower the inversion temperature. For q_t = 1.65 ml min^{-1}, the inversion occurred at 47.8°C, whereas it took place at 61.2°C for q_t = 2.90 ml min^{-1}. The equations corresponding to the ratios taken for the experiments run at the two different flows are summarized in Table 1.

The temperature has important effects not only on the splitting of the injected sample volume, through its influence on the splitting of the flow, but also on the viscosity of the streamed solution and on the diffusion coefficient of the substance monitored. The increase in D_1 can only be attributed to a decrease in the flow, q_1, which implies a decrease in V_1 from the expression, $V_1 = q_1 V_i / q_t$, because q_t is constant and because the value of q_2 increases with the expansion of L_2 and with decreased viscosity. The decrease in D_2 can be attributed to, at least, an increase in V_2 with q_2, and to the effect of the temperature on the diffusivity ($D = kT^{2/3}$); increased diffusivity causes increased radial diffusion, thus contributing to a decrease in the overall dispersion phenomenon.

APPLICATIONS

The most immediate application of the configuration suggested is in differential kinetic analysis, as the two sub-samples have different residence times and therefore measurements done on each peak are indeed measurements at different reaction times. The interval can be modified by changing the geometric characteristics of the channels. This concept can be applied to slow reactions either by decreasing the total flow rate or by incorporating a common reactor prior to splitting. The configuration is also applicable to faster reactions (half-life 0.5—3 s).

Several chemical systems have been tested to check the applicability of the configuration suggested. Thus, the simultaneous spectrophotometric determination of cobalt and nickel based on complex formation with 2-hydroxybenzaldehyde thiosemicarbazone has been proposed [14]; formation of the nickel complex is fast, whereas that of the cobalt complex is relatively slow because of the need for previous oxidation of Co(II) to Co(III) by atmospheric oxygen. Mixtures of these ions can be resolved in 1:6 to 6:1 ratios with results perfectly comparable to those obtained by traditional differential kinetic methods.

In another example, Mn(II) and Fe(III) exert a different catalytic action on the oxidation of 2-hydroxybenzaldehyde thiosemicarbazone by hydrogen peroxide in the presence of amines, yielding an intensely fluorescent product. Both ions can be determined by means of the proposed configuration because of their different contributions to the fluorescence. The determination range is 40—600 ng ml^{-1} with an r.s.d. between 1.2—2.5%. The results have been critically compared with those obtained in the sequential determination of both ions by a manifold with a diverting valve [15].

Two methods for the simultaneous fluorimetric determination of pyridoxal and pyridoxal-5-phosphate based on their different rates of oxidation catalyzed by cyanide have been based on this configuration. One of the methods involves the use of a very short reactor so that the first peak is due only to the native fluorescence of pyridoxal whereas the second peak is due to the sum of this fluorescence and that corresponding to the oxidation product of the phosphate derivative. In the other method, the catalyzed oxidation of both compounds is achieved. These compounds can thus be determined in the range of 10^{-3}—10^{-8} M [16].

REFERENCES

1 M. D. Luque de Castro and M. Valcárcel, Analyst (London), 109 (1984) 413.
2 W. D. Basson and J. F. Van Standen, Water Res., 15 (1981) 333.
3 W. D. Basson and J. F. Van Standen, Fresenius Z. Anal. Chem., 302 (1980) 370.
4 L. Anderson, Anal. Chim. Acta, 110 (1979) 123.
5 E. A. G. Zagatto, A. O. Jacintho, L. C. R. Pessenda, F. J. Krug, B. F. Reis and F. H. Bergamin, Anal. Chim. Acta, 125 (1981) 37.
6 M. F. Giné, F. H. Bergamin, E. A. G. Zagatto and B. F. Reis, Anal. Chim. Acta, 114 (1980) 191.
7 H. Kagenow and A. Jensen, Anal. Chim. Acta, 114 (1980) 227.
8 J. W. B. Stewart and J. Růžička, Anal. Chim. Acta, 82 (1976) 137.
9 J. Růžička, J. W. B. Stewart and E. A. G. Zagatto, Anal. Chim. Acta, 81 (1976) 387.
10 J. Růžička and E. H. Hansen, Anal. Chim. Acta, 145 (1983) 1.
11 O. Levenspiel and W. H. Smith, Chem. Eng. Sci., 6 (1957) 227.
12 J. T. Vanderslice, K. K. Stewart, A. G. Rosenfeld and D. J. Higgs, Talanta, 28 (1981) 11.
13 M. A. Gómez-Nieto, M. D. Luque de Castro, A. Martín and M. Valcárcel, Talanta, 31 (1984) in press.
14 A. Fernández, M. D. Luque de Castro and M. Valcárcel, Anal. Chem., 56 (1984) 1146.
15 F. Lázaro, M. D. Luque de Castro and M. Valcárcel, Anal. Chim. Acta, in press.
16 P. Linares, M. D. Luque de Castro and M. Valcárcel, Clin. Chem., in press.

Analytica Chimica Acta, 165 (1984) 227—236
Elsevier Science Publishers B.V., Amsterdam — Printed in The Netherlands

A RANDOM WALK SIMULATION OF FLOW INJECTION ANALYSIS

D. BETTERIDGE[a], C. Z. MARCZEWSKI and A. P. WADE[a]

BP Research Centre, Sunbury-on-Thames, Middlesex, TW16 7LN (Great Britain)

[a]*Department of Chemistry, University College Swansea, Swansea, W. Glam., SA2 8PP (Great Britain)*

(Received 3rd November 1983)

SUMMARY

Dispersion and chemical reaction in a single-channel flow-injection system are modelled by a random walk (stochastic, Markovian chain) method using a microcomputer. The effects of various simulated physical variables are investigated. The model provides valuable insight into the mixing process in flow injection analysis.

In order to gain more insight into the processes at work in flow injection analysis (f.i.a.), some computer simulations based on a random walk (stochastic, Markov chain) model have been carried out on PET and Apple microcomputers. Einstein used the random walk model of diffusion to explain Brownian motion [1]. He showed that a group of molecules taking a series of random steps will finally reach a Gaussian distribution around the origin, the spread being determined by the number of steps and the mean size of each step. For a molecule experiencing laminar flow, the total displacement per step can be considered a combination of the effects of random walk and laminar flow (convection). Giddings [2, 3] showed that the random walk model gave a satisfactory account of the chromatographic process.

For simulation of f.i.a., the random walk model has several advantages, primarily that it deals with individual molecules and not assemblages. Because it is based on the fate of individual molecules, it is easy to simulate the effects of sample size, chemical kinetics and the competing effects of the rate of chemical reaction and physical dispersion. Theories based on physical dispersion which are current in the literature on f.i.a. have difficulty in dealing with these basic points [4—10]. Furthermore, the model, by concentrating on the movement of individual molecules, is conceptually easier than that based on a series of imaginary tanks [4, 8]. An alternative approach to modelling the chemical and physical kinetics has been developed by Painton and Mottola [11]; it is a continuous rather than stochastic model and depends on the solution of a complex set of differential equations.

0003-2670/84/$03.00

Model for physical dispersion

The random walk model for f.i.a. is ideal for computer simulation. For this it is assumed that the "sample" is "injected" as a "plug" of known dimension. (Simulated physical realities are placed in inverted comas, when they are first introduced; thereafter the commas are omitted.) The sample is of 500—3000 "molecules" each with coordinates in three-dimensional space selected so as to fill the "tube" evenly. Then a "flow" commences for a predetermined "time". The new position of each molecule is calculated in two stages. For the first, it is assumed that it has moved downstream in accordance with normal laminar flow [9], so that its position is determined by the flow rate and its initial radial position. Then, from its new position the molecule takes a random step, the average length of which depends on the "diffusion constant" and the time per movement. The process is repeated many times.

It is easily shown that the spread of a sample on the assumption that the molecules take N steps of average length, l, for time, t, at v steps per unit time is given by the probability $\langle y^2 \rangle$ of finding a molecule at a distance y from the origin [12]

$$\langle y^2 \rangle = \frac{1}{2} (\pi Dt)^{-1/2} \int_{-\infty}^{+\infty} y^2 \exp(-y^2/4Dt)\,dy \qquad (1)$$

where D is the diffusion constant for the process, and that $\langle y^2 \rangle = 2Dt = Nl^2 = vtl^2$ [12].

Model for chemical reaction

In order to simulate reaction, sample and reagent concentrations in defined zones are calculated. These are then combined with the reaction-rate constant in accord with the stoichiometry of the reaction to obtain reaction probabilities in the range 0—1. A random number in this range is then generated for each sample molecule. If this is less than the zonal reaction probability then the molecule reacts and its type is changed to product. This ensures that in a given zone the correct proportion of molecules reacts. The random walk model is diffusion-based and similar in its treatment of physical dispersion to Taylor's theory [9], which has formed the basis of interpretation of f.i.a. [5, 6, 13], but it also permits the inclusion of chemical interactions.

EXPERIMENTAL

Method

Each molecule is represented by x, y and z coordinates, constrained within the boundaries of a hypothetical tube of circular cross-section (Fig. 1). The origin of the coordinates is taken as the centre of the sample plug at the centre of the tube; r_0 is the radius of the tube and L_s is the length occupied by the sample. Thus the coordinates of the ith molecule are constrained by

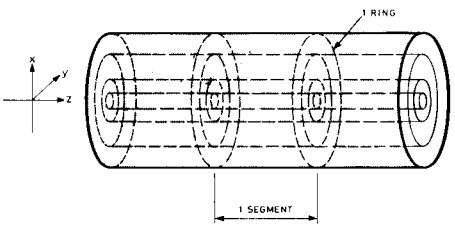

Fig. 1. Simulated flow-through tube.

$0 \leqslant x_i \leqslant r_0$ and $0 \leqslant y_i \leqslant r_0$, such that $0 \leqslant (x_i^2 + y_i^2) \leqslant r_0^2$, and initially, $-0.5L_s \leqslant z_i \leqslant 0.5L_s$. The molecules are placed in the sample space so as to give uniform sample "concentration" (i.e., number of molecules per unit volume). In two-dimensional studies, the y variable is omitted.

The chosen sample size, flow rate and other physical parameters required for the simulation were selected as typical of simple conditions for f.i.a. Each cycle of the simulation was chosen to simulate one second. To avoid confusion between real and simulated time, the term simsec (simulated second) is used. The movements and reaction of 1500 molecules were simulated for 60 simsec after injection.

Calculation of sample plug dispersion without chemical reaction

The molecules are moved so as to simulate both random dispersion similar to Brownian motion (Δd), and longitudinal transport by laminar flow (Δf). Thus, for each cycle, $x_{i\,(\text{new})} = x_{i\,(\text{old})} + \Delta d$; $y_{i\,(\text{new})} = y_{i\,(\text{old})} + \Delta d$; $z_{i\,(\text{new})} = z_{i(\text{old})} + \Delta d + \Delta f$. Without flow, random dispersion causes the initial rectangular injection to become Gaussian, and its spread with respect to time is given by $\sigma_z^2 = 2Dt$, where σ_z^2 is the variance of the Gaussian distribution, D is the sample diffusion constant ($mm^2\ s^{-1}$) and t is the time elapsed since injection (s). A statistical treatment [12] shows the average movement (mm) in t' s in any one dimension to be $l \approx (2Dt')^{1/2}$. This mobility factor is inversely related to viscosity and so is temperature-dependent. It is assumed here that the system is aqueous, for which there is an accurate viscosity (η/cp)/temperature ($T/^\circ C$) expression [14]

$$\log_e (\eta_{20}/\eta_T) = [1.37023\,(T - 20) + 8.36 \times 10^{-4}\,(T - 20)^2]/(109 + T)$$

Water has a viscosity of 1 cp at 20°C and therefore $l = (2Dt')^{1/2}/\eta_T$. The random distance moved in each direction in t' s is then $\Delta d = rns\ rnd\ 2\ l \equiv -2l + 4l\ rnd$, where rnd is a random number uniformly distributed in the range 0—1 and rns is −1 or +1 with equal probability. A new Δd value is obtained for each coordinate.

The flow velocity ($mm\ s^{-1}$) at a distance r from the centre of the tube can be expressed as

$$U_r = 2\bar{U}(1 - r^2/r_0^2)$$

If r_i denotes the r value for the ith molecule, and since $r_i^2 = x_i^2 + y_i^2$.

$$\Delta f = 2t'\overline{U}[1 - (x_i^2 + y_i^2)/r_0^2]$$

Each time that new x_i and y_i are generated, the resultant r_i is calculated ($r_{i\,(\text{new})} = x_{i\,(\text{new})}$ in the two-dimensional system). Should $r_{i\,(\text{new})} \geqslant r_0$, then the coordinates would be outside the tube boundaries; this is prevented by generating new coordinates using $\Delta d = 0$ and $\Delta f(\text{used}) = 0.5\Delta f$.

Calculation of distribution of product of chemical reaction

Given laminar flow, all molecules equidistant from the centre of the tube at any one time will experience the same physical and chemical conditions. The simulated tube (Fig. 1) is divided into several rings of equal area, typically 5, and a number of fixed length segments, to a maximum of 80, depending on the sample spread. Each ring of each segment is referred to as a zone and the numbers of molecules of sample (A) and product (X) in each zone are calculated. Reagent molecules (B) are calculated by difference

$$B = BR(N_0 - A - X) - nX$$

where BR is the initial ratio of reagent concentration (carrier stream) to sample concentration, N_0 is the initial number of molecules per zone and n is the order of the reaction. The formation of one product molecule involves reaction of one sample molecule with n reagent molecules, each product molecule counting $n + 1$ times.

The probability of reaction increases with reaction rate (k_1) and is given by

$$P = (k_1/N_0)t'B/A \quad (0 \leqslant P \leqslant 1)$$

Owing to random fluctuations of B and A, the computed values of P may sometimes be <0 or >1, in which case, they are rounded up or down to 0 or 1. To prevent spurious product concentrations being produced by statistical noise, P is taken as zero when $A \geqslant 0.66N_0$.

Most of the calculations were run with $k_1 = 4$ because this gave a peak height/time relationship similar to that of a real flow-injection system studied earlier [15]. The Arrhenius equation states that the rate constant for a reaction is given by $k = A' \exp(-E_a/RT)$, where A' is the frequency factor, E_a the activation energy, R the gas constant and T the absolute temperature. From collision theory [16], $A' = k'T^{1/2}$, where k' is a proportionality constant. Thus

$$k_1 = k'T^{1/2} \exp(-E_a/RT)$$

An activation energy of 70 kJ mol^{-1} was assumed as typical of fast aqueous chemical reactions. With $k_1 = 4$ (at 20° C), this gave $k' = 6.941 \times 10^{11}$ and an approximate expression for the behaviour of k_1 with temperature.

Output

After each simulation cycle, the (x—z plane) "detector views" of the plug and concentration histograms for sample plug and product are displayed in

low-resolution graphics. A dot matrix printer produces a hard copy of these images (Figs. 2, 3) which are also stored on 5¼-in. floppy disks for later rapid sequential retrieval ("animation"). Also displayed are the positions of the front molecule, the last molecule and the current maximum product concentration, the longitudinal spread of the plug, and the sample dispersion. Levels of concentration are shown as 13 different colours on the Apple CRT and as 16 bit patterns of different density on the hard copy.

Simulations of 1500 molecules over 60 simsec took about 7 h on the Apple microcomputer, which was fitted with an accelerator card using a 3.5-MHz 6502C microprocessor.

RESULTS AND DISCUSSION

The simulated peaks, in the form of histograms, show the molecular distribution along the length of the tube (Figs. 2 and 3). The accuracy of the model increases with the number of molecules used for the simulation; normally 1500 was chosen but useful demonstrations are possible with as few as 50. Calculations with a larger computer have shown that with 15 000 molecules the results are essentially the same as with 1500, but the output approaches a smooth continuous function. For the purpose of evaluation, the peak height H_{max} was plotted against time (simsec) for the variables investigated.

The results of the simulation are in substantial agreement with experiment and the predictions of other theories when physical dispersion is the predominant feature. Additionally, they shed light on the process of mixing and indicate the hitherto unnoticed consequences of combinations of different factors. Thus it is predicted, as expected, that: (i) without chemical reaction, the peak height decreases exponentially with time (Fig. 4); (ii) there is a linear relationship between baseline-to-baseline time dispersion and the distance the plug has travelled [5]; (iii) the larger the diffusion constant, the

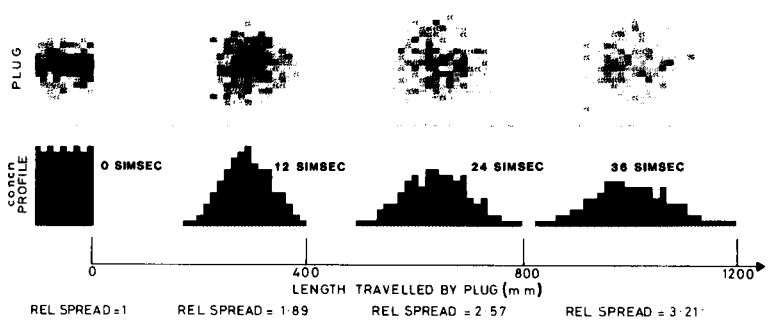

Fig. 2. Simulation of f.i.a. without reaction. Conditions: 1400 molecules; 1 simsec/cycle; flow rate 1 ml min^{-1}; sample size 400 μl; temperature 20° C; tube internal diameter 0.8 mm; diffusion constant 10^{-3} mm^2 s^{-1}.

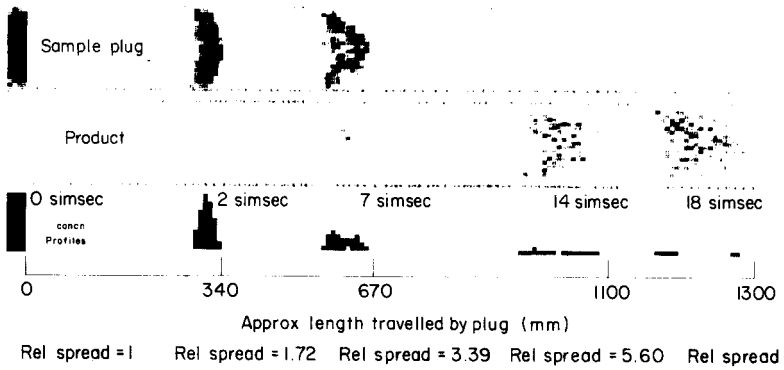

Fig. 3. Simulation of f.i.a. with chemical reaction for reaction $A + B = X$ with $k_1 = 4$. Conditions: 1500 molecules; 1 simsec/cycle; flow rate 1 ml min^{-1}; sample size 100 μl; temperature 20°C; tube i.d. 0.8 mm; diffusion constant 10^{-3} mm^2 s^{-1}. For the concentration profiles, dark areas indicate sample, hatched areas the product.

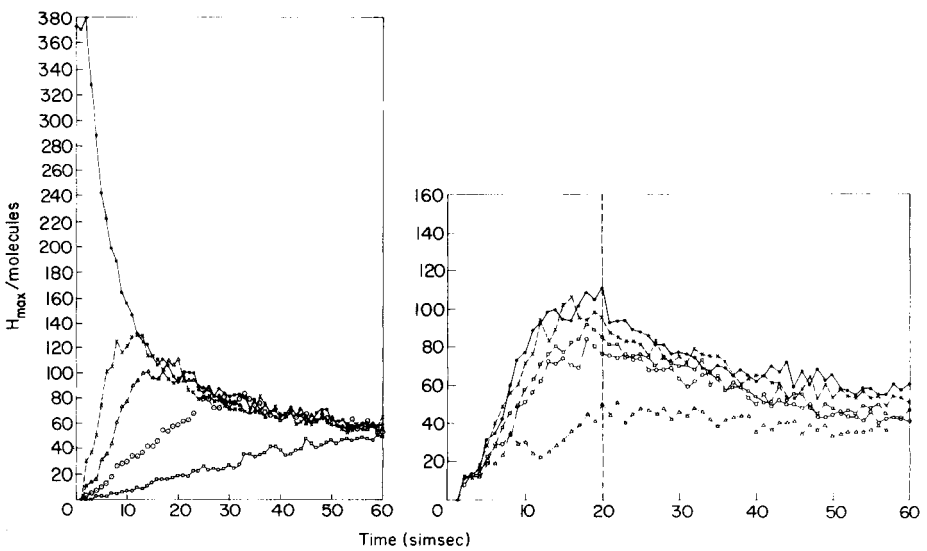

Fig. 4. Simulated effect of rate of reaction for $A + B = X$. (×) $k_1 = 16$; (△) $k_1 = 4$; (○) $k_1 = 1$; (□) $k_1 = 0.25$. (•) All sample (no reaction, dispersion only). Conditions: 1500 molecules (375 per segment initially); otherwise as in Fig. 3.

Fig. 5. Effect of diffusion coefficient with reaction $A + B = X$ ($k_1 = 4$). Diffusion coefficient (mm^2 s^{-1}); (•) 1×10^{-3}; (×) 0.75×10^{-3}; (□) 0.5×10^{-3}; (○) 0.25×10^{-3}; (△) 0. Simulated conditions as for Fig. 4.

greater the rate of mixing and hence peak height (Fig. 5) [9], the plot of peak height squared vs. diffusion constant being linear in agreement with theory [9]; (iv) fast flow rate produces rapid mixing and fast longitudinal dispersion whilst for slow flow rates the converse is true (Fig. 6A); (v) if the conditions

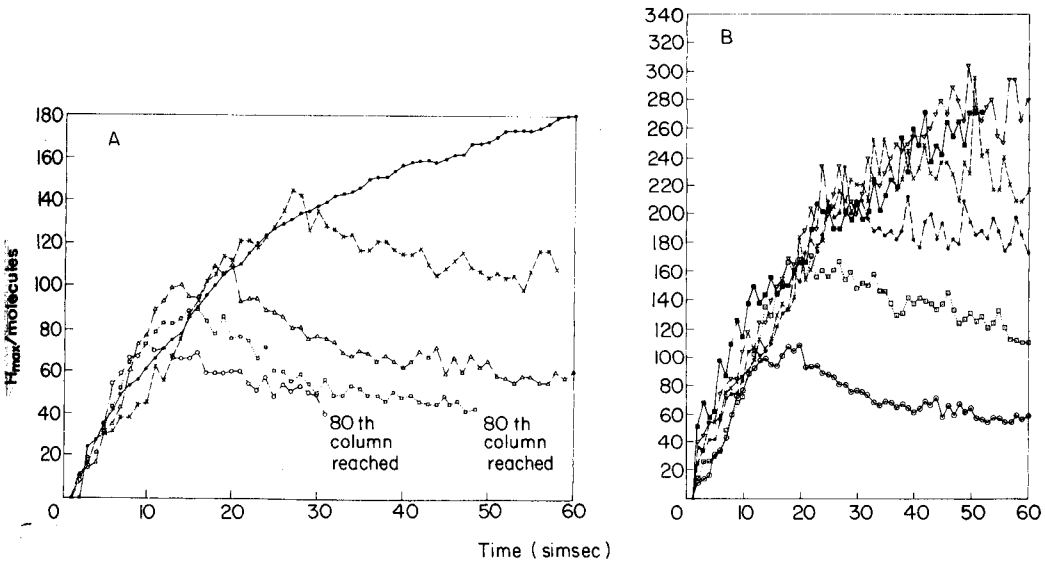

Fig. 6. Random walk model. (A) Effect of flow rate (ml min^{-1}): (•) 0; (×) 0.5; (△) 1.0; (□) 1.5; (○) 2.0. (B) Effect of sample size (μl): (○) 100; (□) 200; (•) 300; (×) 400; (▽) 500; (▪) 600. Other conditions as for Fig. 4.

are such that double peaks are avoided, sensitivity is favoured by large sample size with a practical limit of 500—600 μl for 0.8 mm i.d. tubing (Fig. 6B) [15, 17]. The other findings are discussed separately.

The mixing process

Initially, reaction takes place at the interfaces between the sample plug and reagent carrier stream. For medium or large samples, a double peak is initially observed for the product. The original rectangular sample peak becomes Gaussian (in the absence of flow) or skewed Gaussian (in the presence of flow) as the product double peak increases in height and width until the two humps coalesce to a single shouldered peak. The sample peak collapses as the product peak grows, leaving a few unreacted molecules in the centre of the sample plug head and at the rear of the plug on the walls; the latter molecules then disappear, and finally those in the plug head mix sufficiently to react. Painton and Mottola have shown experimentally that molecules in the head are the last to undergo reaction [18].

Plots of product concentration with time have their maximum at the point where the rate of product formation is equal to the rate of product dispersion. The plots obtained are in agreement with the findings of Růžička and Hansen [17]. For systems where product formation is highly favoured, this occurs when virtually all the sample has reacted. Under identical conditions, slow chemical reactions will take more time to reach this condition, and thus will have undergone more longitudinal dispersion. The simulation correctly

predicts that fast reactions are likely to give higher maximum product concentrations, and in less time (Fig. 4). Thus the observed peak height and shape is a consequence of the interaction of both physical and chemical dispersion and is crucially affected by flow rate and the rate of chemical reaction.

The order of reaction also has an effect in that the reaction $A + 2B = X$ requires twice as much B as the reaction $A + B = X$ to produce the same concentration of X. For the second-order reaction, under conditions where reagent is not greatly in excess, more mixing is obviously required for the reaction to go to completion. The maximum obtainable peak height is therefore lower for the second-order case (Fig. 7), and occurs after a longer time. Of course, the order of reaction has no effect on the dispersive processes, so that the product concentrations are identical once complete reaction has occurred and the same exponential decay curve is followed.

An increase in the ratio of reagent concentration (carrier stream) to sample concentration increases the reaction probability but has no effect on the dispersive processes. The results obtained are therefore similar in shape to those in Fig. 4, but the effect of doubling or halving the reagent concentration is more marked than that of altering the reaction rate constant by the same factor.

Effects of temperature and tubing internal diameter

As expected, an increase in temperature improves the rate of product formation (Fig. 8A). Not only are the chemical kinetics favoured by higher temperatures, but the viscosity decreases, which enhances axial mixing and so decreases the longitudinal dispersion of the sample.

Figure 8B shows the relationship between H_{max} and time for various tubing internal diameters at a constant flow rate of 1 ml min^{-1}. This is a difficult parameter to interpret because of its interactions with flow rate and sample

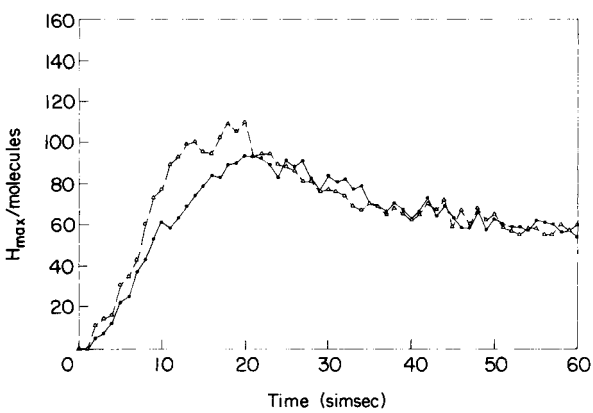

Fig. 7. Effect of order of reaction for $A + nB = X$ ($k_1 = 4$): (△) $n = 1$; (•) $n = 2$. Conditions as for Fig. 4.

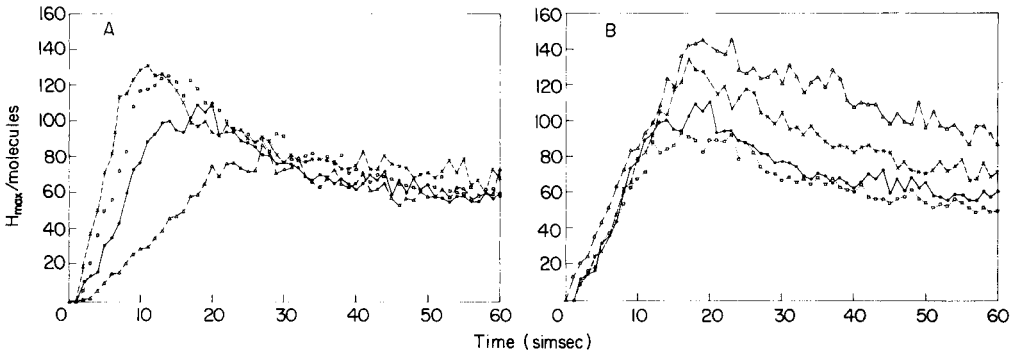

Fig. 8. Random walk model. (A) Effect of temperature (°C) for reaction $A + B = X$ (k_1 is temperature-dependent): (△) 10; (•) 20; (□) 30; (×) 40. (B) Effect of tubing internal diameter (mm) for reaction $A + B = X$ ($k_1 = 4$): (△) 0.2; (×) 0.5; (•) 0.8; (□) 1.0. Other conditions as for Fig. 4.

size. The larger the internal diameter of the tubing, the slower the flow velocity, and hence the higher the maximum found. Small bore tubes and low flow velocities are best suited to reactions requiring longer times, because dispersion is limited.

Conclusions

Obviously, there are limitations to a simulation which uses 10^3 molecules to represent 10^{23}, and the results are subject to statistical noise, as is evident in the figures shown. Nevertheless, the results obtained are much the same as those from a larger-scale calculation and are in substantial agreement with experiment, where experiments have been done. Some further experiments are suggested by the simulation. The complex interaction between temperature, viscosity, flow rate and diffusion coefficient is worthy of closer investigation; a fast diode-array spectrophotometer is currently being used to monitor the process of mixing in f.i.a.

The strengths of the model are that it is straightforward to adapt to other flow-injection processes and systems such as merging zones, extraction and pH-gradients, and that the visual output tends to be a more useful aid for most experimentalists than mathematical functions. Its major weaknesses are that it is time-consuming and that no theory of f.i.a. can take into account realistically the consequences of ill-matching connections, changes in internal diameter, sharp bends in the tubing and all the other factors which differentiate the ideal from the practical system. In practice, optimization is best achieved by some reliable empirical procedure such as the modified simplex method [15, 19] but the random walk (stochastic) model should be a useful addition to those theories which guide experimentalists.

We are grateful to Prof. W. van der Linden, Twente University, for his helpful suggestions and critical comments on the manuscript, and to Dr T. Lilley for assistance with the Apple computer colour graphics.

REFERENCES

1 A. Einstein, Ann. Phys., 17 (1905) 549.
2 J. C. Giddings, J. Chem. Ed., 35 (1958) 588.
3 J. C. Giddings, Dynamics of Chromatography, Part 1, Principles and Theory, Dekker, New York, 1965, pp. 26—35.
4 J. Růžička and E. H. Hansen, Anal. Chim. Acta, 99 (1978) 37.
5 J. T. Vanderslice, K. K. Stewart, A. G. Rosenfeld and D. J. Higgs, Talanta, 28 (1981) 11.
6 R. Tijssen, Anal. Chim. Acta, 114 (1980) 71.
7 J. M. Reijn, W. E. van der Linden and H. Poppe, Anal. Chim. Acta, 123 (1981) 229.
8 O. Levenspiel, Chemical Reaction Engineering, 2nd edn., Wiley, New York, 1972.
9 G. Taylor, Proc. R. Soc. London, Ser. A, 219 (1953) 186.
10 M. J. E. Golay and J. G. Atwood, J. Chromatogr., 186 (1979) 353.
11 C. C. Painton and H. A. Mottola, Anal. Chim. Acta, 158 (1984) 67.
12 A. G. Marshall, Biophysical Chemistry, Wiley, New York, 1978, pp. 140—159.
13 D. Betteridge, Anal. Chem., 50 (1978) 832A.
14 P. W. Atkins, "Physical Chemistry", Wiley, New York, 1978, p. 776.
15 D. Betteridge, T. J. Sly, A. P. Wade and J. E. W. Tillman, Anal. Chem., 55 (1983) 1292.
16 K. J. Laidler, Chemical Kinetics, Tata McGraw-Hill, New Delhi, 1978.
17 J. Růžička and E. H. Hansen, Flow Injection Analysis, Wiley, New York, 1981, p. 18.
18 C. C. Painton and H. A. Mottola, Anal. Chem., 53 (1981) 1713.
19 T. A. H. M. Janse, P. F. A. Van der Weil and G. Kateman, Anal. Chim. Acta, 155 (1983) 89.

Analytica Chimica Acta, 165 (1984) 237—244
Elsevier Science Publishers B.V., Amsterdam — Printed in The Netherlands

DETERMINATION OF UNSATURATED ACIDS BY BROMINATION USING DIRECT INJECTION ENTHALPIMETRY

J. R. MAJER* and M. ELLIS

Department of Chemistry, University of Birmingham, P.O. Box 363, Edgbaston, Birmingham B15 2TT (Great Britain)

(Received 6th October 1983)

SUMMARY

Unsaturated acids (*trans*-2-butenoic acid, 3-phenyl-2-propenoic acid and *trans,trans*-2,4-hexadienoic acid) in water or water-methanol are determined by direct injection enthalpimetry. The method is based on bromination with a bromate-bromide mixture injected into a hydrochloric acid solution of the analyte. The double-injection technique allows a reliable estimate of the temperature rise to be made. Linear regression equations are given for different ranges. The relative standard deviations are in the 1—5% range for concentrations down to 10^{-4} M. The method is also applicable to 1-propen-3-ol.

Hydrogenation is probably the most widely applicable method for the determination of unsaturation and is often regarded as the standard (reference) procedure [1]. It has the advantage of being unaffected by errors from substitution reactions, but rates of reaction vary widely and the standard methods can be time-consuming. Halogenation reactions also provide numerous methods of determining unsaturation, but possible substitution reactions and effects arising from the oxidising power of the halogens can be serious disadvantages. In general, chlorine is considered too reactive unless generated coulometrically and the methods most used are based on bromine, iodine chloride and iodine bromide. Compounds of relatively high reactivity may be titrated directly with a solution of a halogenating agent, the end-point being detected by the electrometric dead-stop method [2]. With less reactive substances, back-titration is needed; the reaction is often left to proceed at low temperature in the dark, in order to reduce side-reactions. Complete reaction may require several hours and catalysts such as mercury(II) ions may be needed [1, 3], but substitution rates are then also increased, so that optimisation of the conditions can be difficult.

The solutions of halogen or interhalogens used as titrants frequently suffer from instability or volatility and so require constant standardisation. Bromine was the first halogenating agent used for the determination of unsaturation; acetic acid or tetrachloromethane is the usual solvent. The stability of solutions of bromine in acetic acid can be improved by the addition of 0.1 M sulphuric acid and 0.0075 M pyridine [4]. Bromine solutions can also be

0003-2670/84/$03.00

stabilised by adding bromide to give tribromide ions. In one method, a small excess of bromate-bromide solution is added to the cooled solution of analyte in acetic acid made 0.24 M in hydrochloric acid, and is back-titrated iodimetrically. Direct titration, with mercury(II) as catalyst, has also been used, but both these methods give high results and an uncatalysed method is preferable for the determination of unsaturation in hydrocarbon mixtures [5].

Iodine interhalogen compounds are often used. The Wijs reagent [6], iodine chloride in acetic acid, is fairly stable and reactive and is widely used to determine unsaturation in unconjugated fatty oils. A 0.2 M solution of iodine bromide in acetic acid [7] is even more stable; precise results can be obtained for unconjugated aliphatic compounds, if the reaction proceeds for 30 min and the excess is back-titrated iodimetrically. With a large excess of reagent, quantitative addition to all three double bonds in conjugated unsaturated oils can be achieved [8]. Bromine chloride can be prepared by the action of excess of hydrochloric acid on a 2:1 bromide-bromate solution. The reaction is rapid [9] and has been used in the submicro determination of unsaturation [10] but if a mercury(II) catalyst is used, there is some substitution.

The present paper is concerned with the reaction of unsaturated acids in aqueous solution with bromine generated by the oxidation of bromide with bromate in dilute hydrochloric acid. The concentration of the unsaturated acid is estimated from the temperature rise, i.e., enthalpimetrically.

EXPERIMENTAL

Apparatus and solutions

A Dewar flask (ca. 67 mm in diameter, 240 mm deep) was used as a calorimeter. It was enclosed in a cylindrical metal container packed with expanded polystyrene granules. A teflon stopper supported a thermistor (Type F23D, STaC, Ltd.), a heater consisting of a 12-V, 5-W capless bulb cemented on to glass tubing, and a length of 1.5-mm bore teflon tubing for the introduction of solutions. A glass stirrer passed through the stopper and was driven by a variable-speed electric motor. The thermistor was connected as one arm of a Wheatstone bridge supplied with 2.52 V by a precision voltage reference source. The bridge was balanced by means of a 20-kohm, 10-turn potentiometer. The out-of-balance voltage from the bridge was amplified by a 725CN operational amplifier with a gain of approximately 500 and the output was recorded on a Servoscribe chart recorder (Smith Industries) set at a speed of 10 mm min^{-1}. The heater power supply was controlled by a 1.2—37-V, 5-A adjustable voltage regulator, the voltage and current through the heater bulb being measured with digital voltmeters. The reagent was injected from a bulb pipette.

The following solutions were prepared and diluted as necessary: aqueous 0.04 M and 0.1 M *trans*-2-butenoic acid (crotonic acid); 0.04 M in 1:1

methanol/water and 0.1 M in methanol solutions of 3-phenyl-2-propenoic acid (cinnamic acid); 0.04 M and 0.1 M solutions of *trans,trans*-2,4-hexadienoic acid (sorbic acid) in 1:1 methanol/water; aqueous 0.1 M *cis*-butendioic acid (maleic acid); aqueous 0.120 M 1-propen-3-ol (allyl alcohol); aqueous 0.1 M tris(hydroxymethyl)aminomethane (Tris base); 0.7 M sodium bromate in 3.5 M sodium bromide; and 0.14 M sodium bromate in 0.7 M sodium bromide.

Procedure

Double injections (2 ml each) of a solution containing 0.7 M sodium bromate and 3.5 M sodium bromide were made into 200-ml volumes of a series of solutions, each containing approximately 1 M hydrochloric acid and a range of concentrations (usually 2×10^{-2}—5×10^{-3} M) of *trans*-2-butenoic acid). Before the injections, the solution in the calorimeter was allowed to attain constant temperature (constant recorder deflection). Several (3—5) determinations were made at each concentration, the amplifier output being recorded on the 5-V range at a chart speed of 10 mm min^{-1}.

The Wheatstone bridge was balanced before the second injection of reagent. Tangents were drawn to the approximately linear portions of the recorder trace, before and after the injection of reagent, and the distance between them was measured. The difference in height between the deflections produced by the first and second injections was measured. The first deflection corresponds to the heat released by the oxidation of bromide, the bromination of the unsaturated acids and the dilution of the bromate/bromide mixture, while the second deflection corresponds only to the heat released by the oxidation of bromide and the dilution. Thus the difference between the two deflections is considered to correspond to the heat released by the bromination of the unsaturated acid.

A further series of determinations was done with concentrations over the range 4×10^{-3}—2×10^{-4} M *trans*-2-butenoic acid and the 0.14 M sodium bromate/0.7 M sodium bromide reagent. The signals were recorded with the recorder on the 1-V range with a chart speed of 10 mm min^{-1}.

Similar procedures were used for 3-phenyl-2-propenoic acid, *trans,trans*-2,4-hexadienoic acid, 1-propen-3-ol and *cis*-butendioic acid. For the first two, it was necessary to dissolve the samples in 1:1 methanol/water and to use 30 ml of methanol in the 200 ml of working solution, to ensure that the compound remained in solution.

Calibration

With 200 ml of distilled water in the calorimeter, the heater voltage was set at 12 V and the heater was switched on for varying times from 10 s to 1 min. The recorder was set to the 5 V range. A calibration curve of recorder deflection against heat input was constructed.

The apparatus was also calibrated by means of the protonation reaction of Tris base. Double injections (1 ml each) of concentrated hydrochloric acid

were made into solutions containing 0.02 M, 0.01 M or 0.005 M Tris base and a blank, with three replicates at each concentration. The recorder was set to the 5 V range. A calibration curve was constructed of recorder deflection against the heat input calculated from the known heat of protonation of Tris base.

RESULTS AND DISCUSSION

Production of the brominating reagent

The reaction of bromine with olefinic linkages has often been used to determine unsaturation in organic compounds. In the present work, the heat of reaction of the addition of bromine to unsaturated acids was used to estimate their concentration. Marik-Korda and Eckhart [11] injected a bromine solution to determine allyl alcohol and two pharmaceuticals (quinine and vasalgin) containing olefinic double bonds, obtaining linear relationships between the temperature rise and the concentration of analyte. They also noted a difference in the rates of reaction between *cis* and *trans* isomers, e.g., maleic and fumaric acids and also oleic and elaidic acids.

Because of the instability and volatility of solutions of bromine, it was decided to generate the bromine immediately before use. There are two possible methods, coulometric generation or the use of oxidising agents. The latter method was preferred, because it was more appropriate for enthalpimetry. In the production of bromine with an oxidising agent, the reagent produced depends on the relative concentrations of the bromide present and upon the acidity [12]. With a bromide/bromate ratio of 5:1, molecular bromine is produced

$$BrO_3^- + 5Br^- + 6H^+ = 3Br_2 + 3H_2O$$

With excess of bromide, the tribromide ion is produced

$$BrO_3^- + 8Br^- + 6H^+ = 3Br_3^- + 3H_2O$$

With a bromide/bromate ratio of 2:1 and an excess of hydrochloric acid, bromine monochloride is formed

$$BrO_3^- + 2Br^- + 3Cl^- + 6H^+ = 3BrCl + 3H_2O$$

To control the bromide/bromate ratio, either the bromide and bromate are placed in solution with the analyte and acid is injected, or a solution of bromide and bromate is injected into a solution of analyte containing an excess of hydrochloric acid. In the former method, the unsaturated acid would have to be neutralised to prevent premature release of bromine and so the second possibility was adopted.

In order to avoid the necessity for applying corrections for changes in heat capacity, it is usual in direct injection enthalpimetry (d.i.e.) to employ a volume ratio of reagent to analyte of $\geqslant$1:100. Therefore, for 200 ml of say 0.025 M unsaturation, 2 ml of a solution about 0.8 M in bromate and 4.0 M

in bromide would be necessary. The solubility of potassium bromate is too low for this to be achieved, but it is possible to make a solution 0.7 M in bromate and 3.5 M in bromide from the sodium salts.

Selection of optimum conditions and statistical data

The bromate/bromide solution (2 × 2 ml) was injected into 200-ml portions of solutions 0.01 M in *trans*-2-butenoic acid and containing various excesses of hydrochloric acid. The recorder deflections were all of the same order, but the outputs for solutions containing 0.5 M hydrochloric acid were noticeably rounded compared with those for the 0.75, 1.0 and 1.5 M hydrochloric acid solutions. This suggested that the rate of reaction was reduced in the 0.5 M acid, and it was decided to use 1 M hydrochloric acid.

After the analyte solution had been placed in the Dewar flask, it was usually necessary to allow a short period of time to enable the solution to approach thermal equilibrium with the calorimeter. When the 5-V range of the recorder was used, 5 min was usually sufficient, but 15 min was often required for the 1-V range. If the injections were made at a time when the temperature of the solution was still falling, the recorder traces were easier to measure.

The linear regression of nett recorder chart deflection on molar concentration was calculated for the range of each compound examined by the least-squares method. Detailed results for *trans*-2-butenoic acid are given in Table 1. The formulae of the regression lines for all compounds studied are given in Table 2. The correlation coefficients and their 99% confidence limits [13] are also listed. It is evident from the correlation coefficients that the relationship between nett chart deflections and the concentration of analyte is close to being linear over the range of concentrations examined. The distributions of the experimental results for the other unsaturated compounds examined were of a very similar form to that for *trans*-2-butenoic acid. The lower limits

TABLE 1

Trans-2-butenoic acid (crotonic acid)

Concentration (M)	Nett deflection D (mm)				
2×10^{-2}	120.8	119.0	120.2	121.2	
	124.4	121.8			
1.5×10^{-2}	95.0	94.4	92.4	90.6	
	89.8				
1.0×10^{-2}	60.6	60.2	59.6	63.5	
	62.0	62.2	60.3	65.0	
5×10^{-3}	32.5	31.5	32.1	31.9	
	32.0	31.2			
2.5×10^{-3}	14.3				
1×10^{-3}	5.3				
Blank	−1.9	−1.5	−2.4	−2.9	−3.2

of concentration which can be calculated with acceptable accuracy were taken as those for which the 95% confidence limits [13] would be ± one third of the calculated values, each nett chart deflection used being the mean of three determinations. These limits are given in Table 2 together with relative standard deviations for each range of each compound. The latter were calculated from the deviations from the linear regression lines and expressed as a percentage of the mean values of chart deflections.

Marik-Korda and Eckhart [11] did not give any statistical information about their results. Rogers [14] reported standard deviations of 0.9—2.3% for several olefins, and Rogers and Sasiela [15] reported 1.3—3.2% for various allylic and vinyl compounds, all determined by hydrogenation. In comparison, Braae [2] reported a precision of about 3% for several monoolefins determined by direct titration with a bromine solution in carbon tetrachloride with mercury(II) chloride as catalyst and dead-stop electrometric end-point detection. Walisch and Ashworth [16] obtained a reproducibility of ±0.3% for the microdetermination of unsaturated compounds by cumulative coulometric titration. Belcher and Fleet [10] reported average deviations of 0.2—1.54% for the submicro determination of olefinic unsaturation with bromine chloride, which was back-titrated iodimetrically. In the present work, the standard deviations for most determinations were in the 2—3% range.

Because of the low solubility of 3-phenyl-2-propenoic acid, the reaction was done in aqueous methanol. The blank determinations showed no evidence of any interaction between the methanol and the bromine. The relative standard deviation of the results for this acid at the 5-V range was 8.5%, which is considerably higher than the values for the other compounds. This is probably due to the lower solubility of this substance. In general, the relative standard deviations on the 1-V range are higher than those on the 5-V range.

Trans,trans-2,4-hexadienoic acid also has limited solubility in water and was dissolved in 1:1 water/methanol to make the 0.1 M stock solution. A further 15 ml of methanol was added before injection of hydrochloric acid. In order to examine the possibility of determining other water-soluble unsaturated compounds, the bromination of 1-propen-3-ol was investigated. No methanol was required to enhance solubility and the reaction was sufficiently fast to give good recorder deflections. Concentrations higher than those listed in Table 2 gave off-scale deflections for both these compounds.

In the case of *cis*-butendioic acid, injection of hydrochloric acid into a solution 0.01 M in the acid, 0.02 M in bromate and 0.1 M in bromide, produced a chart trace in which the initial step (production of bromine) was followed by a very slow rise caused by the slow bromination. When the solution was neutralised with sodium hydroxide before the injection of hydrochloric acid, the temperature continued to increase after the initial jump at a noticeably higher rate and was still rising after 10 min. Thus the bromination of *cis*-butendioic acid took place very slowly, which agrees with the work of Critchfield [17] who suggested that because of the depletion of the π-electrons

TABLE 2

Regression lines and analytical data for the unsaturated compounds tested

Compound	Concentration range (M)	Regression line	Corr. coeff.	99% conf. limits	LD[c] (M)	RSD (%)
Trans-2-butenoic acid	1×10^{-3}—2×10^{-2} [a]	$D = -0.444 + 6146.3C$	0.999	0.997—0.9996	1.3×10^{-3}	3.3
	2×10^{-4}—4×10^{-3} [b]	$D = -2.607 + 31153.7C$	0.998	0.997—0.999	2.8×10^{-4}	4.6
3-Phenyl-2-propenoic acid	2.5×10^{-3}—2×10^{-2} [a]	$D = -1.653 + 5810.9C$	0.995	0.9827—0.9988	3.0×10^{-3}	8.5
	1×10^{-3}—4×10^{-3} [b]	$D = -0.9299 + 29455.8C$	0.9998	0.999—1.000	1.8×10^{-4}	2.0
Trans,trans-2,4-hexadienoic acid	2.5×10^{-3}—1.5×10^{-2} [a]	$D = -1.683 + 7312.4C$	0.9996	0.9984—0.9999	6.9×10^{-4}	2.3
	1×10^{-3}—4×10^{-3} [b]	$D = -1.887 + 34216.7C$	0.9995	0.9976—0.9999	1.9×10^{-4}	3.1
1-Propen-3-ol	3×10^{-3}—1.2×10^{-2} [a]	$D = -1.373 + 7806.7C$	0.9999	0.9994—1.000	3.6×10^{-4}	1.3
	6×10^{-4}—3.6×10^{-3} [b]	$D = -3.152 + 38654C$	0.9994	0.9978—0.9998	1.9×10^{-4}	2.8

[a] 5-V range. [b] 1-V range. [c] Limit of determination with relative standard deviation (see text).

by the two electrophilic groups in the undissociated form, the free acid brominates very slowly. It is not possible to determine *cis*-butendioic acid by bromination and the d.i.e. method, but it is possible to determine unsaturated mono-acids in its presence.

REFERENCES

1 S. T. Hirozawa, in I. M. Kolthoff and P. J. Elving (Eds.), Treatise on Analytical Chemistry, Part II, Vol. 14, Wiley, New York, 1971.
2 B. Braae, Anal. Chem., 21 (1949) 1461.
3 B. Hubl, J. Soc. Chem. Ind. London, 3 (1884) 641.
4 ASTM 1966 Book of ASTM Standards, Designation D1541-60.
5 E. G. Unger, Anal. Chem., 30 (1958) 375.
6 J. J. A. Wijs, Ber. Dtsch. Chem. Ges. A, 31(1) (1898) 750.
7 J. Z. Hanus, Untersuch. Nahr.-u. Genussm, 4 (1901) 913.
8 J. D. Mikusch and C. Frazier, Ind. Eng. Chem. Anal. Ed., 13 (1941) 782.
9 K. Bürger and E. Schulek, Talanta, 7 (1960) 46.
10 R. Belcher and B. Fleet, J. Chem. Soc., (1965) 1740.
11 P. Marik-Korda and E. Eckhart, J. Therm. Anal., 17 (1979) 171.
12 E. Schulek, K. Burger and J. Laszlowsky, Talanta, 7 (1960) 51.
13 G. W. Snedecor and W. G. Cochran, Statistical Methods, 7th edn., Iowa State University Press, 1980, p. 169.
14 D. W. Rogers, Anal. Chem., 43 (1971) 1468.
15 D. W. Rogers and R. J. Sasiela, Talanta, 20 (1973) 232.
16 W. Walisch and M. R. F. Ashworth, Mikrochim. Acta., (1959) 497.
17 F. E. Critchfield, Anal. Chem., 31 (1959) 1406.

Analytica Chimica Acta, 165 (1984) 245—256
Elsevier Science Publishers B.V., Amsterdam — Printed in The Netherlands

EXTRACTION OF ORGANIC ACIDS BY ION-PAIR FORMATION WITH TRI-n-OCTYLAMINE
Part 3. Influence of Counter-ion and Analyte Concentration

M. PUTTEMANS, L. DRYON and D. L. MASSART*

Pharmaceutical Institute, Vrije Universiteit Brussel, Laarbeeklaan 103, B-1090 Brussels (Belgium)

(Received 9th April 1984)

SUMMARY

Various acids of pharmaceutical interest are extracted into chloroform as ion-pairs with tri-n-octylamine. The influence of the counter-ion concentration on the extraction efficiency is investigated as a function of the concentration of the analyte. Side-reactions such as the formation of adducts take place and permit high recoveries to be obtained even for hydrophilic substances.

As shown in earlier papers [1—3], acids can be extracted into chloroform by ion-pair formation with tri-n-octylamine (TnOA). In Part 1 [3], the effects of the pH and the ionic strength of the extraction medium were discussed. This paper describes the influence of the counter-ion on the extraction yield at different concentration levels of the analyte. The above-cited effects are evaluated as a function of the structure of the extracted substances.

The extraction recovery is evaluated for a variety of acids of pharmaceutical interest, to investigate whether or not the extraction scheme developed for dyes [2, 4, 5] is also applicable for other compounds.

EXPERIMENTAL

Apparatus and reagents

A Perkin-Elmer Hitachi 200 spectrophotometer was used with 10- or 50-mm quartz cells (Hellma). The pH was measured with an Orion 601 Ionalyser and a combined glass/calomel electrode. The shaker was from Orlando Valentini (Milano, Italy).

The following compounds were used as received: 3-hydroxybenzoic acid, 2,5-dihydroxybenzoic acid and potassium sorbate (all analytical grade, Fluka); 4-hydroxybenzoic acid (99% pure), 3,4-dihydroxybenzoic acid (97% pure), tri-n-octylamine (Aldrich Europe); sodium benzoate (analytical grade), cinnamic acid and its hydroxy derivatives (reagent grade), phthalic acid (analytical grade) and gallic acid (pure) (all Merck); acetylsalicylic acid,

0003-2670/84/$03.00

sodium *p*-aminosalicylate, nicotinic acid, potassium guaiacol sulfonate (thiocol) (all pharmaceutical grade products, Bios-Coutelier, Brussels); sodium thiomersal (pharmaceutical grade, Federa, Brussels); indomethacine (pharmaceutical grade, Merck, Sharp & Dohme); sodium saccharin (pharmaceutical grade, BDH). Penicillins were pharmaceutical grade (Beecham Belgium and Bristol Belgium).

All other reagents were analytical-grade products (Merck). Chloroform was freed from ethanol and saturated with water by shaking with an equal volume of water. The buffers were prepared from sodium phosphates. All buffer solutions were saturated with chloroform. The TnOA solutions were prepared in chloroform and were saturated with water.

Extraction

Extractions were done in glass, screw-capped, centrifuge tubes with equal volumes (10 ml) of aqueous and organic phases. The aqueous phase, consisting of a solution of the acid at a given concentration in a phosphate buffer of ionic strength 0.1 M, was shaken for 30 min at room temperature with the TnOA solution in chloroform. After phase separation, the concentration of the acid was determined in the aqueous phase by u.v. photometry. Each partition experiment was conducted in triplicate.

THEORY

The following equilibria compete in the distribution of an acid HX between an aqueous (subscript w) and an organic (subscript o) phase, the latter containing an amine A [1, 3].

1. Dissociation of HX

$$HW_w \rightleftharpoons H_w^+ + X_w^- \quad (1)$$

The acidity constant is $K_a = [H^+]_w[X^-]_w/[HX]_w$

2. Distribution of HX

$$HX_w \rightleftharpoons HX_o \quad (2)$$

The liquid-liquid distribution constant of HX is $K_d = [HX]_o/[HX]_w$

3. Extraction of X^- by ion-pair formation with A

$$A_o + H_w^+ + X_w^- \rightleftharpoons AHX_o \quad (3)$$

The conditional ion-pair extraction constant is $K_{ex} = [AHX]_o/[A]_o[H^+]_w[X^-]_w$. The exact ion-pair extraction constant is E_{ahx}, and if no side-reactions occur,

$$K_{ex} = E_{ahx}$$

4. Formation of amine adducts

$$nA_o + H_w^+ + X_w^- \rightleftharpoons AHX \cdot A_{n-1} \quad (4)$$

The extraction constant when amine adducts are formed is K_{add} =

$[AHX \cdot A_{n-1})]/[A]^n[X^-]_w[H^+]_w$. The formation of amine adducts can also be described by $K_{AHX \cdot A_{n-1}}$, the stability constant for an adduct of AHX containing $(n-1)$ moles of A. The stability constant is defined by

$$K_{AHX \cdot A_{n-1}} = [AHX \cdot A_{n-1}]_o/[AHX]_o[A]_o^{n-1} \quad (5)$$

5. Formation of acid adducts

$$A_o + H_w^+ + X_w^- + mHX_o \rightleftharpoons AHX \cdot HX_{mo} \quad (6)$$

The extraction constant when acid adduct formation takes place is $K_{aa} = [AHX \cdot HX_m]_o/[A]_o[H^+]_w[X^-]_w[HX]_o$.

6. Dimerization of ion-pairs

$$2AHX_0 \rightleftharpoons A_2H_2H_{20} \quad (7)$$

The dimerization constant of the ion-pair AHX is $K_{dim} = [A_2H_2X_2]_o/[AHX]_o^2$. The extraction efficiency is expressed either as a % or as a distribution ratio D: D = total concentration in the organic phase/total concentration in the aqueous phase.

RESULTS AND DISCUSSION

Effect of the TnOA concentration

The relation between the distribution ratio D and the counter-ion concentration, $[A]_o$, is given [3] by

$$D = K_{ex}[H^+]_w[A]_o \quad (8)$$

when no side-reactions take place. Equation 8 is obtained from Eqn. 3. If undissociated acid HX is present, its liquid—liquid distribution will influence the distribution ratio

$$D = K_aK_{ex}[A]_o/(1 + K_a/[H^+]_w) + K_d/(1 + K_a/[H^+]_w) \quad (9)$$

Equation 9 is obtained from Eqns. 1—3. As described by earlier workers [6—9], long-chain amines can form adducts which increase the efficiency of the extraction. If amine adducts are formed, the relation between the distribution ratio and the amine concentration is given by

$$\log D = n \log [A]_o + \log [K_aK_{add}/(1 + K_a/[H^+]_w)] \quad (10)$$

Equation 10, obtained from Eqns. 1, 2 and 4, is valid when the extraction of undissociated HX is negligible.

Extraction yields were determined for various acids at six counter-ion concentrations ranging from 0 to 0.1 M. The recoveries, expressed as distribution ratios, were evaluated as a function of the counter-ion concentration ($[A]_o$) by fitting them to Eqns. 9 and 10. The values of the factors a and b of the regression line $y = ax + b$ were calculated by linear regression (least squares). Depending on the variables that were entered (D or $\log D$, $[A]_o$ or $\log [A]_o$), linear plots were obtained the slopes and intercepts of which yield

a number of constants. A plot of D vs. $[A]_o$ results in a slope of $K_a K_{ex}/(1 + K_a/[H^+]_w)$, from which K_{ex} may be calculated if K_a is known. The K_a values used were taken from the literature [10—25]. In contrast, a logarithmic plot (log D vs. log $[A]_o$) has a slope of n, the number of moles of amine in the complex formed, for 1 mole of HX, and an intercept of log $[K_a K_{add}/(1 + K_a/[H^+]_w)]$. Again, K_{add} may be calculated if K_a is known. These calculated values are listed in Table 1, which also contains the percentage recoveries obtained with 0.1 and 0.01 M TnOA. From Table 1, it can be seen that the logarithm of K_{ex} is highly correlated with the % extracted with 0.01 M TnOA ($r = 0.97$).

If one considers the logarithmic plot, it appears that in the group of benzoic acid and its hydroxy derivatives, only the derivatives substituted on position 3 or 4 form amine adducts, which means that n is larger than 1. If a hydroxyl function is present on both positions 3 and 4, a much higher value of n is obtained ($n = 4.1$). The nature of the substituent in position 4 is important: if an amino group is substituted on salicylic acid, a value of 0.79 is obtained for n. This corresponds to an increase by 0.46. Substitution of a hydroxyl group on position 4 of benzoic acid raises n from 0.30 to 1.34. Substitution of a hydroxyl group on position 5 of salicylic acid raises n from 0.33 to 0.98. With cinnamic acid, the same phenomenon is observed; the 4-hydroxy derivative has $n = 1.57$, whereas the other derivatives all have n values less than 1. In contrast to the benzoic acid derivatives, the 3-substituted cinnamic acid derivative does not differ significantly from the other hydroxy derivatives.

In Table 1, the log K_{ex} column also has values given in parentheses. These were calculated by Eqn. 8 whereas the other values were calculated from Eqn. 9. The slope of the graph D vs. $[A]_o$ is equal to $K_a K_{ex}/(1 + K_a/[H^+]_w)$ which is also equal to $K_a K_{ex}[H^+]_w/(K_a + [H^+]_w)$. If $[H^+]_w$ can be neglected compared to K_a, the slope becomes $K_a K_{ex}[H^+]_w/K_a = K_{ex}[H^+]$, which is the same as Eqn. 8. The two values of log K_{ex} (Table 1) are very similar, which indicates that, for the substances investigated, it is possible to neglect $[H^+]_w$ compared to K_a (pH 5.5).

Table 1 also contains extraction data for a heterogeneous group of acids, of which only indomethacine forms amine adducts. For thiomersal, an organomercury antiseptic, linearity of D vs. $[A]_o$ and log D vs. log $[A]_o$ plots was observed up to 0.01 M TnOA. Higher concentrations had no effect on the extraction yield and gave similar, very high, recoveries. Acceptable extraction yields were obtained for all these compounds except for gallic acid (3,4,5-trihydroxybenzoic acid). Compared to the other hydroxy derivatives of benzoic acid, substitution by one more hydroxy group drastically changes the extraction characteristics. With regard to 3,4-dihydroxybenzoic acid, log K_{ex} decreases from 5.68 to 4.28 and n falls from 4.12 to 0.10, which means that the extraction is much less effective and that the extracted acid forms a different complex with the counter-ion.

The effectiveness of the TnOA extraction was also investigated for a

number of penicillins. The extraction conditions used (pH 5.5) are of practical interest because penicillins are labile substances and are most stable in solutions at pH 5—7 [11]. Lower or higher pH values facilitate hydrolysis reactions. Extractions were done at pH 5.5 or 6.5 with TnOA concentrations of 0—0.1 M. For all the compounds investigated, a linear relationship was obtained between D and the amine concentration (or their logarithms) between 0 and 0.01 M TnOA. At pH 5.5 some penicillins show linearity up to 0.1 M TnOA but for others (benzylpenicillin, cloxacillin, dicloxacillin, propicillin, clometocillin, phenoxymethylpenicillin and oxacillin), no increase in extraction yield is obtained when the counter-ion concentration is increased from 0.01 to 0.1 M. At pH 6.5, this conclusion is no longer valid for benzylpenicillin, cloxacillin and dicloxacillin. When the data obtained at pH 5.5 and 6.5 are compared, it can be seen that n is higher at pH 6.5 than at pH 5.5 for most of these compounds.

In order to confirm the different composition of the extracted complexes at different degrees of ionization, the 3-hydroxy, 4-hydroxy, and 3,4-dihydroxy derivatives of benzoic acid, which very clearly formed amine adducts at pH 5.5, were extracted at pH 2.5 with counter-ion concentrations of 0—0.1 M. The effect was most important for the 3,4-dihydroxy derivative: the number of moles of amine in the complex fell from 4.12 to 1.48. The other two acids showed only small changes, from 1.47 to 1.44 for the 3-hydroxy derivative and from 1.34 to 1.30 for the 4-hydroxy derivative. This confirms the conclusion already reached for the penicillins that at a higher degree of ionization, higher amine adducts are formed.

From the data given in Table 1, it can be deduced that the extraction characteristics depend strongly on the structure of the analyte investigated. It is well known [12] that the solubility of the analyte influences the extraction yield. The extraction constants given in Table 1 are compared with log P values found in the literature; P is the octanol/water distribution constant, a quantitative measure of the hydrophobicity of the analyte. As can be seen in Table 2, only the correlation between log K_{ex} and log P is significant. Correlations were calculated for various groups: benzoic acid and its hydroxy derivatives, penicillins, various acids (sorbic acid, indomethacine, ..., phthalic acid), benzoic acid plus its hydroxylated derivatives plus cinnamic acid, sorbic acid and indomethacine. Finally, the correlation was also calculated for the entire group of substances.

The most significant correlation is observed for benzoic acid and its hydroxy derivatives (p = 0.01), both alone and together with a few other acids. For the penicillins, a significant correlation is obtained at the 5% level, whereas the significance is only at the 10% level for the whole group. This indicates, as expected, that correlation is highest when the solutes are closely related. For benzoic acid and its hydroxy derivatives, it can be seen that log K_{add} is not correlated with log P, whereas log K_{ex} is highly correlated (p = 0.01) with log P, which means that log P can be used to predict the efficiency of the ion-pair extraction.

TABLE 1

Extraction characteristics of acids at pH 5.5
(K_{ex}: ion-pair extraction constant calculated by Eqn. 9; values in parentheses were calculated by Eqn. 8; K_{add}: amine adduct extraction constant calculated by Eqn. 10; Penicillins were also extracted at pH 6.5; the corresponding characteristics of Eqns. 9 and 10 are given in square brackets; Log P is the octanol/water distribution constant)

Name	Characteristics of Eqn. 9: $D = f([A]_o)$			Characteristics of Eqn. 10: $\log D = f(\log [A]_o)$			Recovery (%) (M TnOA)		Log P	Ref.
	Slope	Intercept	log K_{ex}	Slope	Intercept	log K_{add}	10^{-2}	10^{-1}		
Benzoic Acid	53.34	2.22	7.25 (7.23)	0.30	1.17	6.69	81.7 ± 3.4	87.8 ± 1.2	1.87	13
Salicylic Acid	3392.05	17.69	9.03 (9.03)	0.33	2.29	7.79	98.3 ± 0.2	98.4 ± 0.3	2.26	14
Acetylsalicylic Acid	43.57	1.93	7.14 (7.14)	0.34	1.14	6.64	79.9 ± 0.5	85.5 ± 2.0	1.23	14
p-Aminosalicylic Acid	73.23	0.83	(7.36)	0.79	1.78		66.7 ± 1.4	88.8 ± 2.8		
2-Hydroxybenzoic Acid	4.86	0.01	6.23 (6.19)	1.34	1.27	6.80	3.5 ± 0.4	48.5 ± 0.6	1.15	15
3-Hydroxybenzoic Acid	9.37	0.03	6.49 (6.47)	1.47	1.57	7.09	4.7 ± 0.9	47.6 ± 0.4	2.50	13
3,4-Dihydroxybenzoic Acid	1.50	0.02	5.72 (5.68)	4.12	5.01	10.55	0.0 ± 0.0	11.6 ± 0.6		
2,5-Dihydroxybenzoic Acid	68.17	0.01	7.33 (7.33)	0.98	1.80	7.30	40.1 ± 0.3	87.2 ± 0.1	1.74	16
Cinnamic Acid	662.09	7.16	8.35 (8.32)	0.74	2.69	8.23	95.4 ± 0.1	98.6 ± 0.4	2.37	17
2-Hydroxycinnamic acid	20.09	0.02	(6.80)	0.88	1.08		14.4 ± 0.3	66.7 ± 0.7		
3-Hydroxycinnamic acid	20.28	0.08	(6.81)	0.90	0.98		8.7 ± 0.7	66.4 ± 0.4		
4-Hydroxycinnamic acid	53.20	0.56	(7.23)	1.57	2.22		12.1 ± 1.8	82.7 ± 0.4		
3,4-Dihydroxycinnamic acid	4.01	0.04	(6.10)	0.83	0.48		5.8 ± 0.5	30.3 ± 1.2		
Saccharin	130.12	9.27	7.61 (7.61)	0.23	1.64	7.14	94.5 ± 0.6	95.7 ± 2.3	0.91	18
Phthalic Acid	144.58	3.14	7.66 (7.66)	0.66	1.99	7.49	86.5 ± 0.9	94.4 ± 1.4	1.66	13
Nicotinic Acid	57.70	0.27	7.35 (7.26)	0.94	1.78	7.37	49.0 ± 0.2	85.6 ± 0.8	−0.20	19
Gallic Acid	0.06	0.01	4.31 (4.28)	0.10	1.65	7.18	0.5 ± 0.1	1.7 ± 1.0	0.70	20
Thiocol	32.87	0.12	(7.02)	0.80	1.34		36.5 ± 0.3	77.1 ± 0.4		
Thiomersal	26332.90	5.48	(9.92)	0.11	2.01		98.6 ± 0.4	98.5 ± 0.8		
Sorbic Acid	235.70	0.70	7.94 (7.87)	0.83	2.21	7.78	76.8 ± 0.6	96.0 ± 0.1	1.33	20
Indomethacin	103.02	0.49	(7.51)	1.85	0.81		65.1 ± 0.7	91.1 ± 0.6	3.08	21
Benzylpenicillin	1859.81	2.70	8.77 (8.77)	0.18	1.43	6.93	92.0 ± 0.2	92.1 ± 0.7	1.83	22
	[434.44]	[2.66]		[0.68]	[2.31]		[92.8 ± 1.1]	[98.0 ± 1.2]		

Cloxacillin	**2924.60**	**3.59**	**8.97 (8.97)**	**0.11**	**1.65**	**7.15**	**96.8 ± 0.5**	**96.2 ± 0.5**	**2.43**	**23**
	[68.32]	[5.16]		[0.10]	[1.17]		[87.8 ± 0.6]	[92.2 ± 0.7]		
Dicloxacillin	770.02	44.73	8.39 (8.39)	0.08	2.12	7.62	98.9 ± 0.5	99.1 ± 1.4	2.91	23
	[254.21]	[7.09]		[0.32]	[1.78]		[88.0 ± 0.8]	[93.1 ± 0.5]		
Ampicillin	24.44	0.01	6.89 (6.89)	1.02	1.45	6.96	23.1 ± 0.8	71.3 ± 0.6	1.35	24
	[17.71]	[0.04]		[1.22]	[1.50]		[13.7 ± 1.0]	[63.8 ± 1.5]		
Methicillin	557.30	7.17	8.25 (8.25)	0.32	1.97	7.47	94.6 ± 1.4	98.5 ± 1.6	1.30	23
	[98.58]	[1.70]		[0.49]	[1.53]		[79.6 ± 0.4]	[91.4 ± 0.4]		
Carbenicillin	98.10	0.33	(7.49)	0.85	2.10		84.4 ± 0.7	90.7 ± 1.8		
	[71.77]	[0.12]		[1.31]	[2.17]		[22.1 ± 1.0]	[87.3 ± 1.1]		
Amoxycillin	0.09	0.00	4.47 (4.45)	0.18	1.77	7.29	0.5 ± 0.2	1.4 ± 0.7	0.87	24
	[0.00]	[0.00]					[0.0 ± 0.0]	[0.0 ± 0.0]		
Epicillin	18.07	0.11	(6.76)	0.65	0.87		22.4 ± 3.0	66.8 ± 0.4		
	[13.90]	[0.05]		[1.03]	[1.25]		[17.8 ± 0.3]	[57.2 ± 1.7]		
Bayercillin	1011.54	15.15	8.51 (8.51)	0.23	2.12	7.62	98.3 ± 0.4	97.6 ± 0.7	2.70	23
	[1118.78]	[4.35]		[0.19]	[1.52]		[91.1 ± 0.5]	[93.4 ± 0.5]		
Phenoxymethylpenicillin	21096.75	4.44	9.83 (9.82)	0.12	1.95	7.45	98.4 ± 0.1	98.3 ± 0.3	2.03	25
	[1138.25]	[3.17]		[0.33]	[1.80]		[89.4 ± 1.4]	[92.8 ± 0.5]		
Clometocillin	499864.99	1295.00	(11.20)	0.62	4.91		97.8 ± 0.4	98.8 ± 0.6		
	[3222.72]	[6.08]		[0.14]	[1.64]		[92.1 ± 1.1]	[94.7 ± 0.5]		
Oxacillin	198667.20	0.33	10.80 (0.80)	1.39	6.48	11.98	99.0 ± 0.1	100.0 ± 0.1	2.38	25

TABLE 2

Correlation between log P values from literature and experimental constants (significance levels [26] are given in parentheses)

	N	Correlation between log P and						
		log K_{ex}	log E_{ahx}	log K_{add}	log $K_{AHX \cdot A}$	log K_{dim}	log K_{aa}	m
Benzoic acid and hydroxy derivatives = A	7	0.974 (1%)	0.797 (5%)	−0.079	0.961 (1%)	0.749 (10%)	0.582	0.333
A + cinnamic acid, sorbic acid, indomethacin	10	0.756 (2%)		0.460				
Penicillins	9	0.670		0.287				
All acids investigated	24	0.369 (10%)						

Correlations were also calculated between log P and the constants given in Tables 4 and 5 (see below). From the data obtained (Table 2), it can be concluded that log P is correlated with log E_{ahx} (p = 0.05) and log K_{dim} (p = 0.10). It is also observed that log $K_{AHX \cdot A}$ (the stability constant of the adduct AHX·A) is highly correlated with log P (p = 0.01). In this case, a negative slope is obtained for the regression line, meaning that more stable amine adducts are formed when the analyte is less hydrophobic, which confirms the earlier conclusions.

Effect of the HX concentration

As the above results indicated that the extracted complex usually contains more acid than amine, (i.e., $n < 1$), further tests were done to see if the complexes formed were indeed acid adducts, which would explain the higher acid content of the complex. Accordingly, the effect of increasing acid concentration (initial concentrations in the aqueous phase of 10—1000 mg l^{-1}) on the distribution ratio at constant pH and counter-ion concentration (0.1 M) was investigated for benzoic acid and its hydroxy derivatives. The relation between the distribution ratio and the HX concentration in the organic phase is given by

$$\log D = m \log [HX]_o + \log (K_{aa}[H^+]_w[A]_o) \quad (11)$$

The concentration of HX in the organic phase was calculated from K_a, K_d [3] and $[H^+]_w$.

The results listed in Table 3 indicate that the extraction yield is increased when higher concentrations of analyte are present. As given by Eqn. 11, the slope and the intercept of the plot of log D vs. log $[HX]_o$ permit the calculation of the number of moles of acid in the complex formed as well as the equilibrium constant. The values of m and log K_{aa} are given in Table 4. For an extraction at pH 5.5, the value of m decreases as a function of the

TABLE 3

Extraction efficiency as a function of the initial concentration in the aqueous phase (pH 5.5, ionic strength 0.1 M, 0.1 M TnOA)

	Extraction (%) at various initial concentrations (mg l^{-1})					
	10	100	250	500	750	1000
Benzoic acid	87.75 ± 1.15	99.17 ± 0.32	99.32 ± 0.44	99.94 ± 0.09	99.98 ± 0.03	99.07 ± 0.16
Salicylic acid	98.38 ± 0.47	98.93 ± 0.15	98.93 ± 0.55	99.87 ± 0.23	99.78 ± 0.08	99.47 ± 0.23
3-Hydroxybenzoic acid	48.47 ± 0.57	51.96 ± 0.28	55.82 ± 0.34	61.26 ± 1.93	64.95 ± 0.15	68.09 ± 0.35
3-Dihydroxybenzoic acid	47.56 ± 0.43	51.30 ± 0.17	54.20 ± 0.10	63.30 ± 0.20	68.13 ± 0.35	72.03 ± 0.40
3,4-Dihydroxybenzoic acid	11.58 ± 0.55	17.93 ± 0.81	18.23 ± 0.60	23.23 ± 0.75	30.18 ± 1.34	31.27 ± 0.67
2,5-Dihydroxybenzoic acid	87.18 ± 0.13	88.80 ± 0.17	89.40 ± 0.17	90.50 ± 0.17	89.73 ± 0.0	90.73 ± 0.23

TABLE 4

Formation of acid adducts

Acid	m	log K_{aa}	Acid	m	log K_{aa}
Benzoic acid	1.56	3.43	4-Hydroxybenzoic acid	0.29	−4.42
Salicylic acid	0.69	0.73	3,4-Dihydroxybenzoic acid	0.07	−4.95
3-Hydroxybenzoic acid	0.28	−4.55	2,5-Dihydroxybenzoic acid	0.68	−3.46

decreasing acidity constant of the extracted analyte. This means that the number of moles of acid in the complex diminishes as the fraction of undissociated acid in the solution decreases. The values of log K_{aa} given in Table 4 indicate that the formation of acid adducts at pH 5.5 is negligible except for benzoic acid and salicylic acid. This is easily explained by the fact that benzoic acid and salicylic acid are extracted to a significant, but low, extent by chloroform, which is not the case for the other acids.

As already stated [3], the optimum yield for the ion-pair extraction is obtained at a pH of pK_a + (1—1.5). Under these circumstances, the degree of ionization is 90—97%, which allows the formation of acid adducts.

Combined effects of counter-ion and analyte concentration

The determination of the distribution ratio at different counter-ion and analyte concentrations enables constants to be calculated for ion-pair extraction, amine adduct formation and the formation of dimers or higher associates [6—9]. Partition experiments were done for benzoic acid and its hydroxy derivatives at TnOA concentrations of 0.01—0.1 M and analyte concentrations of 0.001—0.01 M. According to the principles extensively described by Modin and co-workers [6—8] and Schroder-Nielsen [9], the constants obtained for ion-pair formation (E_{ahx}), dimerization (K_{dim}) and adduct formation (formation of AHX·A) are given in Table 3. The constants given are only approximate because the formation of higher adducts (e.g., AHX·A2,..), tetramers or adducts such as $A_2H_2X_2 \cdot A$ were not taken into account. The main aim of this study was to investigate the effect of the structure of the extracted anion on the extraction recovery and not to determine the equilibrium constants of all the side-reactions that might occur.

The ion-pair extraction constant (K_{ex}, Table 1) is highly correlated with E_{ahx} (r = 0.98); K_{ex} is a conditional constant which is valid only in the absence of side-reactions, whereas E_{ahx} takes into account possible side-reactions. The difference between log K_{ex} and log E_{ahx} reflects the occurrence of side-reactions. For benzoic acid, salicylic acid and 2,5-dihydroxybenzoic acid, the log E_{ahx} values are 24.7, 21.4 and 25.5%, respectively, lower than log K_{ex}. These values are 35.9, 41.2 and 54.9% for the 3-hydroxy, 4-hydroxy and 3,4-dihydroxy derivatives. This means that the hydroxy derivatives substituted on positions 3 and/or 4 are more prone to side-reactions, which confirms earlier conclusions [3].

TABLE 5

Extraction (E_{ahx}), adduct formation ($K_{AHX \cdot A}$) and dimerization constants of benzoic acid and derivatives

Acid	log E_{ahx}	log $K_{AHX \cdot A}$	log K_{dim}
Benzoic acid	5.42	—	3.47
Salicylic acid	7.10	—	3.09
3-Hydroxybenzoic acid	4.16	1.57	0.83
4-Hydroxybenzoic acid	3.63	1.50	0.70
3,4-Dihydroxybenzoic acid	2.58	2.30	0.01
2,5-Dihydroxybenzoic acid	5.46	0.30	2.20

As can be seen in Table 5, the type of side-reaction is different for the analytes investigated. The benzoic acid and salicylic acid ion-pairs strongly dimerize whereas the derivatives substituted on position 3 and/or 4 also form amine adducts. Here again the 2,5-dihydroxy derivative has an intermediate behaviour.

Analytical potential of the ion-pair extraction with TnOA

Table 1 shows that for some compounds (thiomersal, sorbic acid, saccharin, salicylic acid, cinnamic acid and most penicillins), satisfactory recoveries are obtained. For substances such as benzoic acid,acetylsalicylic acid, nicotinic acid, thiocol, indomethacin, the recovery is not so high but minor modifications of the extraction conditions should improve the yield and make the extraction useful for quantitative work. These changes could include an increase of the ionic strength to 0.5 [3]. For the hydroxy derivatives of benzoic acid, it is clear that the pH of the extraction medium should be lowered in order to obtain high yields. With 0.1 M TnOA, the extraction recoveries for the 3-, 4- and 3,4-dihydroxy derivatives are 47.6, 48.5 and 11.6% at pH 5.5; at pH 2.5, these values are 99.1, 94.6 and 87.4%. In both cases, extraction with chloroform alone is negligible.

In conclusion, it may be stated that, for a large series of acids, ion-pair formation with tri-n-octylamine can produce satisfactory extraction yields. It is, however, not possible to propose a generally applicable extraction scheme. With a 0.1 M counter-ion concentration, the pH and the ionic strength should be adjusted as a function of the acidity constant of the analyte. Nevertheless, the conditions used for dyes, i.e, a pH of 5.5, a TnOA concentration of 0.1 M in chloroform and an ionic strength of 0.1, may be proposed as the system which has the highest probability of yielding good extraction yields.

The authors acknowledge financial help from the Fund for Medical Scientific Research and thank A. Langlet-De Schrijver and K. Broothaers-Decq for technical assistance. The Belgian offices of Beecham and Bristol are gratefully acknowledged for gifts of penicillin standards.

REFERENCES

1 M. Puttemans, L. Dryon and D. L. Massart, Anal. Chim. Acta, 113 (1980) 307.
2 M. Puttemans, L. Dryon and D. L. Massart, J. Assoc. Off. Anal. Chem., 65 (1982) 737.
3 M. Puttemans, L. Dryon and D. L. Massart, Anal. Chim. Acta, 161 (1984) 221.
4 M. Puttemans, L. Dryon and D. L. Massart, J. Assoc. Off. Anal. Chem., 66 (1983) 670.
5 M. Puttemans, L. Dryon and D. L. Massart, J. Assoc. Off. Anal. Chem., 66 (1983) 1039.
6 R. Modin and A. Tilly, Acta Pharm. Suec., 5 (1968) 311.
7 R. Modin, Acta Pharm. Suec., 8 (1971) 509.
8 R. Modin and M. Schroder-Nielsen, Acta Pharm. Suec., 8 (1971) 573.
9 M. Schroder-Nielsen, Acta Pharm. Suec., 13 (1976) 439.
10 R. C. Weast (Ed.), Handbook of Chemistry and Physics, CRC Press, Cleveland, OH, 1975—1976.
11 Martindale, in A. Wade (Ed.), The Extra Pharmacopoeia, The Pharmaceutical Press, London, 1978.
12 G. Schill, Separation Methods for Drugs and Related Organic Compounds, Apotekarsocieteten, Stockholm, 1978.
13 T. Fujita, J. Iwasa and C. Hansch, J. Am. Chem. Soc., 86 (1964) 5175.
14 C. Hansch and S. Anderson, J. Org. Chem., 32 (1967) 2583.
15 W. Butte, C. Fooken, R. Klussmann and D. Schuller, J. Chromatogr., 214 (1981) 59.
16 K. A. Herzog and J. Swarbrick, J. Pharm. Sci., 60 (1971) 1666.
17 T. Chan and C. Hansch, Pomona College, unpublished results.
18 D. Soderberg and C. Hansch, Pomona College, unpublished results.
19 N. Ho, J. Y. Park, W. Morozowich and W. I. Higuchi, in E. B. Roche (Ed.), Design of Biopharmaceutical Properties Through Prodrugs and Analogs, American Pharmaceutical Association — Academy of Pharmaceutical Sciences, 1977, p. 136.
20 I. Boyd and E. Beveridge, Microbios, 24 (1979) 173.
21 W. J. Dunn, J. Med. Chem., 16 (1973) 484.
22 A. Bird and A. Marshall, Biochem. Pharm., 16 (1967) 2275.
23 A. Tsuji, O. Kubo, E. Miyamoto and T. Yamana, J. Pharm. Sci., 66 (1977) 1675.
24 T. Yamana, A. Tsuji, E. Miyamoto and O. Kubo, J. Pharm. Sci., 66 (1977) 747.
25 A. Ryrfeldt, J. Pharm. Pharmacol., 23 (1971) 463.
26 Fischer and Yates, Statistical Tables for Biological, Agricultural and Medical Research, Oliver and Boyd, Edinburgh.

Analytica Chimica Acta, 165 (1984) 257—261
Elsevier Science Publishers B.V., Amsterdam — Printed in The Netherlands

Short Communication

DETERMINATION OF RUBIDIUM IN BLOOD BY FLAME EMISSION SPECTROMETRY

P. ALLAIN*, C. TAFFOREAU, Y. MAURAS and G. LEBLONDEL

Laboratoire de Pharmacologie, Centre Hospitalier Universitaire, 49036 Angers Cedex (France)

(Received 4th January 1984)

Summary. Rubidium in plasma and whole blood was determined by flame atomic emission spectrometry after dilution 10× and 100× respectively with a 2.5 g Cs l^{-1} solution used as an ionization suppressor. The method is more sensitive than inductively coupled plasma, and much simpler than, e.g., neutron activation analysis.

Iyengar et al. [1] give 13 references for the rubidium concentration in human blood with a mean value of 2.49 mg l^{-1}, 10 references for rubidium in serum with a mean value of 0.2 mg l^{-1} and 2 references for erythrocytes with values of 4.18 and 5.3 mg l^{-1}. Since this compilation, the rubidium concentration in human serum and red blood cells has been determined by Versieck et al. [2] by neutron activation analysis. Their values are 0.17 mg l^{-1} for serum and 4.28 mg l^{-1} for cells. The rubidium content in human blood has also been measured by Lombeck et al. [3] by neutron activation analysis but their results given in dry weight are difficult to compare with the others. Recently, Schulten et al. [4] determined rubidium in human serum by field desorption mass spectrometry; they obtained a mean value of 1.96 μmol l^{-1} (0.168 mg l^{-1}).

Because flame atomic emission spectrometry is very sensitive (5), the conditions necessary for reliable determination of rubidium in blood by this method have been studied, and its sensitivity compared with inductively-coupled plasma emission spectrometry.

Experimental

For flame emission spectrometry, an Instrumentation Laboratories IL 151 spectrophotometer was used equipped with a Hamamatsu R 928 sensitive photomultiplier tube. A standard air—acetylene flame and single-slot burner were employed for all the measurements. The emission line was at 780.0 nm with a slit-width of 80 μm.

For inductively-coupled plasma (i.c.p.) emission spectrometry, the same emission line was selected by a Jobin-Yvon H 20 monochromator, specially blazed for near-i.r. measurements, and the intensity measured by a Hamamatsu

0003-2670/84/$03.00

photomultiplier tube model R 928 connected to the simultaneous multi-element JY 48 spectrometer. The source used was 1.5 kW (Plasmatherm). The signals were analysed by a PDP 11 computer. Rubidium salts were obtained from Prolabo.

Detection limits were calculated as the concentration corresponding to twice the background standard deviation. The rubidium concentration in blood cells was calculated knowing plasma and blood concentrations and hematocrit values.

Results

Figure 1 shows calibration graphs for rubidium in water and in presence of other elements (Ca, Mg, Fe, Li, Sr, Na, K, Cs) added separately at concentration of 5×10^{-3} M. As expected, all the elements studied enhanced the rubidium intensity; the maximum effect is observed with cesium and potassium which have low ionisation potentials and the least with iron, calcium and magnesium. The background emission measured without rubidium but with 5×10^{-3} M of the enhancing elements is very low, so ionization suppression is the major source of the signal enhancement.

Because the maximum increase in rubidium emission signal is observed with cesium, the influence of increasing concentrations of this element has been studied. Figure 2 shows that a low concentration of cesium (0.125 g l^{-1}) gives a large increase in signal, and maximum enhancement is obtained with Cs 1 g l^{-1}.

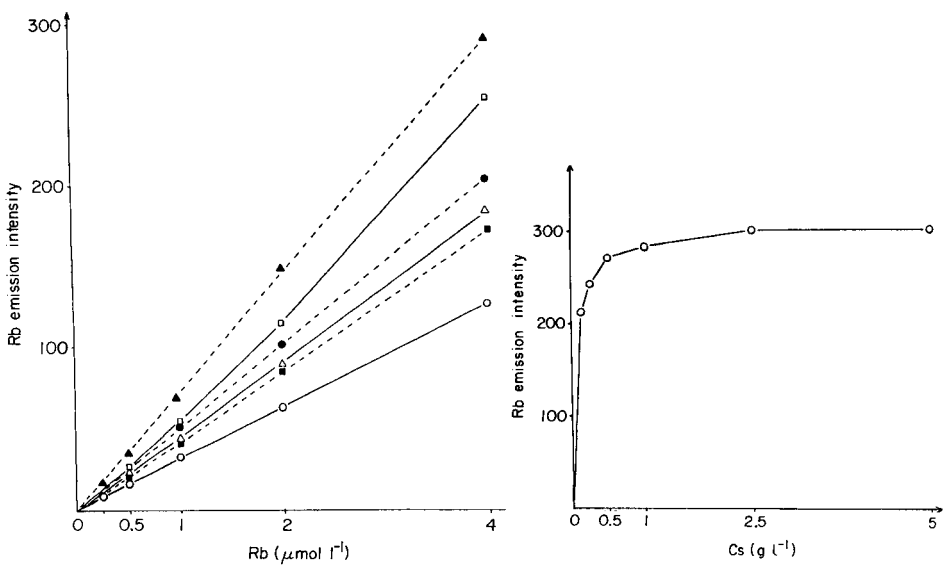

Fig. 1. Calibration graphs for Rb in the presence of 5×10^{-3} M: (▲) Cs; (□) K; (●) Na, Li, Sr; (△) Ca, Mg; (■) Fe; (○) water.

Fig. 2. Effect of Cs concentration on rubidium emission intensity (5 μmol l^{-1} Rb).

These results suggest that the matrix effect can be accommodated by dilution of the sample with a solution containing 2.5 g l^{-1} of cesium, as well as increasing the sensitivity. Figure 3 demonstrates that the signal intensity of rubidium in demineralised water and in a matrix similar to human blood plasma in Na, K, Ca, Mg, Fe, Cu and Zn composition is very different without cesium, but after addition of cesium, the two calibration graphs are superimposed.

For rubidium determination plasma samples were diluted 10-fold and whole blood samples 100-fold with a solution containing 2.5 g l^{-1} of cesium, before nebulization into the flame of the atomic spectrometer. Standard solutions were prepared by adding 5 and 50 μmol l^{-1} respectively, of rubidium to a synthetic matrix having a composition similar to plasma and blood in Na, K, Ca, Mg, Fe, Cu and Zn. The blank for zeroing the spectrometer is measured on the synthetic matrix, without rubidium, diluted with cesium. The detection limit under these conditions was 3.5 nmol l^{-1} (0.3 μg l^{-1}). Reproducibility as measured by 5 determinations on different days on the same sample was better than 3% for plasma or whole blood.

Under these analytical conditions, rubidium recovery studies after addition of 1 and 10 μmol to ten plasmas and ten different blood samples, respectively gave 1.05 ± 0.08 and 9.87 ± 0.5 μmol. The following values for rubidium concentrations in μmol l^{-1} in human plasma, blood cells and whole blood of 27 male controls, age 32 ± 9 years, hematocrit 47.8 ± 5.2 were 2.29 ± 0.29 μmol l^{-1} (0.196 ± 0.025 mg l^{-1}), 74.57 ± 10.37 (6.37 ± 0.89) and 36.79 ± 5.90 (3.14 ± 0.50), respectively. For 17 female controls, age 32 ± 13, hematocrit 39.8 ± 5.0, the results were 1.96 ± 0.46 μmol l^{-1} (0.168 ± 0.039 mg l^{-1}),

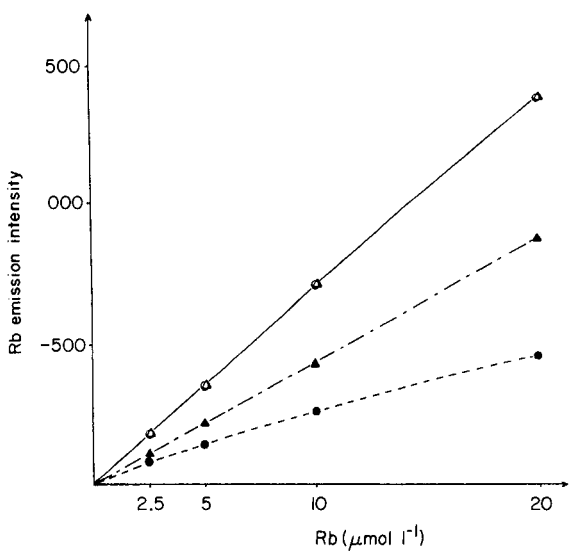

Fig. 3. Calibration graphs for Rb: (•) alone; (▲) in mineral matrix similar to human plasma; (○) with 2.5 g Cs l^{-1} in water; (△) with 2.5 g Cs l^{-1} in above plasma matrix.

72.22 ± 12.76 (6.17 ± 1.09) and 30.19 ± 6.11 (2.58 ± 0.52), respectively. The ± values are standard deviations. The blood cells to plasma rubidium ratio was 32.67 ± 3.51 for males and 38.36 ± 9.13 for females.

With the i.c.p., the best results were obtained at a low incident power of 0.8 kW and a nebulization pressure of 30 p.s.i. at a 1 l min^{-1} argon flow. The detection limit was 8.6 $\mu g\ l^{-1}$ as compared with 0.3 $\mu g\ l^{-1}$ for flame emission.

Discussion

Flame emission spectrometry for rubidium determination was used because trials with flame atomic absorption spectrometry showed poor sensitivity.

Assays with the i.c.p. gave poorer results than flame emission, nevertheless better results could have been achieved with a monochromator capable of improving the signal-to-background ratio and with an automatic background measurement system. Moreover, the low incident power used is not sufficient for sensitive determination of many other elements, so would not be compatible with the simultaneous multielement utilization of the JY 48 spectrometer. Under these conditions, the best instrument for determination of rubidium is a standard atomic absorption/emission spectrometer used in the emission mode, with narrow slits and a photomultiplier sensitive in the near infra red.

Three matrix correction possibilities can be used in emission spectrometry, i.e., to calibrate on a matrix identical to the samples, to add a large amount of an interference suppressor or to use a standard addition procedure. Here, the first two possibilities were used, by calibrating on a matrix similar to plasma and blood in inorganic constitution and by adding a large amount of cesium, which has a lower ionization potential than the analyte and has the greatest power of enhancing the signal intensity.

The rubidium concentrations measured are in good agreement with literature mean values for plasma and whole blood but they have been obtained by a much simpler method than neutron activation analysis or field desorption mass spectrometry. For blood cells, the present value is higher (6.3 and 6.1 mg l^{-1}) than the three literature values (4.18–4.28 mg l^{-1}), but the present value has been calculated from plasma and blood concentrations and the hematocrit value, and thus it is a measure of intracellular rubidium and

TABLE 1

Plasma rubidium concentration ($\mu mol\ l^{-1}$) in controls, mentally depressed and hemodialyzed patients[a] (values are mean ± standard deviation)

Controls		Mentally depressed		Hemodialyzed	
Males (27)	Females (17)	Males (12)	Females (15)	Males (18)	Females (22)
2.29 ± 0.29	1.96 ± 0.46	2.79 ± 0.91	2.50 ± 0.51	1.61 ± 0.26	1.63 ± 0.46

[a]The values in parentheses correspond to the numbers of patients tested.

rubidium adsorbed on the cell membranes. The method is also applicable to rubidium determinations in urine after a 100-fold dilution with cesium.

The method has also been used for diagnostic measurements. For example (Table 1), there is a statistically significant diminution of plasma rubidium in hemodialyzed patients with chronic renal insufficiency and an increase in mentally depressed patients.

The authors are indebted to Mrs. Laisne for typing and Fondation Langlois for its support.

REFERENCES

1 G. V. Iyengar, W. E. Kollmer and H. J. M. Bowen, The Elemental Composition of Human Tissues and Body Fluids, Verlag-Chemie, Weinheim, New York, 1978.
2 J. Versieck, J. Hoste, F. Barbier, H. Michels and J. De Rudder, Clin. Chem., 23 (1977) 1301.
3 I. Lombeck, K. Kasperek, L. E. Feinendegen and H. J. Bremer, in Biological Trace Elements, The Human Press, 1980, 217.
4 H. R. Schulten, P. B. Monkhouse, C. Achenbach and R. Ziskoven, Experientia, 39 (1983) 736.
5 F. J. Fernandez and D. C. Manning, At. Absorpt. Newsl., 11 (1972) 3, 67.

Analytica Chimica Acta, 165 (1984) 263—268
Elsevier Science Publishers B.V., Amsterdam — Printed in The Netherlands

Short Communication

THE ACCURATE DETERMINATION OF GOLD AND SILVER IN ORES AND CONCENTRATES BY WET-CHEMICAL ANALYSIS OF THE LEAD ASSAY BUTTON

A. DIAMANTATOS
Rand Refinery Ltd., Germiston (South Africa)
(Received 27th March 1984)

Summary. Hydroquinone or formic acid can be used as reductant for the quantitative precipitation of gold in the lead perchlorate solution obtained after the lead assay button has been parted with perchloric acid. Silver chloride can be completely precipitated by dilution and overnight standing of the parting solution, thus both gold and silver can be isolated by filtration for the final measurement. The proposed lead-wet chemical method was successfully applied to ores, concentrates, dusts, etc.

The classical lead-cupellation pyrotechnique is not a recommended method for the accurate determination of gold and silver in ores and concentrates. Although their collection in the lead button is practically complete, the subsequent steps, i.e., cupellation and nitric acid parting of the prill, introduce losses and errors. Early research by Lodge [1] showed that in cupellation of 200 mg of gold with 10 g of lead, the loss of gold was 0.155% at 775° C, 1.435% at 1000° C and 2.990% at 1075° C. A radiochemical study by Coxon et al. [2] confirmed that close control of the cupellation temperature is of the utmost importance; a shift of 100° C in the cupellation temperature, for a 6-mg bead, resulted in an increased gold absorption by the cupel of 0.5%. Wall and Chow [3] reported losses ranging from 0.56% to 0.86% for cupellation temperatures between 925 and 1090° C. The cupellation time is also important. Popova et al. [4] showed that an increase in the weight of the lead button from 30 to 50 g was associated with increased cupellation time which increased the relative loss of gold from 1.04 to 3.1%. Yaguchi and Kuneko [5] showed that cupellation is impossible if >3 g of copper and >0.03 g of nickel are present in a 30-g lead button, and that >0.5 g of selenium or >0.2 g of tellurium increases the cupellation losses.

In an informative study of losses of silver in the classical fire assay, Faye and Inman [6] showed that the temperature and time of cupellation and the amount of silver present had a significant influence; the losses of silver varied from 5 to 10% and were never, even under optimum conditions, less than 2%. With samples of low silver content (2—0.1 mg), Nakamura and Fukami [7] reported losses ranging from 5 to 30%.

Errors in parting the silver—gold prill obtained after cupellation have also been reported [8, 9]. It seems to be agreed that even when silver is added up to a silver:gold ratio of 4:1, the nitric acid attack on the prill still does not separate these two noble metals quantitatively. A little gold is lost to the parting acid, but some silver resists dissolution in the nitric acid and remains in the final gold prill; the resulting gain of gold values is generally accepted to be about 1.25% [9]. Wall and Chow [3] found that the silver retained by the gold bead (20—30 mg of gold), varied from 0.1 to 0.5 mg. The gold gained in parting and lost in cupellation compensate to some degree. Radiochemical tests by Trokowicz [10] on the silver content of the final gold prill showed a systematic error of +0.1% for gold.

Although gold and silver losses during cupellation have been widely studied, little has been done to develop methods for determining these two metals collected in lead by non-cupellation procedures. Recently, it was shown [11] that disintegration of the lead button with perchloric acid, followed by dilution with water, results in complete precipitation of silver as silver chloride on standing. Because gold in solution is easily reduced to the metal, it was decided to investigate the possibility of recovering gold from the diluted lead perchlorate solution with common reducing agents.

Experimental

Equipment and reagents. The fire-assay furnace and related equipment, the atomic-absorption spectrometer and the lead flux, were the same as described recently [11]. The hydroquinone was of analytical grade and the formic acid was 98—100%.

Recommended procedure. Mix thoroughly 1—50 g of the sample (roasted if sulphur is present) with 150—180 g of lead flux and transfer to a No. 2 fireclay crucible. Fuse at 1200° C for 1 h and then pour the molten fluid into a conical iron mould. After cooling, detach the lead button from the slag by tapping. Place the button in 100 ml of 30% (w/v) sodium hydroxide solution and boil to remove completely any adhering slag. Place the button in a 800-ml squat beaker and add 250 ml of perchloric acid (70%) and 25 ml of acetic acid (anhydrous). Cover the beaker, heat to 185° C and maintain at 180 ± 5° C until all the lead has dissolved. Allow to cool to about 100° C and dilute the perchlorate solution gradually with 250 ml of water. Bring this solution to boiling and add carefully 100 mg of hydroquinone dissolved in a little water or add 20 ml of formic acid (98—100%). (An almost instantaneous mauve colour indicates precipitation of gold by hydroquinone; with formic acid a pink colour develops after boiling for 3 min.) Keep boiling gently for 1 h. Cool in water for 15—20 min. (If silver is also required, stir the cooled solution and leave standing overnight in a dark place.)

Filter the solution through a Millipore filter apparatus using a 0.45-μm filter and wash 3—4 times with water. Place the filter disc with the retained precipitate (gold metal and silver chloride) in the original 800-ml beaker, add 40 ml of aqua regia and boil until the filter paper has dissolved. Evaporate to

incipient dryness in the presence of a little sodium chloride. Add 20 ml of hydrochloric acid (10 M) and 5—6 drops hydrogen peroxide (100 vol.) and boil gently. Cool, transfer to an appropriate volumetric flask (to give 5—20 mg l^{-1} gold and 1—5 mg l^{-1} silver) and dilute to volume with 3 M hydrochloric acid. Measure the atomic absorption of gold and silver at 242.8 nm and 328.1 nm, respectively.

In the case of rich materials, determine gold and silver gravimetrically. Treat the filter with the retained precipitate with 40 ml of aqua regia to dissolve both gold and filter. Evaporate to ca. 5 ml, dilute to 200 ml with water and heat gently for 1 h to coagulate the silver chloride. Filter on a weighed sintered-glass crucible, dry at 130°C and weigh the silver chloride. In the filtrate, precipitate gold by reduction with hydroquinone or ascorbic acid, filter, ignite and weigh the metallic gold.

Results

The choice of reducing agent. The first experiments were conducted on a fan dust concentrate with a high content of gold and silver (8730 mg kg^{-1} Au and 8700 mg kg^{-1} Ag). The sample (20 g) was fused with 180 g of the lead flux and treated further exactly as described above up to dilution to 500 ml. The diluted solution was boiled for 2—3 min, cooled in water for 15—20 min and left overnight in the dark. Filtration (as described) removed all the silver (174 mg) as silver chloride [11] and some spongy gold (45 mg) precipitated by the hydrogen evolved during parting of the lead button. The filtrate, containing 129.6 mg of gold, was transferred to a 1-l volumetric flask and diluted to the mark with water. Five 100-ml aliquots of this solution were diluted to 500 ml with 225 ml of perchloric acid (70%) and 175 ml of water. These solutions were brought to the boil and one of the following reductants was added while stirring: hydroquinone (0.2 g in 20 ml of water), ascorbic acid (0.2 g in 20 ml of water), oxalic acid (0.2 g in 20 ml of water), 5 ml of formic acid (98—100%) or 5 ml of formaldehyde solution (40%). After the addition of the reductant, the boiling was continued for 1 h. Hydroquinone produced an immediate black suspension which precipitated after 3—4 min of boiling. Ascorbic acid produced a slimy black precipitate, unsuitable for filtration. The addition of formic acid and formaldehyde resulted in a pink solution after ca. 5 min of boiling, and gold metal precipitated later. With oxalic acid, gold precipitated after $\geqslant$30 min of boiling.

After cooling in water for 20 min, each solution was filtered (as described) and the filtrates were examined for gold. For this purpose, each filtrate was evaporated to complete dryness; the residue was boiled with 40 ml of 10 M hydrochloric acid, again evaporated to dryness, and then boiled for 5 min with 40 ml of hydrochloric acid (10 M) and 5—6 drops of hydrogen peroxide. The solutions were cooled completely, and filtered to remove the bulk of lead chloride, and then checked for gold by atomic absorption spectrometry (a.a.s.). No gold was detected in the filtrate from the solution treated with

hydroquinone; only traces of gold were found after the treatment with formic acid. However, 22.9% and 50.4% of the original gold content were found in the filtrates after treatment with formaldehyde and oxalic acid, respectively. Hydroquinone and formic acid were therefore chosen for further work.

Effect of the boiling time on precipitation of gold. To find the boiling time necessary for complete precipitation of gold, another 1 l of lead perchlorate solution was prepared exactly as described above. Four 100-ml aliquots of this solution, each containing 11.84 mg of gold, were diluted with 225 ml of perchloric acid (70%) and 175 ml of water, boiled and treated with hydroquinone as described above. Each solution was boiled for different periods of time (30, 45, 60, 90 min). After cooling, the precipitated gold was filtered off and the filtrates were analysed as described above. No gold was detected in any filtrate, which confirmed complete precipitation of gold with hydroquinone after boiling for 30 min. Analogous tests with formic acid (as specified) showed that boiling for 45 min was needed for complete precipitation. A boiling time of 60 min was chosen for both reductants.

Effect of reductant and acid concentrations. Six 500-ml lead perchlorate/perchloric acid solutions, similar to those used for the boiling time tests, were used to examine the precipitation of gold with different amounts of hydroquinone (50, 100, 200 mg) and formic acid (5, 10, 20 ml) after boiling for 1 h; 50 mg of hydroquinone or 10 ml of the formic acid sufficed for complete precipitation of $\leqslant 12$ mg of gold. With 5 ml of formic acid, about 1.7% of the total gold content was not precipitated.

Similar tests showed that the use of 150, 200 or 250 ml of perchloric acid (70%) in the dilution step (to 500 ml) did not affect matters. Gold was completely precipitated from all the perchloric acid concentrations examined.

Effect of foreign elements. The fate and effect of elements likely to be present in some gold-bearing materials, were also considered. Thus, Ir, Ru and Os remain unattacked by the perchloric acid [12]; Ni, Cu, Cr, Co, Te and Fe are not precipitated by the reductants used but Pt, Pd and Rh are. Selenium is precipitated by hydroquinone but not by formic acid. These co-precipitations, however, do not affect the a.a.s. determination of gold and silver if uranium [13] or copper—cadmium [14] buffer is added. It is, however, essential to remove any sulphur present in the sample. When a gold ore containing pyrites was directly fused with lead flux and the button was parted with perchloric acid, a white turbidity of lead sulphate appeared. This precipitation, which complicates the subsequent determination of the noble metals, was easily eliminated by roasting the sample at 750° C for 1 h before mixing it with the lead flux.

Accuracy and precision. The accuracy and precision of the method was assessed by spiking lead fluxes with known quantities of gold and fusing them before the above procedure was applied. The results given in Table 1 demonstrate high accuracy and precision.

Precipitation of silver. Complete precipitation of silver as silver chloride is attained after dilution and overnight standing of the parting solution [11].

TABLE 1

Recovery of gold from spiked lead fluxes

Au added (mg)	0.250	1.00	5.00	10.00
Au found (mg)	0.245	1.02	4.92	10.05
	0.248	1.00	4.98	9.96

In order to check any effect of the reduction step, 35-g lead buttons, each obtained by fusing 37.8 mg of silver nitrate with 150 g of lead flux, were treated as in the recommended procedure. After overnight standing and filtration, the filter with the precipitate was heated with 1 ml of concentrated hydrochloric acid and then with 50 ml of ammonia liquor. The precipitate was completely dissolved; this test and subsequent analysis of the ammoniacal solution for silver by a.a.s. [11], confirmed complete precipitation of silver chloride by the proposed method.

Determination of gold and silver in various samples and comparison with the classical fire assay. Different samples were analysed for gold and silver by the proposed wet method and by the standard cupellation method. For comparative purposes, all the final measurements were done by a.a.s., thus eliminating any errors which might have been arisen from the use of different final measurement techniques. The results (Table 2) clearly demonstrate the higher efficiency of the method, and give a general indication of the magnitude of the cupellation losses in the classical fire assay.

Discussion

In mine laboratories, large numbers of samples of very similar composition are analysed for gold (and silver) by the classical assay method and correction factors are applied to compensate for losses, mainly during cupellation, by using control standards. The proposed wet method could be very useful as an arbitration method to establish accurate correction factors.

The recommended method is substantially shorter if only gold is to be determined, because there is no need for overnight standing of the perchlorate parting solution before its filtration.

Two variations of the classical fire assay may be compared with the method described here. Fishkova et al. [15] suggested a method in which the original lead button weighing 20—30 g is reduced to 0.5—2 g by incomplete cupellation at 870—950°C in magnesite-cement cupels; the lead bead is treated with nitric acid and both gold and silver are determined by a.a.s. The reported relative errors for gold and silver were 20% and 10%, respectively. In another variation [16], the lead assay button (30—45 g) is reduced to approximately 2 g by double scorification, the small button is treated with diluted nitric acid and, after further treatment and separation, gold and silver are determined by a.a.s. Experience in this laboratory, however, suggests that both scorification and partial cupellation are inadmissible for accurate

TABLE 2

Comparison of lead wet chemical and cupellation methods

Sample	Method	Results (mg kg^{-1})	
		Au	Ag
Gold ore	Wet analysis	16.3	8.1
(50 g)	Cupellation	15.0	7.3
Gold ore	Wet analysis	9.9	2.4
(50 g)	Cupellation	9.3	2.1
Mine dump concentrate	Wet analysis	1110	128
(10 g)	Cupellation	1046	111
Fan dust	Wet analysis	8990	8910
(1 g)	Cupellation	8730	8700
Carbon leader	Wet analysis	707	75
(5 g)	Cupellation	658	71
Refinery borax slag	Wet analysis	594	3080
(5 g)	Cupellation	588	2890
Refinery borax slag	Wet analysis	733	440
(5 g)	Cupellation	702	424
Liners	Wet analysis	1770	1950
(5 g)	Cupellation	1690	1893
Jeweller sweeps	Wet analysis	20150	22780
(0.5 g)	Cupellation	19920	22660

analysis. The proposed method is simpler to handle and improves on the classical assay by eliminating the cupellation.

The author thanks Mr. I. J. Leibbrandt for his assistance with the preparation of the lead buttons. He is also indebted to the General Manager of Rand Refinery, Mr. E. F. Statham, for permission to publish this work.

REFERENCES

1 R. W. Lodge, Notes on Assaying 1904, p. 142.
2 C. H. Coxon, C. J. Verwey and D. N. Lock, J. S. Afr. Inst. Mining Metall., 62 (1962) 546.
3 S. G. Wall and A. Chow, Anal. Chim. Acta, 69 (1974) 439.
4 N. N. Popova, E. P. Zdorova and M. A. Kondulinskaya, Zavod. Lab., 40 (1974) 1061.
5 K. Yaguchi and J. Kuneko, Bunseki Kogaku, 21 (1972) 601.
6 G. H. Faye and W. R. Inman, Anal. Chem., 31 (1959) 1072.
7 Y. Nakamura and K. Fukami, Japan Analyst, 6 (1957) 687.
8 W. A. Sinclair, J. S. Afr. Inst. Mining Metall., 64 (1964) 333.
9 H. Britten, Laboratory Control, 7th Commonwealth Metallurgical Congr., 1961.
10 J. Trokowicz, Chem. Anal., 15 (1970) 1147.
11 A. Diamantatos, Anal. Chim. Acta, 148 (1983) 293.
12 A. Diamantatos, Anal. Chim. Acta, 90 (1977) 179; 91 (1977) 281.
13 R. C. Mallett, D. C. G. Pearton, E. J. Ring and T. W. Steele, Talanta, 19 (1972) 181.
14 M. M. Schnepfe and F. S. Grimaldi, Talanta, 16 (1969) 591.
15 N. L. Fishkova, E. P. Zdorova and N. N. Popova, Zh. Anal. Khim., 30 (1975) 806.
16 P. E. Moloughney, Talanta, 24 (1977) 135.

Analytica Chimica Acta, 165 (1984) 269—273
Elsevier Science Publishers B.V., Amsterdam — Printed in The Netherlands

Short Communication

SPECTROFLUORIMETRIC ASSAY FOR ACYL CoA-CHOLESTEROL ACYLTRANSFERASE

CHIZUKO HAMADA and MASATAKE IWASAKI

Daiichi College of Pharmaceutical Sciences, Tamagawa, Minami-ku, Fukuoka 815 (Japan)

KIYOSHI ZAITSU and YOSUKE OHKURA*

Faculty of Pharmaceutical Sciences, Kyushu University 62, Maidashi, Higashi-ku, Fukuoka 812 (Japan)

(Received March 1st 1984)

Summary. A sensitive assay for acyl CoA-cholesterol acyltransferase (EC 2.3.1.26) in rat liver microsomal and mitochondrial preparations is described. The lowered cholesterol concentration in the enzyme reaction with oleoyl CoA is determined spectrofluorimetrically by using the cholesterol oxidase/peroxidase/*p*-hydroxyphenylpropionic acid system. The assay requires as little as 20 μg of protein in the enzyme preparation.

Acyl CoA-cholesterol acyltransferase (ACAT; EC 2.3.1.26) catalyses the esterification of cholesterol with a long chain fatty acid in the presence of ATP and CoA, or acyl CoA in liver [1, 2], aorta [3] and adrenal glands [4, 5]. The enzyme activity in the arterial intima increases in atherosclerotic aortas compared to the normal [6]. The activity of ACAT has been assayed only by radiochemical methods. When endogenous cholesterol in biological samples is used as one of the substrates for ACAT, the sample is incubated (at 37—39°C for 15 min—15 h) with a ^{14}C-labelled fatty acid in the presence of cofactors, ATP and CoA [4, 7] or ^{14}C-labelled acyl CoA [8—10]. Alternatively, when an endogenous fatty acid is utilized as one of the substrates, the sample is incubated with ^{3}H- [11] or ^{14}C-labelled cholesterol [12] in the presence of the cofactors. The activity of ACAT in the sample is assayed by measuring the isotope incorporated enzymatically into the cholesterol ester after extraction of lipids and thin-layer chromatographic separation. These methods require complicated procedures.

In a previous paper [13], a highly sensitive fluorimetric method was reported for the assay of cholesterol in serum and high-density lipoprotein (HDL) based on an enzymatic method using the cholesterol oxidase (COD)/peroxidase system with tyramine as a fluorogenic substrate of peroxidase. It was later found that *p*-hydroxyphenylpropionic acid (HPPA) was a much more effective fluorogenic substrate for peroxidase than tyramine [14]. This communication describes a sensitive spectrofluorimetric method for the assay of ACAT with a simple procedure based on endogenous cholesterol.

0003-2670/84/$03.00

The biological sample is incubated with oleoyl CoA and the decrease in free cholesterol concentration is determined spectrofluorimetrically by the enzymatic method using the COD/peroxidase system with HPPA as the substrate for peroxidase. Rat liver microsomal and mitochondrial preparations were employed as model preparations of ACAT to establish a general assay procedure because ACAT activity is high in these particulate fractions [15].

Experimental

Reagents and solutions. All chemicals were of reagent grade unless otherwise noted. Double-distilled water and isopropanol were used. An oleoyl CoA/bovine serum albumin (BSA) solution (100 nmol ml^{-1} and 6 mg ml^{-1}, respectively) was prepared from 8 mg of oleoyl CoA (Sigma) and 600 mg of BSA (Wako, Osaka), dissolved in 100 ml of 0.1 M Tris/hydrochloric acid buffer (pH 7.4). The solution was usable for 1 week when stored at 4°C. A COD/peroxidase solution (6.9 mU ml^{-1} and 1 purpurogallin unit ml^{-1}, respectively) was prepared from COD (30 μl of COD suspension, 23 U ml^{-1}, from *Nocardia*; Miles Laboratories, Elkhart, U.S.A.) and 0.4 mg of peroxidase (300 purpurogallin unit mg^{-1}, from horseradish; Sigma), dissolved in 100 ml of 0.3 M potassium phosphate buffer (pH 7.4). The solution was stable for more than 1 month when stored at 4°C. The HPPA (3 mmol, 0.5 g; Dojindo Laboratories, Kumamoto) was dissolved in 100 ml of 0.3 M potassium phosphate buffer (pH 7.4) and stored at 4°C. The solution was used within 1 week.

Apparatus. Uncorrected fluorescence excitation and emission spectra and intensities were measured with a Hitachi MPF-4 spectrofluorimeter using quartz cells of 10 × 10 mm optical path length. The spectral band-widths were 2 nm in the excitation monochromator and 10 nm in the emission monochromator. The pH was measured with a Hitachi-Horiba M-7 pH meter at 25°C.

Enzyme preparations. Fed male Donryu rats, 5 weeks old, were killed by decapitation, livers were removed, and microsomal and mitochondrial preparations were obtained as described by Deykin and Goodman [16]. The enzyme preparations could be stored at −20°C for at least 1 month without loss of ACAT activity. The protein concentration was measured by the method of Lowry et al. [17], with BSA as the standard protein.

Procedure. To 0.5 ml of the oleoyl CoA/BSA solution placed in a glass-stoppered 10-ml test-tube, 5 μl of enzyme preparation (0.02—0.5 mg of protein, 1.6—14.0 nmol of cholesterol) was added and incubated at 37°C for 60 min. The incubated mixture was added to 3.5 ml of methanol/chloroform (1:2, v/v) to stop the enzyme reaction. The mixture was shaken with a vortex-type mixer for 10 min and centrifuged at 1000*g* for 5 min. The lower, organic layer (2.5 ml) was evaporated to dryness below 25°C under vacuum. The residue was dissolved in 3.0 ml of 0.3 M potassium phosphate buffer (pH 7.4) containing 0.025% Triton X-100 (Wako). The

COD/peroxidase solution and HPPA solution (exactly 0.1 ml each) were added, and the mixture was warmed at 37°C for 20 min to develop the fluorescence (mixture A). To determine the initial concentration of free cholesterol in the enzyme preparation, the same procedure was carried out except that the enzyme preparation and oleoyl CoA/BSA solution were added to the methanol/chloroform mixture, incubation being omitted (mixture B). The fluorescence intensities of mixtures A and B were measured at 404 nm with excitation at 320 nm. The difference in the fluorescence intensity between A and B was calculated, and the loss of chloesterol was determined from a calibration graph prepared by treating 5-μl samples of cholesterol standard solutions (520—3100 nmol ml^{-1}, 200—1200 μg ml^{-1}, in isopropanol) by the given procedure. The ACAT activity was expressed as nmol of cholesterol lost per h per mg protein at 37°C.

Results and discussion

Cholesterol in the enzyme preparations can be determined in the same way as in the fluorimetric enzymatic method for the assay of cholesterol in serum and HDL [13] after the extraction of cholesterol with methanol/chloroform mixture, except that HPPA is used as the fluorogenic substrate for peroxidase in place of tyramine. Maximum and constant fluorescence intensity was achieved with 30 μmol ml^{-1} HPPA and peroxidase-equivalent to 1 purpurogallin unit ml^{-1}. Cholesterol (3.9 nmol) added to the microsomal or mitochondrial preparation could be extracted almost completely with 3.5 ml of the methanol/chloroform mixture (recovery 94.6 ± 2.1%, mean ± standard deviation (SD), $n = 5$).

The activity of ACAT in the enzyme preparations was greatest at pH 7.4 in 0.1 M potassium phosphate buffer. Large amounts of ATP and CoA inhibited the peroxidase-mediated reaction. Therefore, acyl CoA was used as the substrate of ACAT. The ACAT was activated more by oleoyl CoA than by palmitoyl CoA, and so oleoyl CoA was preferred. Oleoyl CoA gave maximum and almost constant ACAT activity at concentrations of 75 μM and greater; the observed value of the Michaelis constant was 22.8 μM, as can be extracted from the Lineweaver—Burk plot (Fig. 1); 100 μM was therefore employed in the recommended procedure. No inhibition of peroxidase with CoA formed in the ACAT-catalyzed reaction was detected even at the 10 nmol level. The rate of the ACAT-mediated reaction was proportional to the amount of protein in the enzyme preparation up to at least 1 mg. Cholesterol added to the incubation mixture produced neither stimulation nor suppression of ACAT activity at concentrations of 500—1300 nmol ml^{-1} even in the enzyme preparation with a low cholesterol concentration (1300 nmol ml^{-1}).

Bovine serum albumin was added to the incubation mixture in the assay of ACAT, because the large amount of free fatty acid usually present in biological samples inhibits the esterification of cholesterol; BSA eliminates this inhibition [15] and also enhances the esterification [18]. Maximum

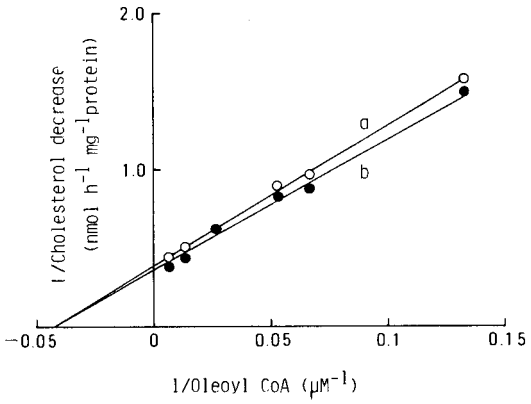

Fig. 1. Lineweaver—Burk plots of the dependency of oleoyl CoA concentration on ACAT activity. Portions (5 μl) of (a) microsomal and (b) mitochondrial preparations, were treated as recommended with various concentrations of oleoyl CoA.

and constant ACAT activity was attained at BSA concentrations of ⩾3.2 mg ml^{-1}; 6 mg ml^{-1} was used as the optimum. The enzyme activity was constant with time for at least 120 min when incubated at 37°C.

The fluorescence excitation (maximum, 320 nm) and emission (maximum, 404 nm) spectra for the final mixtures (A and B) were identical to those obtained with cholesterol standards. The calibration graph for cholesterol was linear up to at least 3100 nmol ml^{-1} and passed through the origin.

Recoveries of cholesterol (4 nmol) added to the incubation mixtures with the microsomal and mitochondrial preparations were 95.3 ± 4.3 and 95.6 ± 4.3% (mean ± SD, n = 7 and 6), respectively. The relative standard deviation was 1.9% (n = 10) for the mitochondrial preparation with a mean ACAT activity of 2.69 units. The limit of detection for cholesterol decreased enzymatically was 1.6 nmol. This corresponds to the amount of cholesterol lowered by 20 μg of protein in the microsomal or mitochondrial preparation. The limit was defined as the amount giving a fluorescence intensity twice that of the final reaction mixture obtained as in the recommended procedure except that the COD/peroxidase solution was replaced with a peroxidase solution (1 purpurogallin unit ml^{-1}).

The ACAT activities in the specified rat liver microsomal and mitochondrial preparations assayed by the present method were 2.71 ± 1.00 and 2.49 ± 1.22 units (mean ± SD, n = 9 each), respectively. These results are similar to those reported by other workers [12]. This method may also permit the assay of ACAT in rat liver and aorta homogenates.

This study provides the first fluorimetric method for the assay of ACAT. The procedure takes less than 4 h, and more than 20 samples can be assayed simultaneously. The method is precise and does not require radioactive substrate.

REFERENCES

1 S. Mukherjee, G. Kunitake and R. B. Alfin-Slater, J. Biol. Chem., 230 (1958) 91.
2 C. A. Dervon, D. B. Weinstein and D. Steinberg, J. Biol. Chem., 255 (1980) 9128.
3 R. W. St. Clair, H. B. Lofland and T. B. Clarkson, Circ. Res., 27 (1970) 213.
4 G. Shyamala, W. J. Lossow and I. L. Chaikoff, Biochim. Biophys. Acta, 116 (1966) 543.
5 F. P. Bell, Biochim. Biophys. Acta, 666 (1981) 58.
6 S. Hashimoto, S. Dayton, R. B. Alfin-Slater, P. T. Bui, N. Baker and L. Wilson, Circ. Res., 34 (1974) 176.
7 J. W. Proudlock and A. J. Day, Biochim. Biophys. Acta, 260 (1972) 716.
8 M. S. Brown, S. E. Dana and J. L. Goldstein, J. Biol. Chem., 250 (1975) 4025.
9 F. P. Bell and E. V. Hubert, Biochim. Biophys. Acta, 619 (1980) 302.
10 K. E. Suckling, G. S. Boyd and C. G. Smellie, Biochim. Biophys. Acta, 710 (1982) 154.
11 D. E. Brenneman, T. Kaduce and A. A. Spector, J. Lipid Res., 18 (1977) 582.
12 K. T. Stokke and K. R. Norum, Biochim. Biophys. Acta, 210 (1970) 202.
13 C. Hamada, M. Iwasaki, Y. Mibuchi, K. Zaitsu and Y. Ohkura, Chem. Pharm. Bull. (Tokyo), 28 (1980) 3131.
14 K. Zaitsu and Y. Ohkura, Anal. Biochem., 109 (1980) 109.
15 D. S. Goodman, D. Deykin and T. Shiratori, J. Biol. Chem., 239 (1964) 1335.
16 D. Deykin and D. S. Goodman, Biochem. Biophys. Res. Commun., 8 (1962) 411.
17 O. H. Lowry, N. J. Rosebrough, A. L. Farr and R. J. Randall, J. Biol. Chem., 193 (1951) 265.
18 C. R. Treadwell, L. Swell and G. V. Vahouny, Fed. Proc. Fed. Am. Soc. Exp. Biol., 21 (1962) 903.

Analytica Chimica Acta, 165 (1984) 275—279
Elsevier Science Publishers B.V., Amsterdam — Printed in The Netherlands

Short Communication

EXTRACTION-SPECTROPHOTOMETRIC DETERMINATION OF MERCURY WITH 1,2,4,6-TETRAPHENYLPYRIDINIUM PERCHLORATE

T. PÉREZ-RUIZ*, J. A. ORTUÑO and M. C. TORRECILLAS
Department of Analytical Chemistry, University of Murcia (Spain)
(Received 7th March 1984)

Summary. The characteristics of 1,2,4,6-tetraphenylpyridinium perchlorate (TPPP) as a reagent for the formation of ion-pair complexes with metal-bromide anions, and its application to the spectrophotometric determination of mercury are described. This reagent forms a 1:1 complex with bromomercurate(II) ions that is slightly soluble in water and can be extracted with isopentyl acetate. The optimum conditions are about 0.5 M sulphuric acid and 0.03 M potassium bromide. Mercury can be determined at 310 nm in the range 0.04—0.5 $\mu g\ ml^{-1}$; the apparent molar absorptivity is $2.63 \times 10^4\ l\ mol^{-1}\ cm^{-1}$, and the conditional stability constant is $\log K = 4.7 \pm 0.1$ at 20° C. The main interferences are easily removed. Mercury can be determined in sphalerites and zinc amalgams.

1,2,4,6-Tetraphenylpyridinium perchlorate (TPPP) forms ion-pair complexes with a small number of metal/halogen anions. These complexes can be used for the spectrophotometric determination of the metal after extraction with the appropriate solvents. Extraction of the relevant chloro complexes has been applied to the spectrophotometric determination of thallium(III) and gold(III) [1, 2]. This communication deals with the formation and extraction of the metal/bromide complexes with TPPP. A new spectrophotometric method for the determination of mercury(II) is proposed. Although various reagents [3—7] have been introduced for spectrophotometric determinations of mercury, dithizone is still commonly used [8—10]. The advantage of the method proposed over the dithizone method is its much higher selectivity which allows direct mercury determinations in complicated samples.

Experimental

Reagents and apparatus. All solutions were prepared from analytical-grade chemicals. Doubly-distilled water was used throughout.

Synthesis of TPPP was as before [1]. An ethanolic 10^{-3} M solution was used; this solution is stable for several weeks if protected from light. Mercury(II) standard solution (0.01 M) was prepared by dissolving mercury(II) nitrate in 0.1 M nitric acid and standardized by titration with EDTA [11]. Working standards were prepared from this solution as required.

0003-2670/84/$03.00

A Pye-Unicam SP8-100 spectrophotometer with 1-cm silica cells was used.

Procedure. To a volume of sample solution in a separating funnel containing up to 25 μg of mercury(II), add 5 ml of 5 M sulphuric acid, 3 ml of 0.5 M potassium bromide solution and 2 ml of 7×10^{-4} M TPPP solution. Dilute to 50 ml with water and extract with 5 ml of isopentyl acetate with vigorous shaking for 2 min. Allow the phases to separate for 10 min, transfer the organic layer to a centrifuge tube and centrifuge to give an organic layer free from water. Measure the absorbance of the organic layer at 310 nm against a reagent blank prepared in a similar way.

Prepare a calibration graph by using different volumes of the standard solution of mercury(II) treated in the same way. Beer's law is obeyed over the concentration range 0.04—0.5 μg ml^{-1} mercury.

Results and discussion

Preliminary studies. Some metal ions react with TPPP in an acidic medium containing an excess of bromide to form ion-pair complexes that can be extracted into isopentyl acetate. The percentage extractions are listed in Table 1 for selected conditions. Gold(III), mercury(II) and thallium(III) have high extraction efficiencies whereas the other metal ions are only slightly extracted. The percentage extractions of the corresponding chloro complexes with TPPP are also high for gold(III) and thallium(III) but low for mercury [1, 2]. The bromomercurate(II) system is thus of interest for mercury determination whereas there is no advantage in using these complexes for thallium(III) and gold(III) determinations.

Figure 1 shows the absorption spectra of TPPP in ethanol (curve 1) or isopentyl acetate (curve 3), and an isopentyl acetate extract of the ion-pair complex obtained with mercury(II) (curve 2). Only a small shift of the 311-nm absorption maximum of the reagent is observed for the complex in isopentyl acetate.

Effect of reaction variables. The effect of acidity on the formation of the ion-pair complex and its extraction into isopentyl acetate was studied for fixed concentrations of mercury(II) (0.4 μg ml^{-1}) and potassium bromide

TABLE 1

Percentage extraction of metal-bromide complexes with TPPP in isopentyl acetate[a]

Metal ion	E (%)	Metal ion	E (%)	Metal ion	E (%)
Au(III)	100	Pt(IV)	0.75	Pb(II)	0.01
Hg(II)	95.9	Sb(V)	0.29	Mn(II)	0.009
Tl(III)	89.7	In(III)	0.20	Zn(II)	0.007
Ag(I)	17.3	Fe(III)	0.04	Cr(III)	0.005
Bi(III)	3.5	Cd(II)	0.03	Cu(II)	0.002

[a]Conditions: 0.03 M potassium bromide, 0.5 M sulphuric acid, 2.8×10^{-5} M TPPP, 10:1 ratio of aqueous phase to isopentyl acetate.

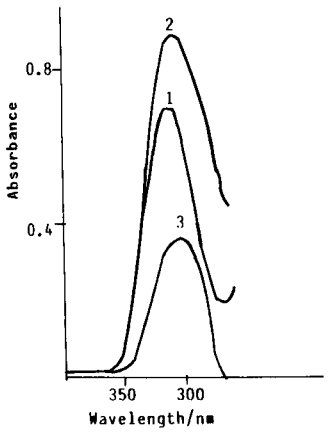

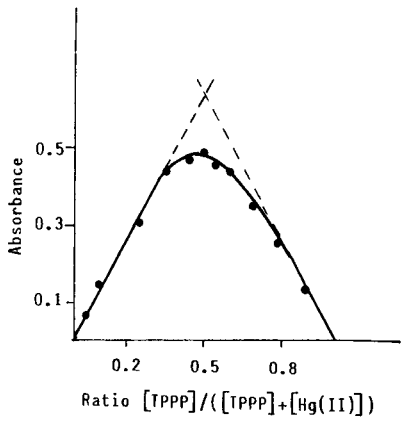

Fig. 1. Absorption spectra: (1) 2×10^{-5} M TPPP in ethanol; (2) the TPPP $HgBr_3$ complex extracted with 5 ml of isopentyl acetate (50 ml of aqueous solution with 2×10^{-6} M Hg(II), 2.6×10^{-5} M TPPP, 0.03 M KBr and 0.5 M sulphuric acid); (3) TPPP in isopentyl acetate.

Fig. 2. Stoichiometry of mercury-TPPP complex determined by Job's method. Concentration of mercury(II) plus ligand, 7×10^{-6} M.

(0.03 M) by varying the sulphuric acid concentration from 0.5×10^{-4} to 2.5 M. Varying the acidity in this range caused only a slight change in absorbance.

The influence of varying bromide ion concentrations in the range 10^{-4}—1 M was studied for 0.4 μg ml^{-1} mercury(II) in 0.5 M sulphuric acid. Increasing the bromide ion concentration in this range caused an increase in absorbance with a maximum at 0.03 M; the absorbance decreased again for higher bromide concentrations.

Composition of the complex. Job's method of continuous variations [12, 13] and the mole ratio method [14] were used to determine the stoichiometry of the ion-pair complex. Job's method showed that the stoichiometric ratio of TPP^+ to $HgBr_3^-$ is 1:1 (Fig. 2). This was confirmed by the mole ratio method, which also showed that a [TPPP]/[Hg(II)] ratio higher than 10 is necessary for complete complex formation. The apparent stability constant of the complex was calculated from the results of the molar ratio and continuous variation methods [15, 16]; the average value was $\log K = 4.7 \pm 0.1$ at 20° C.

Extraction efficiency, stability and calibration range. The ratio by volume of aqueous phase to isopentyl acetate selected was 10:1. The extraction efficiency was 95.9%. The absorbances of the ion-pair complex extracted into isopentyl acetate remain constant if the solution is kept away from sunlight and ultraviolet radiation which affect the tetraphenylpyridinium cation [17].

When the recommended procedure is used, Beer's law is obeyed over the concentration range 0.04—0.5 μg ml^{-1} mercury. The optimum concentration range for spectrophotometric determinations, estimated by Ringbom's method is 0.15—0.4 μg ml^{-1}. The Sandell sensitivity is 7.6 × 10^{-3} μg cm^{-2}. The molar absorptivity is 2.63 × 10^{4} l mol^{-1} cm^{-1}. The standard deviations for 0.2 and 0.4 μg ml^{-1} mercury(II) (ten determinations each) were 0.0061 and 0.0065, respectively, and the relative errors were ±2.17% and ±1.15%, respectively.

Effect of other ions and application to sphalerites and zinc amalgams. For the determination of 0.4 μg ml^{-1} mercury(II) by this method, extraneous ions can be tolerated at the levels given in Table 2. The limiting value of the concentration of foreign ion was taken as that value which caused an error of not more than 2.5% in the absorbance values. Cations were added as chlorides, nitrates or sulphates, and anions as their sodium or potassium salts.

In order to increase the tolerance for iron(III), which is present in many mineral samples with mercury, tetrasodium diphosphate solution (0.05 M) can be added to the separating funnel and the absorbance measured against a reagent blank prepared in a similar way. Under these conditions iron(III) does not interfere up to a Fe(III):Hg(II) molar ratio of 10 000.

Gold(III) and thallium(III) cause the largest interferences. These interferences can be avoided by reducing the ions to gold metal and thallium(I), respectively. The best results were obtained with the use of hydroxylamine as a reducing agent for thallium in 0.05 M sulphuric acid, and sodium nitrite for reduction of gold(III); the excess of nitrite must be eliminated with urea.

The method was applied satisfactorily to the determination of mercury in different materials. For the analysis of sphalerites, the sample was dissolved in aqua regia, then sulphuric acid was added and the solution was boiled to white fumes. After transference of the solutions to calibrated flasks, mercury was determined by the recommended procedure. For one sample, the result was 0.0643% mercury, comparative with a result of 0.0640% obtained by

TABLE 2

Interference of other ions in the determination of mercury(II) (0.4 μg ml^{-1})

Ion added	Molar ratio [ion added]/[Hg(II)]	Ion added	Molar ratio [ion added]/[Hg(II)]
Sb(V)	20	Mn(II)	100
Bi(III)	2	Pt(IV)	10
Cd(II)	10	Ag(I)	0.1
Cr(III)	20 000	Tl(III)	0.02
Cu(II)	10 000	Zn(II)	10 000
Au(III)	0.02	Chloride	100 000
In(III)	1	Nitrate	1 000
Fe(III)	300	Perchlorate	1
Pb(II)	100	Sulphate	15 000

atomic absorption spectrometry. For the analysis of zinc amalgams, the sample was dissolved in nitric acid, and treated with sulphuric acid as before. For a typical amalgam, the result was 0.433% in agreement with a result of 0.438% obtained by a dithizone method.

REFERENCES

1 T. Pérez-Ruiz, C. Sánchez-Pedreño and J. A. Ortuño, Analyst (London), 107 (1982) 185.
2 J. A. Ortuño, T. Pérez Ruiz, C. Sánchez-Pedreño and P. Molina Buendía, Microchem. J., 30 (1984) 71.
3 B. Das and S. C. Shome, Anal. Chim. Acta, 35 (1966) 345.
4 F. Kai, Anal. Chim. Acta, 44 (1969) 242.
5 M. Tsubouchi, Anal. Chem., 42 (1970) 1087.
6 J. Holzbecher and D. E. Ryan, Anal. Chim. Acta, 64 (1973) 333.
7 K. Nakamura and T. Ozowa, Anal. Chim. Acta, 86 (1976) 147.
8 S. S. Yamamura, Anal. Chem., 32 (1960) 1896.
9 H. Woidich and W. Pfannhauser, Z. Anal. Chem., 261 (1972) 31.
10 M. Nabrzyski, Anal. Chem., 45 (1973) 2438.
11 G. Schwarzenbach and H. Flaschka, Complexometric Titrations, Methuen, London, 1969, p. 271.
12 P. Job, Liebigs Ann. Chem., 9 (1928) 113.
13 H. Irving and T. B. Pierce, J. Chem. Soc., (1959) 2565.
14 J. H. Yoe and A. L. Jones, Ind. Eng. Chem., Anal. Ed., 16 (1944) 111.
15 K. Momoki, J. Sekino, H. Sato and N. Yamaguchi, Anal. Chem., 41 (1969) 1286.
16 W. Likussar and D. F. Boltz, Anal. Chem., 43 (1971) 1265.
17 T. Pérez-Ruiz, C. Sánchez-Pedreño, J. A. Ortuño and P. Molina-Buendía, Analyst (London), 108 (1983) 733.

Analytica Chimica Acta, 165 (1984) 281—284
Elsevier Science Publishers B.V., Amsterdam — Printed in The Netherlands

Short Communication

THE STABILITY OF SULPHIDE ANTI-OXIDANT BUFFER

M. G. GLAISTER, G. J. MOODY, T. NASH and J. D. R. THOMAS*

Department of Applied Chemistry, Redwood Building, UWIST, PO Box 13, Cardiff CF1 3XF (Great Britain)

(Received 8th May 1984)

Summary. Chromatographic and titrimetric stability studies have been made of sulphide anti-oxidant buffer compositions incorporating ascorbic acid used as a sacrificial reducing agent in determinations of sulphide with a sulphide ion-selective electrode. The quality of the buffer is maintained for prolonged periods (4 weeks or more) by anaerobic storage under nitrogen.

Sulphide anti-oxidant buffer (SAOB), based on ascorbic acid in sodium hydroxide, is an important high-pH antioxidant medium for maintaining the level of sulphide ions in calibration standards and test samples during analysis with sulphide ion-selective electrodes. In the original specification from Orion Research (1969, 1970), SAOB was called standard anti-oxidant buffer and consisted of sodium hydroxide (80 g dm^{-3}), sodium salicylate (320 g dm^{-3}) and ascorbic acid (72 g dm^{-3}) in deionized water. The sodium salicylate is for masking some heavy metals by complexation [1] but Baumann [2] excluded it because it can contain copper and chromium impurities which would react with dissolved sulphide. Instead, she used an alkaline EDTA/ascorbate solution for sample treatment in the direct determination of sulphide at >30 $\mu g\ l^{-1}$ with the ion-selective electrode.

When used in analytical work involving sulphide, the ascorbic acid of SAOB prevents the oxidative loss of sulphide by its own oxidation to dehydroascorbic acid. By injecting aliquots of sulphide standards into a SAOB (20 g dm^{-3} ascorbic acid in 1 M sodium hydroxide) under a blanket of nitrogen, it is possible to calibrate an Orion 94-16A silver sulphide membrane electrode to ca. 2×10^{-7} M sulphide ions [3]. In this respect, Mosey and Jago [4] confirmed that at high pH (>12) the reducing power of ascorbic acid is adequate to prevent loss of sulphide by oxidation. However, concern over the short lifetime of SAOB prompted Donaldson and McMullan [5] to prepare and store SAOB under nitrogen. This study was, therefore, aimed at establishing the storage lifetimes of SAOB.

0003-2670/84/$03.00

Experimental

All materials were of the best analytical grades. Unless otherwise stated, the SAOB investigated consisted of sodium hydroxide (2 M) containing L-ascorbic acid (20 g dm^{-3}). The ascorbic acid content of the SAOB was determined by titration and paper chromatography was used to detect the presence of dehydroascorbic acid produced by spoilage. Deionized water was used throughout.

The paper chromatograms on Whatman No. 1 paper were developed under nitrogen with the upper layer of a butan-1-ol/acetic acid/water (4:1:5, v/v) mixture; they were visualized by first spraying with aqueous silver nitrate (0.1 M) and acetone (1:1, v/v) followed by aqueous sodium hydroxide (1 M) and 96% ethanol (1:1 v/v), and then exposing to the atmosphere for 1 h [6]. Visualization of chromatograms by exposure to iodine vapour was effective for ascorbic acid but not for dehydroascorbic acid.

The 2,6-dichlorophenolindophenol titrant (0.400 g dm^{-3} in water) used to determine ascorbic acid was standardized to the first permanent pink end-point against 10-cm^3 aliquots of a freshly prepared solution of L-ascorbic acid (0.200% w/v; BDH AnalaR grade) in nitrogen-saturated aqueous metaphosphoric acid solution (5% w/v). The titrimetric studies of stability were conducted on various solutions (Table 1), stored in stoppered containers, under nitrogen.

Ultraviolet-visible absorption spectra of ascorbic acid (6.2×10^{-5} M) in

TABLE 1

Ascorbic acid solutions used for titrimetric stability studies

Designation	Specification[a]
A	L-Ascorbic acid (0.23%) in metaphosphoric acid (5% w/v)
B	As for A but with only 0.11% L-ascorbic acid
C	L-Ascorbic acid (0.20%) in metaphosphoric acid (5% w/v); solution diluted (1 + 1, v/v) with sodium hydroxide (2 M)
D	L-Ascorbic acid (0.11%) in metaphosphoric acid (10% w/v) mixed (1 + 1 v/v) with sodium hydroxide (2 M)
E	L-Ascorbic acid (0.10%) in sodium hydroxide (1 M)
F	SAOB prepared by dissolving L-ascorbic acid (2.0%) in 250 cm^3 of nitrogen-saturated sodium hydroxide solution (2 M) and made up to 1 dm^3 with the same sodium hydroxide solution
G	SAOB prepared as for F but with containers flushed with nitrogen before introducing solutions; storage container also flushed with nitrogen on removal of the samples
H	SAOB prepared by dissolving L-ascorbic acid (8.0%) in nitrogen-saturated solution of 2 M sodium hydroxide also containing 32% sodium salicylate
I	SAOB prepared as in H but with the storage vessel left unstoppered in order to determine the effect of exposure to air

[a] All solutions are aqueous.

TABLE 2

Ascorbic acid contents of solutions shown in Table 1 after storage
(Data are means of 3 determinations with relative standard deviation <1%)

Solution	Storage time (h) and ascorbic acid content found (% w/v)[a]						
A	Time	0.0	0.7	1.9	4.0	5.6	25.4	
	Acid	0.228	0.229	0.231	0.229	0.228	0.225	
B	Time	0.0	0.2	1.3	2.1	5.5	24.3	
	Acid	0.110	0.110	0.109	0.108	0.108	0.107	
C	Time	0.0	0.1	0.4	0.9	1.5	2.0	4.1
	Acid	0.102	0.098	0.096	0.092	0.089	0.080	0.055
D	Time	0.0	0.5	1.1	3.7	23.2		
	Acid	0.106	0.098	0.096	0.093	0.067		
E	Time	0.0	0.5	1.6	2.3	4.8	24.5	
	Acid	0.103	0.102	0.098	0.094	0.086	0.049	
F	Time	0.0	0.1	1.8	3.5	16.8	24.9	49.3
	Acid	2.01	2.00	1.97	1.94	1.91	1.87	1.70
	pH	12.8	—	—	—	—	12.7	12.8
G	Time	0.0	24.7	47.5	165	216	313	673
	Acid	2.00	2.00	1.97	1.91	1.91	1.93	1.92
	pH	12.7	12.6	12.5	12.9	12.6	12.7	12.6
H	Time	0.0	192	360	509	648		
	Acid	8.00	7.54	7.46	7.49	7.69		
I	Time	0.0	192	312	336			
	Acid	8.01	7.52	7.39	7.30			

[a]And pH where varied.

5% metaphosphoric acid solutions with additions of up to 5×10^{-3} M sodium hydroxide were plotted with a Perkin-Elmer 402 spectrophotometer.

Results and discussion

Chromatographic studies. Paper chromatography of L-ascorbic acid (BDH) and dehydroascorbic acid (Fluka) gave R_f values of 0.40 and 0.11, respectively, consistent with previous work [6]. However, dehydroascorbic acid could not be detected in the alkaline SAOB solutions unless the pH was first brought to about 2.7 before the chromatograms were run. Then, paper chromatography gave two spots at 0.39 and 0.13 corresponding to L-ascorbic acid and dehydroascorbic acid, respectively, in SAOB exposed to air for three days, followed by pH adjustment. These data indicate that dehydroascorbic acid is a product of SAOB spoilage.

Titrimetric studies. The various ascorbic acid contents of solutions A to I of Table 1 with time are summarized in Table 2. They show that any stabilizing effect of metaphosphoric acid on L-ascorbic acid (Solutions A and B)

is ineffective under alkaline conditions (Solutions C and D) when, of course, metaphosphate will be present in the excess of sodium hydroxide. It is of interest that the main ultraviolet spectroscopic absorption of ascorbic acid at 244 nm in the presence of metaphosphoric acid alone shifts to 266 nm and intensifies when sodium hydroxide is added. The high intensity and broadness of the band under SAOB conditions causes absorption continuum up to about 500 nm which relates to the yellow to brown colour, according to age, of SAOB solutions. The dehydroascorbic acid absorption band at 193 nm in the presence of metaphosphoric acid and 200 nm when the solution is alkaline is a narrow one.

Solutions of SAOB themselves (Solution F) are fairly stable for periods of up to 24 h. However, the quality of SAOB can be maintained for longer periods by minimizing contact with air and oxygen as for solutions G and H. The recommendation that air and oxygen should be excluded during storage in order to promote stability of SAOB is well demonstrated by the data for solutions F and I when compared with the better preserved solutions, G and H, respectively.

The Science and Engineering Research Council is thanked for a studentship (to M.G.G.) within the CASE scheme in association with Interox Chemicals, Ltd. The authors also thank Mrs. G. E. Ellwell and Mr. J. W. Ogleby, Interox Chemicals, Ltd. for helpful discussions.

REFERENCES

1 H. Clysters and F. Adams, Anal. Chim. Acta, 83 (1976) 27.
2 E. W. Baumann, Anal. Chem., 46 (1974) 1345.
3 D. J. Crombie, G. J. Moody and J. D. R. Thomas, Anal. Chim. Acta, 80 (1975) 1.
4 F. Mosey and D. A. Jago, Water Research Centre, Stevenage Laboratory, Stevenage, Herts., Technical Report TR53, September, 1977.
5 E. L. Donaldson and D. C. McMullan, Anal. Lett., A11 (1978) 39.
6 G. J. Moody and J. D. R. Thomas, J. Food Technol., 14 (1979) 535.

Analytica Chimica Acta, 165 (1984) 285—289
Elsevier Science Publishers B.V., Amsterdam — Printed in The Netherlands

Short Communication

EFFECTS OF CONCENTRATION OF NEUTRAL CARRIER AND ADDITION OF ORGANOPHOSPHORUS COMPOUNDS ON ALKALI METAL ION-SELECTIVITY OF THE DIBENZO-14-CROWN-4 LIQUID-MEMBRANE ELECTRODE

TOSHIHIKO IMATO, MASAHIRO KATAHIRA and NOBUHIKO ISHIBASHI*

Department of Applied Analytical Chemistry, Faculty of Engineering, Kyushu University, Hakozaki, Higashi-ku, Fukuoka, 812 (Japan)

(Received 8th February 1984)

Summary. The lithium ion selectivity of the dibenzo-14-crown-4 (DB14C4) liquid-membrane electrode increases with the concentration of DB14C4 in the membrane. The lithium ion selectivity was enhanced by an addition of organophosphorus compounds such as trioctyl phosphine oxide.

The selectivity of a liquid-membrane electrode which has a sensing membrane consisting of a water-immiscible organic solution with an ion-exchange site and its counter-ion, depends mainly on the nature of the solvent and much less on the kind of ion-exchange site, as long as there is no specific strong interaction (e.g., chelate formation) between the ion-exchange site and the counter-ion [1—3]. However, Fujinaga and co-workers [4, 5] reported that addition of phenol derivatives to the membrane of the organic sulfonate-selective electrode suppressed interferences of inorganic anions. They explained that the hydrogen bonding between the primary sulfonate ion and the phenol derivative enhanced the selectivity of the electrode for sulfonate ions.

The present communication shows that selectivity for lithium ions can be enhanced by adding organophosphorus compounds to the membrane of the neutral-carrier electrode based on dibenzo-14-crown-4 (DB14C4). Olsher [6] described the lithium ion-selective electrode based on DB14C4 but did not study the effect of the carrier concentration in the membrane on the selectivity. Accordingly, this effect was also examined here.

Experimental

Chemicals. Dibenzo-14-crown-4 was synthesized according to Pedersen's procedure [7] and recrystallized twice from n-heptane. Melting point (146—148°C, uncorr.) and carbon/hydrogen results confirmed its purity.

Trioctyl phosphine oxide (TOPO; Dojin Laboratory), tricresyl phosphate (TCP; Kishida Kagaku) and dioctyloctyl phosphonate (DOOP; Daihachi

0003-2670/84/$03.00

Kagaku) were used as received. The other chemicals were of analytical grade and were used without further purification.

Preparation of the liquid membrane and the evaluation of selectivity coefficients. The solutions for the liquid membrane were prepared by dissolving DB14C4 in the concentration range 3.0×10^{-4}—3.0×10^{-2} M and sodium dipicrylaminate in the range 1.0×10^{-5}—1.0×10^{-4} M in nitrobenzene (M ≡ mol dm^{-3}). The organophosphorus compound was added to this nitrobenzene solution in order to examine the effects on the selectivity.

The selectivity coefficient of an ion M with reference to sodium ion, $K^{pot}_{Na,M}$ was evaluated, according to the separate solution method [8], by measurements of the e.m.f. of the following electrochemical cell:

(−)Ag/AgCl/1.0×10^{-3}—1.0×10^{-1} M MCl soln./liquid membrane/1.0×10^{-2} M NaCl soln./AgCl/Ag(+)

where M denotes Li^+, K^+, Rb^+, or Cs^+. Details of the construction of the cell have been given elsewhere [9]. Selectivity coefficients between the lithium ion and another alkali metal ion, $K^{pot}_{Li,M}$, were calculated from the observed $K^{pot}_{Na,M}$ and $K^{pot}_{Na,Li}$ values: $K^{pot}_{Li,M} = K^{pot}_{Li,Na} K^{pot}_{Na,M}$ and $K^{pot}_{Li,Na} = 1/K^{pot}_{Na,Li}$.

Results and discussion

The selectivity coefficients of liquid-membrane electrodes are well-known to vary with the concentrations of the aqueous sample solution and of the ion-exchange site in the electrode membrane. In the present work, however, the following arrangements were made to ensure that the selectivity coefficients were independent of the values of these parameters. Thus, the sodium ion was chosen as the counter-ion to the ion exchanger (dipicrylaminate) in the membrane, as described above. Among the alkali metals, the sodium ion is the least preferred by the DB14C4-containing membrane. Further, the concentration of the sodium ion in the membrane was kept lower than that of the other alkali metal ion in the sample solution. The membrane system thus produced may be considered as a bi-ionic system in which the additivity rule on the membrane potential holds, as has been shown by various workers [10—13].

When the electrode membrane is in contact with a sample solution, the sodium ion initially present as the counter-ion in the membrane may be exchanged with ion M in the aqueous solution. The superficial layer of the membrane next to the sample solution is converted to the M-ion form from the sodium ion form by ion exchange. In contrast, the ionic composition of the interfacial layer of the sample solution does not change essentially, because the amount of the sodium ion displaced from the membrane is very small compared to that of the M ion. Thus, the membrane system is converted.

MCl soln. aqueous phase	M^+ ion form ⋮ Na$^+$ ion form membrane phase	NaCl soln. aqueous phase

In this bi-ionic system, the additivity rule for the membrane potential, and the above equations for $K_{i,j}^{pot}$, have been experimentally confirmed as valid [10—13]. The selectivity coefficients obtained from these equations are shown in Fig. 1 as a function of the concentration of DB14C4, C_S^{tot}, in the membrane. As can be seen, $K_{Li,Na}^{pot}$ is almost constant in the range $10^{-3.5}$—$10^{-2.5}$ M DB14C4. In contrast, $K_{Li,K}^{pot}$, $K_{Li,Rb}^{pot}$ and $K_{Li,Cs}^{pot}$ decrease with increasing concentration of DB14C4 over the same range. The relationship between the selectivity coefficient and the neutral carrier concentration in such membranes has been treated theoretically as well as experimentally by Morf and Simon [3] and Jyo et al. [14]. Because DB14C4 was found to form a 1:1 complex with the lithium ion, by crystallographic analysis [15], then, according to theory [3, 14], the following three relations may hold between $K_{Li,M}^{pot}$ and C_S^{tot}, depending on the composition of the complex formed between M and DB14C4.

For no formation of complexes between M and DB14C4

$$\log K_{Li,M}^{pot} = \text{const.} - \log C_S^{tot} \tag{1}$$

For formation of the 1:1 complex

$$\log K_{Li,M}^{pot} = \text{const.} \tag{2}$$

For formation of the 2:1 complex

$$\log K_{Li,M}^{pot} = \text{const.} + \log C_S^{tot} \tag{3}$$

Therefore, the result shown in Fig. 1 indicates that the sodium ion forms the 1:1 complex with DB14C4, while the potassium, rubidium and cesium ions

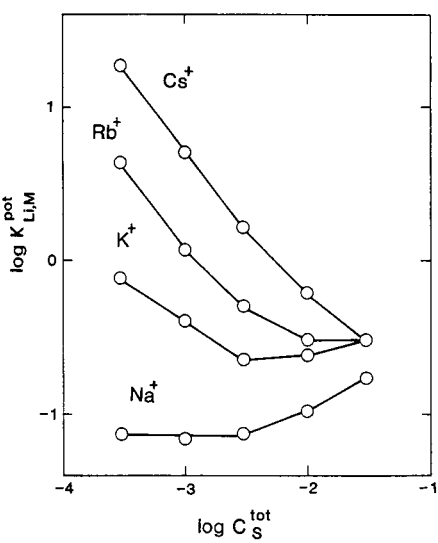

Fig. 1. Dependence of selectivity coefficients, $K_{Li,M}^{pot}$, on the concentration of DB14C4 in the membrane.

virtually do not form complexes in the DB14C4 concentration range below $10^{-2.5}$ M.

The situation is different at concentrations higher than $10^{-2.5}$ M. The value of $K^{pot}_{Li,Na}$ tends to increase with increasing concentration of DB14C4, which probably reflects the increasing tendency to formation of the 2:1 complex for the sodium ion, from the relations described above. Formation of the 2:1 complex has generally been observed when the cavity of a crown ether is smaller than the metal ion [16, 17]. Such observations led to the development of the potassium ion-selective electrode based on naphtho-15-crown-5, which has a selectivity almost the same as that of the valinomycin-based electrode [18]. In the present case, the cavity size of DB14C4 (1.2—1.5 Å [17]) is smaller than the crystallographic diameter of the sodium ion (1.9 Å). The $K^{pot}_{Li,Rb}$ and $K^{pot}_{Li,K}$ reach constant values at high concentrations of DB14C4. This suggests that rubidium and potassium ions form 1:1 complexes with DB14C4 at those concentration ranges.

The effects of the addition of TOPO, TCP and DOOP to the DB14C4-based membrane on the selectivity for lithium are shown in Table 1. The concentration of DB14C4 in the membrane was kept at 1.0×10^{-2} M. It is clear that the addition of these organophosphorus compounds enhances the lithium ion selectivity over the other alkali metal ions. This is presumably due to a synergic increase in the extractability of the complex by the organophosphorus compounds. Such synergic effects in liquid—liquid extraction have been observed for the systems dibenzo-18-crown-6/TOPO [19] and 15-crown-5/tributyl phosphate (TBP) [20]. Two molecules of TOPO or one molecule of TBP were found to be coordinated to Ag^+—DB18C6 or to Rb^+— and Cs^+—15C5 complexes and the extractability of the complexes was increased. In the present case, it may be considered that the lithium ion enters

TABLE 1

Effect of organophosphorus compounds on the selectivity of the DB14C4-based liquid-membrane electrode for lithium over other alkali metals[a]

Added compound	Concentration (M)	$K^{pot}_{Li,M}$			
		Na^+	K^+	Rb^+	Cs^+
None		0.10	0.25	0.30	0.60
TOPO	1.0×10^{-3}	0.063	0.13	0.17	0.30
	5.0×10^{-3}	0.036	0.062	0.075	0.14
	1.0×10^{-2}	0.027	0.044	0.048	0.082
TCP	1.0×10^{-2}	0.087	0.19	0.25	0.55
	5.0×10^{-2}	0.041	0.052	0.052	0.082
DOOP	1.0×10^{-2}	0.066	0.13	0.15	0.31
	5.0×10^{-2}	0.046	0.062	0.071	0.12

[a]Concentration of DB14C4 in the membrane is 1.0×10^{-2} M.

the cavity of DB14C4 and the resulting cationic complex is coordinated with an oxygen atom of the organophosphorus compound. The coordination of the organophosphorus compounds may be stronger for the lithium ion complex because of its higher charge density compared to the other cations.

The sequence of enhancement for the lithium ion selectivity is TOPO > DOOP > TCP, which is in accordance with the basicity of the oxygen atom of the organophosphorus compounds. Further detailed investigations are in progress.

The authors are grateful to Daihachi Kagaku Co., for the supply of DOOP, and to the Ministry of Education and the Asahi Garasu Kogyo Gijutsu Shoreikai for financial support.

REFERENCES

1 W. E. Morf, D. Amman, E. Presch and W. Simon, Pure Appl. Chem., 36 (1973) 421.
2 A. Jyo, H. Mihara and N. Ishibashi, Denki Kagaku, 44 (1976) 268.
3 W. E. Morf and W. Simon, in H. Freiser (Ed.), Ion-Selective Electrode in Analytical Chemistry, Vol. 1, Plenum Press, 1978, p. 211.
4 T. Fujinaga, S. Okazaki and H. Hara, Chem. Lett., (1978) 1201.
5 H. Hara, S. Okazaki and T. Fujinaga, Bull. Chem. Soc. Jpn., 53 (1980) 3610.
6 U. Olsher, J. Am. Chem. Soc., 104 (1982) 4006.
7 C. J. Pedersen, J. Am. Chem. Soc., 89 (1967) 7017.
8 G. J. Moody and J. D. R. Thomas, Selective Ion Sensitive Electrode, Merrow, Watford, Herts., 1971, p. 13.
9 N. Ishibashi and H. Kohara, Anal. Lett., 4 (1971) 785.
10 G. Shean and K. Sollner, J. Membr. Biol., 9 (1972) 297.
11 G. M. Shean, J. Membr. Sci., 2 (1977) 133.
12 A. Jyo, M. Torikai and N. Ishibashi, Bull. Chem. Soc. Jpn., 47 (1974) 2862.
13 N. Yoshida and N. Ishibashi, Bull. Chem. Soc. Jpn., 50 (1977) 3189.
14 A. Jyo, H. Seto and N. Ishibashi, Nippon Kagaku Kaishi, (1980) 1423.
15 G. Shoham, W. N. Lipscom and U. Olsher, J. Chem. Soc., Chem. Commun., (1983) 208.
16 C. J. Pedersen and H. K. Frensdorff, Angew. Chem. Int. Ed. Engl., 11 (1972) 16.
17 C. J. Pedersen, J. Am. Chem. Soc., 92 (1970) 386.
18 M. Yamauchi, A. Jyo and N. Ishibashi, Anal. Chim. Acta, 136 (1982) 399.
19 Y. Hasegawa, K. Suzuki and T. Sekine, Chem. Lett., (1981) 1075.
20 Y. Takeda, Bull. Chem. Soc. Jpn., 54 (1981) 526.

Analytica Chimica Acta, 165 (1984) 291—296
Elsevier Science Publishers B.V., Amsterdam — Printed in The Netherlands

Short Communication

FLOW INJECTION ANALYSIS FOR GLUCOSE BY THE COMBINED USE OF AN IMMOBILIZED GLUCOSE OXIDASE REACTOR AND A PEROXIDASE ELECTRODE

TOSHIO YAO*, MINORU SATO, YOSHIAKI KOBAYASHI and TAMOTSU WASA

Department of Applied Chemistry, College of Engineering, University of Osaka Prefecture, Mozu-Umemachi, Sakai 591 (Japan)

(Received 20th February 1984)

Summary. The amperometric peroxidase electrode measures hexacyanoferrate(III), produced by hydrogen peroxide, which is generated by injecting a 2-μl sample into a reactor of immobilized glucose oxidase covalently bound to silica gel. The peak current is linearly related to the glucose concentration in the range 0.05—10 g l^{-1}; sample throughput is about 100 h^{-1}. Ascorbic acid ($\leq$ 0.5 mM) does not interfere.

Recently, several enzymatic methods for glucose determination in flow systems have been reported [1—5], and glucose oxidase is frequently employed because of its high selectivity for β-D-glucose. The immobilization of glucose oxidase provides a preparation that combines high selectivity with increased stability. In addition, if the immobilized enzyme is used in a continuous flow system, handling is minimized, reproducibility is enhanced and the enzyme can be re-used.

The glucose is oxidized in the presence of glucose oxidase, producing hydrogen peroxide. In the commonest methods, the hydrogen peroxide is monitored electrochemically at flow-through solid electrodes [3, 6]. As the anodic oxidation of the hydrogen peroxide is irreversible, the electrodes operate at a high potential (0.6—0.7 V vs. Ag/Ag^+ [7]). At such a potential, other electroactive species (ascorbic acid, uric acid, etc.) in biological fluids are oxidized. Therefore, to remove such interfering substances, a precolumn packed with copper(II) dithiocarbamate-modified silica gel [6, 8] or an electrolytic column [9] should be positioned just before the flow-through electrode.

In this communication, the hydrogen peroxide generated by the glucose oxidase reactor produces hexacyanoferrate(III) at a peroxidase electrode, constructed by cross-linking peroxidase with bovine serum albumin using glutaraldehyde on a platinum sheet silanized with 3-aminopropyltriethoxy silane.

$$H_2O_2 + 2Fe(CN)_6^{4-} + 2H^+ \xrightarrow{\text{peroxidase}} 2H_2O + 2Fe(CN)_6^{3-}$$

$$Fe(CN)_6^{3-} + e^- \rightarrow Fe(CN)_6^{4-}$$

The hexacyanoferrate(III) is measured amperometrically. As the electrode operates at a low potential (ca. —50 mV vs. Ag/Ag^+), there is little interference from other constituents normally present in biological fluids. Also, this peroxide electrode has a fairly rapid response, long-term stability and good reproducibility as an electrochemical detector in a flow-injection system.

Experimental

Reagents. Glucose oxidase (EC.1.1.3.4, 43.4 I.U. mg^{-1}, from *Aspergillus niger*) and peroxidase (EC.1.11.1.7, 100 I.U. mg^{-1}, from Horseradish) were obtained from Amano Pharmaceutical Co. and Boehringer-Mannheim Yamanouchi K.K., respectively. Bovine serum albumin (BSA, 96—99% albumin), glutaraldehyde and 3-aminopropyltriethoxysilane were as described previously [6]. ORTHO control sera (Ortho Diagnostic Systems) were used as standards. Aqueous stock solutions (10 g l^{-1}) of D-glucose were allowed to mutarotate overnight before use. All other chemicals were of analytical-reagent grade.

Preparation of glucose oxidase reactor. The method was similar to that described previously [10]. Silica gel (Wakogel C-200) previously boiled in 6 M hydrochloric acid was refluxed with stirring in a 10% (v/v) solution of 3-aminopropyltriethoxysilane in toluene. The resulting alkylamino-bonded silica gel was activated before glucose oxidase was bound by reaction with an aqueous 5% (v/v) solution of glutaraldehyde. The preparation was packed into glass tubing (5 mm × 4 mm i.d.), and glucose oxidase was loaded covalently by circulating a 5-ml solution of enzyme (43 U ml^{-1}) in acetate buffer solution (0.1 M, pH 5.5) at 1.0 ml min^{-1} for 12 h at room temperature. The total activity of the resulting reactor was 0.55 U.

Preparation of peroxidase electrode. On one side of a platinum sheet (1 × 2 cm), silanized as described previously [11], 2 μl of aqueous 10% (w/v) BSA and a 4 μl of 4% (w/v) peroxidase in 0.1 M phosphate buffer, pH 7.0, were mixed with 2 μl of aqueous 4% (v/v) glutaraldehyde. The solutions were spread and the membrane was allowed to form for 2 h at room temperature, open to the air. In this way, peroxidase cross-linked with BSA was bound by glutaraldehyde to the alkylamino-bonded platinum. The amperometric flow cell was assembled with the peroxidase-BSA membrane attached to the platinum sheet over the glassy carbon working electrode of a Yanagimoto thin-layer electrochemical flow cell, which also had a silver—silver chloride reference electrode and a platinum auxiliary electrode.

Flow system and procedures. The flow system was similar to that described previously [6]. The immobilized glucose oxidase reactor was positioned just after the point of sample injection and before the flow-through peroxidase electrode. A constant potential (—50 mV vs. Ag/Ag^+) was applied to the

peroxidase electrode with a Yanagimoto potentiostat (VMD-101), and current was measured with a strip-chart recorder (Hitachi 056-3001). A phosphate buffer (0.1 M, pH 5.5) which was 0.1 M in sodium chloride and 1 mM in potassium hexacyanoferrate(II)) served as the carrier solution and was pumped at 1.5 ml min^{-1}.

Sample solutions (2 μl) were injected with a microsyringe and glucose was estimated from the current peak height. A calibration graph was prepared from the results obtained with standard glucose solutions.

Results and discussion

Optimization of experimental conditions. Experiments were conducted to establish the optimum pH under flow conditions. Acetate and phosphate buffers at various pH values, 0.1 M in sodium chloride and 1 mM in potassium hexacyanoferrate(II), were tested as the carrier solution. Figure 1 shows the effect of pH on peak current. Maximum activity of the peroxidase electrode occurred at a low pH, close to 3.5; the maximum activity of the glucose oxidase reactor was at pH 7.5 [10]. Therefore, maximum response was obtained at pH ca. 5.5 in the present flow system, which comprised the glucose oxidase reactor and the peroxidase electrode; this pH was used in all later work.

The response current in the present system at a constant glucose concentration depended on the concentration of the hexacyanoferrate(II), which acts as the mediator. As its concentration in the carrier solution was raised

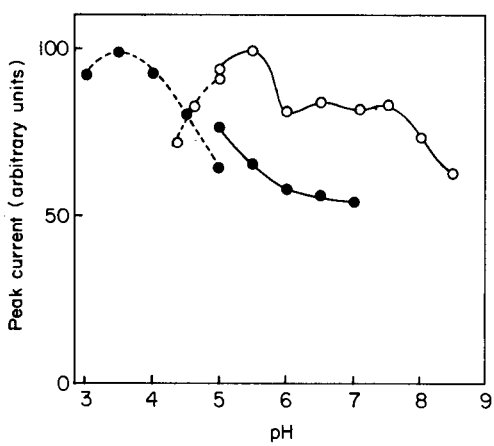

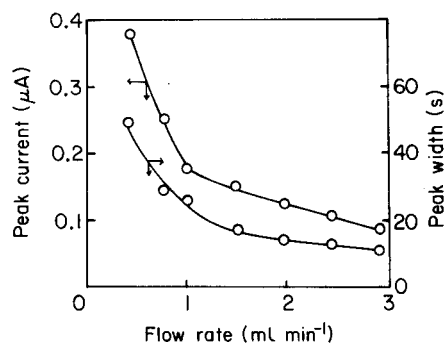

Fig. 1. Effect of pH of the carrier solution on the peak current for (○) glucose and (●) hydrogen peroxide; (——) 0.1 M phosphate buffer; (— — —) 0.1 M acetate buffer. (Flow rate 1.5 ml min^{-1}; applied potential −50 mV vs. Ag/Ag^{+}; 2-μl injections of 1 gl^{-1} glucose and 0.91 mM H_2O_2.)

Fig. 2. Effect of flow rate on peak current and peak width (time to return to baseline for glucose injections).

from 0.1 to 1 mM, the peak current increased, becoming almost constant at higher concentrations. Therefore, 0.1 M phosphate buffer (pH 5.5), 0.1 M in sodium chloride and 1 mM in potassium hexacyanoferrate(II), was selected as the carrier solution.

Figure 2 shows the effect of the buffer solution flow rate on the peak current and on the peak width. As the flow rate decreased, the peak current increased. However, the time required for determination became excessive at low flow rates and a flow rate of 1.5 ml min^{-1} is recommended. This provides relatively good sensitivity and reasonable sample throughput (ca. 180 h^{-1}).

Calibration. Figure 3 is a typical recording of 2-μl injections of standards, and sera and spiked urine samples under the recommended conditions. There was no carry-over from high to low concentrations. A linear calibration graph was obtained over the range 0.05—10 g l^{-1} for 2-μl injections; the slope, y-intercept and linear correlation coefficient (6 results) were 56.4 nA l g^{-1}, —1.99 nA and 0.9998, respectively.

Selectivity and interferences. Glucose oxidase is specific for β-D-glucose, so this method offers high selectivity for glucose over other sugars; the selectivity coefficient was less than 10^{-4} for glucose over fructose, lactose, sucrose, galactose, mannose, xylose and arabinose. However, because oxidizable species in the serum may reduce some of the hexacyanoferrate(III) that is produced enzymatically by the peroxidase electrode, these substances were

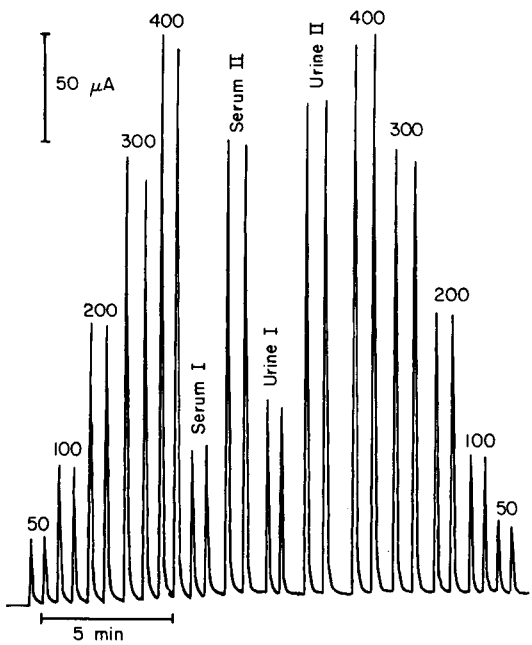

Fig. 3. Typical signals for duplicate 2-μl injections of five standard solutions of glucose (50—400 mg dl^{-1}) followed by two sera and two urine samples spiked with a standard solution, and repetition of the five standards.

studied for interferences with the amperometric enzymatic assay for glucose. The results are shown in Table 1. It can be seen that there is no interference from substances other than ascorbic acid. A normal value for ascorbic acid in human serum is 0.01—0.11 mM, and concentrations (>0.5 mM) much higher than this normal value do interfere, presumably by reducing the hexacyanoferrate(III) that is to be measured electrochemically.

Reproducibility and accuracy. The reproducibility of the results was tested by measurements on repeated 2-μl injections of glucose standard solutions, control sera and human urine spiked with glucose, at an injection rate of 100 samples h^{-1} (Table 2). The relative standard deviation was less than 2% for all samples. Also, the average amount of glucose found in the control sera closely agreed with the manufacturer's data.

Glucose levels in human blood serum were determined by the proposed method and with a commercial glucose analyzer (Glucoroder-S, Analytical Instruments Co., Tokyo) which is routinely used at some hospitals. The Pearson correlation coefficient between the two methods was found to be

TABLE 1

Effect of addition of other substances on the response to a 1 g l^{-1} glucose solution

Substance added	Level tested (mM)	Relative response	Substance added	Level tested (mM)	Relative response
None	—	100	Ascorbic acid	0.2	100.0
Uric acid	1.0	100.3		0.4	99.8
Glutathione	1.0	99.6		0.6	97.8
Tyrosine	1.0	100.0		1.0	91.2
Cysteine	1.0	101.4		1.8	80.4
Bilirubin	10.0[a]	101.2			

[a]mg l^{-1}.

TABLE 2

Reproducibility and accuracy of measurements on glucose solutions, control sera and human urine spiked with glucose (10 measurements on each solution)

Sample type	Glucose standard			Control serum		Urine	
Glucose taken (mg dl^{-1})	50	100	300	96.7 ± 7	317 ± 15	100	300
Glucose found (mg dl^{-1})							
Mean	29.0[a]	61.7[a]	189[a]	104	322	103	306
S.d.	0.6	0.5	2.3	1.8	5.2	1.6	4.0
R.s.d. (%)	2.1	0.8	1.2	1.8	1.6	1.6	1.3

[a]Calibration data; mean and s.d. given in nA.

0.998 (20 pairs of results). The slope obtained by linear regression was 0.968 and the y-intercept was 0.03 g l^{-1}.

The enzyme reactor and peroxidase electrode were used repeatedly to assess their stability with time. When not in use, they were stored at 4° C in 0.1 M phosphate buffer (pH 6.0). Stability was good; even after repetitive use for 6 months for the glucose oxidase reactor and for 2 months for the peroxidase electrode, they retained over 90% of their original activities.

REFERENCES

1 M. D. Joseph, D. J. Kasprzak and S. R. Crouch, Clin. Chem., 23 (1977) 1033.
2 C. M. Wolff and H. A. Mottola, Anal. Chem., 50 (1978) 94.
3 B. Watson, D. N. Stifel and F. E. Semersky, Anal. Chim. Acta, 106 (1979) 233.
4 D. Pilosof and T. A. Nieman, Anal. Chem., 54 (1982) 1698.
5 P. J. Worsfold, Anal. Chim. Acta, 145 (1983) 117.
6 T. Yao, Anal. Chim. Acta, 153 (1983) 175.
7 G. G. Guilbault and G. J. Lubrano, Anal. Chim. Acta, 64 (1973) 439.
8 T. Yao, Anal. Chim. Acta, 153 (1983) 169.
9 T. Yao, Y. Kobayashi and M. Sato, Anal. Chim. Acta, 153 (1983) 337.
10 T. Yao and Y. Kobayashi, Bunseki Kagaku, 32 (1983) 253.
11 T. Yao, Anal. Chim. Acta, 148 (1983) 27.

Analytica Chimica Acta, 165 (1984) 297—301
Elsevier Science Publishers B.V., Amsterdam — Printed in The Netherlands

Short Communication

SEGMENTED APPROXIMATION OF INTERFERENCE EFFECTS IN ATOMIC ABSORPTION SPECTROMETRY

P. KOŚCIELNIAK and A. PARCZEWSKI*
Department of Analytical Chemistry, Jagiellonian University, Krakow (Poland)
(Received 5th March 1984)

Summary. A segmented approximation method is used for empirical modelling of interference effects in atomic absorption spectrometry. First- and second-degree polynomials are used in the modelling. The examples presented concern the determination of iron in presence of sodium, and calcium in the presence of strontium. In each case, the split polynomial models are more accurate and reliable than the single high-degree polynomial models.

The relationship between a measured analytical signal (or its function), R, and the concentrations of n sample components, $c_1, \ldots, c_n$, can be approximated by the following empirical polynomial model [1, 2]

$$\hat{R} = \sum_{i=0}^{n} B_i \bar{c}_i + \sum_{\substack{i,j=1 \\ (i \leqslant j)}}^{n} B_{ij} \bar{c}_i \bar{c}_j + \ldots \qquad (\bar{c}_0 \neq 1) \tag{1}$$

where $\bar{c}_i = f_i(c_i)$ $(i = 1, \ldots, n)$. The regression coefficients B in model (1) are evaluated on the basis of the results of measurements done on standard solutions with compositions corresponding to a selected plan, e.g., a $k_1 \times k_2 \times \ldots \times k_n$ (in particular k^n) factorial [2].

In the conventional approach, linear relations of $\bar{c}_i$ and c_i are applied:

$$\bar{c}_i = (2c_i - c_i^{(u)} + c_i^{(l)})/(c_i^{(u)} - c_i^{(l)}) \tag{2}$$

where $c_i^{(l)}$ and $c_i^{(u)}$ denote the assumed lower and upper concentration levels of the ith component. Recently, nonlinear (e.g., logarithmic) functions f_i have been applied [1, 2]

$$\bar{c}_i = \log_{q_i}\{[(q_i^2 - 1)(c_i - c_i^{(l)}) + (c_i^{(u)} - c_i^{(l)})]/q_i(c_i^{(u)} - c_i^{(l)})\} \tag{3}$$

where q_i is an empirical parameter. Both Eqns. 2 and 3 satisfy the following coding conditions: $\bar{c}_i^{(l)} = f_i(c_i^{(l)}) = -1$, $\bar{c}_i^{(u)} = f_i(c_i^{(u)}) = 1$, and $\bar{c}_i^{(o)} = f_i(c_i^{(o)}) = 0$ for the linear relation (2), where $\bar{c}_i^{(o)} = (c_i^{(l)} + c_i^{(u)})/2$, or $\bar{c}_i^{*} = f_i(c_i^{*}) = 0$ for Eqn. 3, where $\bar{c}_i^{*} = (c_i^{(u)} + c_i^{(l)} \cdot q_i)/(q_i + 1)$. The coordinate c_i^{*} is the counterpart of the geometrical centre, $c_i^{(o)}$, of the conventional plan. The unconventional plans are asymmetrical in the coordinates system of actual

concentrations, c_i, but can be made symmetrical in the system of coded coordinates, $\bar{c}_i$, by formulae such as Eqn. 3.

Model (1) proved to be very effective in approximation of the "regular" responses $R = f(c_1, \ldots, c_n)$. However, it usually fails when the dependence of R on the concentration of interfering species is complex, especially when broad concentration ranges are considered. In Figs. 1 and 2, the measured dependences of R on c (concentration of an interfering species) are presented by solid lines [3] and the models $\hat{R}$ are presented by dashed lines. These examples are concerned with interferences in atomic absorption spectrometry (a.a.s.). Clearly, the models $\hat{R}$, based on logarithmic concentrations (Eqn. 3), fit the experimental lines more accurately than the conventional models.

In general, the approximation of complex responses such as those shown in Figs. 1 and 2 by a single polynomial model $\hat{R}$ is ineffective. Accordingly, the application of segmented approximation based on experimental design is proposed here; the method was previously applied in examination of the homogeneity of solids [4]. The method is illustrated in Figs. 1B and 2B.

Experimental

Method. As indicated above, the concentration space (intervals of concentrations of the sample components) is divided into segments and the response

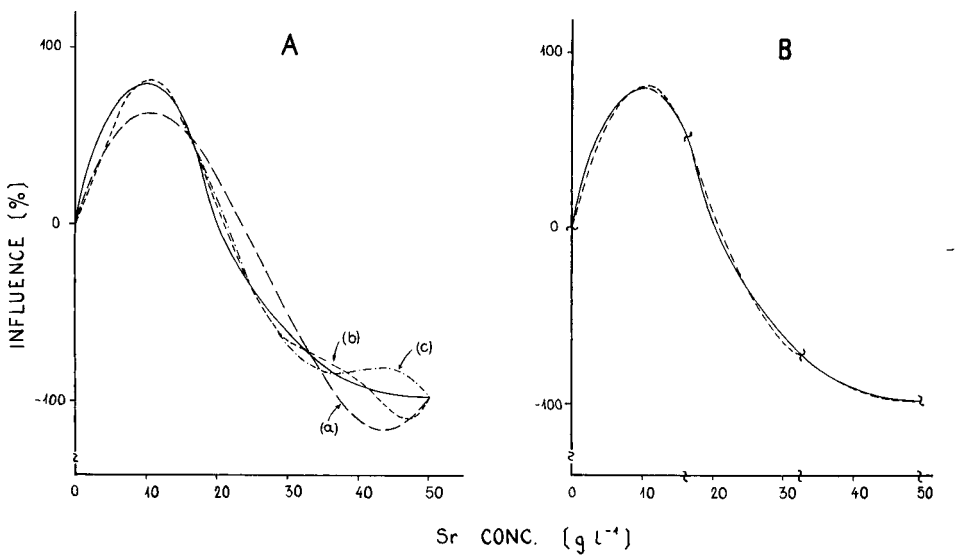

Fig. 1. Interfering effect of strontium on the determination of calcium by a.a.s.: (—) experimental; (---) calculated from the empirical model $\hat{R}$. (A) Curves: (a) conventional third-degree model based on a symmetrical 4^1 factorial; (b) conventional sixth-degree model (symmetrical 7^1 factorial); (c) unconventional sixth-degree model (asymmetrical 7^1 factorial with logarithmic strontium concentrations as in Eqn. 3 with q = 1.95). (B) Segmented approximation by three conventional second-degree models (dashed lines), each model being based on 3^1 factorials; the division points are marked by wavy lines.

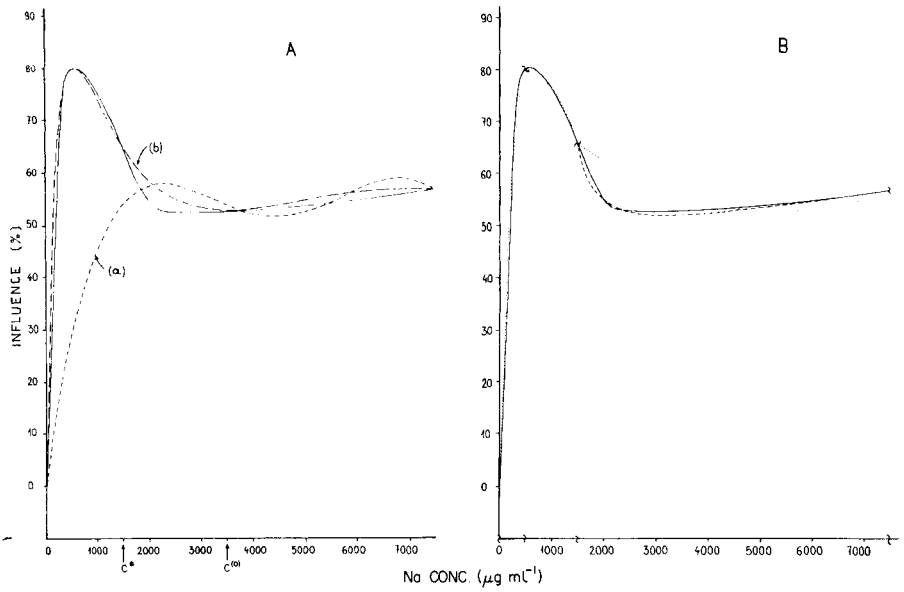

Fig. 2. Interference of sodium on the determination of iron by a.a.s.: (—) experimental; (---) calculated from the empirical model $\hat{R}$. (A) Curves: (a) conventional fourth-degree model based on symmetrical 5^1 factorial; (b) unconventional fourth-degree models based on asymmetrical 5^1 factorials with logarithmic sodium concentration as in Eqn. 3 for $q = 4$. (B) Segmented approximation: (—) experimental line; (···) approximation by three conventional second-degree polynomials; (---) unconventional model applied in the 1500—7500 μg ml^{-1} range.

$R = f(c_1, \ldots, c_n)$ is approximated in each segment separately by a simple polynomial (of the first or second degree). For example, in Fig. 1B the interval 0—50 g l^{-1} strontium is divided into three segments (0—1.66, 1.66—3.33, 3.33—5); in each segment (sub-interval) the relationship R vs. c_{Sr} is approximated by the conventional second-degree model on the basis of three experimental results in each interval (in all, seven results were used in the modelling). In Fig. 2B, the concentration interval 0—7500 μg ml^{-1} sodium is divided into three unequal intervals (0—500, 500—1500, 1500—7500). In each interval, the experimental line is approximated by the conventional second-degree model; the third segment (interval 1500—7500) is also approximated by the unconventional second-degree model based on logarithmic sodium concentration (Eqn. 3). The segmented approximation presented in Fig. 1B should be compared with the single model presented in Fig. 1A, based also on seven experimental results.

The efficiency of the segmented approximation depends not only on how the concentration intervals are divided into segments but also on the degree of the models applied and on the composition of standards (applied plans) used in formulation of these models. The split models meet each other at the

border lines indicated on the figures only when all possible terms (regression coefficients B) in the models of the same degree are taken into account (no degrees of freedom for lack of fit); if not, discontinuity appears at the border lines (see below).

Examples. An atomic absorption spectrometer (AAS-1; C. Zeiss, Jena) was used under standard conditions with an air—acetylene flame. Triplicate readings of the absorbance of iron at 259.9 nm were taken for each solution. The compositions of the standard samples used in formulation of the models $\hat{R}$ and in testing of these models are presented in Fig. 3.

The following two $\hat{R}$ models were tested ($c_1 = c_{Fe}$, $c_2 = c_{Na}$)

$$\hat{R}_1 = B_0 + B_1\bar{c}_1 + B_2\bar{c}_2 + B_{12}\bar{c}_1\bar{c}_2 \tag{4}$$

based on the 2^2 factorial, and

$$\hat{R}_2 = B_0 + B_1\bar{c}_1 + B_2\bar{c}_2 + B_{12}\bar{c}_1\bar{c}_2 + B_{22}\bar{c}_2^2 + B_{122}\bar{c}_1\bar{c}_2^2 \tag{5}$$

based on 2×3 factorial [2], where $\bar{c}_1$ and $\bar{c}_2$ are related to c_1 and c_2, respectively, as in Eqn. 2. In the segmented approximation, the response R was approximated by two models: (a) Eqn. 5 in the concentration ranges 2.5—10 μg ml^{-1} iron and 0—2.5 μg ml^{-1} sodium, and (b) Eqn. 4 in the concentration ranges 2.5—10 μg ml^{-1} iron and 2.5—25 μg ml^{-1} sodium. In Fig. 4, the results of segmented approximation are compared with the simple second-degree model (Eqn. 5) spread over the whole (original) concentration ranges of 2.5—10 μg ml^{-1} iron and 0—25 μg ml^{-1} sodium.

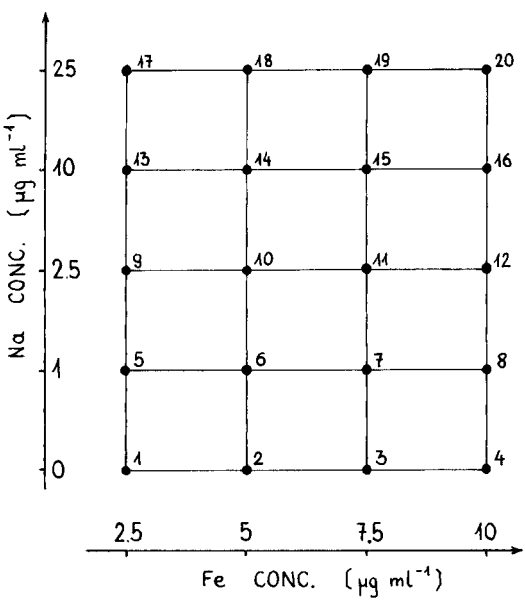

Fig. 3. The compositions of standard solutions used in the tests.

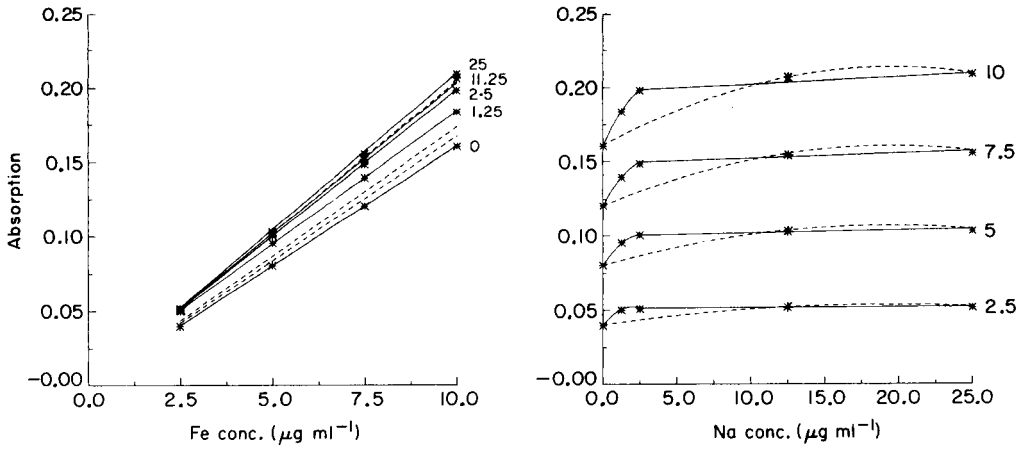

Fig. 4. Approximations of the response $R = f(c_{Fe}, c_{Na})$ by a single second-degree model (dashed lines) based on 2 × 3 factorial (solutions 1, 4, 13, 16, 17, and 20 in Fig. 3), and two models (solid lines): a second-degree model (Eqn. 5) based on a 2 × 3 factorial (solutions 1, 4, 5, 8, 9, and 12), and a first-degree model (Eqn. 4) based on a 2^2 factorial (solutions 9, 12, 17, and 20). Experimental results are denoted by asterisks.

Discussion

The segmented approximation method makes it possible to use experimental designs and simple polynomial models of the first and/or second-degree in empirical modelling. The method is especially useful in approximation of a complex response surface. The regression coefficients in the models are readily calculated with a simple calculator. Programs for the computer (programmable calculator) are easily prepared and handled.

The high efficiency of segmented approximation in modelling of interference effects in a.a.s. is clearly seen in Figs. 1 and 2, where the single polynomial models of high (up to sixth) degree are compared with the split function composed of three second-degree models. The adequacy and reliability of the segmented model are clearly better than those of the single polynomial model. Obviously, some preliminary information on the response surface is necessary to make the segmented approximation fully successful, but this requirement is relevant to all methods of empirical modelling.

REFERENCES

1 P. Kościelniak and A. Parczewski, Anal. Chim. Acta, 153 (1983) 103, 111.
2 P. Kościelniak and A. Parczewski, Chem. Anal. (Warsaw), in press.
3 M. Pinta, Spectrometrie D'Absorption Atomique, Masson, Paris, 1971.
4 A. Parczewski, Anal. Chim. Acta, 130 (1981) 221.

ANALYTICA CHIMICA ACTA, VOL. 165 (1984)

AUTHOR INDEX

ACA announcements

ANNOUNCEMENTS OF MEETINGS

36th PITTSBURGH CONFERENCE AND EXPOSITION ON ANALYTICAL CHEMISTRY AND APPLIED SPECTROSCOPY, NEW ORLEANS, LA, U.S.A., FEBRUARY 25–MARCH 1, 1985

The following symposia have already been arranged for the 1985 technical programme: ASTM E-42 Small Area Solid and Surface Analysis; Analysis of Toxic Wastes Combined with Water Pollution Analysis; Near Infrared Analysis; New Dimensions in Particle Size and Shape Technologies; Flow Injection Analysis; New Advances in Raman Spectroscopy; Analytical Applications of Micellar Solutions; Reaction Detectors in Liquid Chromatography; Fiber Optics/Lasers; Computers; Planar Chromatography; Biomedical Spectroscopy.

The Pittsburgh Conference and Exposition is the forum for presentation of major awards to distinguished scientists. The Awards symposia planned for the 1985 Pittsburgh Conference and Exposition are: (1) Pittsburgh Spectroscopy Award sponsored by the Spectroscopy Society of Pittsburgh; (2) Pittsburgh Analytical Chemistry Award sponsored by the Society for Analytical Chemists of Pittsburgh; (3) Charles N. Reilley Award sponsored by the Society for Electroanalytical Chemistry; (4) The Williams-Wright Industrial Spectroscopist Award sponsored by the Coblentz Society; (5) Maurice F. Hasler Award sponsored by Spectroscopy Systems, Division of Bausch and Lomb.

Further information: David R. Weill III, Publicity Chairman, Shady Side Academy, 423 Fox Chapel Road, Pittsburgh, PA 15238, U.S.A.

AMSTERDAM SUMMERSCHOOL ON HPLC, AMSTERDAM, THE NETHERLANDS, JUNE 17–21, 1985

The above-mentioned course will be held at the University of Amsterdam.

This international course will provide a coherent overview of high-performance liquid chromatography as analytical and preparative technique.

Fundamental aspects on theory and instrumentation will be treated in main lectures and seminars by leading international experts in the field. The course includes practical experiments in order to illustrate the potential of the technique. The Summerschool will be organized by the separation group of Prof. H. Poppe and Dr. J.C. Kraak. The official language will be English.

Information and registration through the Municipal Congress Bureau, Oudezijds Achterburgwal 199, 1012 DK Amsterdam, The Netherlands. Tel.: 020 - 552.3458/59.

STATISTICAL METHODS IN ANALYTICAL CHEMISTRY, INTERNATIONAL SUMMER SCHOOL, MERSEBURG, G.D.R., JUNE 24–29, 1985

The "Carl Schorlemmer" Technical University of Leuna-Merseburg will hold a Summer School in "Statistical Methods in Analytical Chemistry". The main problems will be: the evaluation of analytical procedures; the treatment of analytical data.

After a short revision of fundamental mathematical procedures the following themes will be discussed: measurements and quality of products through the estimation of confidence intervals; deriving decisions from statistical tests; planning and evaluation of a round robin; treatment of linear and non-linear calibration functions; detection of systematic errors.

Possibilities of application are the main topic, and they will be demonstrated by examples from the chemical industry. Additional lectures will provide information on developments and experience in special fields, e.g.: application of pattern recognition; statistical optimization in analytical chemistry; possibilities of auto-correlation and cross-correlation functions; queuing problems for optimizing the organisation of a laboratory; description of analytical procedures by a graph; testing homogeneity.

The Summer School will include a micro symposium on June 28th in order to present and to discuss new results of research.

The Summer School will be under the guidance of Dr. sc. nat. K. Doerffel, Professor of the Department of Chemistry and leader of the group "Chemimetrics" in the G.D.R. All lectures at the Summer School will be held in English.

8th INTERNATIONAL CONFERENCE ON THERMAL ANALYSIS, BRATISLAVA, CZECHOSLOVAKIA, AUGUST 19–23, 1985

The 8th International Conference on Thermal Analysis will be organized in Czechoslovakia by decision of the International Confederation for Thermal Analysis (ICTA). It has the sponsorship of the International Union of Pure and Applied Chemistry. The conference will include the 10th Czechoslovak Conference on Thermal Analysis (TERMANAL '85). The International Conferences on Thermal Analysis, with their twenty years of tradition, are concerned with recent progress in the field of thermal analysis and its application. Material scientist and engineers, solid-state physicists, physical chemists, metallurgists, ceramists, mineralogists as well as chemists working in various fields of organic and macromolecular chemistry and technology find topics of interest.

The conference language will be English. Plenary and award lectures are expected. The majority of papers will be presented as posters. All papers – not exceeding four papers – will be published in the Proceedings of the Conference.

Accommodation will be provided in the University student hostels and hotels satisfying international standards. The conference programme will include ladies and social programmes. All services including travels, accommodation, pre- and post-conference programme will be arranged by the travel agency TATRATOUR, Bratislava.

Further information: Organizing Committee of the 8th ICTA, c/o Slovak Technical University, 812 43 Bratislava, Czechoslovakia.

CALENDAR OF FORTHCOMING MEETINGS

Feb. 25–March 1, 1985 New Orleans, LA, U.S.A.	**36th Pittsburgh Conference and Exposition on Analytical Chemistry and Applied Spectroscopy** Contact: David R. Weill III, Shady Side Academy, 423 Fox Chapel Road, Pittsburgh, PA 15238, U.S.A. Tel.: (421) 781-2400 X258.
Apr. 15–19, 1985 Pretoria, South Africa	**2nd International Symposium on Analytical Chemistry in the Exploration, Mining and Processing of Materials** Contact: The Symposium Secretariat S.328, CSIR, Box 395, Pretoria, 0001 South Africa. Tel.: (012) 86-9211 ext. 4412 or 2077. Telex: 3-21312 SA.
April 28–May 3, 1985 Miami Beach, FL, U.S.A.	**189th National Meeting of the American Chemical Society** Contact: Meetings Department, American Chemical Society, 1155 Sixteenth Street, NW, Washington, DC 20036, U.S.A.
May 7–9, 1985 Gaithersburg, MD, U.S.A.	**OM 85. Topical Conference on Basic Properties of Optical Materials** Contact: Robert S. Levine, B260 Polymers Building, NBS, Gaithersburg, MD 20899, U.S.A. Tel.: 301/921-3845.
May 14–16, 1985 Riva del Garda, Italy	**6th International Symposium on Capillary Chromatography** Contact: Dr. P. Sandra, Laboratory of Organic Chemistry, University of Ghe Krijgslaan 281 (S.4), B-9000 Ghent, Belgium.
June 3–6, 1985 Oslo, Norway	**21st International Symposium on Advances in Chromatography** Contact: Prof. A. Zlatkis, Chemistry Department, University of Houston, Houston, TX 77004, U.S.A. Tel.: (713) 713) 749-2623. Telex.: 762878. (Further details published in Vol. 162.)

ıne 9–15, 1985 rankfurt am Main, F.R.G.	**ACHEMA 85, 21st Exhibition-Congress on Chemical Engineering** Contact: DECHEMA, Organisation ACHEMA, Postfach 970146, D-6000 Frankfurt am Main 97, F.R.G. Tel.: (06 11) 75 64-0241/242. Telex: 412 490 dcha d.
une 17–19, 1985 aithersburg, MD, U.S.A.	**International Conference on Chemical Kinetics** Contact: John T. Herron, A147 Chemistry Building, NBS, Gaithersburg, MD 20899, U.S.A. Tel.: 301/921-2792.
une 17–21, 1985 msterdam, he Netherlands	**Amsterdam Summerschool on HPLC** Contact: The Municipal Congress Bureau, Oudezijds Achterburgwal 199, 1012 DK Amsterdam, The Netherlands. Tel.: (020) 552.3458 or (020) 552.3459.
une 19–21, 1985 nowmass, CO, U.S.A.	**Silanes, Surfaces and Interfaces** Contact: Mail Stop CO2430, Dow Corning Corporation, Midland, MI 48640, U.S.A.
une 24–29, 1985 erseburg, G.D.R.	**Statistical Methods in Analytical Chemistry, International Summer-School** Contact: "Carl Schorlemmer" Technical University, c/o Post-graduate Education, Otto-Nuschke-Strasse, DDR-4200 Merseburg, G.D.R.
uly 1–5, 1985 dinburgh, Scotland, J.K.	**9th International Symposium on Column Liquid Chromatography** Contact: J.H. Knox, Department of Chemistry, University of Edinburgh, Edinburgh EH 9 3JJ, Scotland, U.K.
ug. 19–23, 1985 ratislava, zechoslovakia	**8th International Conference on Thermal Analysis** Contact: Organizing Committee of the 8th ICTA, c/o Slovak Technical University, 812 43 Bratislava, Czechoslovakia.
ept. 3–7, 1985 ansas City, MO, U.S.A.	**2nd International Symposium on the Synthesis and Applications of Isotopically Labeled Compounds** Contact: Dr. D. Wilk, Symposium Coordinator, School of Pharmacy, 5100 Rochill Road, Kansas City, MO 64110, U.S.A. Tel.: (816) 276-16160. (Further details published in Vol. 162.)
ept. 5–8, 1985 irmingham, U.K.	**Flow Analysis III – An International Conference on Flow Analysis** Contact: Flow Analysis III, Dr. A.M.G. Macdonald, Department of Chemistry, The University, P.O. Box 363, Birmingham B15 2TT, U.K. (Further details published in Vol. 159.)
ept. 8–13, 1985 hicago, Il, U.S.A.	**190th National Meeting of the American Chemical Society** Contact: Meetings Department, American Chemical Society, 1155 Sixteenth Street, NW, Washington, DC 20036, U.S.A.
ept. 9–13, 1985 anchester, U.K.	**30th International Congress of Pure and Applied Chemistry** Contact: The Royal Society of Chemistry, Burlington House, London WIV 0BN, U.K. (Further details published in Vol. 155.)
ept. 15–21, 1985 armisch–Partenkirchen, .R.G.	**Colloquium Spectroscopicum Internationale XXIV** Contact: CSI XXIV, Organisationsbüro, Institut für Spektrochemie und angewandte Spektroskopie, Postfach 778, D 4600 Dortmund 1, F.R.G.
Sept. 16–19, 1985 Bradford, U.K.	**Particle Size Analysis 1985** Contact: Dr. T. Allen, School of Powder Technology, University of Bradford, Bradford, West Yorkshire BD7 1DP, U.K. Tel.: (0274) 733466 ext. 382/380.

Oct. 9–11, 1985 Gaithersburg, MD, U.S.A.	**1st International Symposium on Fire Safety Science** Contact: J. Quintiere, A345 Polymers Building, NBS, Gaithersburg, MD 20899, U.S.A. Tel.: 301/921-3242.
Oct. 24–25, 1985 Freiburg, F.R.G.	**2nd Symposium on Handling of Environmental and Biological Samples in Chromatography** Contact: Workshop Office IAEAC, M. Frei-Hausler, Postfach 46, CH-4123 Allschwil 2, Switzerland. (Further details published in Vol. 162.)
Nov. 11–16, 1985 Yalta, U.S.S.R.	**5th Danube Symposium on Chromatography** Contact: Dr. L.N. Kolomiets, The Scientific Council of Chromatography, Academy of Sciences of the U.S.S.R., Institute of Physical Chemistry, Lenin-Prospect 31, Moscow 117312, U.S.S.R.
Jan. 3–10, 1986 Maui, HI, U.S.A.	**1986 Winter Conference on Plasma Spectrochemistry** Contact: 1986 Winter Conference, c/o ICP Information Newsletter, Department of Chemistry, GRC Towers, University of Massachusetts, Amherst, MA 01003-0035, U.S.A. Tel.: (413) 545-2294.
Apr. 22–24, 1986 Noordwijkerhout, The Netherlands	**Anatech '86 – An International Symposium on Applications of Analytical Chemical Techniques to Industrial Process Control** Contact: Prof. W.E. van der Linden, Laboratory for Chemical Analysis, Department of Chemical Technology, Twente University of Technology, P.O. Box 217, 7500 AE Enschede, The Netherlands.
May 18–23, 1986 San Francisco, CA, U.S.A.	**New Frontiers in HPLC. 10th International Symposium on Column Liquid Chromatography** Contact: Ms. Shirley Schlessinger, 400 E. Randolph Drive, Chicago, IL 60601, U.S.A.
July 20–26, 1986 Bristol, U.K.	**SAC 86 – International Conference and Exhibition on Analytical Chemistry** Contact: Miss P.E. Hutchinson, Royal Society of Chemistry, Analytical Division, Burlington House, London W1V 0BN, U.K. Tel.: (01) 734-9971.
Aug. 25–29, 1986 Antwerp, Belgium	**10th International Symposium on Microchemical Techniques** Contact: Dr. R. Dewolfs, University of Antwerp (UIA), Department of Chemistry, Universiteitsplein 1, B-2610 Wilrijk, Belgium. Tel.: 03/828.25.28 (ext. 204). Telex: 33646

(Continued from outside back cover)

CONTENTS

(Abstracted, Indexed in: Anal. Abstr.; Biol. Abstr.; Chem. Abstr.; Curr. Contents Phys. Chem. Earth Sci.; Life Sci.; Index Med.; Mass Spectrom. Bull.; Sci. Citation Index; Excerpta Med.)

(Continued on inside back